

**DEVELOPMENT OF NOVEL FUNCTIONALIZED
SOLID PHASE EXTRACTION (SPE) SORBENTS
AND SOLID PHASE MICROEXTRACTION (SPME)
FIBER COATINGS FOR ANALYTICAL
APPLICATIONS**

**A Thesis Submitted to
the Graduate School of Engineering and Sciences of
İzmir Institute of Technology
In Partial Fulfillment of the Requirements for the Degree of
DOCTOR OF PHILOSOPHY**

in Chemistry

**by
Ezel BOYACI**

**December 2011
İZMİR**

ACKNOWLEDGEMENTS

I would like to acknowledge the help of many people during the course of my study. Firstly, I would like to thank my supervisor Prof.Dr. Ahmet E. Erođlu for providing invaluable insights, timely encouragement as well as guidance, balanced by the freedom to express myself throughout this research work.

I am thankful to Prof.Dr. O.Yavuz Ataman, Prof.Dr. Emür Henden, Assist.Prof.Dr. Ritchie Eanes and Assist.Prof.Dr Ali Çađır who readily agreed to be members of my thesis examining committee. I also thank Assoc.Prof.Dr. Talal Shahwan and Assoc.Prof.Dr. Mustafa Demir for their constructive comments on the thesis.

I would like to extend my sincere thanks to Handan Gaygısız for her valuable helps on studies performed in hyphenation of HPLC with ICP-MS, to Dr. Hüseyin Özgener for providing help on elemental analysis, to the research scientists at the Center for Materials Research (IZTECH) for their help on facilities TGA, XRD and SEM, and also to the research scientists Esra Yücel, Sanem Ezgi Kınal and Filiz Kurucaovalı at the Environmental Research Centre for ICP-MS analyses. My special thanks to Prof. Dr. Klaus Albert (University of Tübingen, Germany) for useful discussions during the XI. National Spectroscopy Congress and providing solid state NMR spectra of sorbents. I am thankful to Dr. Sinem Bezirciliođlu (Academic Writing Center) for her help during the review of the thesis. I would like to thank Polat Bulanık from Chemistry Department for supplying my endless last minute chemical requirements.

I would like to acknowledge The Scientific and Technological Research Council of Turkey (TÜBİTAK) for the support of this work through the project 108T798 and also İzmir Institute of Technology for the support of the thesis by project 2009İYTE18. Thanks to HES Kablo for kindly donating the fiber optic cables.

My special thanks go to my sisters Meral Karaca, Ayşegül Şeker, Merve Demirkurt, Esen Dönertaş and Semira Ünal. I am thankful to all the present and past members of our research group especially to Dr. Arzu Erdem, Dr. Aslı Erdem, Dr. Müşerref Yersel, Dr. Öznur Kaftan and Deniz Bölek, to Dr. Murat Erdoğan and Dr. Betül Öztürk for their friendships and instructive advice. Many thanks go to Nesrin Horzum for timeless insightful conversations and helpful comments in electrospinning process.

Finally, this thesis would not have been possible without the continuous support of my family. I dedicate this work to my family.

ABSTRACT

DEVELOPMENT OF NOVEL FUNCTIONALIZED SOLID PHASE EXTRACTION (SPE) SORBENTS AND SOLID PHASE MICROEXTRACTION (SPME) FIBER COATINGS FOR ANALYTICAL APPLICATIONS

In the first part of the study, amino-, mercapto- and bifunctional silica-based solid phase extraction (SPE) sorbents were developed, characterized and utilized for sorption and speciation of inorganic As(III)/As(V). Critical parameters on sorption and desorption of species were investigated. The proposed methodology was validated through the analysis of a standard reference material. The subsequent studies were concentrated on the transfer of the experience gained during the modification of silicate surface for preparation of SPE sorbents to the preparation of SPME coatings.

The second part of the thesis includes the development, characterization and use of solid phase microextraction (SPME) fibers for the speciation of inorganic and organometallic arsenic compounds. SPME fiber coatings have been prepared by two routes, namely, sol-gel synthesis and nanoparticle immobilization. Fibers having amino functionality synthesized through the sol-gel process were used in the speciation of As(III), As(V), monomethyl arsonic acid (MMA) and dimethyl arsinic acid (DMA). HPLC-HGAAS or HPLC-ICPMS was used in the measurements. Speciation of arsenic compounds was also realized using SPME fibers modified with zero valent iron nanoparticles embedded into an agarose matrix. The detection of the solid phase microextracted analytes was realized by HPLC-ICPMS. Prepared fibers have shown superior extraction for arsenicals. The effect of several parameters on the extent of extraction of arsenic species; namely, solution pH, extraction time, agitation speed and ionic strength were investigated. Validity was checked via the application of the proposed methodology on real samples (tap water, bottled water and geothermal water, urine samples) and standard reference materials.

ÖZET

ANALİTİK UYGULAMALAR İÇİN İŞLEVSELLEŞTİRİLMİŞ YENİ KATI FAZ EKSTRAKSİYON (SPE) VE KATI FAZ MİKROEKSTRAKSİYON (SPME) FİBER KAPLAMALARININ GELİŞTİRİLMESİ

Çalışmanın ilk kısmında, amino-, merkapt- ve her iki fonksiyonel grubu içeren (bifonksiyonel) silika bazlı katı faz ekstraksiyon (SPE) sorbentleri hazırlanmış, karakterize edilmiş ve inorganik As(III)/As(V) türleme çalışmalarında kullanılmıştır. Arsenik türlerinin sorpsiyonu ve çözeltiye geri alınmasındaki kritik parametreler araştırılmıştır. Önerilen metot standart referans madde analizi ile valide edilmiştir. Sonraki çalışmalar, silika yüzeyinin işlevselleştirilmesi ve SPE sorbentlerinin hazırlanması sırasında edinilen tecrübenin, SPME kaplamalarının geliştirilmesinde kullanılması üzerine yoğunlaşmıştır.

Tezin ikinci kısmı, katı faz mikroekstraksiyon (SPME) fiberlerinin geliştirilmesini, karakterizasyonunu ve inorganik/organometalik arsenik bileşiklerinin türleme çalışmalarında kullanılmasını kapsamaktadır. SPME fiber hazırlanmasında sol-jel sentezi ve nanoparçacık immobilizasyonu olmak üzere iki farklı rota izlenmiştir. Sol-jel metodu ile amino- fonksiyonel grupları içerecek şekilde hazırlanan fiberler As(III), As(V), monometil arsonik asit (MMA) ve dimetil arsinik asit (DMA) türlemesinde kullanılmıştır. Ölçümler, HPLC-HGAAS veya HPLC-ICPMS ile yapılmıştır. Arsenik türlerinin ayrılmasında ayrıca agaroz matriksinde sabitlenen sıfır değerlikli demir nanoparçacıklarıyla kaplı SPME fiberleri de kullanılmış, ekstrakte edilen analitler HPLC-ICPMS ile tayin edilmiştir. Hazırlanan fiberler arsenik türleri için yüksek ekstraksiyon göstermiştir. Çözelti pH'sı, ekstraksiyon süresi, karıştırma hızı ve iyonik güç gibi parametrelerin arsenik türlerinin ekstraksiyonuna olan etkisi incelenmiştir. Metodun validasyonu, musluk suyu, şişe suyu, jeotermal su ve çeşitli standart referans maddelerin analiz edilmesiyle test edilmiştir.

TABLE OF CONTENTS

LIST OF FIGURES	xii
LIST OF TABLES	xvii
LIST OF ABBREVIATIONS.....	xix
CHAPTER 1. INTRODUCTION	1
1.1. Solid Phase Extraction (SPE) and Solid Phase Microextraction (SPME).....	1
1.2. Types of SPME	3
1.3. Advantages and Disadvantages of SPME.....	4
1.4. Commercially Available Fibers	5
1.5. Fiber Coatings Developed in Literature.....	5
1.6. Theoretical Aspects of SPME.....	11
1.7. Effect of Various Parameters	12
1.7.1. Thickness of Coating.....	12
1.7.2. Type of Coating.....	12
1.7.3. Type of Analyte and Matrix.....	13
1.7.4. pH of Solution	13
1.7.5. Extraction Time.....	13
1.7.6. Ionic Strength	14
1.8. Detection with SPME	14
1.9. Sol-Gel Chemistry for Thermally Stable Coatings	15
1.9.1 Sol-Gel Coating Steps	16
1.9.1.1. Hydrolysis	16
1.9.1.2. Polycondensation.....	16
1.9.1.3. Condensation	17
1.9.1.4. Surface Bonding.....	17
1.10. Arsenic	20
1.10.1. Occurrence and Toxicity of Arsenic	20
1.10.2. Determination and Speciation of Arsenic	21

1.11. Aim of the Study	25
CHAPTER 2. NEW SPE SORBENTS: SOLID PHASE EXTRACTION	
OF ARSENIC WITH MODIFIED SILICA	26
2.1. Experimental	26
2.1.1. Instrumentation and Apparatus	26
2.1.2. Reagents and Solutions	27
2.1.3. Synthesis of Sorbents	28
2.1.4. Characterization of Sorbents	30
2.1.5. Sorption Studies	31
2.1.6. Sorption Isotherm Model: Dubinin–Radushkevich (D–R)	
Isotherm Model	31
2.1.7. Desorption Studies	33
2.1.8. Reusability of the Sorbents	33
2.1.9. Method Validation	34
2.2. Results and Discussion	34
2.2.1. Characterization of Sorbents	35
2.2.2. Sorption Studies	42
2.2.2.1. Effect of pH on the Sorption of As(III) and As(V)	42
2.2.2.2. As(III) Sorption	47
2.2.2.2.1. pH = 1.0	48
2.2.2.2.2. pH = 9.0	49
2.2.2.2.3. pH = 3.0	51
2.2.2.3. As(V) Sorption	53
2.2.3. Sorption Capacity (Dubinin–Radushkevich Isotherm Model).....	58
2.2.4. Desorption Studies	59
2.2.4.1. Desorption of As(III).....	59
2.2.4.2. Desorption of As(V).....	60
2.2.5. Reusability of the Sorbents	61
2.2.6. Method Validation	63
CHAPTER 3. NEW SPME SORBENTS: SOLID PHASE MICROEXTRACTION	
OF ARSENIC	65
3.1. Experimental	65

3.1.1. Instrumentation and Apparatus	65
3.1.1.1. HPLC-HGAAS.....	65
3.1.1.2. HPLC-ICPMS	66
3.1.1.3. Characterization and Microextraction Studies	68
3.1.2. Reagent and Solutions.....	68
3.1.3. Preparation of the SPME Fibers.....	72
3.1.3.1. Sol-Gel Based SPME Fiber Coatings.....	72
3.1.3.2. Sol-Gel Based Electrospun Amine-Modified SPME Fiber Coating	73
3.1.3.3. Capillary Template Method for Immobilization of Zerovalent Iron Nanoparticles.....	74
3.1.3.4. Electrospun Nanofibers Coated SPME Fibers	76
3.1.3.4.1. Electrospun ZnO Nanofibers	77
3.1.3.4.2. Electrospun Fe ₂ O ₃ Nanofibers	77
3.1.4. Arsenic Speciation with Sol-Gel Based SPME Fibers.....	78
3.1.4.1. Extraction of Arsenic Species	78
3.1.4.2. Extraction of Arsenic Species: Further Improvement on the Fibers	78
3.1.4.3. Optimization of Extraction Parameters for Electrospun Coated Amine-Modified SPME Fibers	79
3.1.4.3.1. Effect of pH on Extraction of Arsenic Species.....	79
3.1.4.3.2. Effect of Agitation Time/Speed on Extraction of Arsenic Species.....	79
3.1.4.3.3. Effect of Salt Concentration (Ionic Strength) on Extraction of Arsenic Species.....	80
3.1.4.3.4. Effect of Solution Temperature on Extraction of Arsenic Species.....	80
3.1.4.3.5. Repetitive Use of the Fibers and Fiber Reproducibility.....	80
3.1.5. Arsenic Speciation with Nanoparticle Immobilized (Capillary Template) SPME Fibers	81
3.1.5.1. Extraction of the Arsenic Species	81
3.1.5.2. Optimization of Extraction Parameters	81
3.1.5.2.1. Effect of pH on Extraction of Arsenic Species.....	81

3.1.5.2.2. Effect of Agitation Time/Speed on Extraction of Arsenic Species.....	82
3.1.5.2.3. Effect of Salt Concentration (Ionic Strength) on Extraction of Arsenic Species.....	82
3.1.5.3. Interference Studies.....	83
3.1.5.4. Analytical Performance of the Method.....	83
3.1.5.5. Method Validation.....	84
3.2. Results and Discussions.....	84
3.2.1. Characterization of Prepared SPME Fibers.....	84
3.2.1.1. Sol-Gel Based SPME Fiber Coatings.....	85
3.2.1.2. Nanoparticles Immobilized SPME Fibers Prepared by Capillary Template Method.....	90
3.2.1.3. Electrospun Nanofiber Immobilized SPME Fibers.....	94
3.2.1.3.1. Electrospun ZnO Nanofibers.....	94
3.2.1.3.2. Electrospun Fe ₂ O ₃ Nanofibers.....	97
3.2.1.3.2.1. Effect of Amount of FeCl ₃ .6H ₂ O.....	97
3.2.1.3.2.2. Effect of the Solvent.....	105
3.2.1.3.2.3. Effect of the Feeding Rate.....	110
3.2.2. Arsenic Speciation with Sol-Gel Based SPME Fibers.....	117
3.2.2.1. Optimization of Chromatographic Separation and Hydride Generation of Arsenic Species (HPLC-HGAAS).....	117
3.2.2.2. Speciation of Arsenic with Amine-Modified Fibers (Manual Coated).....	119
3.2.2.3. Speciation of Arsenic with Amine-Modified Fibers: Further Improvement on the Fibers.....	122
3.2.2.3.1. Optimization of Chromatographic Parameters for HPLC-ICPMS.....	122
3.2.2.3.2. Optimization of Fiber Coating.....	125
3.2.2.3.3. Optimization of Extraction Parameters.....	130
3.2.2.3.3.1. Effect of pH on Extraction of Arsenic Species.....	130
3.2.2.3.3.2. Effect of Agitation Time/Speed on Extraction of Arsenic Species.....	133

3.2.2.3.3.3. Effect of Salt Concentration (Ionic Strength) on Extraction of Arsenic Species.....	137
3.2.2.3.3.4. Effect of Solution Temperature on Extraction of Arsenic Species.....	139
3.2.2.3.4. Repetitive Use of the Fibers and Fiber Reproducibility	140
3.2.3. Arsenic Speciation with Nanoiron-Agarose SPME Fibers	141
3.2.3.1. Optimization of Desorption Parameters.....	142
3.2.3.2. Optimization of Extraction Parameters.....	144
3.2.3.2.1. Effect of pH on Extraction of Arsenic Species.....	144
3.2.3.2.2. Effect of Agitation Time/Speed on Extraction of Arsenic Species	146
3.2.3.2.3. Effect of Salt Concentration (Ionic Strength) on Extraction of Arsenic Species.....	149
3.2.3.3. Interference Studies.....	152
3.2.3.4. Analytical Performance of the Method.....	155
3.2.3.5. Method Validation	157
 CHAPTER 4. CONCLUSIONS	 162
 REFERENCES	 166

LIST OF FIGURES

<u>Figure</u>	<u>Page</u>
Figure 1.1. Summary of micro extraction techniques.....	2
Figure 1.2. Typical SPME device	3
Figure 1.3. SPME extraction modes	4
Figure 1.4. Hydrolysis reaction.....	16
Figure 1.5. Polycondensation reaction.....	16
Figure 1.6. Condensation reaction	17
Figure 1.7. Surface bonding of the network	18
Figure 1.8. Deactivation process.....	18
Figure 2.1. Synthesis steps of modified silica gel.....	29
Figure 2.2. TGA curves of a) (SH)silica b) (NH ₂ +SH)silica, c)unmodified silica, and d) (NH ₂)silica	36
Figure 2.3. ²⁹ Si CP/MAS of activated silicate	38
Figure 2.4. ²⁹ Si CP/MAS of (NH ₂)silicate	39
Figure 2.5. ²⁹ Si CP/MAS of (SH)silicate.....	39
Figure 2.6. ²⁹ Si CP/MAS of (NH ₂ +SH)silicate.....	40
Figure 2.7. ¹³ C CP/MAS NMR spectra of (NH ₂)silicate	40
Figure 2.8. ¹³ C CP/MAS NMR spectra of (SH)silicate	41
Figure 2.9. ¹³ C CP/MAS NMR spectra of (NH ₂ +SH)silicate.....	41
Figure 2.10. Effect of pH on the sorption of 100.0 µgL ⁻¹ a) As(III) and b) As(V)	44
Figure 2.11. Effect of pH on the sorption of 100.0 µgL ⁻¹ (●) As(III) and (▼) As(V) ...	44
Figure 2.12. Speciation diagram of As(III).....	47
Figure 2.13. Speciation diagram of As(V).....	47
Figure 2.14. Effect of a) sorbent amount, b) reaction time, c)temperature on the sorption of 100.0 µgL ⁻¹ As(III).....	48
Figure 2.15. Effect of a) sorbent amount, b) reaction time, c)temperature on the sorption of 100.0 µgL ⁻¹	50
Figure 2.16. Effect of a) sorbent amount, b) reaction time, c)temperature on the sorption of 100.0 µgL ⁻¹ As(III)	52
Figure 2.17. Effect of the sorbent amount on the sorption of 100.0 µgL ⁻¹ As(V)	54

Figure 2.18. Effect of the amount of (NH ₂)silica on the sorption of 100.0 µgL ⁻¹ As(V) in (Δ) unbuffered and (▲) buffered solutions	55
Figure 2.19. Variation in the solution pH as a function of reaction time for different amounts of (NH ₂)silica.....	55
Figure 2.20. Effect of the reaction time on the sorption of 100.0 µgL ⁻¹ As(V).....	56
Figure 2.21. Effect of the reaction time on the sorption of 100.0 µgL ⁻¹ As(V) by (NH ₂)silica in (Δ) unbuffered and (▲) buffered solutions	57
Figure 2.22. Effect of the reaction temperature on the sorption of 100.0 µgL ⁻¹ As(V)	58
Figure 3.1. HPLC-ICPMS system	67
Figure 3.2. Dip coating method	74
Figure 3.3. Coating procedure of silica fiber	76
Figure 3.4. Experimental set-up used in electrospinning process.....	76
Figure 3.5. SEM images of various manually coated sol-gel based SPME fibers	86
Figure 3.6. SEM images of amine-functionalized fibers (10 mm/min removal speed, single layer coating).....	87
Figure 3.7. SEM images of amine-functionalized fibers (10 mm/min removal speed, double layer coating)	87
Figure 3.8. SEM images of amine-functionalized fibers (1 mm/min removal speed, single layer coating).....	88
Figure 3.9. SEM images of amine-functionalized fibers (1 mm/min removal speed, double layer coating).....	89
Figure 3.10. SEM images of amine-functionalized fibers (1 mm/min removal speed, single layer coating, high viscosity PDMS) ..	89
Figure 3.11. EDX spectrum of amine-functionalized fibers.....	90
Figure 3.12. SEM images of a) bare silica fiber b) and c) agarose coated silica fiber ...	91
Figure 3.13. SEM images of nZVI-agarose fibers at various magnifications	92
Figure 3.14. SEM images of the synthesized zerovalent iron nanoparticles	92
Figure 3.15. EDX spectra of a) bare silica fiber and b) agarose coated silica fiber and c) nanoiron-agarose coated silica fiber	93
Figure 3.16. XRD pattern of the a) agarose powder, b) nZVI, c) ground silica fiber and d) ground nanoiron-agarose fiber.....	94
Figure 3.17. SEM images of electrospun coated fiber before calcination	95

Figure 3.18. SEM images of electrospun fibers after calcination.....	96
Figure 3.19. SEM images of PVP+FeCl ₃ electrospun fibers (11.50 g PVP/ 0.50 g FeCl ₃ .6H ₂ O)	98
Figure 3.20. SEM images of PVP+FeCl ₃ electrospun fibers (11.50 g PVP/ 1.00 g FeCl ₃ . 6H ₂ O)	99
Figure 3.21. SEM images of PVP+FeCl ₃ electrospun fibers (11.50 g PVP/ 1.50 g FeCl ₃ . 6H ₂ O)	99
Figure 3.22. SEM images of PVP+FeCl ₃ electrospun fibers (11.50 g PVP/ 2.50 g FeCl ₃ . 6H ₂ O)	100
Figure 3.23. SEM images of PVP+FeCl ₃ electrospun fibers after calcination.....	101
Figure 3.24. TGA curves of a) PVP, b) PVP+FeCl ₃ , and c) PVP+FeCl ₃ after calcination.....	102
Figure 3.25. XRD pattern of the a) PVP, b) PVP+FeCl ₃ , and c) PVP+FeCl ₃ after calcination.....	104
Figure 3.26. SEM images of PVP+FeCl ₃ electrospun fibers prepared in ethanol (20.0 mLh ⁻¹)	106
Figure 3.27. SEM images of PVP+FeCl ₃ electrospun fibers prepared in ethanol (10.0 mLh ⁻¹)	107
Figure 3.28. SEM images of PVP+FeCl ₃ electrospun fibers prepared in ethanol (5.0 mLh ⁻¹)	108
Figure 3.29. SEM images of PVP+FeCl ₃ electrospun fibers prepared in ethanol (1.0 mLh ⁻¹)	109
Figure 3.30. SEM images of PVP+FeCl ₃ electrospun fibers prepared in ethanol (0.5 mLh ⁻¹)	110
Figure 3.31. SEM images of PVP+FeCl ₃ electrospun fibers (20.0 mLh ⁻¹)	111
Figure 3.32. SEM images of PVP+FeCl ₃ electrospun fibers after calcination (20.0 mLh ⁻¹)	112
Figure 3.33. SEM images of PVP+FeCl ₃ electrospun fibers (10.0 mLh ⁻¹).....	112
Figure 3.34. SEM images of PVP+FeCl ₃ electrospun fibers after calcination (10.0 mLh ⁻¹)	113
Figure 3.35. SEM images of PVP+FeCl ₃ electrospun fibers (5.0 mLh ⁻¹)	113
Figure 3.36. SEM images of PVP+FeCl ₃ electrospun fibers after calcination (5.0 mLh ⁻¹)	114

Figure 3.37. SEM images of PVP+FeCl ₃ electrospun fibers a) before calcination b) and c) after calcination (1.0 mLh ⁻¹).....	114
Figure 3.38. SEM images of PVP+FeCl ₃ electrospun fibers (0.5 mLh ⁻¹)	115
Figure 3.39. SEM images of PVP+FeCl ₃ electrospun fibers after calcination (0.5 mLh ⁻¹).....	115
Figure 3.40. SEM images of PVP+FeCl ₃ electrospun fibers (0.1 mLh ⁻¹)	116
Figure 3.41. SEM images of PVP+FeCl ₃ electrospun fibers after calcination (0.1 mLh ⁻¹).....	116
Figure 3.42. Optimization of hydride formation conditions of arsenic species.....	118
Figure 3.43. Callibration plot for As(V) extraction	120
Figure 3.44. Callibration plot for DMA extraction.....	121
Figure 3.45. Callibration plot for MMA extraction	121
Figure 3.46. Optimization of chromatographic conditions in HPLC-ICPMS	124
Figure 3.47. Chromatograms obtained after extraction with endcapped amine-modified fibers.....	126
Figure 3.48. Chromatograms obtained after extraction with non endcapped amine-modified fibers.....	127
Figure 3.49. Effect of APTES amount in the sol-gel solution on extraction of the As(V) in dip coated fibers.....	129
Figure 3.50. Effect of APTES amount in the sol-gel solution on extraction of the As(V) in electrospun coated fibers.	129
Figure 3.51. Proposed coating mechanisms for a) electrospinning and b) dip coating methods.....	130
Figure 3.52. Effect of solution pH on extraction of As(V).....	131
Figure 3.53. Effect of solution pH on extraction of DMA	132
Figure 3.54. Effect of solution pH on extraction of MMA.....	132
Figure 3.55. Effect of agitation time on extraction of As(V)	134
Figure 3.56. Effect of agitation time on extraction of DMA	134
Figure 3.57. Effect of agitation time on extraction of MMA	135
Figure 3.58. Effect of agitation speed on extraction of As(V)	135
Figure 3.59. Effect of agitation speed on extraction of DMA	136
Figure 3.60. Effect of agitation speed on extraction of MMA	136
Figure 3.61. Effect of NaCl concentration on extraction of As(V).	137
Figure 3.62. Effect of NaCl concentration on extraction of DMA.....	138

Figure 3.63. Effect of NaCl concentration on extraction of MMA	138
Figure 3.64. Effect of solution temperature on extraction of the arsenic species.....	139
Figure 3.65. Repetitive use of the same fiber	140
Figure 3.66. Fiber-to-fiber reproducibility	141
Figure 3.67. Effect of KH_2PO_4 concentration on arsenic peaks	143
Figure 3.68. Repetitive desorption of As species from the same fiber.....	143
Figure 3.69. Effect of solution pH on extraction of As species by nanoiron-agarose fiber	145
Figure 3.70. Effect of solution pH on extraction of As species by agarose fiber	146
Figure 3.71. Effect of agitation speed on extraction of the As species.....	148
Figure 3.72. Effect of agitation time on extraction of the As species.....	148
Figure 3.73. Effect of ionic strength on the extraction of the As species.....	150
Figure 3.74. Chromatograms obtained with SPME-HPLC-ICPMS after inserting fiber into 0.010 M NaCl solution	150
Figure 3.75. Chromatograms obtained after injection of 0.010 M NaCl to HPLC-ICPMS	151
Figure 3.76. Selected ion monitoring chromatograms at m/z: 78 for selenium elution from HPLC-ICPMS	154
Figure 3.77. Selected ion monitoring chromatogram at m/z: 51 for vanadium elution from HPLC-ICPMS	155
Figure 3.78. Selected ion monitoring chromatogram at m/z: 121 for antimony elution from HPLC-ICPMS	155
Figure 3.79. Chromatograms obtained from validation.....	158

LIST OF TABLES

<u>Table</u>	<u>Page</u>
Table 1.1. Summary of SPME fiber coatings developed in literature	7
Table 1.2. Reagents used for a typical sol-gel based fiber coatings	19
Table 1.3. Arsenic speciation with SPME	24
Table 2.1. Certified values for Natural Water – Trace Elements (SRM 1640)	28
Table 2.2. Summary of the parameters and ranges used throughout the study	31
Table 2.3. Surface area and pore width results	36
Table 2.4. Elemental analysis results	36
Table 2.5. Summary of Dubinin-Radushkevich coefficients	59
Table 2.6. Desorption of As(III) using 0.050 M KIO ₃ in 2.0 M HCl	60
Table 2.7. Desorption of As(III) using 0.50 M NaOH	60
Table 2.8. Desorption of As(V) with various eluent	61
Table 2.9. Repetitive use of (NH ₂)silica for sorption of As(V)	62
Table 2.10. Repetitive use of (NH ₂ +SH)silica and (NH ₂)silica+(SH)silica for sorption of As(V)	63
Table 2.11. Repetitive use of (NH ₂ +SH)silica and (NH ₂)silica+(SH)silica for sorption of As(III)	63
Table 2.12. Spike recovery results obtained using (NH ₂ +SH)silica for a drinking water sample	64
Table 3.1. Operation conditions for HPLC-HGAAS	66
Table 3.2. Operation conditions for HPLC-ICPMS	67
Table 3.3. Reagents used through the preparation of SPME fiber coatings	70
Table 3.4. Certified values for Trace Elements in Natural Waters (SRM 1643e)	72
Table 3.5. Arsenic species used throughout the study	119
Table 3.6. Summary of the interference study	153
Table 3.7. Typical calibration line equations obtained with prepared SPME fibers	156
Table 3.8. Typical calibration line equations obtained with HPLC-ICPMS without extraction with SPME fiber	156
Table 3.9. Relative standard deviations obtained for inter-day and intra-day extractions	157
Table 3.10. Method validation with novel SPME fibers	161

Table 3.11. Sample applications with novel SPME fibers.	161
--	-----

LIST OF ABBREVIATIONS

AAS	atomic absorption spectrometry/spectrometer
APTES	3-Aminopropyltriethoxysilane
AsB	arsenobetaine
AsC	arsenocholine
BTEX	benzene, toluene, ethylbenzene, and xylenes
CE	capillary electrophoresis
CP/MAS NMR	cross polarization and magic angle spinning nuclear magnetic resonance
CW/DVB	carbowax/divinylbenzene
DCM	dichloromethane
DMA	dimethyl arsenic acid
D-R	Dubinín–Radushkevich
EDX	energy-dispersive X-ray spectroscopy/spectrometer
EPA	Environmental Protection Agency
ESI-MS	electrospray ionization mass spectrometry/spectrometer
GC	gas chromatography/chromatograph
GC-ECD	gas chromatography electron capture detection/detector
GC-FID	gas chromatography flame ionization detection/detector
GC-FPD	gas chromatography flame photometric detection/detector
GC-MS	gas chromatography mass spectrometry/spectrometer
GC-MS-PFPD	gas chromatography mass spectrometry pulsed flame photometric detection/detector
GC-PFPD	gas chromatography pulsed flame photometric detection/detector
GC-TDS	gas chromatography thermionic specified detection/detector
HG	hydride generation
HG-AAS	hydride generation atomic absorption spectrometry/spectrometer
HG-AFS	hydride generation atomic fluorescence spectrometry/ spectrometer
HPLC-ESI-MS	high performance liquid chromatography electrospray ionization mass spectrometry/spectrometer

HPLC-HGAAS	high performance liquid chromatography hydride generation atomic absorption spectrometry/spectrometer
HPLC-ICPMS	high performance liquid chromatography inductively coupled plasma mass spectrometry/spectrometer
HR-XPS	high resolution X-ray photoelectron spectroscopy/spectrometer
IC	ion chromatography/chromatograph
ICP-MS	inductively coupled plasma mass spectrometry/spectrometer
IEP	iso electric point
IZTECH	İzmir Institute of Technology
LC-ESI-MS/MS	liquid chromatography electrospray ionization tandem mass spectrometry/spectrometer
LC- MS/MS	liquid chromatography coupled with tandem mass spectrometry
LLE	liquid liquid extraction
LOD _{3s}	limit of detection
LOQ _{10s}	limit of quantification
LPME	liquid phase microextraction
MALDI-IMS	matrix-assisted laser desorption/ionization imaging mass spectrometry/spectrometer
MALDI-TOF	matrix-assisted laser desorption/ionization-time of flight
MALDI-TOF-MS	matrix-assisted laser desorption/ionization time of flight mass spectrometry/spectrometer
MMA	monomethyl arsonic acid
MPTMS	(3-Mercaptopropyl) trimethoxysilane
MTMOS	methyltrimethoxysilane
(NH ₂)silica	3-Aminopropyltriethoxysilane treated silica
(NH ₂ +SH)silica	3-Aminopropyltriethoxysilane and (3-Mercaptopropyl) trimethoxysilane treated silica
NIST	National Institute of Standards and Technology
NMR	nuclear magnetic resonance
nZVI	nano zerovalent iron
OH-TSO	hydroxyl terminated silicone oil
PA	polyacrylate
PAH	polycyclic aromatic hydrocarbons
PDMDPS	polydimethyldiphenylsiloxane

PDMS	polydimethylsiloxane
PDMS/DVB	polydimethylsiloxane/divinylbenzene
PEG	polyethylene glycol
PFA	perfluoroalkoxy
PhAs	phenylarsonic acid
PMHS	poly(methylhydrosiloxane)
PPY	polypyrrole
PVA	polyvinyl alcohol
PVP	polyvinylpyrrolidone
RSD	relative standard deviation
RT	room temperature
SBSE	stir bar sorptive microextraction
SDME	single drop microextraction
SEM	scanning electron microscopy/microscope
SFI-HGAAS	segmented flow injection hydride generation AAS
(SH)silica	(3-Mercaptopropyl) trimethoxysilane treated silica
SPE	solid phase extraction
SPME	solid phase microextraction
SRM	standard reference material
TeMA	tetramethylarsonium ion
TEOS	tetraethyl orthosilicate
TFA	trifluoroacetic acid
TFME	thin film microextraction
TG/DTA	thermo gravimetry/differential thermal analyzer
THF	tetrahydrofuran
TMAO	trimethylarsine oxide
TMOS	tetramethyl orthosilicate
upw	ultra pure water
VOCs	volatile organic compounds
WHO	World Health Organization
XRD	x-ray diffraction/diffractometer

CHAPTER 1

INTRODUCTION

1.1. Solid Phase Extraction (SPE) and Solid Phase Microextraction (SPME)

Solid-phase extraction (SPE) is a widely used sample preparation method. Acting mechanism of SPE depends on partition of analyte between solid active phase and sample matrix. This method is very similar to liquid liquid extraction (LLE) which suffers from drawbacks such as requirement for large amounts of organic solvents and long extraction times and in some cases, from incomplete extraction of analytes. SPE was introduced in early 1970s to eliminate classical LLE problems (Fritz 1999). Benefits of the method are preconcentration of analyte to detection threshold values and enrichment of valuable compounds, sample clean up, purification, and removal of toxics from environmental samples (Huck and Bonn 2000). Although it was introduced to overcome classical LLE problems, requirement of less toxic reagents or minimized handling of the solvents as well as obstructions resulting from multistep extraction and elution, demands the development of new and more environmentally compatible methods. For this purpose, the solid-phase microextraction (SPME) was introduced in early 1990s. SPME, incorporates several sampling, extraction, concentration and sample introduction processes into a single step (Kataoka 2010; Zhang et al. 1994). In addition to time saving features of single (multi purpose) step, the other advantage of SPME is that it is a solvent free method for desorption in gas chromatography (GC). Generally, only two essential steps exist: partitioning of the analyte between coating and sample matrix and desorption of the extracted analyte into an analytical instrument (Zhang et al. 1994). In addition to SPME, other microextraction related techniques were also developed by extending this technology. The generalized form of microextraction related methods is summarized in Figure 1.1.

The first studies about SPME were started by Janusz Pawliszyn to develop a solvent free solid-phase extraction method for volatile organic compounds (Zhang et al. 1994). The major problem associated with plugging in the classical solid-phase

extraction method focused on the studies on head space extractive sorbents. This approach did not suffer from plugging limitations. Coatings of commercial GC capillary columns were the examples of the first developed SPME active phases for extraction of the volatile organic compounds (VOCs) (Lord and Pawliszyn 2000). Figure 1.2 illustrates the general view of a commercial solid-phase microextraction fiber and fiber holder. The fiber consists of a fused silica core coated with an active outside layer. The fiber with the extracting phase is protected within stainless steel piercing needle for repetitive use. The stainless steel needle is contained in special designed syringe like fiber holder.

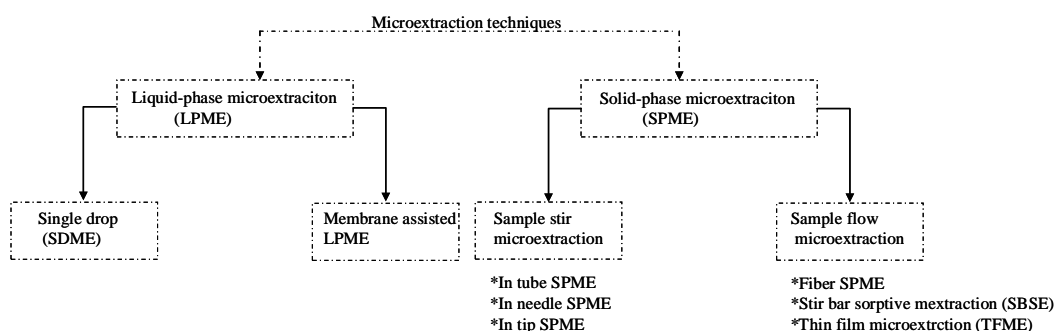


Figure 1.1. Summary of micro extraction techniques
(Source: Kataoka 2010)

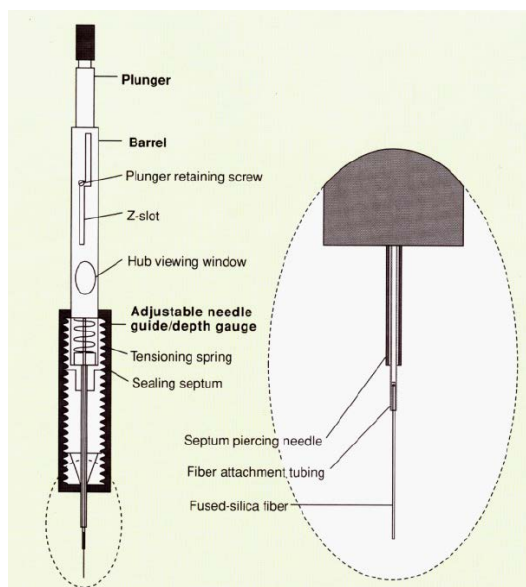


Figure 1.2. Typical SPME device
(Source: Zhang et al. 1994)

1.2. Types of SPME

SPME can be used in two general approaches, namely, direct mode and headspace mode (Koning et al. 2009). Direct mode (Figure 1.3a) depends on the direct immersion of the fiber active phase in the solution containing the non volatile analyte(s). When equilibrium is established, the fiber is withdrawn and the concentrated analytes are introduced into the sample introduction port of an analytical instrument such as high performance liquid chromatograph (HPLC), inductively coupled plasma mass spectrometer (ICP-MS) or capillary electrophoresis (CE). Primarily, the headspace mode is used for volatile analytes. Extraction of the analyte(s) from the sample is achieved just by inserting the active phase of the fiber on the top of the sample without direct contact with the solution (Figure 1.3b). Extracted analyte(s) are thermally desorbed on injection port of a GC which provides both qualitative and quantitative information (Mester et al. 2001). The headspace mode includes extraction and sequential desorption (to GC) steps and eliminates elution step with solvents. There are various derivatization agents which make possible the headspace extraction of some non volatile and semi-volatile analytes. The acting mechanism depends on the changing polarity (which also affects the volatility) of the analyte. In addition, derivatization has a function of enabling better chromatographic separations.

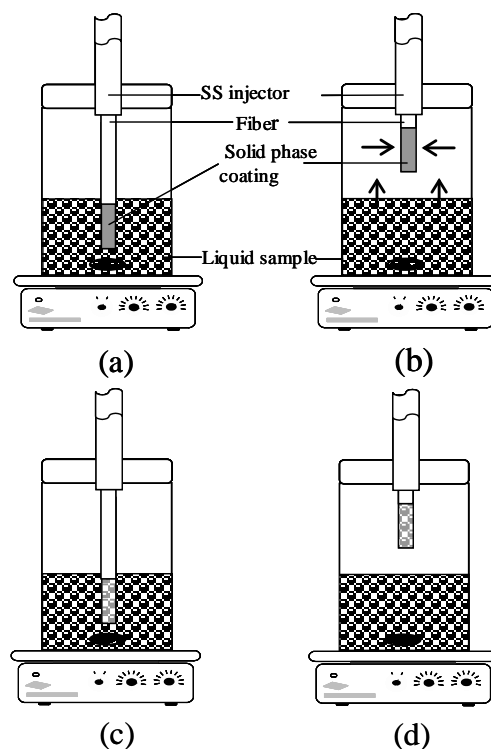


Figure 1.3. SPME extraction modes a) direct extraction, b) headspace extraction, c) equilibrium in direct mode, d) equilibrium in headspace mode

1.3. Advantages and Disadvantages of SPME

SPME is a solvent free technique which is one of the most important benefits of the method. In addition, short application time, analyte concentration ability, improved detection limits, repetitive use of the same fiber (up to 100 extractions) and selectivity are other important features. Moreover, it is practical to use with a wide range of samples such as air samples, solid samples, food samples and aqueous samples (Risticvic 2009). In contrast to the great deal of advantages limitations arise especially with lack of analyte specific fiber coatings. Since commercially available fibers are limited to some polar, non polar and semi-polar characters the extraction of a fiber is similar for analogous compounds (Nerin et al. 2009; Zhang et al. 1994). Other drawbacks are poor reproducibility in analysis and production of fibers (Dietz et al. 2006).

1.4. Commercially Available Fibers

Commercially available fibers are divided into three major categories, namely, polar, semi-polar and nonpolar fibers. The coatings are inspired from commercial gas chromatographic capillary column fillings. Polydimethylsiloxane (PDMS) is the most popular non polar coating for SPME. Polydimethylsiloxane/Divinylbenzene (PDMS/DVB) is semi-polar coating. Polar coatings are polyacrylate (PA) and Carbowax/Divinylbenzene (CW/DVB) (Mester et al. 2001; 2005). Production of fibers with distinctive coatings reduces the possibility of extracting interferences and increases the extraction selectivity. Another classification of the coatings depends on homogeneity of the active phase. One of them is homogeneous pure polymer coatings (Pawliszyn 1999). PDMS and PA are examples of homogeneous coatings. The stability of these coatings via organic solvents is enhanced by cross linking (bonding) of polymers. The second type of coatings is the porous particles embedded in a partially cross-linked polymeric phase. These coatings are not robust as homogeneous types but they are more selective. Examples of blended coatings are PDMS/DVB, CW/DVB and PDMS/Carboxen. Blending of the polymer enhances the total capacity of the fiber by increasing the porosity of the coatings. In addition, increasing the porosity of the polymer particles in fiber amplifies analyte retention on fiber. Moreover, pore size of the polymer particle in coating affects selectivity of the fiber (Pawliszyn 1999).

1.5. Fiber Coatings Developed in Literature

Development of a new type of fiber coating is a growing area in SPME technologies, especially to extend the application areas, matrixes and analyte types. Generally, commercial fibers are convenient for GC applications, but the main drawback is the thermal instability of the phase during desorption. Some fibers can also be used with HPLC (PDMS). However, desorption into HPLC requires solvents which destroy surface coating. The studies related to production of the new fiber coatings are extended to develop solvent-resistive and thermally stable active coatings as well as to enhance mechanical strength of the phase. In addition, developing the new functionality enhances the selectivity for specific analytes. Especially, sol-gel route offers the opportunity for attachment of various functionalities to the fiber which expands the

working area of SPME to biological applications. Table 1.1 summarizes the recent methods applied in the literature for development of new SPME coatings. It can be mentioned that, the major working areas are sol-gel based modifications of fiber surface by attachment of sol-gel active functional groups onto fused silica. Molecular imprinting is another surface modification method frequently used especially to prepare analyte selective coatings. Furthermore, immobilization of nanoparticles, particularly carbon nanotubes, is promising in SPME coatings (Augusto et al. 2010).

Table 1.1. Summary of SPME fiber coatings developed in literature

Coating	Analyte	Detection	Reference
Titania sol-gel coated (anodized) alumina fiber (Tetrabutylortitanate, PEG)	BTEX	GC-FID	Farhadi et al. 2009
NiTi alloy coated with ZrO ₂ (electrodeposition)	BTEX, alcohols and trihalomethanes	GC-FID	Budziak et al. 2007
Ionic liquid coated fused silica capillary (1-butyl-3-methylimidazolium hexafluorophosphate)	PAH	GC-FID	Huang et al. 2009
Physically incorporated extraction phase (PDMS) containing 3% vinyl, Methyltrimethoxysilane, Poly(methylhydrosiloxane)	BTEX, organophosphorous pesticides	GC-FID, GC-TDS	Liu et al. 2006
Membrane SPME (PEG, PDMS)	phenols	GC-FID	Kloskowski and Pilarczyk 2009
Ionic liquid-mediated bis[(3-methylmethoxysilyl)propyl] polypropylene oxide-based polar sol-gel coating	direct extraction of polar and nonpolar analytes	GC-FID	Shearrow et al. 2009
Various types of coated silica (octadecyl, polar embedded (RP-Amide C16 (RPA)) and cyano) particles	drug analysis	LC-MS/MS	Vuckovic et al. 2009
Nanostructured titania coating in situ on the surface of titanium wire	dichlorodiphenyltrichloroethane and its degradation products	GC-ECD	Cao et al. 2008
Highly porous solid-phase microextraction fiber coating based on poly(ethylene glycol)-modified ormosils (Carbowax 20M ormosil)	BTEX	GC-FID	Silva and Augusto 2005
Multiwalled carbon nanotubes/Nafion coating	polar aromatic compounds	GC-FID	Chen et al. 2009
Sol-gel based coatings with C8-TEOS and MTMOS	diphenylmercury; triphenylarsine; trimethylphenyltin	HPLC-UV	Gbatu et al. 1999
Phosphonate modified silica nanoparticle-deposited capillary	phosphopeptides	MALDI-TOF	Wu et al. 2010

(cont. on next page)

Table 1.1. (cont.)

Coating	Analyte	Detection	Reference
A sol-gel-based amino functionalized fiber with 3-(trimethoxysilylpropyl) amine, PDMS, PMHS	organophosphorus pesticides	GC-MS	Bagheri et al. 2010
A novel sol-gel-based amino-functionalized fiber for headspace solid-phase microextraction	phenol and chlorophenols	GC-MS	Bagheri et al. 2008
Homemade OH/TSO (Hydroxylterminated silicone oil)-PMHS fiber	antiestrogens	GC-MS	Liu et al. 2009
Home made (C8-TEOS): methyltrimethoxysilane (MTMOS) coated fiber	arson	GC-FID	Ahmad et al. 2008
NiTi alloy coated with ZrO ₂ (electrodeposition)	haloanisoles	GC-ECD	Budziak et al. 2009
Biocompatible coatings based on polyacrylonitrile	verapamil, loperamide, diazepam, nordiazepam, and warfarin	HPLC	Musteata et al. 2007
Carbon nanotube-coated metal fiber based on sol-gel technique	BTEX and phenols, PAH	GC-MS	Jiang et al. 2009
Silica HDK20, pyrogenic Aerosil, SC16. Silica xerogel, Silica aerogel coatings	isoamyl acetate, ethyl hexanoate, phenylethyl alcohol, ethyl octanoate, 2-phenylethyl acetate, and ethyl decanoate,	GC-MS	Biazon et al. 2009
Electrochemically deposited boronate affinity extracting phase (poly- 3-aminophenylboronate (polyAPBA))	cis-diol biomolecules	HPLC-UV	He et al. 2009
Polypropylene microporous membrane	halogenated toluenes	GC-ECD GC-MS	Carpinteiro et al. 2009
Metal-organic frameworks 199 Films	benzene homologues	GC-FID	Cui et al. 2009
Molecularly imprinted polymer (MIP)-coated solid-phase microextraction	ascorbic acid	Preanodized MIP-modified HMDE sensor	Prasad et al. 2008

(cont. on next page)

Table 1.1. (cont.)

Coating	Analyte	Detection	Reference
Polyphosphate-doped polypyrrole coated on steel fiber	organochlorine pesticides	GC-ECD	Mollahosseini and Noroozian 2009
Ametryn-imprinted polymer (Methacrylic acid (functional monomer), ethylene glycol dimethacrylate (cross linker) ametryn (template))	triazine herbicides	GC-MS	Djozan et al. 2009
Molecularly imprinted solid-phase microextraction fibers	bisphenol A	HPLC	Tan et al. 2009
NiTi fibers coated with functionalised silica (C-18) particles HO-PDMS, TEOS, VTEOS C-18	benzaldehyde, acetophenone and dimethylphenol, BTEX	GC-FID	Azenha et al. 2009
Poly(pyrrole) film coated fibers	antidepressants	HPLC-UV	Chaves et al. 2009
Amino ethyl-functionalized nanoporous fiber	essential oil	GC-MS	Hashemi et al. 2009
Tosyl-functionalized carbon nanoparticles	benzophenone-3 and triclosan	Voltam.	Vidal et al. 2008
Magnesium oxinate nanoparticle-modified carbon paste electrode	copper(II)	Cyclic voltammetry	Zhu et al. 2010
Polymeric negative photoresist, SU-8 2100 -nanofibers	benzene, toluene, ethylbenzene, o-xylene, phenol, 4-chlorophenol and 4-nitrophenol	GC-FID	Zewe et al. 2010
Silica nanoparticle -deposited capillary modified with octadecyl groups	endocrine disruptors and polycyclic aromatic hydrocarbons	HPLC	Li et al. 2009
AS-16® latex particles possessing quaternary ammonium functionalities	fluoride, chloride, nitrite, bromide, nitrate, sulfate and phosphate	IC	Kaykhaiii et al. 2011
TiO ₂ nanoparticle	phosphopeptides	LC-ESI-MS/MS	Lin et al. 2008

(cont. on next page)

Table 1.1. (cont.)

Coating	Analyte	Detection	Reference
Carbon monolith prepared from styrene and divinylbenzene precursors and dodecanol as a porogen during polymerization	phenols	GC-MS	Shi et al. 2009
Sol-gel based polymer-functionalized single-walled carbon nanotubes	polybrominated diphenyl ethers	GC-ECD	Zhang et al. 2009
Sol-gel based coatings with Allyloxy bisbenzo 16-crown-5 trimethoxysilane (precursor) for sol-gel -derived bisbenzo crown ether/hydroxylterminated silicone oil	organophosphorous pesticides	GC-FPD	Yu et al. 2004
Silica nanoparticle-deposited capillary bonded by 3-(triethoxysilyl) propyl methacrylate and then modified with poly(N-isopropylacrylamide) .	diethylstilbestrol	HPLC	Yu et al. 2011

1.6. Theoretical Aspects of SPME

SPME is not an exhaustive but equilibration method. Mainly, three phase equilibrium is established in SPME. Equilibria in fiber coating (c), gas phase (h) and sample matrix (s). Analyte distributes itself through each phase until equilibrium is reached (Mester and Sturgeon 2005).

$$C_0V_0 = C_cV_c + C_hV_h + C_sV_s \quad (1.1)$$

Equation 1.1 describes total mass of analyte, where C_0 and V_s are initial concentration of analyte in the sample and volume of the sample, respectively. Mass of analyte adsorbed on fiber is given by Equation 1.2, where K_{hs} and K_{ch} are distribution coefficients for gas phase-sample (hs) and coating-gas phase (ch), respectively.

$$n = \frac{K_{ch}K_{hs}V_cC_0V_s}{K_{ch}K_{hs}V + K_{hs}V_h + V_s} \quad (1.2)$$

The definition of distribution coefficient of coating-sample (K_{cs}) is given by Equation 1.3, which simplifies the expression of the mass of the analyte extracted on the fiber for head space (Eqn. 1.4) and for direct extraction (Eqn. 1.5). The equation relating the amount of the analyte extracted by headspace shows that this amount is independent of the position of the fiber (no terms related to K_{ch}).

$$K_{cs} = K_{ch}K_{hs} \quad (1.3)$$

$$n = \frac{K_{cs}V_cC_0V_s}{K_{cs}V_c + K_{hs}V_h + V_s} \quad (1.4)$$

$$n = \frac{K_{cs}V_cC_0V_s}{K_{cs}V_c + V_s} \quad (1.5)$$

Generally, the volume of the coating is much smaller than the volume of the sample and Eqn. 1.5 simplifies to Eqn. 1.6. This means that there is no need to exactly know the sample volume since the extracted amount of the analyte is independent of the sample volume. The simplified equation clearly demonstrates the dependence of the extracted amount of analyte on the active fiber coating volume, initial concentration of the analyte in the sample and affinity of the coating and the sample matrix for the analyte.

$$n = K_{cs} V_c C_0 \quad (1.6)$$

1.7. Effect of Various Parameters

1.7.1. Thickness of Coating

The volume of the active phase on the fiber directly affects the sensitivity of the SPME method. Although increasing the thickness of the coatings results in slower mass transfer of analyte through the fiber (which means the longer extraction time), increasing coating thickness or increasing the length of the active phase also results in enhanced analyte extraction. This constructively affects sensitivity (Zhang et al. 1994).

1.7.2. Type of Coating

In a typical microextraction, analyte affinity of the fiber coating and type of sample matrix are important. A large partition coefficient, K_{cs} , is essential for adequate extraction of the analyte. This can be achieved with proper coating; the general rule is “like dissolves like” (Pawliszyn 1999). Nowadays, SPME fibers with novel functional extracting phases with more selective recognition sites or specific binding groups are introduced for various applications.

1.7.3. Type of Analyte and Matrix

The nature of sample matrix is crucial in extraction of the analyte. Additionally, the volatility of the analyte has a significant effect. In case of the volatile analytes, headspace extraction works well, while semi-volatiles need heating to overcome the kinetics of the mass transfer (Zhang et al. 1994). The headspace determination of nonvolatile analytes usually requires derivatization which results in volatile products (Lambropoulou 2007). For relatively clean sample matrixes, the direct extraction mode also results in rapid mass transfer. In the case of complex matrixes, the direct mode does not work well and requires headspace extractions.

1.7.4. pH of Solution

Solution pH may play an important role in the sensitivity of the method (Zhang et al. 1994). In the case of non-ionic polymer fiber coatings, the partition of the analyte is larger on the fiber in its neutral form. Thus, in principle, it is important to adjust the sample pH to obtain neutral forms when analytes are in acidic or basic forms in the original sample.

1.7.5. Extraction Time

Extraction time is controlled by mass transfer phenomena. Generally, mass transfer depends on diffusion of analyte from sample matrix and through coatings. Commonly, efficient agitation results in non restricted analyte diffusion from sample matrix (Zhang et al. 1994). In that case mass transfer depends closely on diffusion of the sample into fiber coatings. Equilibrium is achieved more rapidly with thin fiber coatings when analyte diffusion to fiber is the only rate determining step for mass transfer. The most favorable approach for extraction time is approaching the time where there is no significant increase in extracted analyte. This means reaching equilibrium between sample and fiber. In quantitative analyses, attaining equilibrium conditions are vital since non equilibrium conditions result in significant variations on extracted amount of analyte. In addition, agitation conditions strictly control the extraction equilibrium.

Sonication decreases extraction equilibration time with respect to magnetic stirring. Additionally, temperature also has an effect on extraction time. Mass transfer is faster at higher temperature and equilibrium is established rapidly.

1.7.6. Ionic Strength

Large partition coefficients (K) of analytes are needed for SPME. The K for the analyte depends on the interaction of the analyte with the fiber and with the sample matrix. In general, modification of matrix decreases the matrix analyte interaction and results in large partition coefficients. In the case of polar organic compounds, salting the sample matrix increases ionic strength and decreases the matrix analyte interaction (Zhang et al. 1994). This is not valid for ionic compounds.

1.8. Detection with SPME

Choosing detection system to be connected to SPME fiber after desorption is crucial. Efficient coupling between SPME and detector requires an efficient interface design. Commonly, SPME detection systems are gas chromatography coupled to mass detector or flame ionization detector for head space extraction of volatile organic compounds (Farhadi et al. 2009; Ahmad et al. 2008; Mester and Sturgeon 2005). Volatile analytes are thermally desorbed in the GC injector port. When the analyte is a non volatile or semi-volatile species, derivatization is applied for GC determination (Kaur et al. 2006). In addition, HPLC and ICP-MS are other common methods used after direct mode SPME (Gbatu et al. 1999). Metals and organometals are determined also after derivatization with various detection systems, namely, GC, ICP-MS, gas chromatography pulsed flame photometric detector (GC-PFPD) and HPLC (Mester and Sturgeon 2005). Moreover, volatile organometallic species had been directly introduced into ICP-MS and atomic absorption spectrometer (AAS) with special interfaces (Dietz et al. 2003). Coupling with capillary electrophoresis is another successful strategy (Pawliszyn 1999). In addition to the hyphenated techniques mentioned above, numerous other methods had been used in combinations to provide better detection. These have included direct introduction to electrospray ionization mass spectrometry (ESI-MS) (Mester and Pawliszyn 1999), high performance liquid chromatography electrospray

ionization mass spectrometry (HPLC-ESI-MS) (Wu et al. 2000), matrix-assisted laser desorption/ionization time of flight mass spectrometry (MALDI-TOF-MS) (Bail et al. 2009) and matrix-assisted laser desorption/ionization imaging mass spectrometry (MALDI-IMS) (Tong et al. 2002).

1.9. Sol-Gel Chemistry for Thermally Stable Coatings

As aforementioned, commercial SPME coatings are inspired from GC capillary column packings. The active filling inside the wall of the GC column is not chemically bonded. Mostly, static coatings are applied. For SPME fibers, the same approach has limitations for thermal stability of the phase (Pawliszyn 1999). Thus, SPME fibers commonly suffer from limitation due to the repetitive use. Another drawback is due to film coating thinner than what is needed. To overcome these weaknesses of the method, the active phase should be chemically bonded onto the surface of the fiber. The best approach for the preparation of the stable coatings is the sol-gel based coating methods (Bagheri et al. 2010). This approach provides strong adhesion of the coating onto a silica surface which improves the stability against solvent and heating. The porosity of the silicate matrix presents a large surface area for extraction sites. Moreover, selectivity of the fibers can easily be varied with the nature of the coatings (Yu et al. 2002; Alhooshani et al. 2005). Sol-gel active reagents make it possible to extend variation in coating as well as in controlling the volume of the coating.

Generally, the sol-gel based coatings are utilized as follows: the bare silica fiber is dipped into an alkoxide-based sol-gel precursor under acid catalyst. This results in hydrolysis of the precursor and formation of the polymer network attached onto surface of the silica via reaction of surface silanol groups with siloxane groups (Gbatu et al. 1999; Kumar et al. 2008). The addition of a hydroxy terminated sol-gel active polymer and surface derivatizing agent to the sol-gel solution produces a porous organic-inorganic hybrid chemically bonded phase on the surface of the fiber. The functional groups can vary according to the analytes. The thickness of the coating is simply controlled by the number of times of successive dippings of the fiber into the sol-gel solution.

1.9.1 Sol-Gel Coating Steps

1.9.1.1. Hydrolysis

The first step in the sol-gel process is the hydrolysis reaction which occurs while the alkoxide precursor is mixed with water in the presence of alcohol to achieve sufficient homogenization. Hydrolysis leads to the formation of silanol groups. Intermediates produced in the alcohol–water medium include silanols, ethoxy silanols and oligomers of low molecular weight which were formed during the first stages of the process. Hydrolysis reactions can be catalyzed by either acid or base. Two hydrolysis processes give different structures and morphology; acid catalysis forms linear weakly cross-linked polymer whereas base catalysis forms more highly branched clusters as a result of rapid hydrolysis step (Brinker et al. 1990).

Figure 1.4 illustrates the hydrolysis reaction that occurs under acid catalysis of the alkoxide based precursor.

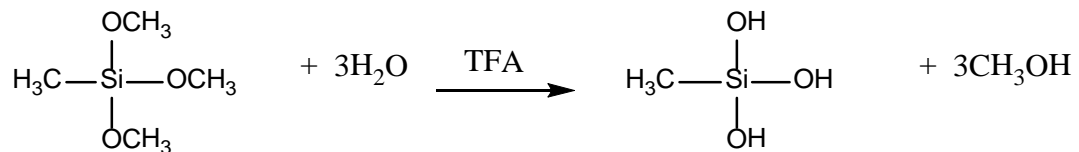


Figure 1.4. Hydrolysis reaction

1.9.1.2. Polycondensation

The second step of sol-gel synthesis is the polycondensation between the two silanol groups and condensation reaction between silanol and alkoxyde groups by releasing a water or alcohol unit, respectively (Figure 1.5).

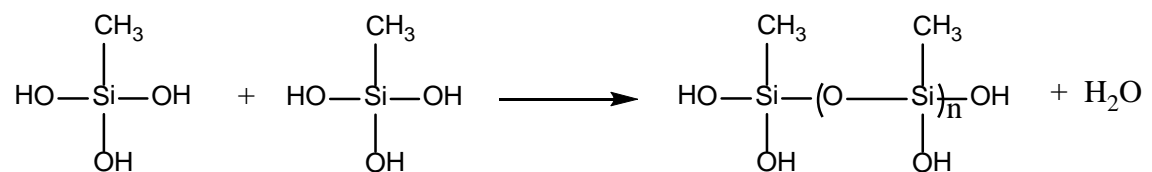


Figure 1.5. Polycondensation reaction

1.9.1.3. Condensation

Further condensation of the silica network with sol-gel active hydroxy terminated organic polymer results in organic- inorganic network (Figure 1.6).

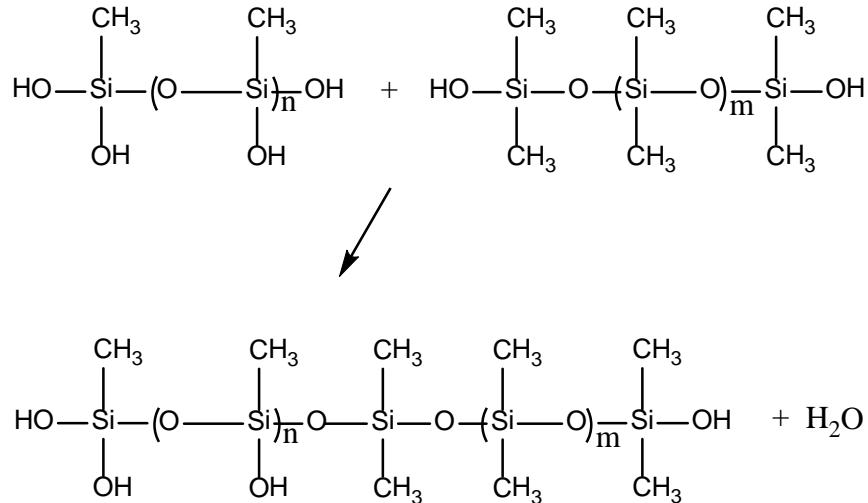


Figure 1.6. Condensation reaction

1.9.1.4. Surface Bonding

Surface bonding on silica fiber is achieved simply by dipping the bare fiber into produced viscous sol-gel. Chemical bonding of polymer network to silica surface occurs through condensation of the surface silanol groups with silanol or siloxane groups in the organic-inorganic polymer network (Figure 1.7).

The final step of the process is deactivation (or derivatization) of the silanol groups using Poly(methylhydrosiloxane) (Figure 1.8). Deactivation process is completed after thermal curing of the resulting fiber. In addition to the deactivation process, the PMHS also controls the polarity of the resulting coating.

Numerous sol-gel based coatings are summarized in the literature (Bagheri et al. 2008; Bianchi et al. 2008; Yu et al. 2004; Zeng et al. 2001; Wang et al. 2000). The most widely used are organic/inorganic based sol-gel approaches. In addition, only inorganic sol-gel with various functional groups is also given. The major reagent and their functionalities in the process are summarized in Table 1.2.

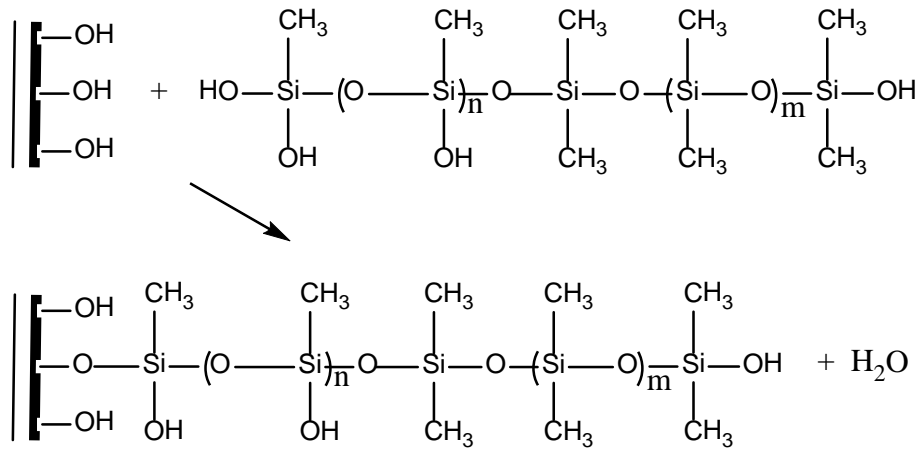


Figure 1.7. Surface bonding of the network

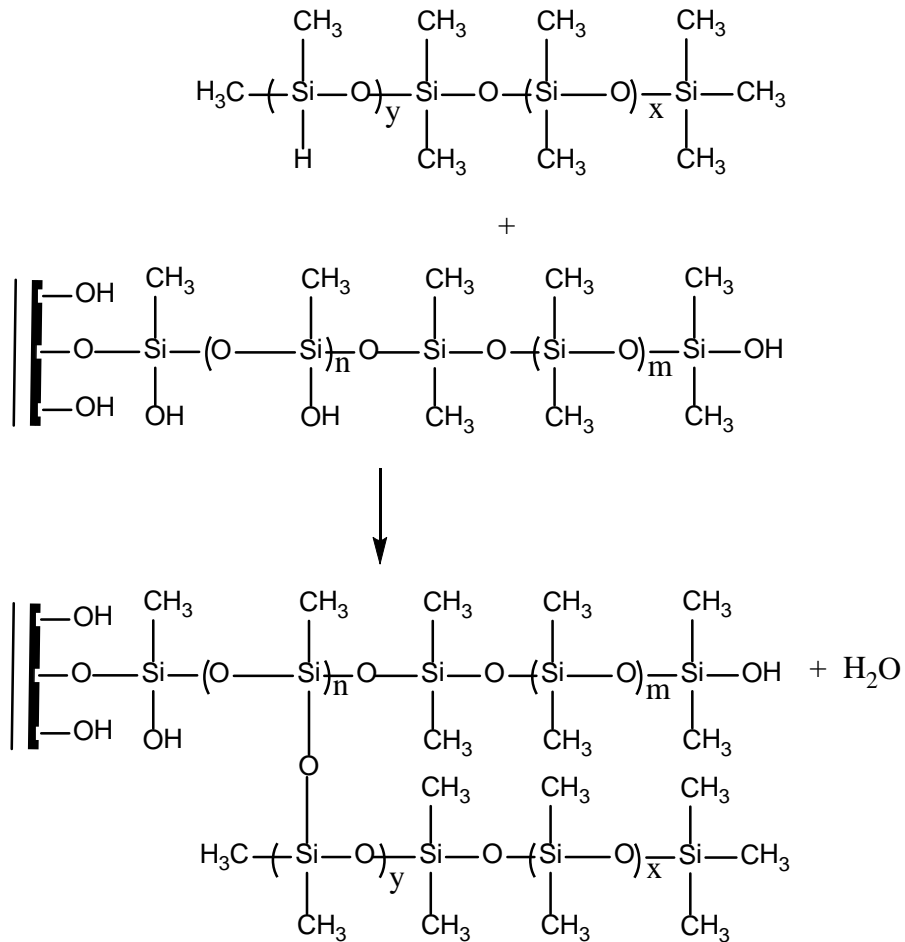


Figure 1.8. Deactivation process

Table 1.2. Reagents used for a typical sol-gel based fiber coatings

	Chemical name	Structure	Function
Sol-gel precursor	Methyltrimethoxysilane (MTMOS) (Pawliszyn 1999)		Source of inorganic component in network, provide active silanol groups for coating
	Tetraethyl orthosilicate (TEOS) (Shearrow et al. 2009)		
	Tetramethyl orthosilicate (TMOS) (Dietz et al. 2006)		
	3-Aminopropyltriethoxysilane (APTES) (Bagheri et al. 2008)		
Organic polymer with sol gel active terminal	polydimethylsiloxane (PDMS) (Pawliszyn 1999)	$\text{HO}-\underset{\text{CH}_3}{\overset{\text{CH}_3}{\text{Si}}}-\text{O}-\left(\underset{\text{CH}_3}{\overset{\text{CH}_3}{\text{Si}}}-\text{O}\right)_m-\underset{\text{CH}_3}{\overset{\text{CH}_3}{\text{Si}}}-\text{OH}$	Provide the organic component of hybrid network
	Polydimethyldiphenylsiloxane (PDMDPS) (Shearrow et al. 2009)	$\text{HO}-\left(\underset{\text{CH}_3}{\overset{\text{CH}_3}{\text{Si}}}-\text{O}\right)_m-\underset{\text{CH}_3}{\overset{\text{CH}_3}{\text{Si}}}-\text{O}-\left(\underset{\text{C}_6\text{H}_5}{\overset{\text{C}_6\text{H}_5}{\text{Si}}}-\text{O}\right)_n-\text{H}$	
	Polyethylene glycol (PEG) (Wang et al. 2000)	$\text{HO}-\left(\underset{\text{H}}{\overset{\text{H}}{\text{C}}}-\underset{\text{H}}{\overset{\text{H}}{\text{C}}}-\text{O}\right)_m-\text{H}$	
	n-Octyltriethoxysilane (Gbatu et al. 1999)		
	Hydroxyl terminated silicone oil (OH-TSO) (Yu et al. 2004)	$\text{C}_{60}-\text{(OH)}_n$	

(cont. on next page)

Table 1.2. (cont.)

	Chemical name	Structure	Function
Deactivation reagent	Poly(methylhydrosiloxane) PMHS (Pawlyszin 1999)	$\text{H}_3\text{C}-\text{Si}(\text{CH}_3)_2-\text{O}-\left(\text{Si}(\text{CH}_3)_2-\text{O}\right)_y-\left(\text{Si}(\text{CH}_3)_2-\text{O}\right)_x-\text{Si}(\text{CH}_3)_2-\text{CH}_3$	Deactivate silanol groups.
Sol-gel catalyst	Trifluoroacetic acid (TFA) (Pawlyszin 1999)	$\text{F}_3\text{C}-\text{C}(=\text{O})-\text{OH}$	Catalyze the sol gel process
	HCl (Gbatu et al. 1999)		
Solvents	Dichloromethane (DCM) (Shearrow et al. 2009)	$\text{Cl}-\text{CH}_2-\text{Cl}$	Provide a homogeneity in the sol gel process
	Methanol (Gbatu et al. 1999)	$\text{C}-\text{OH}$	

1.10. Arsenic

1.10.1. Occurrence and Toxicity of Arsenic

Arsenic is a metalloid present in the earth's crust, in seawater, and in the human body. Its natural existence in the environment and its release by anthropogenic sources result in an inevitable increase of accumulated arsenic in water resources. The element exists in the environment in two primary forms, organic and inorganic. Inorganic arsenic is mainly found at higher oxidation state, As(V), in most surface waters where oxidizing conditions are prevailing, and the lower oxidation state, As(III), predominantly occurs in ground waters where reducing conditions exist (EPA 1999). Organoarsenical species are formed through biotransformation of inorganic species by living organisms. The most common species are monomethyl arsonic acid (MMA), dimethyl arsinic acid (DMA), trimethylarsine oxide (TMAO), tetramethylarsonium ion (TeMA), arsenobetaine (AsB), arsenocholine (AsC) and arseno-sugars (Leermakers et

al. 2006). Although arsenic is regarded as one of the most toxic elements in the world, its toxicity depends on the oxidation state and the methylation order (Mandal and Suzuki 2002). Among organoarsenic species, AsB, AsC and arseno-sugars are known as non-toxic and frequently found in foodstuff as a result of bioaccumulation of inorganic arsenic species in waters by marine organisms (Leermakers et al. 2006; Kumaresan and Riyazuddin 2001). Several methylated biotransformation products of arsenic are known to be produced by various microorganisms in waters or sediments containing inorganic arsenic (Kumaresan and Riyazuddin 2001). A primary route of exposure of human body to arsenic occurs through the consumption of contaminated water and marine food which may give rise to acute and chronic poisoning. It has been reported that long term exposure to arsenicals results in keratosis, gangrene or development of cancer (EPA 1999; Choong et al. 2007). Acute poisoning shows symptoms such as bloody diarrhea and vomiting (Mohan and Pittman 2007). Recent studies about the toxicity of arsenic species on humans classify inorganic arsenic as a primary carcinogen (Calatayud et al. 2010). However, the results of animal experiments indicated evidences for cancer and non-neoplastic lesions formation as a result of exposure to DMA and MMA, respectively (Calatayud et al. 2010). Moreover, cytotoxic activity studies for the arsenic species revealed that the trivalent methylated species are even more toxic than inorganic As(III) and As(V) (Shen et al. 2009). The fact that the variation in the oxidation state and the methylation process affect the toxicity of the arsenic species necessitates the individual determination of each species rather than their total concentration.

1.10.2. Determination and Speciation of Arsenic

Various methods employed for the speciation of arsenic have been reviewed by various researchers in the field. For example, voltammetric and spectrophotometric methods have been used for speciation of inorganic arsenic compounds, while electrophoretic methods have been used to determine both inorganic and organometallic arsenic species (Kumaresan and Riyazuddin 2001). Nowadays, the most widely used arsenic speciation methods are hydride generation (HG) and chromatography. The formation of hydride species under selective reaction conditions with NaBH_4 derivatization is used to determine As(III), As(V), MMA and DMA by atomic detection methods (Bundaleska et al. 2005). Among the chromatographic methods, HPLC is the

most important tool for speciation of arsenical compounds. Since many of these compounds are ionic species, ion-exchange or ion-pair chromatography are used for separation (Day et al. 2002; Ackley et al. 1999). The detection of the species separated by liquid chromatography is mainly performed by atomic detection with ICP-MS (Afton et al. 2008; Ammann 2010; Kannamkumarath et al. 2004), hydride generation atomic absorption spectrometry (HG-AAS) (Sur and Dunemann 2004; Niedzelski et al. 2004; Tsalev et al. 2000) and hydride generation atomic fluorescence spectroscopy (HG-AFS) couplings (Bohari et al. 2002; Perez et al. 2008). However, the reliable quantification of arsenical species in biological matrixes generally requires more complicated preliminary sample preparation steps because of the possible oxidation of As(III) and transformation of organoarsenicals to inorganic forms.

Speciation of inorganic arsenic can also be achieved through selective adsorption of the species onto SPE sorbents. Depending on the selectivity of the sorbent toward the lower or higher oxidation step, a pre-oxidation or pre-reduction step is necessary before sorption. For example, in a recent study, As(V) was selectively adsorbed on a solid phase adsorbent and the total inorganic arsenic content was determined after pre-oxidation of As(III) to As(V) (Tüzen et al. 2008). Although this has been a practical strategy in speciation studies, the search of new sorbents capable of retaining both species under different conditions has been an important area. An example of these types of sorbents was described by Huang et al. (Huang et al. 2007) using dimercaptosuccinic acid-modified mesoporous titanium. In the study, both arsenic species were retained onto sorbent under neutral conditions while only arsenite was retained quantitatively at pH 10-11. Alternatively, modification of the available substrates with more than one functional group can be a promising strategy for speciation studies. Functionalization of the solid supports can be realized by functional silane coupling reagents. The polysiloxane sorbents functionalized with mercapto and amine groups are revealed in literature as effective in the removal of metal ions (Jal et al. 2004; El-Nahhal et al. 2000; El-Nahhal et al. 2001; El-Nahhal et al. 2002; El-Nahhal et al. 2007; El-Ashgar et al. 2005; Blitz et al. 2007) and Hg(II) (Ho et al. 2003; Puanngam and Unob 2008). In addition, bifunctional sorbents containing two functionalities (amine and mercapto) on the same sorbent had been prepared and used for the removal of metal ions (Burke et al. 2008). The advantage of the bifunctionalization can also be seen by the extraction of a wide spectrum of the hard and soft metal ions by the prepared sorbents.

Among the sample preparation techniques, SPME is, currently, a prevailing sample preparation technique. The advantages and disadvantages of the method have been discussed in previous parts of this chapter. Although the SPME-based sample preparation methods have been widely used and gained more recognition, there have been a few studies in literature which are summarized in Table 1.3. For instance, Mester et al. used commercial SPME fibers coated with PDMS/Carboxen for the extraction of As(III) after hydride generation with NaBH₄ and determined the extracted analyte using ICP-MS (Mester et al. 2000). Szostek et al. evaluated the extraction of dimethylarsinic acid, phenylarsonic acid and 2-chlorovinylarsonous acid by using commercial SPME fiber after dithiol derivatization (Szostek et al. 1998). Moreover, thioglycol methylate derivatization was used for the determination of DMA and MMA in human urine after extraction with commercial SPME fibers (Mester and Pawliszyn 2000). The requirement of additional derivatization step for arsenic determination can be regarded as one of the disadvantages of some SPME fibers. To overcome such a mandatory step, various home-made coatings for SPME were also proposed. Polypyrrole coated capillary was one of the successful examples of in tube SPME of DMA, MMA, AsB and AsC, which allows direct detection with liquid chromatography-electrospray ionization mass spectrometry (LC-ESI-MS) (Wu et al. 2000). Yates et al. and Tamer et al. proposed electro-synthesis of organic conducting polymers poly(3-dodecylthiophene) (Yates et al. 2002) and poly(3-octylthiophene) (Tamer et al. 2003), respectively, for the determination of AsB, while Gbatu et al. proposed similar SPME coating based on poly(3-methylthiophene) (Gbatu et al. 1999) for the determination of As(V) species. Among the limited number of studies for SPME of arsenicals, the major drawback arises from the lack of a method for extraction and quantification of each fundamental inorganic and organoarsenic species (As(III), As(V), DMA and MMA) by a single fiber at once.

Table 1.3. Arsenic speciation with SPME

Extraction phase	Analyte	Derivatization	Detection	Reference
100- μm PDMS, 85- μm PA, 65- μm Carbowax-DVB	DMA, PhAs, <i>trans</i> -2-chlorovinyl arsonous acid	dithiol derivatization	GC-MS	Szostek and Aldstadt 1998
Poly(3-dodecylthiophene)	AsB	-	HPLC-ICP-MS	Yates et al. 2002
Carboxen/PDMS 85- μm	dimethylchloroarsine	-	GC-MS	Killelea and Aldstadt 2002
PDMS 100 - μm , PDMS-CAR 75 μm , and PDMS-CAR-DVB 50/30 μm .	DMA, MMA, TMAO	NaBH ₄	GC-MS	Kösters et al. 2003
65- μm PDMS-DVB	Roxarsone, DMA, MMA	1,3-propanedithiol	GC-MS-PFPD	Roerdink and Aldstadt 2004
Ordered mesoporous Al ₂ O ₃	As(III)/As(V)	-	ICP-MS	Hu et al. 2008
PDMS	DMA, MMA	thioglycol methylate	GC-MS	Mester and Pawlyszyn 2000
Polypyrrole (PPY) coated capillary	MMA, DMA, AsB, AsC	-	LC-ESI-MS	Wu et al. 2000

1.11. Aim of the Study

The general aim of this thesis is to develop novel functionalized SPE sorbents and SPME fiber coatings for analytical applications. Since the scope of the study is relatively broad, the thesis includes several chapters. The first part of the thesis includes the preparation of mercapto-, amino-, and both functional groups (bifunctional) containing silica as a solid phase extraction materials. This part deals with the synthesis, characterization and application of the sorbent for As(III) and As(V) speciation. The second part of the thesis is related to the development of new SPME fiber coatings. As explained in related parts of the introduction section, the main drawback encountered with the commercial SPME fibers is the production of analyte-specific fiber coatings. Other critical point in SPME process is the stability problem that arises during thermal and solvent desorption. The second part of the thesis includes several sections with the major aim of the preparation of robust, easily prepared and selective SPME coatings. The experience gained during the sol-gel synthesis route applied in the preparation of SPE sorbents was transferred to subsequent studies for preparation of thermally stable/solvent resistive and selective SPME coatings. In this part, sol-gel based amino functionalized SPME fibers and nanoiron-functionalized SPME fibers were aimed to be prepared by various coating approaches. Among the limited number of studies for SPME of arsenicals, the major drawback arises from the lack of a method for extraction and quantification of each fundamental inorganic and organoarsenic species (As(III), As(V), DMA and MMA) by a single fiber at once. Thus, prepared fibers were used to develop novel SPME-HPLC-ICPMS methodologies for the simultaneous microextraction/speciation/determination of the metabolically critical inorganic and organoarsenic species, namely, As(III), As(V), DMA, and MMA in natural waters such as drinking and geothermal waters, and biological fluids such as urine.

CHAPTER 2

NEW SPE SORBENTS: SOLID PHASE EXTRACTION OF ARSENIC WITH MODIFIED SILICA

2.1. Experimental

2.1.1. Instrumentation and Apparatus

An inductively coupled plasma mass spectrometer (ICP-MS, Agilent 7500ce Series, Tokyo, Japan) was employed in the determination of arsenic concentrations at m/z : 75. In order to prevent the possible matrix-based polyatomic interference of $^{40}\text{Ar}^{35}\text{Cl}^+$ on $^{75}\text{As}^+$ signal, chloride-containing acids or solvents were not used in the preparation of solutions except during desorption with KIO_3 which also contained HCl. Still, in case the use of any chloride species would be inevitable in the pre-measurement steps, the optimization of ICP-MS parameters was carried out in the collision mode in octopole reaction system with He gas.

In batch sorption studies, GFL 1083 water bath shaker (Burgwedel, Germany) equipped with a microprocessor thermostat was used for mixing. The pH of the solutions was adjusted with 0.01-1.0 M HNO_3 and 0.01-1.0 M NH_3 using Ino Lab Level 1 pH meter (Weilheim, Germany). The elemental composition of sorbents was determined by a LECO-CHNS-932 elemental analyzer (Mönchengladbach, Germany). Microimages of sorbents were obtained utilizing a Philips XL-30S FEG scanning electron microscope (Eindhoven, The Netherlands). The thermal properties of sorbents were examined using a Perkin Elmer Pyris Diamond TG/DTA (Boston, MA, USA). Surface area measurements of the sorbents were performed with Micromeritics Gemini V Series Surface Area Analyzer (Norcross, USA). ^{29}Si and ^{13}C NMR spectra of the prepared sorbents were acquired using ^{29}Si cross polarization magic angle spinning nuclear magnetic resonance (CP/MAS NMR) spectrometer: ASX 300 Bruker (Milton, Ontario, Canada) and ^{13}C CP/MAS NMR spectrometer: Avance 200 Bruker (Germany).

2.1.2. Reagents and Solutions

All the chemicals were of analytical reagent grade. Deionized ultrapure water (18.2 M Ω .cm) was used throughout the study. Glassware and plastic containers were cleaned by soaking in 10% (v/v) nitric acid for 24 h and rinsed with deionized water prior to use.

Stock standard solutions of As(V) and As(III), were prepared by dissolving required amounts of As₂O₅ (Merck, product code: 1.09939, CAS no.: [1303-28-2]) and As₂O₃ (Fischer, CAS no.: [1327-53-3]), respectively, in ultrapure water in order to obtain 2000.0 mgL⁻¹ arsenic in final solutions. Lower concentration standard solutions were prepared daily by appropriate dilution from their stock standards before use.

Silica gel was purchased from Merck (product code: 1.10184, CAS no.: [7631-86-9]) and activated with acetic acid (Riedel-de Haen, product code: 27225, CAS no.: [64-19-7]). Functionalization of silica gel was realized with 3-(Triethoxysilyl) propylamine (APTES) (Merck, product code: 8.26619, CAS no.: [14814-09-6]) and (3-Mercaptopropyl) trimethoxysilane (MPTMS) (Fluka, product code: 63800, CAS no.: [4420-74-0]), respectively. Toluene, (Riedel-de-Haen, product code: 24529, CAS no.: [108-88-3]) was used both as a reaction solvent and for removal of the unreacted reagent after modification step; and acetone (Merck, product code: 1.00014, CAS no.: [67-64-1]) as a further washing solvent. Nitric acid (Merck, product code: 1.00456, CAS no.: [7697-37-2]) was employed for the acidification of samples prior to ICP-MS determination. L-cysteine (Merck, product code: 1.02838, CAS no.: [52-90-4]) at a concentration of 1.0% (w/v) was used as the eluent for the desorption of As(V) whereas the eluent for As(III) desorption was 0.050 M KIO₃ (Merck, product code: 1.02404, CAS no.: [7758-05-6]) in 2.0 M HCl (Merck, product code: 1.00314, CAS no.: [7647-01-0]).

SRM from NIST, Natural Water – Trace Elements, Cat. No. 1640 were used to validate the proposed methodology. The composition of SRM 1640 is given in Table 2.1.

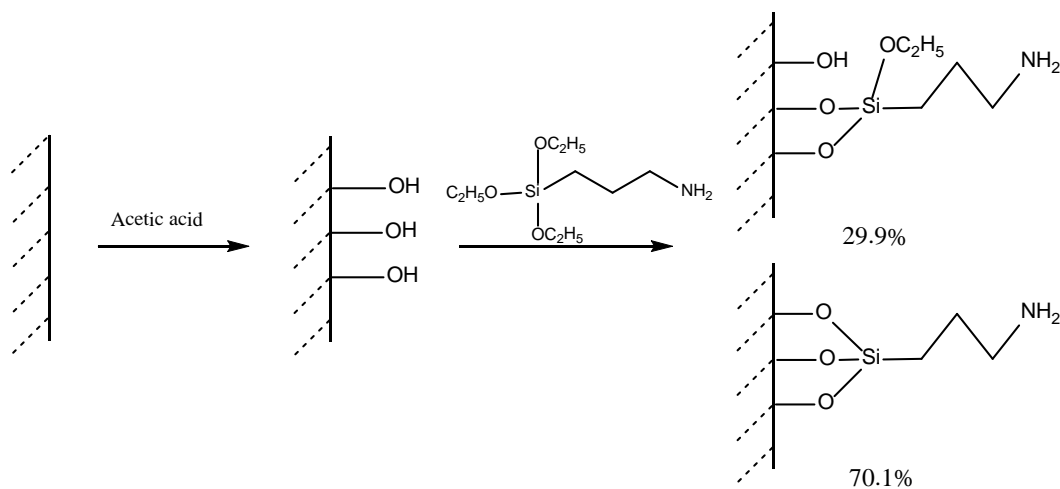
Table 2.1. Certified values for Natural Water – Trace Elements (SRM 1640)

Elements	Concentration (μgL^{-1})	Elements	Concentration (μgL^{-1})
Na	29350 \pm 310	Se	22.0 \pm 0.51
Mg	5819 \pm 56	Rb	2.00 \pm 0.02
K	994 \pm 27	Sr	124.2 \pm 0.7
Ca	7045 \pm 89	Ba	148 \pm 2.2
V	13.0 \pm 0.37	Pb	27.89 \pm 0.14
Cr	38.6 \pm 1.6	Bi	n/a
Mn	122 \pm 1.1	Tl	n/a
Fe	34.3 \pm 1.6	Y	n/a
Co	20.3 \pm 0.31	Br	n/a
Ni	27.4 \pm 0.8	Ti	n/a
Cu	85.2 \pm 1.2	S	n/a
Zn	53.2 \pm 1.1	Cl	n/a
As	26.7 \pm 0.41		

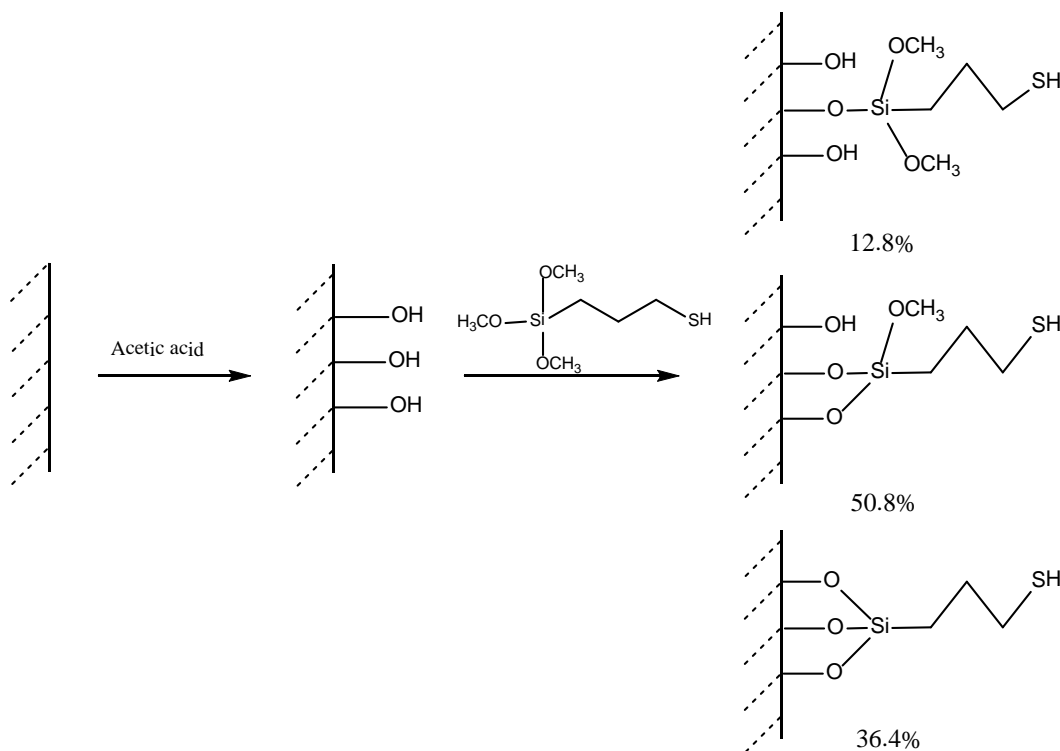
2.1.3. Synthesis of Sorbents

The procedure utilized in the functionalization of the silica surface was compiled from literature (Liu et al. 2002) with some modifications. The outline of the functionalization of silica gel surface is illustrated in Figure 2.1. The first step is the activation of the silica surface to convert the siloxane groups to silanol. For this purpose, 5.00 g of silica was treated with 50.0 mL of 0.010 M acetic acid for 1 h and then washed with ultrapure water until a neutral filtrate was obtained. This step was completed after drying the activated silica at 120 °C for 24 h in an oven. The amine modification step was carried out by mixing 5.0 g of activated silica, 3.0 mL of APTES and 9.0 mL toluene in a two necked 25 mL flask. A condenser having anhydrous CaCl_2 drying tube at the top was connected to the reaction flask. The reaction was proceeded under an inert atmosphere provided with N_2 bubbled through the side arm of the flask. The mixture was stirred for 24 h at 100 rpm under constant reflux in an oil bath at a temperature of 110 °C. After the reaction had been completed, amine-treated silica was washed sequentially with 10.0 mL portions of acetone and toluene and then dried in an oven at 50 °C overnight. The same procedure was applied for mercapto-modification of the silica using MPTMS instead of APTES. Bifunctionalization of the silica was

realized with the simultaneous addition of the same amounts of both functional silanes into the reaction mixture under the same experimental conditions.



(a)



(b)

Figure 2.1. Synthesis steps of modified silica gel a) (NH₂)silica, b) (SH)silica and c) (NH₂+SH)silica

(cont. on next page)

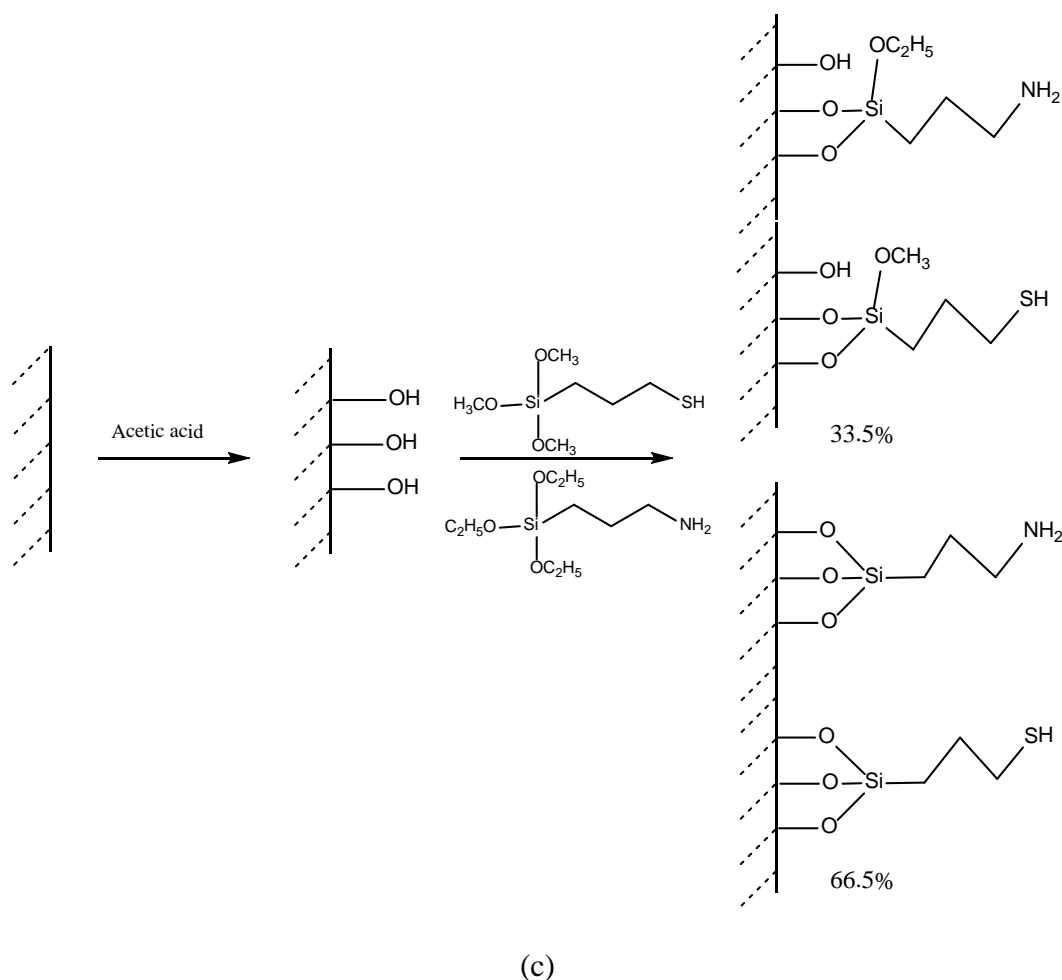


Figure 2.1. (cont.)

2.1.4. Characterization of Sorbents

A variety of methods were applied for the characterization of the modified silica samples. Elemental analysis was used for the determination of nitrogen, sulfur and carbon contents. Images and elemental mapping of unmodified silica (silica), mercapto-modified silica ((SH)silica), amine-modified silica ((NH₂)silica) and mercapto-amine bifunctionalized silica ((NH₂+SH)silica) were obtained using scanning electron microscopy (SEM). Surface area and thermal gravimetric degradation behavior of the sorbents were also investigated. In addition, ¹³C NMR and ²⁹Si NMR Spectroscopy were applied to prepared sorbents in order to realize the bonding of the functional silane coupling agents onto silica surface.

2.1.5. Sorption Studies

Sorption studies were performed through a batch process for all the sorbents prepared; namely, silica, (SH)silica, (NH₂)silica and (NH₂+SH)silica. In order to examine the possible changes in the sorption of bifunctionalized sorbent, a mechanical (1:1) mixture of amine-modified silica and mercapto-modified silica (NH₂)silica+(SH)silica was also prepared as an alternative sorbent for the bifunctional silica.

Batch sorption studies were carried out at 25 °C with each sorbent separately after the initial pH of solutions was adjusted to 1.0, 2.0, 3.0, 4.0, 5.0, 7.0, 8.0 and 9.0 with dilute HNO₃ or NH₃. After pH adjustment step, 50.0 mg sorbent was added into each of the 50 mL centrifuge tubes containing 20.0 mL aliquots of 100.0 µgL⁻¹ As(V) or 100.0 µgL⁻¹ As(III) solutions. The mixtures were placed in a thermostated water bath shaker and shaken for 30 minutes, then they were filtered through blue-band filter papers. The filtrates were analyzed for arsenic concentration by ICP-MS. Prior to ICP-MS measurements, all samples and standard solutions were acidified with the addition of appropriate amounts of concentrated HNO₃ to produce 1.0% (v/v) HNO₃ in the final solution. The effects of the amount of sorbent, shaking time, solution temperature and repetitive use of the sorbents were investigated throughout the study. The investigated parameters and ranges are summarized in Table 2.2.

Table 2.2. Summary of the parameters and ranges used throughout the study

Parameters investigated	Range
pH of solution	1.0, 2.0, 3.0, 4.0, 5.0, 7.0, 8.0 and 9.0
Amount of sorbent (mg)	5.0, 10.0, 25.0, 50.0 and 100.0
Shaking time (min)	1, 5, 15, 30, 60 and 120
Solution temperature (°C)	25, 50, 75

2.1.6. Sorption Isotherm Model: Dubinin–Radushkevich (D–R) Isotherm Model

An isotherm is a curve describing the functional relationship between analyte and sorbent in a sorption process. Isotherm is obtained by varying the concentration of

the analyte retained onto sorbent under constant temperature. Mainly, it is used to predict the mobility of the substance in the environment (Limousin et al. 2007). Among various isotherm models, the Dubinin–Radushkevich (D–R) isotherm model was chosen to predict the sorption behaviour of the proposed method.

This isotherm model depends on the assumption that the ionic species preferentially are bound to the most energetically favorable sites of sorbent associated with multilayer adsorption of ions (Guibal et al. 1998). D-R isotherm is described by Equation 2.1 (Kavitha and Namasivayam 2007):

$$Q_e = q_s \exp(-B\varepsilon^2) \quad (2.1)$$

Where,

$$\varepsilon = RT \ln \left(1 + \frac{1}{C_e} \right)$$

The D-R parameter, B, gives the information about the mean free energy of sorption per molecule of adsorbate which is required to transfer it to the surface of the solid from infinity in the solution, q_s corresponds to the sorption monolayer capacity (Şeker et al. 2008). Mean free energy of sorption can be calculated from D-R parameter B by Equation 2.2.

$$E = (2B)^{1/2} \quad (2.2)$$

The q_s and B constants are calculated from intercepts and slopes of plots of experimental plot of $\ln q$ versus ε^2 . By reason of the discrete behavior of the sorption characteristics of each analyte under various pHs, D-R model was applied at pH 1.0, 3.0 and 9.0 for As(III) and pH 3.0 for As(V). Due to highly toxic nature of the inorganic arsenic species, the capacity of the sorbents were determined by varying the amount of sorbents used under fixed arsenic concentrations instead of using elevated amount of arsenicals. Sorption conditions were; arsenite or arsenate concentration of $100.0 \mu\text{gL}^{-1}$, solution volume: 20.0 mL, shaking time: 30 min, and reaction temperature: 25 °C.

2.1.7. Desorption Studies

Initial desorption studies were performed on an oxidation-reduction basis of the sorbed As(III) and As(V). For the oxidation of As(III) to As(V), 0.050 M KIO₃ in 2.0 M HCl was used while 1.0% (w/v) L-cysteine solution with pH adjusted to 3.0 was the eluent for the reduction of As(V) to As(III). In addition to the oxidative-reductive eluents, 0.50 M NaOH and 0.50 M HNO₃ were also used as alternative. Before desorption studies, the following parameters were used for As(III) sorption: arsenite ion concentration of 100.0 µgL⁻¹, solution volume of 20.0 mL, sorbent amount of 50.0 mg, shaking time of 30 min, reaction temperature of 25 °C and solution pHs of 1.0, 3.0, 5.0 and 8.0. In the case of As(V), similar sorption parameters were applied at the solution pH of 3.0. Desorption conditions were; shaking time: 60 min, solution volume: 20.0 mL and reaction temperature: 25 °C. The filtrates, both after the sorption step and desorption step were analyzed for arsenic concentration by ICP-MS. Prior to ICP-MS measurements all samples and standard solutions were acidified with the addition of appropriate amounts of concentrated HNO₃ to produce 1.0% (v/v) HNO₃ in the final solution (if desorption matrix had already contained acid this step was ignored). Matrix-matched standardization was applied in each case.

2.1.8. Reusability of the Sorbents

Based on the results of sorption studies, the pH of 3.0 had been chosen as the critical pH for sorption and speciation studies. For this reason, the reusability of the sorbents was tested at pH of 3.0 for each arsenic forms. For As(V), 1.0% (w/v) L-cysteine was used as the eluent for (NH₂)silica, 0.50 M NaOH for (NH₂)silica, (NH₂)silica+(SH)silica and (NH₂+SH)silica, and 0.50 M HNO₃ for (NH₂)silica, (NH₂)silica+(SH)silica and (NH₂+SH)silica. In the case of As(III) sorption, only two sorbents, namely, (NH₂)silica+(SH)silica and (NH₂+SH)silica were investigated for their reusability. Elutions were performed with 0.50 M NaOH, 0.50 M HNO₃ and 0.05 M KIO₃ in 2.0 M HCl. Sorption conditions were; solution pH: 3.0, sorption time: 30 min, sorbent amount: 50.0 mg, sample volume: 20.0 mL, sorption temperature: 25 °C. The mixtures were placed in a thermostated water bath shaker and shaken for specified time, and then they were filtered through blue-band filter papers. The filtrates were

analyzed for arsenic concentration by ICP-MS. Prior to ICP-MS measurements all samples and standard solutions were acidified with the addition of appropriate amounts of concentrated HNO₃ to produce 1.0% (v/v) HNO₃ in the final solution. The analyte retained on the sorbent was desorbed by the prespecified eluent. Applied desorption conditions were; desorption time: 60 min, eluent volume 20.0 mL and desorption temperature: 25 °C). The sorbent that remained on the filter paper was washed with ultra pure water in order to remove any traces of the desorption matrix and it was subjected to the next sorption/desorption cycle. The procedure above was repeated for five successive sorption/desorption cycles.

2.1.9. Method Validation

The proposed methodology was validated both through the analysis of a standard reference material (SRM from NIST, Natural Water – Trace Elements, Cat. No. 1640) and via spike recovery experiments. (NH₂+SH)silica was used in the validation study because of the absence of information about the oxidation state of arsenic in the reference material. Before the sorption/desorption steps, the acid content of the SRM was removed in a way that 5.0 mL of the solution was diluted with 10.0 mL of ultrapure water in a Teflon beaker and the mixture was evaporated to dryness. The residue in the beaker was dissolved in 10 mL of ultrapure water, transferred to a centrifuge tube where pH was adjusted to 3.0, diluted to 15.0 mL, and then used in the sorption/desorption. The expected concentration of the SRM in the final solution was, thus, 8.89 µgL⁻¹.

In addition to SRM analysis, the applicability of the methodology was also tested by spike recovery tests using drinking water. The spike concentration was 30.0 µgL⁻¹ as this value was close to the concentration of SRM (26.67 µgL⁻¹). Moreover, similar dilution and pH adjustment steps were employed before the sorption/desorption cycles.

2.2. Results and Discussion

As explained in Section 2.1.1, the concentration of arsenic species in the final solutions was determined using ICP-MS at m/z ratio of 75. In case the use of any

chloride species would be inevitable in the pre-measurement steps, the optimization of ICP-MS parameters was carried out in the collision mode in octopole reaction system with He gas in order to prevent the possible matrix-based polyatomic interference of $^{40}\text{Ar}^{35}\text{Cl}^+$ on $^{75}\text{As}^+$ signal. Under the studied conditions, the calibration line equation was $y = 1836.5x + 370.3$ with a correlation coefficient of $R^2 = 0.9991$. The limit of detection (LOD_{3s}) and the limit of quantitation (LOQ_{10s}) were $0.041 \mu\text{gL}^{-1}$ and $0.135 \mu\text{gL}^{-1}$, respectively. These figures of merits were considered to be sufficient for the purpose of the study; therefore, no attempt was tried to enhance these values.

2.2.1. Characterization of Sorbents

The results of the surface area and pore width measurements of the prepared sorbents (Table 2.3) indicate that the modification has slightly decreased both the surface area and the pore size of the novel sorbents with respect to the unmodified silica. These results indicate the modification of the silica surface with the employed functional groups. The extent of modification was also followed by the characterization of the functional groups on the basis of surface N, S, C, and H contents. The elemental analysis results are given in Table 2.4. As seen, (NH_2) silica contains 2.14% nitrogen while (SH) silica contains 3.73% sulphur. The bifunctional sorbent containing both mercapto- and amine- groups, on the other hand, has 1.03% nitrogen and 2.52% sulfur. The modification of the silica surface with the organic groups is also indicated by thermal gravimetric analysis (TGA) curves of the sorbents, as given in Figure 2.2. Unmodified silica shows two-stage weight losses at the thermal ranges of 25-200 °C (4%) and 200-600 °C (2.4%). This is possibly caused by the removal of physically adsorbed water, and a further loss caused by the condensation of free silanol groups to siloxane groups on the surface of silica, respectively (Arakaki and Airoidi 2000). (NH_2) silica has a characteristic weight loss (4.6%) between 25 and 200 °C due to the removal of physically adsorbed water, and a second loss (7.1%) between 200 and 600 °C possibly because of the thermal decomposition of the organic functional groups of the modified silica. Similarly, (SH) silica displays 1.5% and 10.2% weight losses in the same temperature range for the same reasons. Similarly, (NH_2+SH) silica has a characteristic thermograph between (SH) silica and (NH_2) silica with weight losses of

3.0% and 9.5% corresponding, respectively, to the removal of physisorbed water and the thermal degradation of organic functional groups.

Table 2.3. Surface area and pore width results

	BET surface area (m ² g ⁻¹)	Average pore size (Å)
silica	253.9	17.3
(NH ₂)silica	168.9	14.1
(SH)silica	189.6	14.1
(NH ₂ +SH)silica	183.9	14.1

Table 2.4. Elemental analysis results, (%)

	C	H	N	S
(NH ₂)silica	6.03	1.63	2.14	–
(SH)silica	5.62	1.31	–	3.73
(NH ₂ +SH)silica	6.48	1.51	1.03	2.52

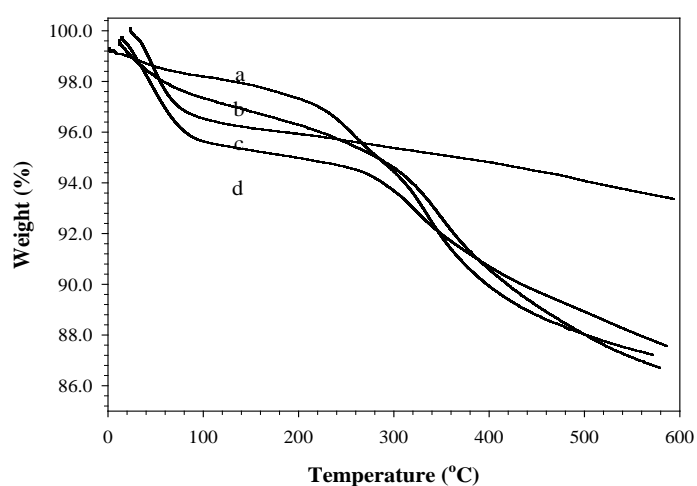


Figure 2.2. TGA curves of a) (SH)silica b) (NH₂+SH)silica, c) unmodified silica, and d) (NH₂)silica

Prepared sorbents were also characterized for their surface species before and after modification steps using ^{13}C and ^{29}Si NMR spectroscopy. Relative amounts of surface species were determined by peak deconvolution of spectra obtained from ^{29}Si CP/MAS NMR. Q and T notation used on the NMR survey refers to the number of oxygen bounded to silicon atom. In case of 'T' three oxygen atoms are bound to a silicon atom. Furthermore, T^1 was used to describe the single bonding of the functional group containing silane coupling agent, while T^2 and T^3 were used to describe the double and triple bonding to silica surface, respectively. On the other hand 'Q' notation defines that four oxygen atoms are bounded to silicon atom. Moreover, Q^2 , Q^3 and Q^4 are described geminal silanol, free silanol and siloxane, respectively. According to Figure 2.3, activated silica surface contains both geminal and free silanol in addition to siloxane bonds. Considering the spectra of activated silica and modified silicas (Figures 2.3, 2.4, 2.5 and 2.6) it can be stated that modification leads to a decrease in the amount of the silanol groups (Q^2 and Q^3). In addition, an increase in the amount of the siloxane groups (Q^4) and appearance of new peaks (T) which corresponds to bonded trifunctional silane coupling agents are observed. Appearance of the T^2 (29.9 %) and T^3 (70.1%) peaks indicate that the APTES mainly bond to surface via triple bonding (Figure 2.4). In case of MPTMS modification T^1 (12.8%), T^2 (50.8%) and T^3 (36.4%) peaks show that the bonding of the MPTMS was not as strong as APTES bonding (Figure 2.5). ^{29}Si CP/MAS NMR spectrum of bifunctional modification (APTES and MPTMS) (Figure 2.6) shows chemical bond formation to silica surface similar to $(\text{NH}_2)\text{silica}$ where T^2 and T^3 percentages were 33.5% and 66.5%, respectively.

^{13}C CP/MAS NMR spectra of $(\text{NH}_2)\text{silicate}$ (Figure 2.7), $(\text{SH})\text{silicate}$ (Figure 2.8) and $(\text{NH}_2+\text{SH})\text{silicate}$ (Figure 2.9) are also used as a supplementary for the surface modification. The spectrum of $(\text{NH}_2)\text{silica}$ is indicative of three different type of carbon in the silica network which appeared as three peaks at δ 45, 24 and 12. The carbon atom directly attached to amine group appeared in the downfield (higher ppm) of the spectrum as a result of the decreased electron density around the atom and deshields the atom from the magnetic field. The carbon atom attached directly to less polar silicon and relatively less polar neighbor carbon appeared in upfield (lower ppm) of the spectrum. The electron density around this carbon atom is relatively high which shields the atom from the magnetic field. Similar chemical shifts were observed in ^{13}C spectrum of $(\text{SH})\text{silica}$ with additional peak appearing in downfield region of spectrum (δ : 52). This peak corresponds to a carbon atom which is deshielded even more than the

sulfur bearing carbon atom. Considering both ^{13}C and ^{29}Si NMR spectra of the (SH)silica, the mentioned peak most probably corresponds to the carbon atom from unbounded metoxysilane fraction of the coupling agent. In the case of the $(\text{NH}_2+\text{SH})\text{silica}$ ^{13}C spectrum shows intense peaks at δ 59, 45, 29, 13 and some smaller peaks. The most deshielded carbon atom is the one directly bonded to metoxysilane which has the most polar atom (oxygen) in the structure. Because of the higher polarity of the nitrogen with respect to sulfur, the carbon bonded to amine group appeared further downfield (δ : 45) than mercapto bonded carbon (δ : 29). More detailed illustrations of chemical shifts of each carbon atom are shown in the insets of the corresponding ^{13}C spectra.

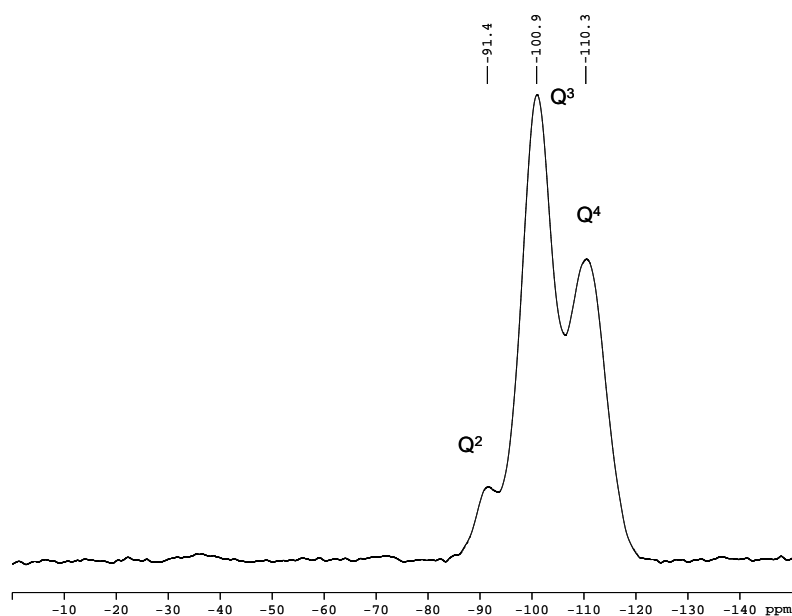


Figure 2.3. ^{29}Si CP/MAS of activated silicate

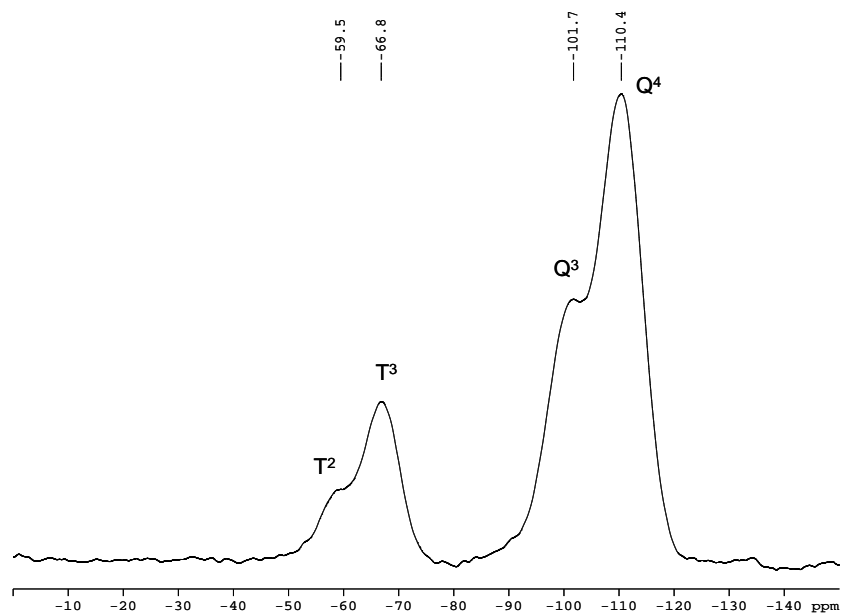


Figure 2.4. ²⁹Si CP/MAS of (NH₂)silicate

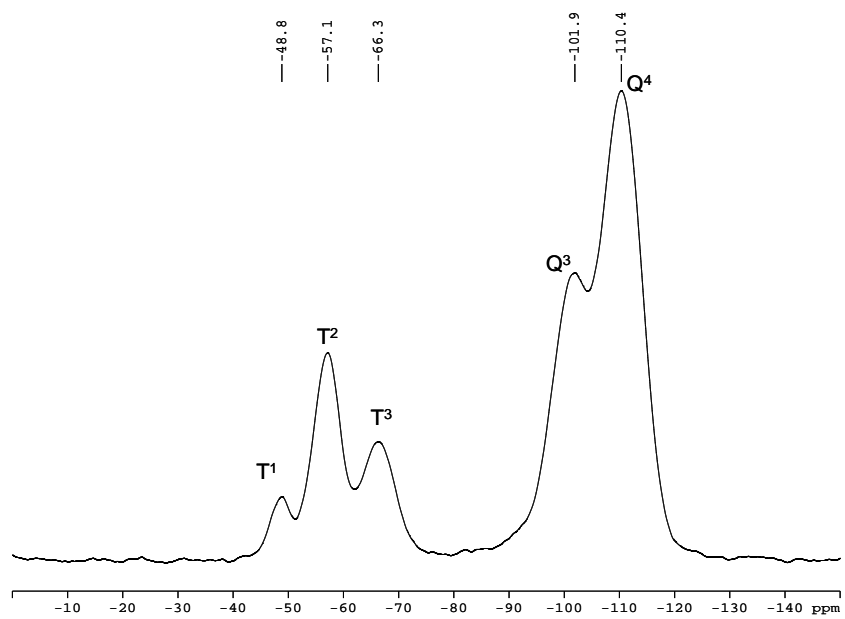


Figure 2.5. ²⁹Si CP/MAS of (SH)silicate

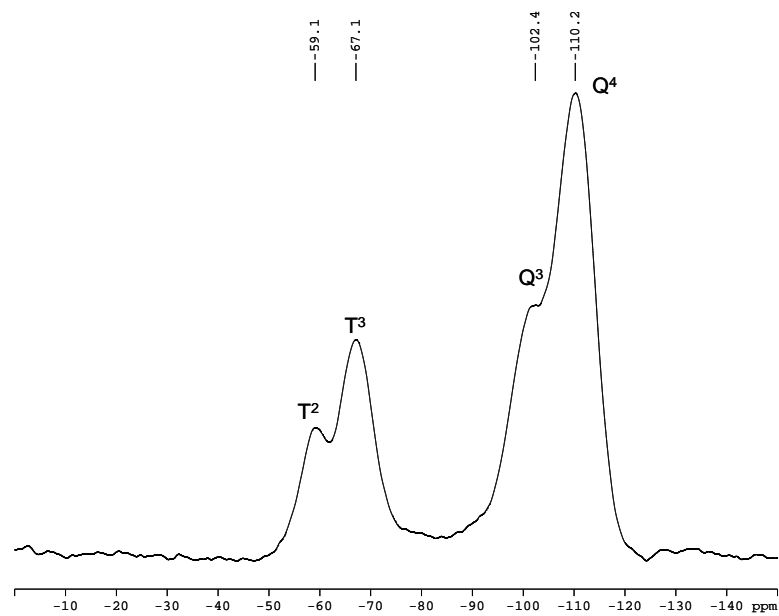


Figure 2.6. ^{29}Si CP/MAS of (NH_2+SH) silicate

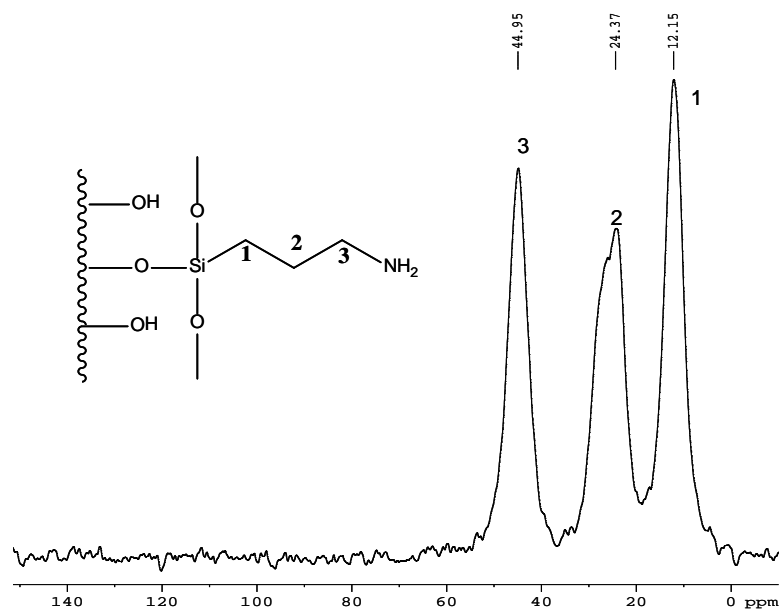


Figure 2.7. ^{13}C CP/MAS NMR spectra of (NH_2) silicate

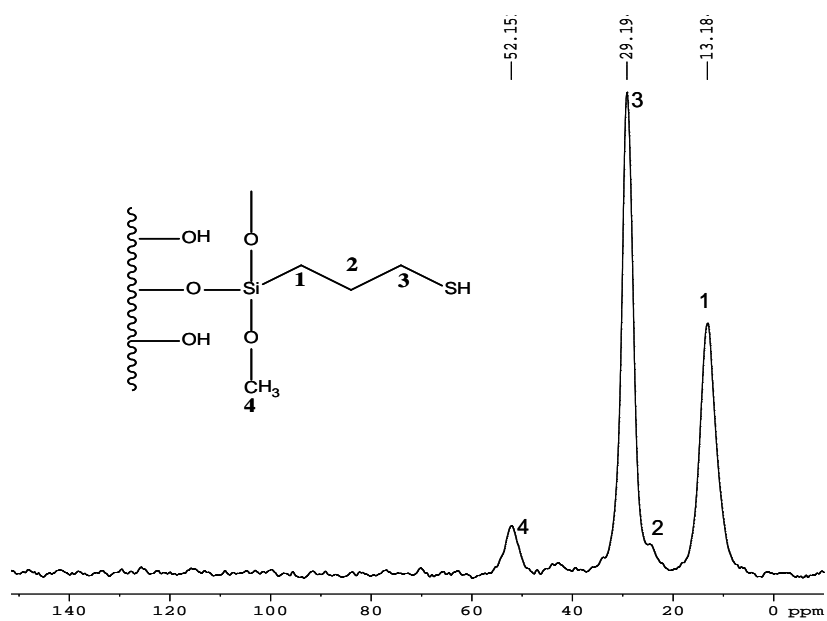


Figure 2.8. ^{13}C CP/MAS NMR spectra of (SH)silicate

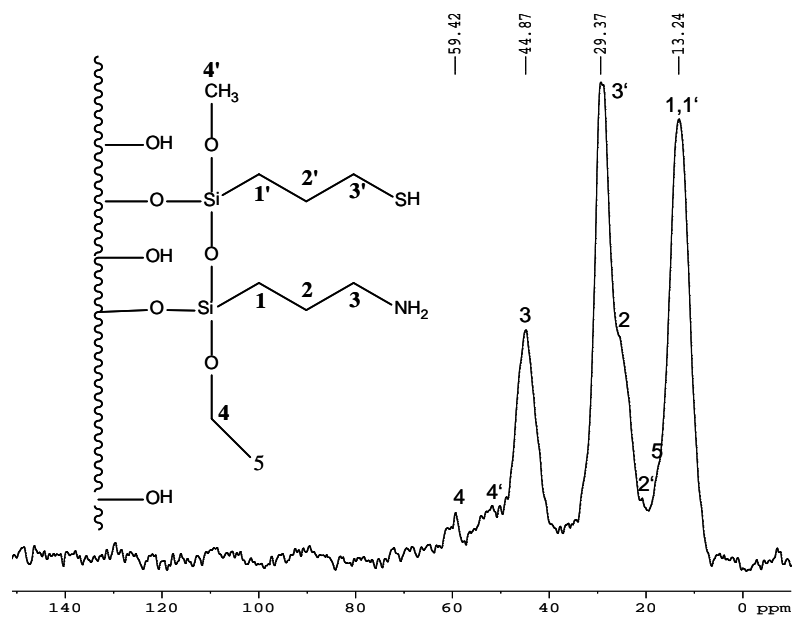


Figure 2.9. ^{13}C CP/MAS NMR spectra of (NH₂+SH)silicate

2.2.2. Sorption Studies

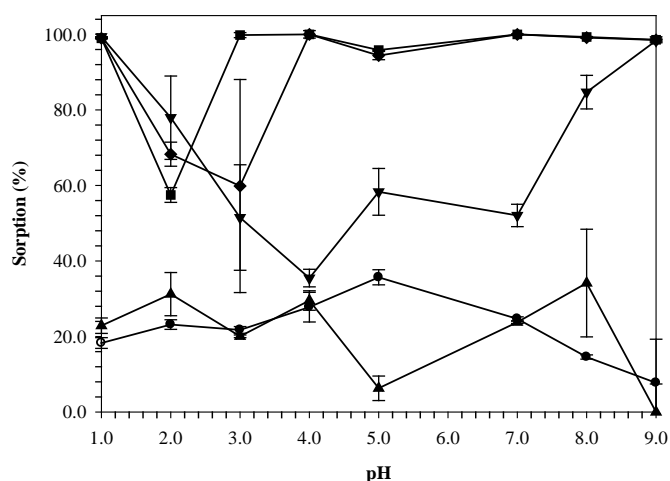
2.2.2.1. Effect of pH on the Sorption of As(III) and As(V)

The sorption percentages of the sorbents towards As(III) and As(V) as a function of pH are shown in Figure 2.10. In order to figure out the sorption characteristics of the sorbents in a simpler manner, Figure 2.10 was also redrawn based on the sorption affinity of the individual sorbents (Figure 2.11). Furthermore, the pH dependent speciation diagrams of As(III) and As(V) are demonstrated additionally in Figure 2.12 and 2.13, respectively, so as to realize the sorption mechanism better. The unmodified silica shows no appreciable sorption to any of the two As species. Alternatively, (SH)silica shows quantitative sorption only to As(III) at the two extreme points in the investigated pH range, namely, pH 1.0 and 9.0 while As(V) is not retained. This result is in accordance with similar literature studies which suggest that mercapto group is selective, generally, to the lower oxidation states of the hydride forming elements (Hao et al. 2009; Dominguez 2002; Erdem and Eroğlu 2005; Zheng and Hu 2009). On the other hand, (NH₂)silica demonstrates selectivity only towards As(V), and this response is indicative of the affinity of the amine functionality to arsenate ion. The nature of sorption at pH 3.0 was suggested, in a previous study, as being the electrostatic attraction between the protonated amine groups of (NH₂)silica and H₂AsO₄⁻ ion, which is the main species at this pH (Boyacı et al. 2010).

As can be deduced from Figure 2.10(a) and 2.10(b), the most striking feature of the bifunctional (NH₂+SH)silica, in contrast to (SH)silica, is its quantitative sorption capability towards As(III) at a relatively wide pH range. The bifunctional sorbent can be used for As(III) sorption from pH 1.0 to at least 9.0 with an exception at pH 2.0 only. This improvement in the sorption percentage of the bifunctional sorbent compared to (SH)silica needs further investigation and, for the present, can be attributed to the synergistic effect of the amine groups on the sorbent in addition to the mercapto groups. Another important property of (NH₂+SH)silica is that it can be applied for the quantitative sorption of As(V) at pH 3.0. From these results, it can be argued that the bifunctional sorbent possesses the efficient features of the two functional groups. In addition, with a simple pH adjustment step (to pHs greater than 4.0) before the sorption, (NH₂+SH)silica can be employed for the sorption of As(III) only; or for the sorption of

both As(III) and As(V) simultaneously at pH 3.0. A similar but less efficient sorption behavior was also observed with the mechanically-mixed (NH₂)silica+(SH)silica. The sorbent mixture can be used for the sorption of As(III) quantitatively at a wide pH range but, in contrast to (NH₂+SH)silica, there is not a single pH for the simultaneous quantitative sorption of As(III) and As(V). The percentage sorption of the sorbent mixture to As(III) at pH 3.0 is not reproducible.

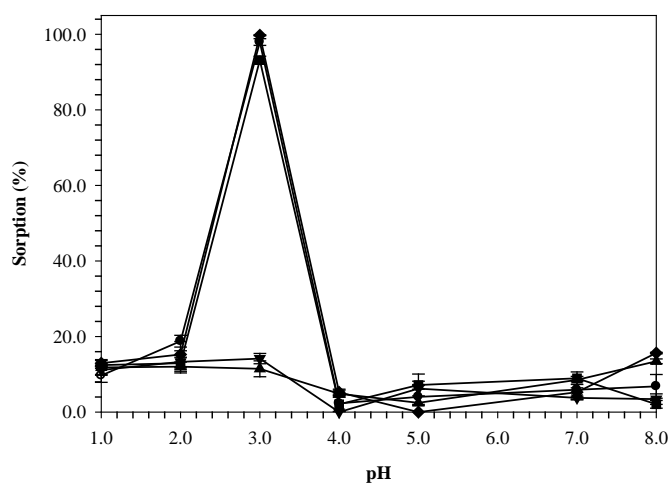
The results outlined in the previous two paragraphs have demonstrated the high flexibility of the sorbent systems developed in the present study. Depending on the purpose of the investigation, that is whether As(III) or As(V) is to be determined, either (NH₂)silica or (SH)silica can be used after a pH adjustment step. In addition to the mono-functionalized silicas, a better strategy could be the application of the bifunctional (NH₂+SH)silica due to its selectivity to either As(III) or both As(III) and As(V) after a simple pH adjustment step.



(a)

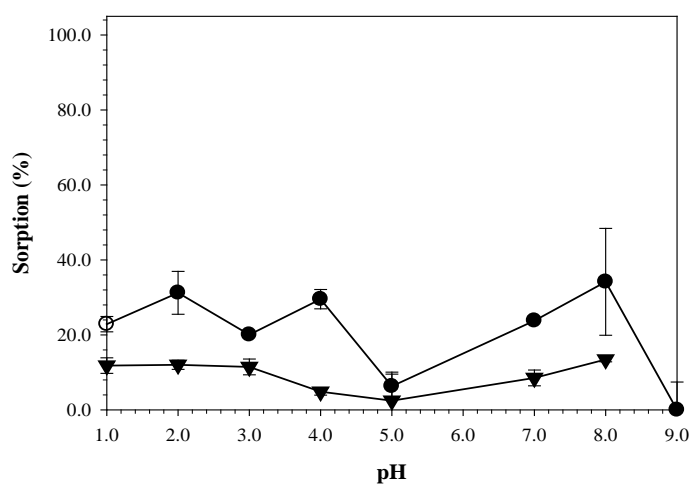
Figure 2.10. Effect of pH on the sorption of 100.0 µgL⁻¹ a) As(III) and b) As(V). (●) (NH₂)silica, (▼) (SH)silica, (■) (NH₂+SH)silica, (▲) unmodified silica and (◆) (NH₂)silica+(SH)silica. (reaction time: 30 min, sorbent amount: 50.0 mg, sample volume: 20.0 mL, sorption temperature: 25 °C, n=3). Error bars indicate the standard deviation of the triplicate measurements at 95% CI.

(cont. on next page)



(b)

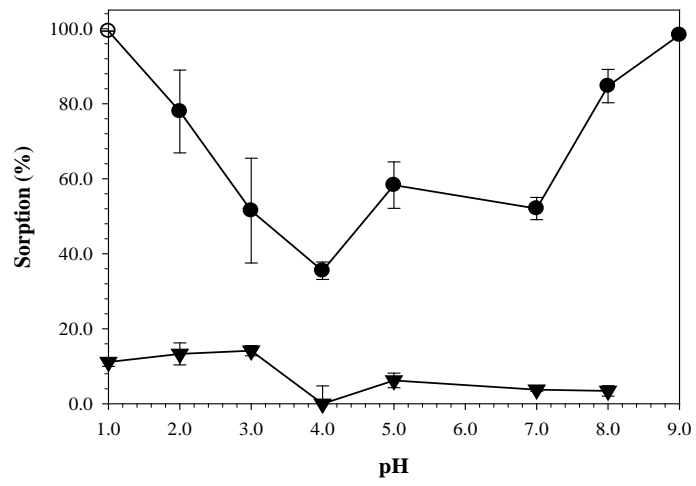
Figure 2.10. (cont.)



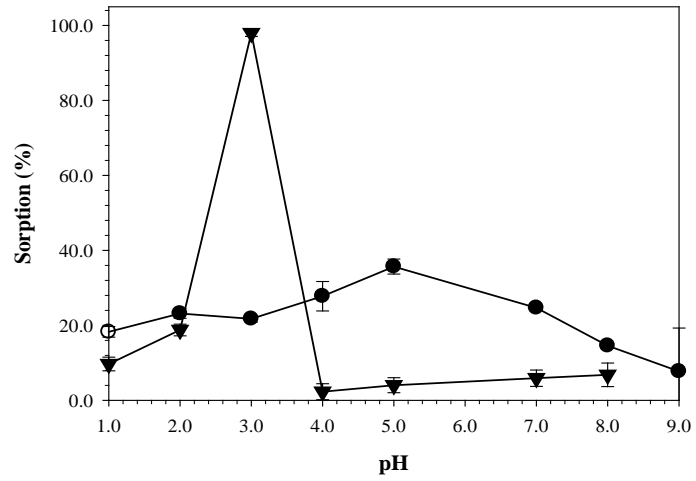
(a)

Figure 2.11. Effect of pH on the sorption of $100.0 \mu\text{gL}^{-1}$ (●) As(III) and (▼) As(V) by a) unmodified silica, b) (SH)silica, c) (NH₂)silica, d) (NH₂+SH)silica, e) (NH₂)silica+(SH)silica. (reaction time: 30 min, sorbent amount: 50.0 mg, sample volume: 20.0 mL, sorption temperature: 25 °C, n=3).

(cont. on next page)



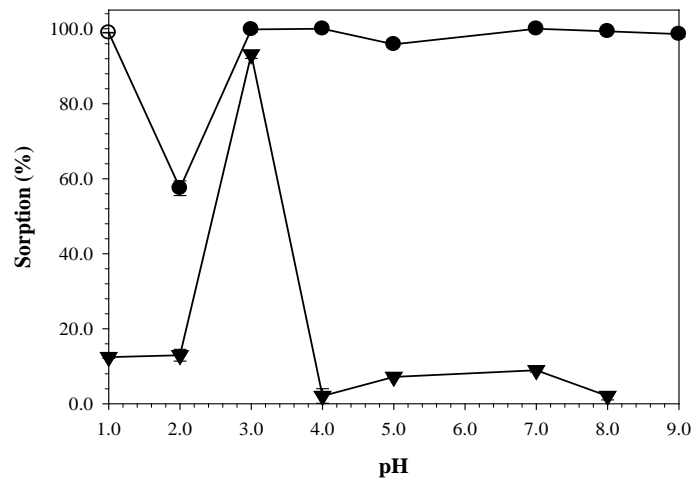
(b)



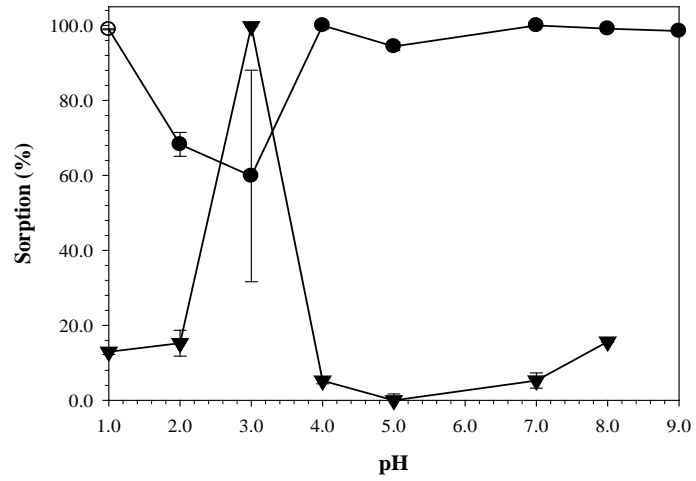
(c)

Figure 2.11. (cont.)

(cont. on next page)



(d)



(e)

Figure 2.11. (cont.)

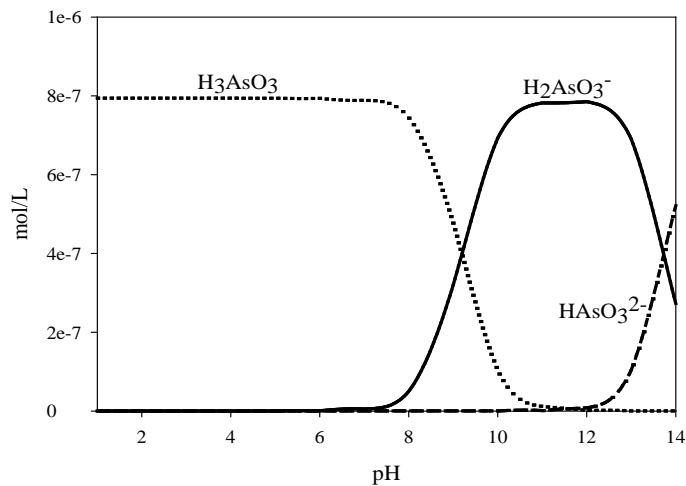


Figure 2.12. Speciation diagram of As(III) (obtained with Visual MINTEQ)

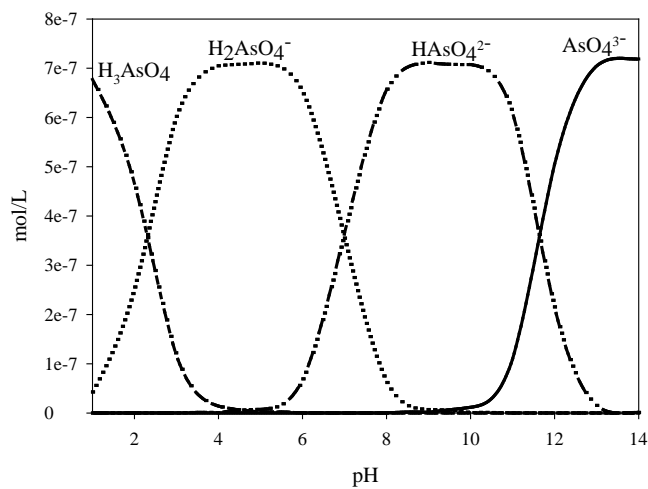


Figure 2.13. Speciation diagram of As(V) (obtained with Visual MINTEQ)

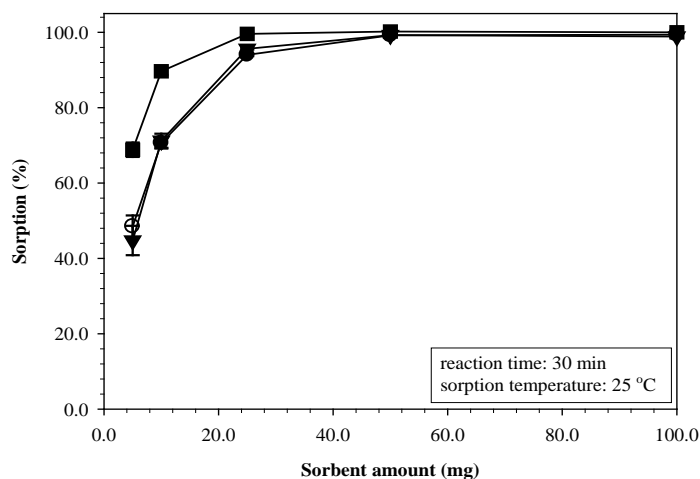
2.2.2.2. As(III) Sorption

The percentage sorption of the mono-functional (SH)silica, the bifunctional (NH₂+SH)silica and the mechanically-mixed (NH₂)silica+(SH)silica towards As(III) was investigated at three pH values decided from Figure 2.10, namely, pH 1.0, 3.0, and 9.0. The solution pH of 1.0 and 9.0 were chosen since the percentage sorption of the

related sorbents was quantitative at these pHs. In addition, the percentage sorption was also examined at pH 3.0 which is a critical pH for As(V) as well. For all pHs, the effects of the sorbent amount, the reaction time, and the reaction temperature were studied.

2.2.2.2.1. pH = 1.0

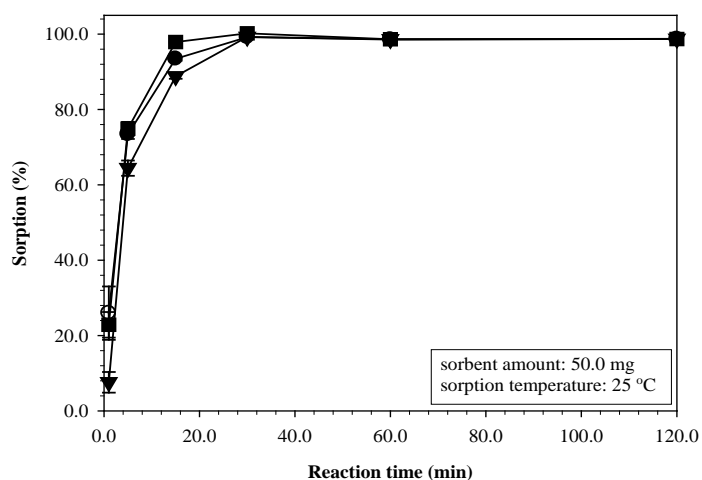
The results of the As(III) sorption studies carried out at pH 1.0 are summarized in Figure 2.14. As can be seen from Figure 2.14(a), the quantitative sorption was obtained at the sorbent amount of 50.0 mg for (NH₂+SH)silica and (NH₂)silica+(SH)silica, whereas a lower amount of (SH)silica (25.0 mg) was sufficient to attain a saturation plateau. The indicated sorbents showed a similar sorption behavior as a function of reaction time, and 30.0 min was sufficient to obtain a quantitative sorption (Figure 2.14(b)). The effect of reaction temperature on sorption is shown in Figure 2.14(c). The graph reveals a slight exothermic nature of the sorption, with the percentage sorption amounting to more than 95% sorption even at 75 °C.



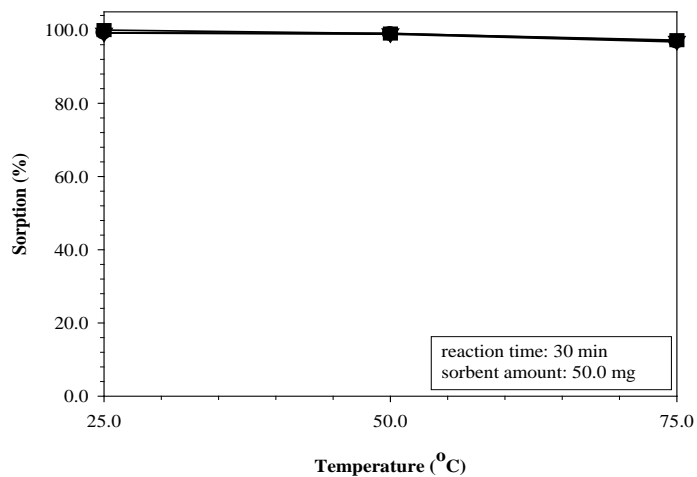
(a)

Figure 2.14. Effect of a) sorbent amount, b) reaction time, c) temperature on the sorption of 100.0 µgL⁻¹ As(III). (■) (SH)silica, (●) (NH₂+SH)silica, (▼) (NH₂)silica+(SH)silica (sample volume: 20.0 mL, solution pH: 1.0, n=3).

(cont. on next page)



(b)



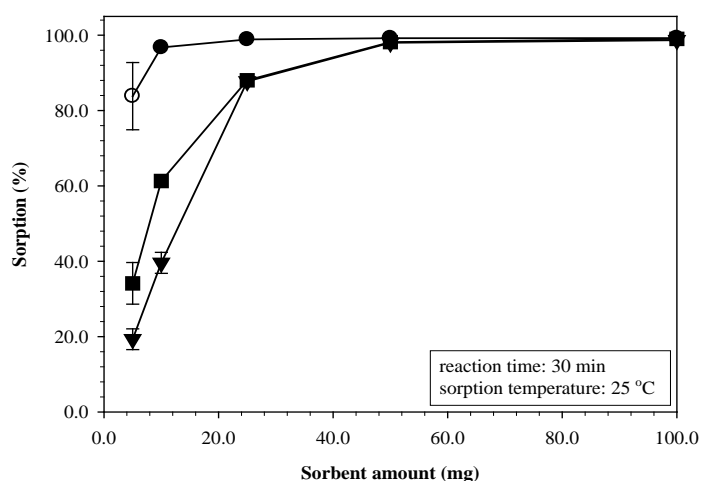
(c)

Figure 2.14. (cont.)

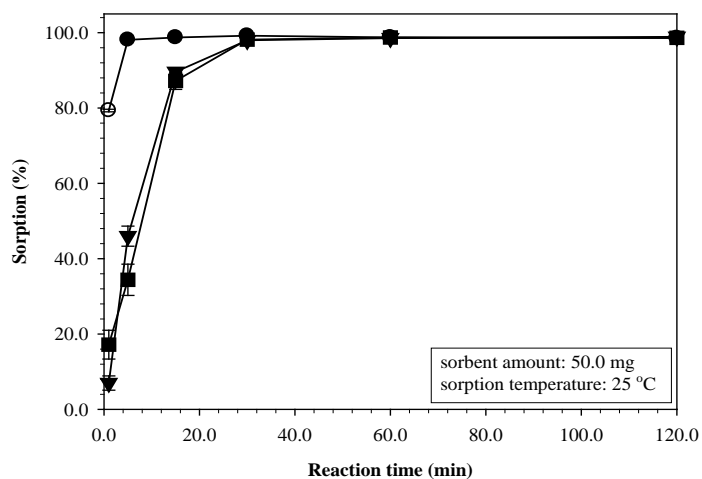
2.2.2.2.2. pH = 9.0

The results of the sorption studies obtained at the solution pH of 9.0 were similar to those at pH 1.0, as shown in Figure 2.15. For (SH)silica and (NH₂)silica+(SH)silica, quantitative sorption was obtained with 50.0 mg sorbent amount, whereas 25.0 mg of (NH₂+SH)silica was sufficient to reach the maximum sorption (Figure 2.15(a)). As seen in Figure 2.15(b), the bifunctional (NH₂+SH)silica demonstrated faster sorption behavior, and even 5.0 min of contact time was sufficient to exceed 96% sorption

percentage. For (SH)silica and (NH₂)silica+(SH)silica, it was necessary to shake the mixture for at least 30.0 min to attain a saturation plateau. The reaction temperature did not have a significant influence on sorption and the percentage sorption was always quantitative at all the examined temperatures (Figure 2.15(c)).



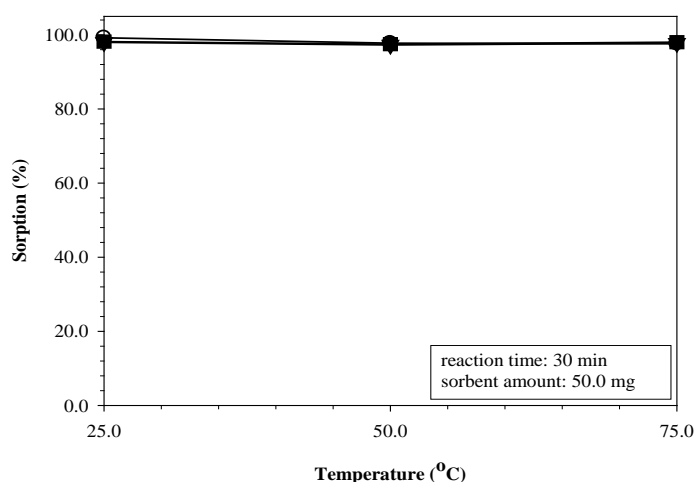
(a)



(b)

Figure 2.15. Effect of a) sorbent amount, b) reaction time, c) temperature on the sorption of 100.0 µgL⁻¹ As(III). (■) (SH)silica, (●) (NH₂+SH)silica, (▼) (NH₂)silica+(SH)silica (sample volume: 20.0 mL, solution pH: 9.0, n=3).

(cont. on next page)



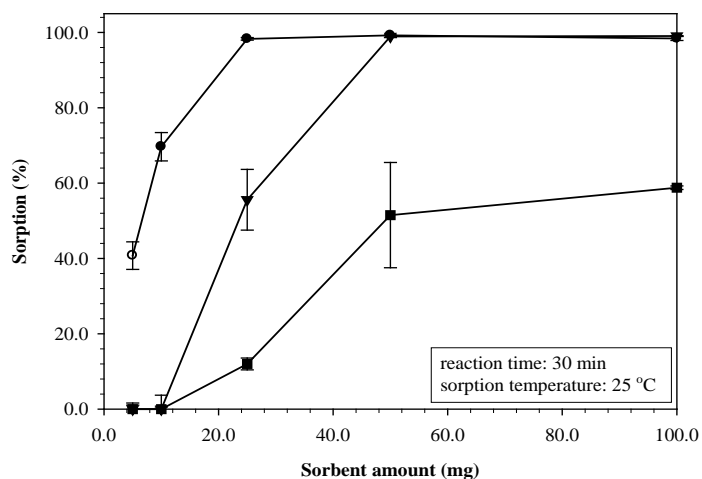
(c)

Figure 2.15. (cont.)

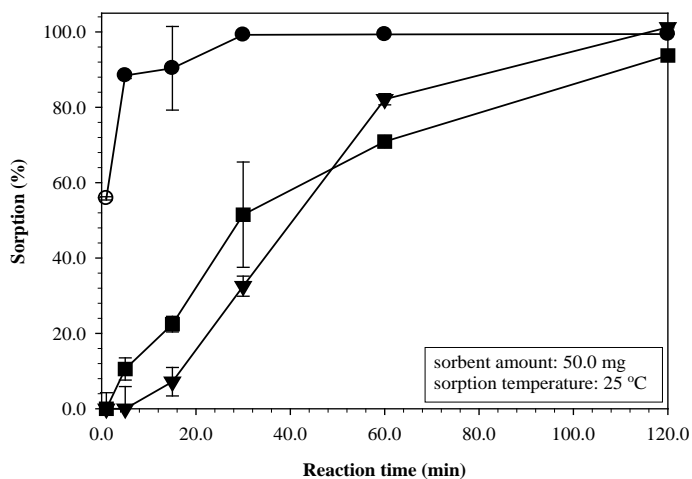
2.2.2.2.3. pH = 3.0

It has been demonstrated in Section 2.2.2.1 that the solution pH of 3.0 deserved a closer examination. Figure 2.10(a) shows that the reproducibility of sorption by the mono-functionalized (SH)silica and the mechanically-mixed (NH₂)silica+(SH)silica was not good at pH 3.0, as can be concluded from the wide error bars whereas the bifunctional (NH₂+SH)silica displayed a better sorption performance. Additional experiments were carried out in order to investigate the sorption behavior of the chosen sorbents at pH 3.0, and the results are summarized in Figure 2.16. As can be seen from the figure, the bifunctional (NH₂+SH)silica always demonstrated a superior sorption behavior over the other two sorbents. A sorbent amount of only 25.0 mg and a reaction time of 30.0 min were sufficient to achieve maximum sorption. In the case of the mechanically-mixed (NH₂)silica+(SH)silica, a higher amount (50.0 mg) and a longer equilibration time (120.0 min) were necessary to attain quantitative sorption. The situation was completely different for the mono-functionalized (SH)silica for which the quantitative sorption was never obtained even with an increase in the sorbent amount. Although longer shaking times increased the sorption percentage, as shown in Figure 2.16(b), quantitative sorption was never approached and the results were irreproducible. The effect of reaction temperature elucidated important differences in the performances of the sorbents. Figure 2.16(c) indicates that the extent of sorption on the bi-functional

(NH₂+SH)silica and the mechanically-mixed (NH₂)silica+(SH)silica were slightly affected by temperature change within the range of 25 °C-75 °C, and tended to display exothermic behavior. On the other hand, the sorption behavior of the mono-functionalized (SH)silica was distinctly endothermic, with the sorption percentage increasing drastically from 52% at 25 °C to about 95% at 75 °C.



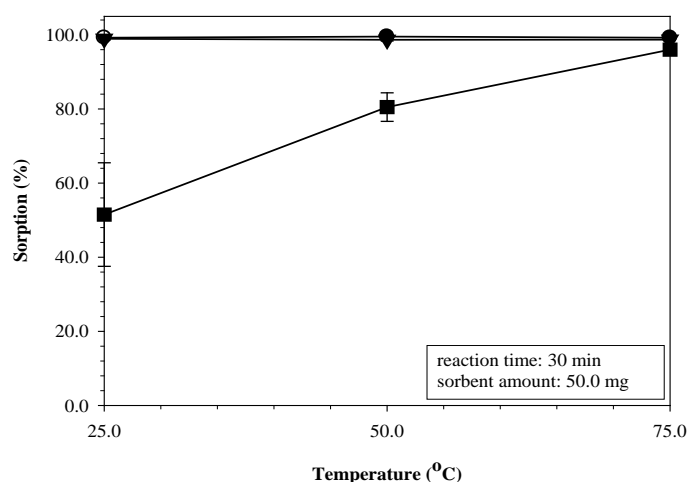
(a)



(b)

Figure 2.16. Effect of a) sorbent amount, b) reaction time, c) temperature on the sorption of 100.0 μgL^{-1} As(III). (■) (SH)silica, (●) (NH₂+SH)silica, (▼) (NH₂)silica+(SH)silica (sample volume: 20.0 mL, solution pH: 3.0, n=3).

(cont. on next page)



(c)

Figure 2.16. (cont.)

2.2.2.3. As(V) Sorption

The percentage sorption of the mono-functional (NH₂)silica, the bifunctional (NH₂+SH)silica and the mechanically-mixed (NH₂)silica+(SH)silica towards As(V) was investigated at pH 3.0. This was the only pH at which (NH₂)silica displayed quantitative sorption (see Figure 2.10(b)) and therefore, any comparison among the selected sorbents containing amine functionality can only be performed at this point. In this context, the effects of the sorbent amount, the reaction time, and the reaction temperature were studied and the results are shown in related figures. The percentage sorption graphs of (NH₂)silica, (NH₂+SH)silica and (NH₂)silica+(SH)silica as a function of sorbent amount demonstrate the different behavior of these sorbents towards As(V) (Figure 2.17). For all the sorbents, 50.0 mg appears to be an optimum quantity for maximum sorption. This amount forms the point at which a saturation plateau was reached for (NH₂+SH)silica and (NH₂)silica+(SH)silica. The most noticeable and unexpected feature of the figure, however, is the decrease of the percentage sorption for the mono-functional (NH₂)silica after 50.0 mg. In order to test whether (or not) this observation is actually due to the increase in sorbent amount, a detailed pH study was performed, bearing in mind the observation that the sorption of (NH₂)silica is restricted to pH 3.0. For this purpose, sorption was carried out in both buffered and unbuffered As(V) solutions. The percentage sorption results are shown in Figure 2.18 together with the

change in the solution pH as a function of the sorbent amount. From these results, it can be argued that the decrease in the sorption percentage occurs as a consequence of the change in the solution pH, rather than being related with the sorbent amount. This finding was further made clear by monitoring the variation in the solution pH as a function of time for different amounts of the sorbent (NH₂)silica (Figure 2.19). As can be deduced from the figure, the solution pH is shifted to even basic pHs in a few seconds in the unbuffered solution, depending on the amount of (NH₂)silica. The reason for the increase in the solution pH must be protonation of the amine functional groups in (NH₂)silica and thereby decreasing the hydronium ion concentration in the solution. Since any pH \geq 4.0 is not suitable for the sorption of As(V), the sorption percentage decreases. Moreover, the amount where the sorption percentage starts to decrease may be affected by the percentage of the amine functional groups used in the modification of the silica surface, and probably also by batch-to-batch variations. This result also demonstrates the superior performance of the bifunctional (NH₂+SH)silica over the mono-functional (NH₂)silica.

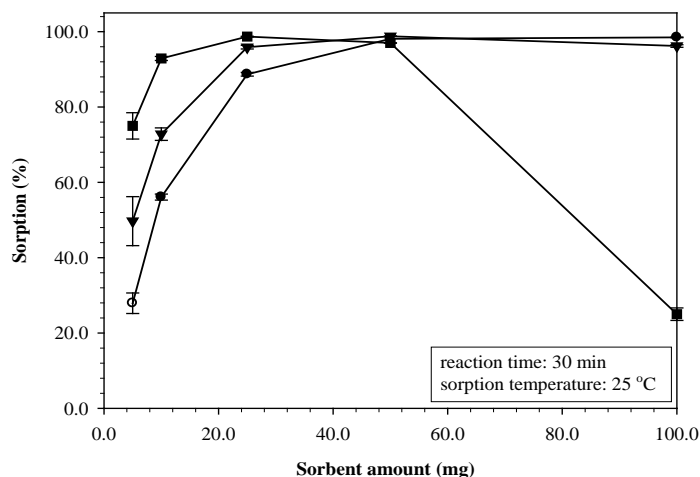


Figure 2.17. Effect of the sorbent amount on the sorption of 100.0 μgL^{-1} As(V) ((■) (NH₂)silica, (●) (NH₂+SH)silica, (▼) (NH₂)silica+(SH)silica, sample volume: 20.0 mL, solution pH: 3.0, n=3).

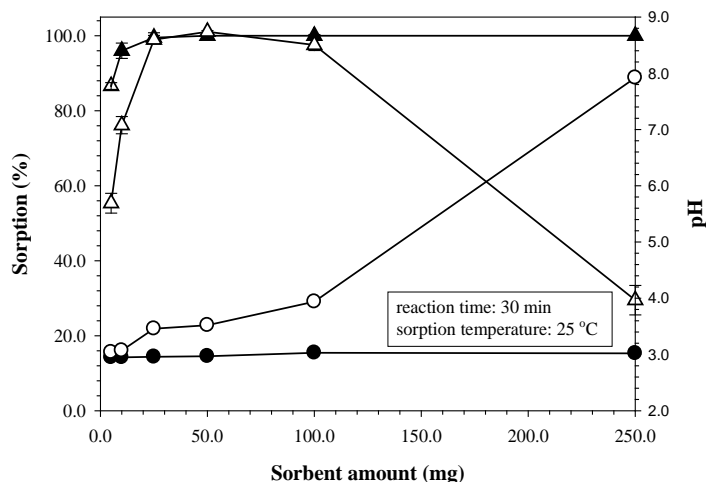


Figure 2.18. Effect of the amount of (NH₂)silica on the sorption of 100.0 µgL⁻¹ As(V) in (Δ) unbuffered and (▲) buffered solutions (variation of pH in (○) unbuffered and (●) buffered solutions), sample volume: 20.0 mL, solution pH: 3.0, n=3.

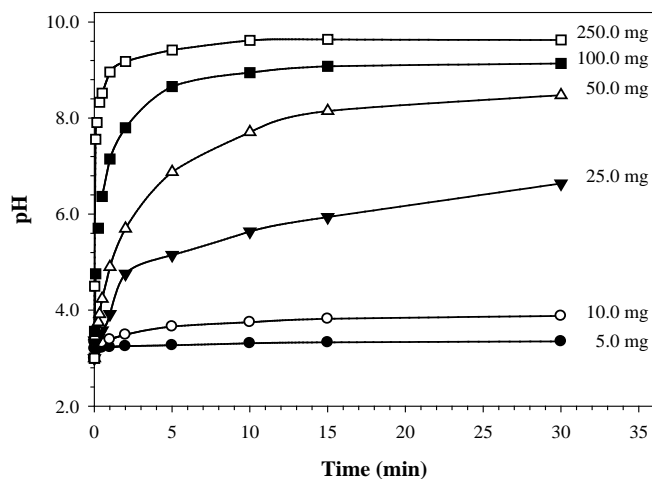


Figure 2.19. Variation in the solution pH as a function of reaction time for different amounts of (NH₂)silica, sample volume: 20.0 mL, solution pH: 3.0 (Experiments were performed under unbuffered conditions).

The effect of the reaction time on the sorption percentages of the selected sorbents, namely, (NH₂)silica, (NH₂+SH)silica and (NH₂)silica+(SH)silica was also investigated and the results are shown in Figure 2.20. As shown in the figure, with small

differences, all three sorbents exhibit similar performance in the time interval of 5-60 min. The sorption percentage is higher than 85% even within the initial 5 min of contact, indicating ease of accessibility to the sorbent groups/sorption sites. As in the previous section, and in relation with the amount of sorbent, the sorption percentage obtained with (NH₂)silica decreases to below 20% in a very short time. In order to enlighten this issue, a detailed pH study was again carried out in both buffered and unbuffered As(V) solutions. The percentage sorption results together with the change in the solution pH in the course of the reaction are shown in Figure 2.21. From these results, it can be suggested that the decrease in percentage sorption can once again be referred to the change in the solution pH, and is not a consequence of the reaction time. This conclusion can also be drawn from Figure 2.19 which shows that depending on the amount of (NH₂)silica in the unbuffered solution, the solution pH was not equal to 3.0, and has immediately shifted to higher values in a matter of seconds where no sorption of As(V) occurs. This result illustrates, once again, the better sorption performance of the bifunctional over the mono-functional silica.

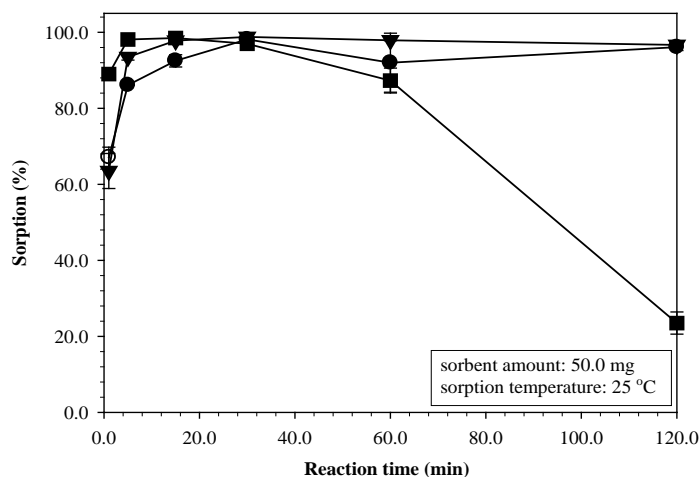


Figure 2.20. Effect of the reaction time on the sorption of 100.0 µgL⁻¹ As(V) ((■) (NH₂)₂silica, (●) (NH₂+SH)silica, (▼) (NH₂)silica+(SH)silica, sample volume: 20.0 mL, solution pH: 3.0, n=3).

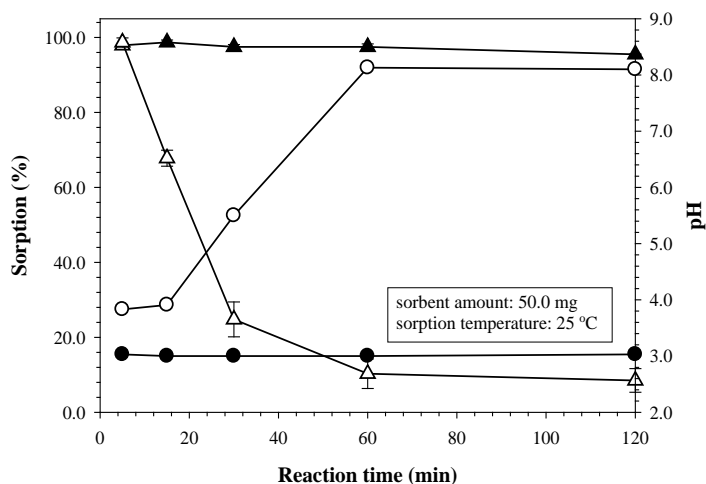


Figure 2.21. Effect of the reaction time on the sorption of $100.0 \mu\text{gL}^{-1}$ As(V) by $(\text{NH}_2)\text{silica}$ in (Δ) unbuffered and (\blacktriangle) buffered solutions (variation of pH in (\circ) unbuffered and (\bullet) buffered solutions), sample volume: 20.0 mL , solution pH: 3.0 , $n=3$)

The effect of reaction temperature on the sorption of As(V) by the selected sorbents is shown in Figure 2.22. As explained in the previous two paragraphs, the sorption percentage is strongly affected by the solution pH, and buffering the solution at pH 3.0 had always a positive influence on the extent of sorption. At $25 \text{ }^\circ\text{C}$ and under the employed experimental conditions, all three sorbents displayed quantitative sorption in both the unbuffered and the buffered solutions although the pHs of the unbuffered solutions after the sorption step had risen to 8.05, 6.90, and 6.50 for $(\text{NH}_2)\text{silica}$, $(\text{NH}_2)\text{silica}+(\text{SH})\text{silica}$ and $(\text{NH}_2+\text{SH})\text{silica}$, respectively. These high sorption results can be ascribed to the fast kinetics of the sorption with the selected sorbents. At $50 \text{ }^\circ\text{C}$, the sorption of $(\text{NH}_2)\text{silica}$ and $(\text{NH}_2)\text{silica}+(\text{SH})\text{silica}$ in the unbuffered solutions have decreased below 10% whereas the respective sorption results were 83% and 76% in the buffered solutions. Although these results are indicative of exothermic nature of sorption with these two sorbents, it seems that the sudden decrease in sorption can be attributed to the increase in the solution pH to values where no sorption occurs, rather than being a thermal effect. Following the sorption step, the pH values of the solutions were 8.50 and 7.83 for $(\text{NH}_2)\text{silica}$ and $(\text{NH}_2)\text{silica}+(\text{SH})\text{silica}$, respectively. This finding also shows the importance of buffering the solutions if $(\text{NH}_2)\text{silica}$ or $(\text{NH}_2)\text{silica}+(\text{SH})\text{silica}$ are planned to be used. The situation for the bifunctional $(\text{NH}_2+\text{SH})\text{silica}$ was different from the two sorbents in a way that the sorption was

again quantitative for both the unbuffered and the buffered solutions. At 75 °C, the sorption decreased to almost 0% for the unbuffered, and below 25% for the buffered solutions, for (NH₂)silica and (NH₂)silica+(SH)silica, respectively. For (NH₂)silica and (NH₂)silica+(SH)silica, the pH values of the unbuffered solutions following the sorption step were 8.70 and 7.76, respectively. On the other hand, the pH did not change in the buffered solutions and the decrease in the sorption percentage can, therefore, be ascribed to exothermic nature of sorption on these two sorbents. The sorption of (NH₂+SH)silica was not affected by the temperature increase and was quantitative even at 75 °C. These results verify the robust nature and the applicability of the bifunctional (NH₂+SH)silica even at such relatively unusual conditions.

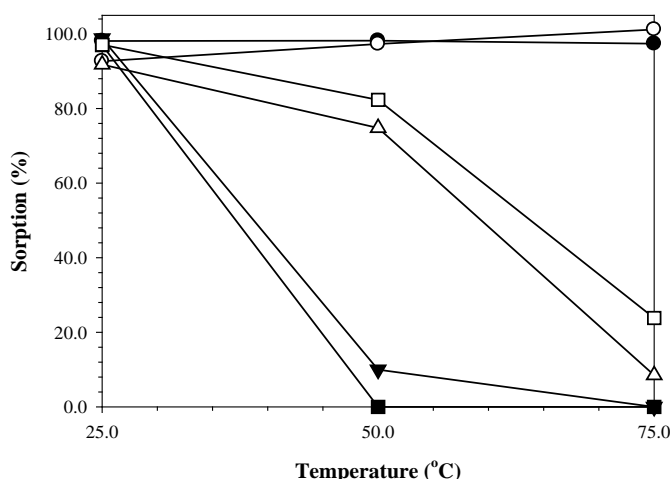


Figure 2.22. Effect of the reaction temperature on the sorption of 100.0 µgL⁻¹ As(V). (■) (NH₂)silica unbuffered solution, (□) (NH₂)silica buffered solution, (▼) (NH₂)silica+(SH)silica unbuffered solution, (Δ) (NH₂)silica+(SH)silica buffered solution, (●) (NH₂+SH)silica unbuffered solution, (○) (NH₂+SH)silica buffered solution (sample volume: 20.0 mL, sorbent amount: 50.0 mg, reaction time: 30.0 min, solution pH: 3.0, n=3).

2.2.3. Sorption Capacity (Dubinin–Radushkevich Isotherm Model)

In addition to the sorption studies with As(III) and As(V), the capacity of the sorbents was determined via D–R isotherm model. The model was applied at pH 1.0, 3.0 and 9.0 for As(III) and pH 3.0 for As(V). The results are summarized in Table 2.5. The linear correlation coefficients (R^2) were generally high, suggesting that the

isotherm is suitable for describing the sorption of both arsenic species. During the sorption studies, the arsenic amount was 0.00053 mmolAs/g sorbent (As initial concentration: 100.0 μgL^{-1} , solution volume: 20.0 mL and sorbent amount: 50.0 mg) and according to the maximum sorption capacity, Q_{max} , values of the sorbents (Table 2.4) only a small fraction of the capacity of the sorbents appears to be used for sorption, which is ascribed to the low initial sorbate concentration. Overall, the calculated values of sorption energy correspond to electrostatic type of interaction.

Table 2.5. Summary of Dubinin-Radushkevich coefficients (Solution volume, shaking time and reaction temperature were 20.0 mL, 30 min and 25 °C, respectively, n = 3).

	Parameter	(SH+NH ₂)silica	(SH)silica+(NH ₂)silica	(SH)silica	(NH ₂)silica	
As(III)	pH 1.0	R ²	0.9802	0.9759	0.9897	
		Q _{max} (mmol/g)	0.0063	0.0072	0.0072	-
		E (kJ/mol)	15.8	15.8	22.4	
	pH 3.0	R ²	0.982	0.9956	0.9974	
		Q _{max} (mmol/g)	0.0360	0.0210	0.0470	-
		E (kJ/mol)	12.9	12.9	9.1	
	pH 9.0	R ²	0.9851	0.861	0.9844	
		Q _{max} (mmol/g)	0.0390	0.0021	0.0044	-
		E (kJ/mol)	12.9	22.4	15.8	
As(V) pH 3.0	R ²	0.9660	0.9966		0.9962	
	Q _{max} (mmol/g)	0.0039	0.0121	-	0.1312	
	E (kJ/mol)	15.8	12.9		11.2	

2.2.4. Desorption Studies

2.2.4.1. Desorption of As(III)

As explained in Section 2.1.7, the first strategy followed for desorption of As(III) from (SH)silica, (NH₂+SH)silica and (NH₂)silica+(SH)silica was to oxidize the adsorbed As(III) to As(V) using the oxidative eluent 0.050 M KIO₃ in 2.0 M HCl. This eluent desorbed As(III) over 89% by oxidizing to As(V) when the sorption was performed at pH values of 1.0 and 3.0; and lower desorption (between 70-77%) was

achieved when sorption was performed at pH of 5.0 and 8.0 (Table 2.6). In the case of 0.50 M NaOH (Table 2.7), almost complete desorption of As(III) was observed which was possibly caused by removal of functional groups of the sorbents when sorption was realized at pH values of 1.0 and 3.0. On the other hand, desorption percentages were between 60 and 70 when sorption was carried out at pH values of 5.0 and 8.0. The wide range of the desorption percentages obtained using the same eluent at different sorption pH values can be ascribed to the different type of interaction of the analyte ion with the functional groups on the modified silicas.

Table 2.6. Desorption of As(III) using 0.050 M KIO₃ in 2.0 M HCl (Sorption condition: sorption time: 30 min, sorbent amount: 50.0 mg, sample volume: 20.0 mL, sorption temperature: 25 °C. Desorption conditions: desorption time: 60 min, eluent volume 20.0 mL and desorption temperature: 25 °C).

Sorbent	Desorption (%)			
	pH 1.0	pH 3.0	pH 5.0	pH 8.0
(SH)silica	101.4 (±7.0)	-	-	-
(NH ₂ +SH)silica	92.5 (±1.7)	93.5 (±8.0)	74.5 (±1.8)	73.4 (±3.4)
(NH ₂)silica+(SH)silica	88.7 (±1.9)	94.6 (±2.3)	76.8 (±4.3)	70.5 (±0.9)

Table 2.7. Desorption of As(III) using 0.50 M NaOH (Sorption condition: sorption time: 30 min, sorbent amount: 50.0 mg, sample volume: 20.0 mL, sorption temperature: 25 °C. Desorption conditions: desorption time: 60 min, eluent volume 20.0 mL and desorption temperature: 25 °C).

Sorbent	Desorption (%)			
	pH 1.0	pH 3.0	pH 5.0	pH 8.0
(SH)silica	89.0 (±1.0)	-	-	69.5 (±2.6)
(NH ₂ +SH)silica	75.8 (±3.7)	104.5 (±8.8)	68.6 (±0.7)	58.6 (±2.0)
(NH ₂)silica+(SH)silica	95.5 (±2.7)	115.0 (±1.6)	64.7 (±3.1)	67.4 (±3.1)

2.2.4.2. Desorption of As(V)

A similar strategy was followed for elution of As(V) from (NH₂)silica, (NH₂+SH)silica and (NH₂)silica+(SH)silica by reducing the adsorbed As(V) to As(III)

with L-cysteine. The results showed that nearly 90% desorption was achieved from (NH₂)silica while (NH₂+SH)silica and (NH₂)silica+(SH)silica underwent only 20% and 57% desorption percentages, respectively (Table 2.8). A possible reason for the lower desorption with mercapto containing sorbents is the affinity of the mercapto group toward As(III) produced after reduction step. The second strategy to elute As(V) from the sorbents was to leach the sorbent with 0.50 M HNO₃ or 0.5 M NaOH. The desorption percentage of the As(V) when HNO₃ is used as eluent from (NH₂)silica and (NH₂)silica+(SH)silica was above 85%, but this eluent was not much effective for (NH₂+SH)silica (43% desorption). 0.50 M NaOH was able to desorb As(V) over 92% from each sorbent. The main reason for desorption of arsenate from the prepared sorbents can be explained by the leaching of the functional groups (amino- and/or mercapto) from the silica surface under basic conditions.

Table 2.8. Desorption of As(V) with various eluent (Sorption condition: solution pH: 3.0, sorption time: 30 min, sorbent amount: 50.0 mg, sample volume: 20.0 mL, sorption temperature: 25 °C. Desorption conditions: desorption time: 60 min, eluent volume 20.0 mL and desorption temperature: 25 °C).

Sorbent	Desorption (%)		
	1.0% L -cysteine	0.50 M NaOH	0.50 M HNO ₃
(NH ₂)silica	88.0 (±1.0)	97.5 (±1.2)	86.8 (±0.3)
(NH ₂ +SH)silica	20.7 (±0.9)	92.0 (±0.8)	42.6 (±2.9)
(NH ₂)silica+(SH)silica	56.8 (±1.4)	97.1 (±5.4)	88.4 (±2.7)

2.2.5. Reusability of the Sorbents

As mentioned in Section 2.1.8, the pH of 3.0 had been chosen as the critical pH for sorption and speciation studies. For this reason, the reusability of the sorbents was tested at pH 3.0 for both arsenic forms. For As(V), 1.0% (m/v) L-cysteine was used as the eluent for (NH₂)silica, 0.50 M NaOH for (NH₂)silica, (NH₂)silica+(SH)silica and (NH₂+SH)silica, and 0.50 M HNO₃ for (NH₂)silica, (NH₂)silica+(SH)silica and (NH₂+SH)silica. The results demonstrate that (Table 2.9) (NH₂)silica can be used at least 5 times when 1.0% (m/v) L-cysteine is used as the eluent since more than 88 % sorption was obtained even after five sorption/elution cycles. When 0.50 M HNO₃ was used for elution (Table 2.10), the sorption percentage decreased gradually from 97 to 78

between the first and the fifth cycles. The highest desorption was obtained using 0.50 M NaOH; however, when this eluent is used the sorbent cannot be used further since the functional groups are deteriorated. In the case of As(III) sorption, only two sorbents, namely, (NH₂)silica+(SH)silica and (NH₂+SH)silica were investigated for their reusability after elution with 0.50 M NaOH, 0.50 M HNO₃ and 0.05 M KIO₃ in 2.0 M HCl (Table 2.11). The results show that only 0.50 M HNO₃, with higher than 80 % sorption after the fifth sorption/elution cycle, can be used if the sorbents are to be reused. On the other hand, 0.50 M NaOH and 0.05 M KIO₃ in 2.0 M HCl can be used only once because of the degradation of the surface functional groups. Nevertheless, these eluents can be used for As(III) and As(V) in many applications where the reusability of the sorbent is not of concern.

Table 2.9. Repetitive use of (NH₂)silica for sorption of As(V) (Sorption condition: solution pH: 3.0, sorption time: 30 min, sorbent amount: 50.0 mg, sample volume: 20.0 mL, sorption temperature: 25 °C. Desorption conditions: desorption time: 60 min, eluent volume 20.0 mL and desorption temperature: 25 °C).

Number of reuse	Sorption (%)		
	1.0% (m/v) L-cysteine	0.50 M NaOH	0.50 M HNO ₃
1	96.7 (± 0.3)	96.4 (± 0.5)	96 (± 0.3)
2	90.9 (± 0.2)	0	94.1 (± 1.1)
3	88.5 (± 2.2)	0	91.2 (± 2.5)
4	89.6 (± 0.1)	0	89.8 (± 1.6)
5	87.7 (± 0.4)	0	83.6 (± 7.7)

Table 2.10. Repetitive use of (NH₂+SH)silica and (NH₂)silica+(SH)silica for sorption of As(V) (Sorption condition: solution pH: 3.0, sorption time: 30 min, sorbent amount: 50.0 mg, sample volume: 20.0 mL, sorption temperature: 25 °C. Desorption conditions: desorption time: 60 min, eluent volume 20.0 mL and desorption temperature: 25 °C).

Number of reuse	Sorption (%)			
	(NH ₂ +SH)silica		(NH ₂)silica+(SH)silica	
	0.50 M NaOH	0.50 M HNO ₃	0.50 M NaOH	0.50 M HNO ₃
1	95.3 (± 0.7)	94.7 (± 1.6)	97.3 (± 1.5)	97.4 (± 0.1)
2	21.3 (± 11.6)	79.5 (± 3.5)	32.6 (± 20.4)	86.0 (± 3.1)
3	0	80.0 (± 6.2)	0	84.5 (± 2.5)
4	0	78.8 (± 4.2)	0	77.9 (± 3.1)
5	0	79.9 (± 3.8)	0	78.0 (± 4.8)

Table 2.11. Repetitive use of (NH₂+SH)silica and (NH₂)silica+(SH)silica for sorption of As(III) (Sorption condition: solution pH: 3.0, sorption time: 30 min, sorbent amount: 50.0 mg, sample volume: 20.0 mL, sorption temperature: 25 °C. Desorption conditions: desorption time: 60 min, eluent volume 20.0 mL and desorption temperature: 25 °C).

Number of reuse	Sorption (%)			
	(NH ₂ +SH)silica		(NH ₂)silica+(SH)silica	
	0.50 M NaOH	0.050 M KIO ₃ in 2.0 M HCl	0.50 M NaOH	0.050 M KIO ₃ in 2.0 M HCl
1	97.9 (± 0.3)	97.5 (± 0.1)	95.1 (± 0.1)	92.5 (± 0.7)
2	8.5 (± 10.8)	13.4 (± 17.9)	0	48.0 (± 15.4)
3	0	16.3 (± 2.2)	0	49.1 (± 8.7)
4	0	3.8 (± 6.8)	0	21.3 (± 11.6)
5	0	0	0	0

2.2.6. Method Validation

As can be deduced from both the sorption and the desorption results, the bifunctional (NH₂+SH)silica is advantageous over the mono-functionalized (NH₂)silica and (SH)silica, and also the mechanically-mixed (NH₂)silica+(SH)silica. It offers better

sorption features for both As(III) and As(V) compared to the other sorbents. For this reason, the accuracy of the method was investigated through the analysis of a standard reference material using (NH₂+SH)silica as the sorbent. The result obtained with the proposed methodology was $27.53 \pm 0.37 \mu\text{gL}^{-1}$ which is in good agreement with the certified value of arsenic in the SRM (NIST 1640, $26.67 \mu\text{gL}^{-1}$). In order to further verify the results of SRM study, statistical t-test was applied. The result of the t-test indicated that there is no difference in the determined and certified value of arsenic at 95% confidence level. In addition, a spike recovery test was applied to drinking water to further test the validity of the method. The percent recovery values given in Table 2.12 indicate that the proposed methodology is practical to use with ultrapure and drinking water with the percentage recovery values of $93.0 (\pm 2.3)$, $86.9 (\pm 1.2)$, respectively.

Table 2.12. Spike recovery results obtained using (NH₂+SH)silica for a drinking water sample (solution pH: 3.0, sorption time: 30 min, sorbent amount: 50.0 mg, sample volume: 15.0 mL, sorption temperature: 25 °C, eluent: 0.5 M NaOH, desorption time: 60 min, n=3).

	Concentration (μgL^{-1})			Recovery (%)
	Initial	Spiked	Determined*	
Ultrapure water	0.0	30.0	$27.9 (\pm 0.7)$	$93.0 (\pm 2.3)$
Drinking water	2.7	30.0	$28.4 (\pm 0.4)$	$86.9 (\pm 1.2)$
Drinking water (1/3 diluted)	0.9	10.0	$9.0 (\pm 0.2)$	$82.6 (\pm 2.1)$
SRM**	26.67	0	$27.53 (\pm 0.37)$	-

* Concentration determined after sorption/desorption steps

** SRM solution (1/3 diluted)

CHAPTER 3

NEW SPME SORBENTS: SOLID PHASE MICROEXTRACTION OF ARSENIC

3.1. Experimental

3.1.1. Instrumentation and Apparatus

3.1.1.1. HPLC-HGAAS

Separation of extracted arsenical species was achieved in Agilent 1200 Series HPLC system with a 250 mm anion exchange column (Hamilton, PRP-X100) using 25 mM phosphate buffer (pH 5.85) as mobile phase at flow rate of 1.0 mLmin⁻¹. From the anion exchange column exit 1.0 mL fractions were collected and detection of each species in the fractions was realized with A Thermo Elemental Solaar M6 Series AAS (Cambridge, UK). An air-acetylene burner was used in arsenic determination utilizing the Segmented Flow Injection Hydride Generation (SFI-HGAAS) unit. An arsenic hollow cathode lamp at the wavelength of 193.7 nm and a deuterium lamp were employed as the source line and for background correction, respectively. The pH adjustment of buffer solution was achieved with Ino Lab Level 1 pH meter (Weilheim, Germany). Operating conditions for the instruments are given in Table 3.1.

Table 3.1. Operation conditions for HPLC-HGAAS

HPLC (Agilent 1200 Series)		HG-AAS (Thermo Elemental Solaar M6)	
Column	Hamilton PRP-X 100	Carrier gas (N ₂) flow rate	200 mLmin ⁻¹
Mobile phase	25 mM phosphate buffer	2.0 % (v/v) HCl flow rate	6.1 mLmin ⁻¹
Thermostat temp.	25 °C	NaBH ₄ concentration	1.0% (w/v)
Injection volume	20 µL	NaBH ₄ flow rate	3.0 mLmin ⁻¹
Mobile phase flow rate	1.0 mLmin ⁻¹	Sample flow rate	6.0 mLmin ⁻¹

3.1.1.2. HPLC-ICPMS

The separation of extracted arsenic species was achieved with Agilent 1200 Series HPLC system with a 250 mm anion exchange column (Hamilton, PRP-X100). Gradients with 10.0 mM and 30.0 mM ammonium carbonate solutions (pH 8.50) were used as mobile phase at flow rate of 1.0 mLmin⁻¹. The detection of each species was realized with ICP-MS, Agilent 7500ce (Tokyo, Japan). Online separation and detection of five arsenic species were accomplished by connecting HPLC column outlet directly to ICP-MS concentric nebulizer. The two instruments were connected by the shortest allowed tubing to prevent the broadening of the peaks (Figure 3.1). The connection was realized with 67 cm long perfluoroalkoxy (PFA) tubing (ID: 0.5 mm). The operating parameters for HPLC and ICP-MS are provided in Table 3.2. The pH adjustments of buffer solutions were achieved with Ino Lab Level 1 pH meter (Weilheim, Germany). Operating conditions for the instruments are given in Table 3.2.



Figure 3.1. HPLC-ICPMS system

Table 3.2. Operation conditions for HPLC-ICPMS

HPLC		Agilent 1200	
Analytical column	PRP-X100 (250 mm x 4.1 mm, 10 μ m)		
Mobile phase	10.0 mM and 30.0 mM $(\text{NH}_4)_2\text{CO}_3$ solutions, pH=8.50		
Flow rate	1.0 mLmin ⁻¹		
Column temperature	25 °C		
Sample loop	100 μ L		
ICP-MS		Agilent 7500ce	
Rf power output	1550 W	Interface	Ni sampler cone (1 mm)
Frequency	27 MHz		Ni skimmer cone (0.4 mm)
Plasma gas flow rate	15 Lmin ⁻¹	Spray chamber temp.	2 °C
Carrier gas flow rate	0.85 Lmin ⁻¹	Nebulizer	Concentric
Collision gas flow rate	4.5 mLmin ⁻¹	Dwell time	100 ms
Octopole reaction system	+	Detected isotope	⁷⁵ As
Collision gas	He	Integration mode	Peak area

3.1.1.3. Characterization and Microextraction Studies

Microimages of bare and coated silica fibers were taken using a Philips XL-30S FEG scanning electron microscope (SEM) (Eindhoven, The Netherlands). The thermal properties of electrospun nanofibers were examined using a Perkin Elmer Pyris Diamond TG/DTA (Boston, MA, USA). The crystallographic structure of the fiber coatings were elucidated by a Philips X'Pert Pro X-Ray Diffractometer (XRD) (Eindhoven, The Netherlands). The feeding rate was kept constant in electrospinning process by microsyringe pump (LION WZ-50C6). The pH of the solutions was adjusted with 0.01-1.0 M HNO₃ and 0.01-1.0 M NH₃ using Ino Lab Level 1 pH meter (Weilheim, Germany). Extractions of arsenic species were performed in multi-position magnetic stirrer RO 10 power IKAMAG.

3.1.2. Reagent and Solutions

All the chemicals were of analytical reagent grade. Ultra-pure water (18.2 MΩ.cm) was used throughout the study. Glassware and plastic containers were cleaned by being soaked in 10% (v/v) nitric acid for 24 h and rinsed with ultra-pure water prior to use.

Stock standard solutions of As(V) and As(III), 2000.0 mgL⁻¹, were prepared by dissolving As₂O₅ (Merck, product code: 1.09939, CAS no: [1303-28-2]) and As₂O₃ (Fischer, CAS no: [1327-53-3]), respectively, in ultra pure water. Dimethylarsinic acid (DMA, 1000.0 mgL⁻¹) and monomethylarsonic acid (MMA, 553.0 mgL⁻¹) were prepared by dissolving dimethylarsinic acid sodium salt trihydrate (Merck, product code: 8.20670, CAS no: [6131-99-3]) and disodium methyl arsonate hexahydrate (Supelco, product no: PS 281, CAS no: [144-21-8]), respectively, in ultra-pure water. A solution of Arsenobetaine (AsB, 1031 mgkg⁻¹) in water (BCR 626) was obtained from BCR (Brussels, Belgium). The concentrations of all the stock solutions described above were given in terms of arsenic. Prepared stock solutions were stored in refrigerator at 4 °C, lower concentrations were prepared daily by diluting appropriate amount of stocks in ultra-pure water. HNO₃ (Merck, product code: 1.00456, CAS no: [7697-37-2]) and NH₃ (Merck, product code: 1.05422) were used to adjust the pH of the solutions.

For HPLC-HGAAS studies, 25.0 mM phosphate buffer solution (pH 5.85) was prepared by daily dissolving a proper amount of HPLC grade KH_2PO_4 (Fluka, product code: 60221, CAS no.: [7778-77-0]) and K_2HPO_4 (Fluka, product code: 17835, CAS no.: [7758-11-4]) in ultra-pure water, and pHs of the solution was adjusted by using various concentrations of HNO_3 and NH_3 . Sodium borohydride solution was prepared for a daily use from fine granular product (Merck, product code: 8.06373, CAS no.: [16940-66-2]) and stabilized by NaOH (Merck, product code: 1.06498, CAS no.: [1310-73-2]) in water. L-Cysteine (Merck, product code: 1.02838, CAS no.: [52-90-4]) was added to collected fractions from anion exchange column to reduce As(V) to As(III) before HG-AAS determination.

For HPLC-ICPMS studies, 10.0 mM and 30.0 mM $(\text{NH}_4)_2\text{CO}_3$ solutions (pH 8.50) were prepared daily by dissolving a proper amount of HPLC grade $(\text{NH}_4)_2\text{CO}_3$ (Fluka, product code: 74415, CAS no.: [506-87-6]) in ultra-pure water, and pHs of the solutions were adjusted by using various concentrations of HNO_3 and NH_3 .

All solutions that were passed from anion exchange column (mobile phase and eluting solvent) was filtered from 0.20 μm cellulose acetate filter paper (Sartorius) and degassed for 15 min in ultrasonic bath.

Fiber optic cable was kindly supplied by HES Kablo (Kayseri, Turkey). Acetone (Merck, product code: 1.00014, CAS no: [67-64-1]) was used for removal of protective polyamide coating of the fibers. Pellet form of NaOH (Merck, product code: 1.06498, CAS no: [1310-73-2]), was used to prepare 1.0 M NaOH solution in order to introduce maximum number of silanol groups on the surface of the bare fiber. 0.1 M HCl (Merck, product code: 1.00314, CAS no.: [7647-01-0]) was used for neutralization of the base. All reagent used in the preparation and synthesis of the SPME fiber coatings were summarized in Table 3.3.

In order to show the effect of the ionic strength on the extraction of arsenic species, NaCl (Riedel-de Haen, product code: 13423, CAS no: [7647-14-5]) solutions were prepared in various concentrations by dissolving appropriate amount of solid NaCl in water.

Arsenic Species in Frozen Human Urine (NIST, SRM 2669) and Trace Elements in Natural Waters (NIST, SRM 1643e) were used to validate the proposed methodology. The composition of SRM 1643e is given in Table 3.4.

Table 3.3. Reagents used through the preparation of SPME fiber coatings

Reagent	Company	Product Code	CAS no.	Purpose of use
NaBH ₄ (granular)	Merck	8.06373	[16940-66-2]	Reducing of Fe(II) to nZVI
FeCl ₂ .4H ₂ O	Sigma Aldrich	22,029-9	[13478-10-9]	Synthesis of nZVI
Absolute Ethanol	Sigma Aldrich	32221	[64-17-5]	Solvent for FeCl ₂ .4H ₂ O
Agarose	Sigma	A5093	[9012-36-6]	Immobilization matrix for nZVI
FeCl ₃ .6H ₂ O	Merck	1.03943	[10025-77-1]	Electrospun Fe ₂ O ₃ nanofibers
PVP	Sigma Aldrich	PVP10	[9003-39-8]	Electrospun Fe ₂ O ₃ nanofibers
PVA				Electrospun ZnO or ZnO-CeO ₂ nanofibers
Ce(NO ₃) ₂ .6H ₂ O	Fluka	22350	[10294-41-4]	Electrospun ZnO- CeO ₂ nanofibers
Zn(CH ₃ COO) ₂ .2H ₂ O	Fluka	96459	[5970-45-6]	Electrospun ZnO nanofibers
3-(Triethoxysilyl) propylamine	Merck	8.26619	[14814-09-6]	Functionalization of silica fiber
(3-Mercaptopropyl) trimethoxysilane	Fluka	63800	[4420-74-0]	Functionalization of silica fiber
3-Choloropropyltrimethoxysilane	Alfa Aesar	42413	[2530-87-2]	Functionalization of silica fiber
Triethoxyvinylsilane	Merck	8.08273	[78-08-0]	Functionalization of silica fiber

(cont. on next page)

Table 3.3 (cont.)

Reagent	Company	Product Code	CAS no.	Purpose of use
Dichloromethane	Riedel-de Haen	24233	[75-09-2]	Solvent in sol-gel process
THF	Sigma Aldrich	87368	[109-99-9]	Solvent in sol-gel process
TFA	Merck	76-05-1	[808260]	Catalyst in sol-gel process
PMHS	Aldrich	81330	[9004-73-3]	Deactivator in sol-gel process
PDMS 25 000 cSt	Aldrich	481339	[70131-67-8]	Organic polymer with sol gel active terminal for SPME coatings
PDMS	Aldrich	432997	[70131-67-8]	Organic polymer with sol gel active terminal for SPME coatings

Table 3.4. Certified values for Trace Elements in Natural Waters (SRM 1643e)

Elements	Concentration (μgL^{-1})	Elements	Concentration (μgL^{-1})
Al	141.8 ± 8.6	Mn	38.97 ± 0.45
Sb	58.30 ± 0.61	Mo	121.4 ± 1.3
As	60.45 ± 0.72	Ni	62.41 ± 0.69
Ba	544.2 ± 5.8	K	$2\ 034 \pm 29$
Be	13.98 ± 0.17	Rb	14.14 ± 0.18
Bi	14.09 ± 0.15	Se	11.97 ± 0.14
B	157.9 ± 3.9	Ag	1.062 ± 0.075
Cd	6.568 ± 0.073	Na	$20\ 740 \pm 260$
Ca	$32\ 300 \pm 1\ 100$	Sr	323.1 ± 3.6
Cr	20.40 ± 0.24	Te	1.09 ± 0.11
Co	27.06 ± 0.32	Th	7.445 ± 0.096
Cu	22.76 ± 0.31	V	37.86 ± 0.59
Fe	98.1 ± 1.4	Zn	78.5 ± 2.2
Pb	19.63 ± 0.21	Mg	$8\ 037 \pm 98$
Li	17.4 ± 1.7		

3.1.3. Preparation of the SPME Fibers

SPME fibers were prepared with two main ways, namely, sol-gel based fiber coatings and nanoparticle immobilized fiber coatings. Sol-gel based coatings were prepared with the insertion of bare fiber into sol-gel solution; after the reaction was completed the functionalized fibers were removed from the solution and dried. The second route of the fiber coating was immobilization of the various nanoparticles onto the surface of the fiber either by immobilization of the nanoparticles into a supporting matrix (capillary template method) or by in situ formation of nanofibers on the surface of the SPME fiber by electrospinning. Details of the methods are given below.

3.1.3.1. Sol-Gel Based SPME Fiber Coatings

The protective polyamide layer of the silica fiber was removed by immersing the piece of 7 cm cut into acetone. Bare fibers were washed with ultra-pure water. Introduction of maximum silanol groups on bare silicate surface which are necessary for

coupling reaction was accomplished by dipping segments of the bare silicate fibers into 1 M NaOH solution for 60 min. This step was followed by dipping the fiber into 0.1 M HCl solution for 30 min to neutralize excess base. Fibers were washed with ultrapure water and thermal curing was applied for 24 h at 120 °C. Coating solutions with different precursors were prepared as follows; 100.0 µL PDMS (hydroxy terminated) and 150.0 µL DCM were mixed in 1.5 mL vial. A precursor with amine functionality (APTES) of 50.0 µL was added into former solution; sequentially 25.0 µL of terminator (PMHS) was added to resulting solution. The sol-gel reaction was started after addition of 50.0 µL TFA (95v TFA+5v water) which was used to catalyze the reaction. The resulting solution was centrifuged for 10 min. Coating process was performed by the immersion of activated silica fiber into prepared solution for 30 min. After reaction period, coated fiber was dried at 60 °C for 30 min. To achieve bulky coatings the procedure can be repeated until desired thickness was obtained. Thermal curing at 120 °C was applied for 24 h, which results in termination of the reactions.

Different coatings were obtained by replacing APTES with mercapto-, cholo- or vinyl-functionality containing sol-gel active compounds.

The same coating process was also applied using dip coater (Figure 3.2) to obtain homogeneous surface coating. Prepared SPME fibers were characterized by scanning electron microscopy (SEM) and energy-dispersive X-ray spectroscopy (EDX).

3.1.3.2. Sol-Gel Based Electrospun Amine-Modified SPME Fiber Coating

The sol-gel solution described in former section was modified and used for electrospun coating of SPME fiber. In a typical procedure 2.0 mL PDMS (hydroxyl terminated, typical viscosity: 25.000 cSt), 3.0 mL tetrahydrofuran (THF), 1.0 mL APTES and 0.50 mL PMHS was mixed in a 20 mL vial. Into the resulting solution 1.0 mL of TFA (95v TFA+5v water) was added and mixed thoroughly. The resulting sol-gel solution was stirred for 48 h at room temperature. In order to achieve viscosity adequate for electrospinning process, some of the solvent (THF) was evaporated from the sol-gel solution at 80 °C for 2 h. Resulting sol-gel solution was loaded into a syringe and electrospinning process was performed at 25 kV potential difference with the feeding rate of 5.0 mL/h. The distance between the syringe and the metal collector was

10 cm. In order to obtain a homogeneous coating on the fiber, the plain silica fiber was attached on rotating drum and constant rotation rate of 300 rpm was applied during coating. The drum was placed between the metal collector and syringe. The distance of rotating drum from syringe was 3 cm. Coated fibers were conditioned at 110 °C overnight to facilitate the endcapping of free silanol groups. Non endcapped amine-modified fibers were prepared by the same procedure excluding the PMHS from the sol-gel solution.

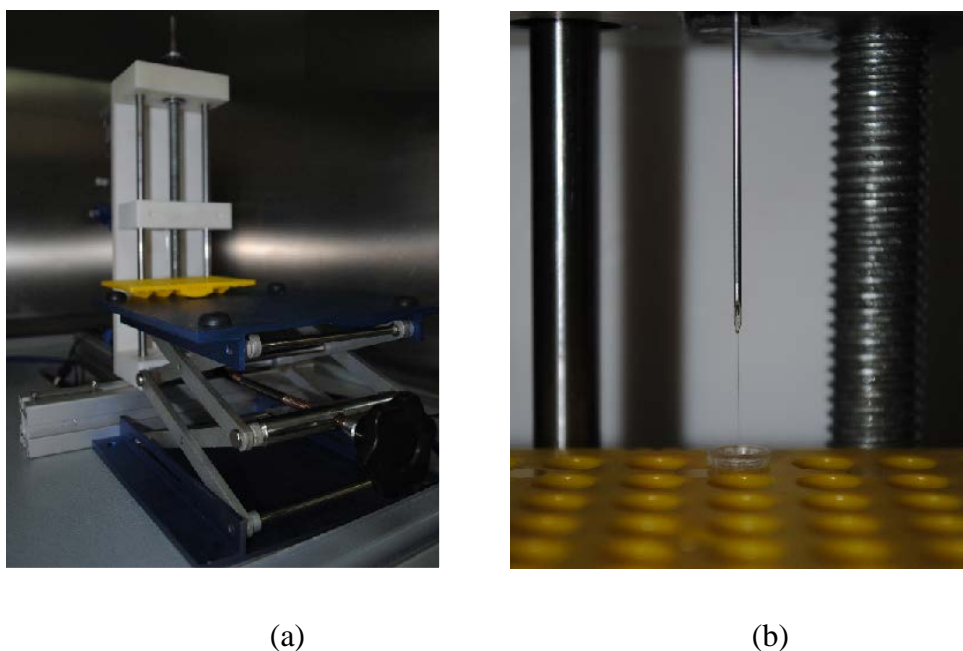


Figure 3.2. Dip coating method a) general view of instrument and b) a typical sol-gel based coating with the dip coater.

3.1.3.3. Capillary Template Method for Immobilization of Zerovalent Iron Nanoparticles

The protective polyamide layer of the silica fiber was removed by immersing the piece of 7 cm cut into acetone. Bare fibers were washed with ultra-pure water. A two step procedure was followed for the functionalization of the fibers. Firstly, nano zerovalent iron (nZVI) particles were synthesized as described in previous reports (Efecan et al. 2009) by drop wise addition of 220.0 mL of 4.0% (w/v) NaBH_4 solution from burette to flask containing 50.0 mL of 1.0 M Fe(II) solution under continuous stirring. After all reducing agent was added, the mixture was stirred for additional 20

min. Obtained nZVI particles were filtered and washed with small amount of ultrapure water and copious amount of ethanol and further dried overnight in oven at 75 °C. Secondly, an immobilization matrix of iron nanoparticles in hot agarose was used for coating the silica fibers. The immobilization matrix was prepared by mixing 0.400 g of agarose and 20.0 mL of ultra-pure water in a 50-mL beaker. The resulting solution was stirred and boiled in a hot plate until a clear solution was obtained. Then, the solution was cooled down to 50 °C and 0.250 g of nZVI was subsequently added. After stirring for 10 min, the mixture was used immediately for coating the fibers at 50 °C. The process of fiber coating is illustrated in Figure 3.3. The first step of coating process was filling up a capillary tubing (i.d.: 1.0 mm, length: *ca* 3 cm, used as a template) with nanoiron-agarose mixture by applying a low vacuum and then immersing a fiber into the filled capillary tubing. After a few minutes, the temperature of the mixture in the capillary tubing dropped down to room temperature and nanoiron-agarose matrix was solidified. The removal of the solidified nanoiron-agarose coated silica fiber from the template capillary tube was easily accomplished by pushing the material inside from the open end of the capillary tube with a small piece of metallic rod. The length of the nanoiron-agarose coating on the fiber was adjusted to 2.0 cm by cutting the excess part from the lower end of the silica fiber and allowing it to air dry at room temperature. Blank SPME fibers were also prepared in the same manner in the absence of iron nanoparticles. Prepared fibers were characterized by SEM, EDX and XRD.

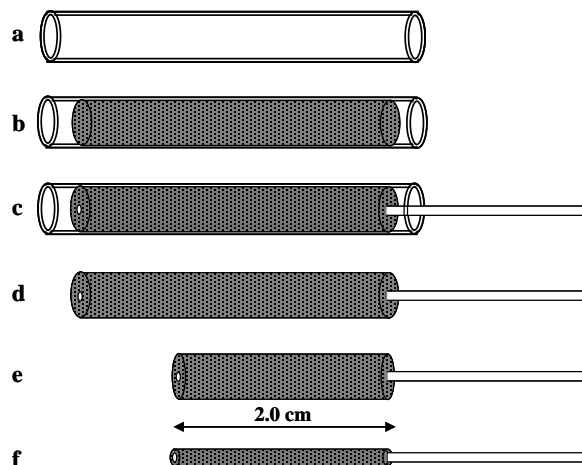


Figure 3.3. Coating procedure of silica fiber; a) empty capillary tubing (*ca* 3 cm), b) capillary tubing filled with nanoiron-agarose matrix (50 °C), c) inserting silica fiber into capillary tubing and cooling for solidification of nanoiron-agarose matrix, d) removal of nanoiron-agarose modified silica fiber, e) cutting the end of the fiber to adjust the length of coating to 2.0 cm, f) air-dried SPME fiber.

3.1.3.4. Electrospun Nanofibers Coated SPME Fibers

In electrospinning method, an electrode is inserted into a polymer solution and the other is attached to a collector, which is grounded. As a high voltage (typically 10–30 kV) is applied, the charge repulsion on the surface of the fluid causes a force directly opposite to the surface tension of the fluid itself. Figure 3.4 shows experimental set-up used for electrospun method. Various electrospun nanofibers were produced throughout the study as candidate materials for SPME fiber coating.



Figure 3.4. Experimental set-up used in electrospinning process

3.1.3.4.1. Electrospun ZnO Nanofibers

For synthesis of ZnO nanofiber coated SPME fiber, a sample of 2.50 g of zinc acetate dihydrate ($\text{Zn}(\text{CH}_3\text{COO})_2 \cdot 2\text{H}_2\text{O}$), was mixed with 4.00 g of polyvinyl alcohol (PVA) solution (18% w/w) and stirred for 5 h in a water bath at 60 °C. To perform the electrospinning process, the prepared solution was loaded into a plastic syringe and a potential difference of 15 kV was applied to the tip of a needle of syringe. The distance between the syringe and the metal collector was 6 cm. The feeding rate was kept constant at $4.5 \text{ mL} \cdot \text{h}^{-1}$ using a microsyringe pump. The obtained electrospun fibers were dried under vacuum at 70 °C for 8 h and calcined for 5 h at 500 °C with a heating rate of $4 \text{ }^\circ\text{C} \cdot \text{min}^{-1}$ in a muffle furnace.

In the synthesis of ZnO-CeO₂ nanofiber coated SPME fiber, the same method was used with addition of 2.00 g Ce(NO₃)₂·6H₂O to described electrospinning solution. Characterizations of fibers were done by scanning electron microscopy.

3.1.3.4.2. Electrospun Fe₂O₃ Nanofibers

For synthesis of Fe₂O₃, nanofibers FeCl₃·6H₂O was employed as an iron source. Since the FeCl₃ is highly soluble in water the polymer that will be used for electrospinning process should be water soluble. Accordingly, polyvinylpyrrolidone (PVP) was chosen as a template polymer for electrospinning process. In a typical experiment, 2.50 g FeCl₃·6H₂O and 11.50 g PVP powder were dissolved in 10.0 mL ultrapure water. The resulting viscous solution was stirred at room temperature overnight. Electrospinning process was performed in a similar manner as had been described in Section 3.1.3.4.1. The potential difference of 35 kV was applied to the tip of a needle of syringe. The distance between the syringe and the metal collector was 10 cm. The feeding rate of microsyringe pump was changed in order to optimize the spinning procedure. The obtained electrospun PVP-FeCl₃ nanofibers were calcined in a muffle furnace at 500 °C for 6 h with a heating rate of $4 \text{ }^\circ\text{C} \cdot \text{min}^{-1}$. The effect of several parameters on electrospinning process was investigated throughout the study. For instance the amount of FeCl₃ was changed between 0.50, 1.00, 1.50 and 2.50 g while PVP concentration was kept constant at 11.50 g. In another experiment, the amount of PVP was varied between 5.00 g and 15.00 g while the amount of FeCl₃·6H₂O was kept

constant at 2.50 g. Another parameter was the effect of the solvent, instead of water ethanol was used as a solvent and in this experiment the amounts of $\text{FeCl}_3 \cdot 6\text{H}_2\text{O}$ and PVP were 2.50 g and 11.50 g, respectively. Also the feeding rate was investigated in the mentioned experiment. Characterizations of Fe_2O_3 nanofibers and PVP- FeCl_3 nanofibers were done by scanning electron microscopy, XRD and TGA.

3.1.4. Arsenic Speciation with Sol-Gel Based SPME Fibers

3.1.4.1. Extraction of Arsenic Species

Solid phase micro extraction was carried out with amine-modified fibers (endcapped amine-modified fibers) in a 20 mL vial containing 15.0 mL of aqueous arsenic mixture (As(III), DMA, MMA and As(V)) which was stirred with magnetic bar. A 200 μL pipette tip was blocked from base by application of heat and used as a desorption container. Initial conditions of extractions were; solution pH: 3.6 (no pH adjustment), arsenic concentration: $1.0 \mu\text{g mL}^{-1}$, stirring speed: 200 rpm, extraction time: 60 min, extraction temperature: RT. Initial desorption conditions were; desorption time: 60 min, desorption volume: 50.0 μL , desorption temperature: RT, eluent: 25.0 mM KH_2PO_4 solution. Extraction parameters such as extraction pH, extraction time, agitation (stirring) speed, ionic strength and desorption conditions were optimized.

3.1.4.2. Extraction of Arsenic Species: Further Improvement on the Fibers

SPME of mentioned arsenic species was carried out with endcapped amine-modified fibers and non endcapped amine-modified fibers. Extractions were performed in a 20-mL vial containing 15.0 mL of aqueous arsenic mixture solution (As(III), DMA, MMA and As(V)) which was stirred with a magnetic bar. Desorption of the analytes was carried out in a container which was prepared from 200- μL pipette tip blocked at the base by application of heat. The conditions for extractions were; solution pH: 4.0, arsenic concentration: $100.0 \mu\text{g L}^{-1}$, stirring speed: 700 rpm, extraction time: 60 min, extraction temperature: RT. For desorption, the conditions were; desorption time: 15

min, desorption volume: 150.0 μL , desorption temperature: RT, eluent: 50.0 mM KH_2PO_4 solution.

3.1.4.3. Optimization of Extraction Parameters for Electrospun Coated Amine-Modified SPME Fibers

3.1.4.3.1. Effect of pH on Extraction of Arsenic Species

The first investigated parameter was solution pH. Extraction studies were carried out at 25 °C after the initial pH of solutions was adjusted to 3.0, 5.0, 7.0 and 9.0 with dilute HNO_3 or NH_3 . The conditions for the extractions were; arsenic concentration: 10.0 μgL^{-1} from each species (AsB, As(III), DMA, MMA and As(V)), stirring speed: 700 rpm, extraction time: 60 min, solution volume: 15.0 mL. Afterwards, desorption of the extracted analytes were performed from the fiber as explained previously. Desorption conditions were; desorption time: 20 min, 150 μL 50.0 mM KH_2PO_4 . Desorption solution was analyzed for its arsenic content and species by HPLC-ICPMS.

3.1.4.3.2. Effect of Agitation Time/Speed on Extraction of Arsenic Species

Effect of agitation time on the extraction of arsenic species by amine-modified fiber was investigated for time intervals of 5, 15, 30 60 and 120 min. The conditions for the extractions were; solution pH: 5.0, arsenic concentration: 10.0 μgL^{-1} from each species (AsB, As(III), DMA, MMA and As(V)), stirring speed: 700 rpm, solution volume: 15.0 mL. Separately, effect of the agitation speed on extraction of the arsenic species was studied at 300, 500, 700 and 1000 rpm stirring speeds. In addition, static extraction of the arsenic species for a 30 min interval was performed to evaluate the effect of the extraction mode. Extraction conditions were; solution pH: 5.0, arsenic concentration: 10.0 μgL^{-1} from each species (AsB, As(III), DMA, MMA and As(V)), extraction time: 30 min, solution volume: 15.0 mL, Desorption conditions for both experiments were; desorption time: 20 min, 150 μL 50.0 mM KH_2PO_4 .

3.1.4.3.3. Effect of Salt Concentration (Ionic Strength) on Extraction of Arsenic Species

Effect of the ionic strength on the extraction of arsenic species was investigated by addition of various amount of NaCl into arsenic containing solution. The investigated concentrations were 1.0 M, 0.10 M, 0.010 M and without addition of NaCl. Extraction conditions for the aforementioned experiment were; solution pH: 5.0, arsenic concentration: $10.0 \mu\text{gL}^{-1}$ from each species (AsB, As(III), DMA, MMA and As(V)), extraction time: 30 min, stirring speed: 700 rpm, solution volume: 15.0 mL. Desorption conditions were; desorption time: 20 min, 150 μL 50.0 mM KH_2PO_4 .

3.1.4.3.4. Effect of Solution Temperature on Extraction of Arsenic Species

The influence of the solution temperature on extraction of arsenicals was scrutinized for prepared amine-modified fibers. The inspected temperatures were 20 °C, 35 °C and 55 °C. In a typical experiment, prepared solution was equilibrated in a thermostated water bath until selected temperature was accomplished. The extractions of arsenic species were performed in the same thermostated water which was placed onto the multiple multi-position magnetic stirrer. Extraction conditions for the mentioned experiment were; solution pH: 5.0, arsenic concentration: $10.0 \mu\text{gL}^{-1}$ from each species (AsB, As(III), DMA, MMA and As(V)), extraction time: 30 min, stirring speed: 700 rpm, solution volume: 15.0 mL. Desorption conditions were; desorption time: 20 min, 150 μL 50.0 mM KH_2PO_4 .

3.1.4.3.5. Repetitive Use of the Fibers and Fiber Reproducibility

The one of the most important task in the SPME fiber production is preparation of stable fiber coatings. The repetitive use of the same fiber is key study for confirmation the stability of the active phase. Extraction conditions were; extraction time: 30 min, As concentration: $10.0 \mu\text{gL}^{-1}$, solution pH: 5.0, stirring speed: 700 rpm, solution volume: 15 mL. Desorption conditions were; desorption time: 20 min, 150 μL 50.0 mM KH_2PO_4 . In order to prevent the carry over of the remaining analytes on the

fibers to the next running, a cleaning step was applied before reuse of the fiber. The cleaning conditions were; 10 min desorption into 15 mL 0.50 M KH_2PO_4 , 5 min cleaning in 15 mL ultra-pure water, 2 min activation in 15 mL 0.10 M HNO_3 and 5 min conditioning at 110 °C. The single fiber was reused for ten successful microextractions.

3.1.5. Arsenic Speciation with Nanoparticle Immobilized (Capillary Template) SPME Fibers

3.1.5.1. Extraction of the Arsenic Species

Microextraction was carried out with nanoiron-agarose and agarose-only fibers (as blank) in a 20-mL vial containing 15.0 mL of aqueous arsenic mixture solution which was stirred with a magnetic bar. Desorption of the analytes was carried out in a container which was prepared from 200- μL pipette tip blocked at the base by application of heat. The initial conditions for extractions were; solution pH: 7.0, arsenic concentration: 10.0 μgL^{-1} , stirring speed: 300 rpm, extraction time: 30 min, extraction temperature: RT. For desorption, the initial conditions were; desorption time: 10 min, desorption volume: 150.0 μL , desorption temperature: RT, eluent: 50.0 mM KH_2PO_4 solution. The HPLC mobile phases and desorption solutions were filtered through 0.20 μm cellulose acetate filter paper (Sartorius) before use. Afterwards, the extractions parameters such as extraction pH, extraction time, agitation (stirring) speed, ionic strength and desorption conditions were optimized. In addition, fiber to fiber reproducibility and repetitive use of the same fiber were also investigated.

3.1.5.2. Optimization of Extraction Parameters

3.1.5.2.1. Effect of pH on Extraction of Arsenic Species

Solution pH is one of the most important parameters on the extraction of arsenic species by the prepared fibers. For this reason, the initial experiments in the optimization of the extraction parameters focused on the investigation of extraction pH with each fiber. Extraction studies were carried out at 25 °C after the initial pH of

solutions was adjusted to 4.0, 7.0 and 10.0 with dilute HNO₃ or NH₃. The conditions for the extractions were; arsenic concentration: 10.0 µgL⁻¹ from each species (AsB, As(III), DMA, MMA and As(V)), stirring speed: 300 rpm, extraction time: 60 min, solution volume: 15.0 mL. Afterwards, desorption of the extracted analytes were performed from the fiber as explained previously. Desorption conditions were; desorption time: 10 min, 150 µL 50.0 mM KH₂PO₄. Desorption solution was analyzed for its arsenic content and species by HPLC-ICPMS.

3.1.5.2.2. Effect of Agitation Time/Speed on Extraction of Arsenic Species

Effect of agitation time on the extraction of arsenic species by nanoiron-agarose fiber was investigated for time intervals of 1, 5, 15, 30 and 60 min. In addition, static extraction of the arsenic species for a 5 min interval was performed to inquire the effect of the extraction mode. The conditions for the extractions were; solution pH: 4.0, arsenic concentration: 10.0 µgL⁻¹ from each species (AsB, As(III), DMA, MMA and As(V)), stirring speed: 700 rpm, solution volume: 15.0 mL. Separately, the effect of the agitation speed on extraction of the arsenic species was studied at 300, 500, 700 and 1000 rpm stirring speeds. Extraction conditions were; solution pH: 4.0, arsenic concentration: 10.0 µgL⁻¹ from each species (AsB, As(III), DMA, MMA and As(V)), extraction time: 60 min, solution volume: 15.0 mL, Desorption conditions for both experiments were; desorption time: 10 min, 150 µL 50.0 mM KH₂PO₄.

3.1.5.2.3. Effect of Salt Concentration (Ionic Strength) on Extraction of Arsenic Species

The effect of the ionic strength on the extraction of arsenic species was investigated by addition of various amount of NaCl into arsenic containing solution. The investigated concentrations were 1.0 M, 0.10 M, 0.010 M and 0.0010 M NaCl. Extraction conditions for the aforementioned experiment were; solution pH: 4.0, arsenic concentration: 10.0 µgL⁻¹ from each species (AsB, As(III), DMA, MMA and As(V)), extraction time: 60 min, stirring speed: 700 rpm, solution volume: 15.0 mL. Desorption conditions were; desorption time: 10 min, 150 µL 50.0 mM KH₂PO₄.

3.1.5.3. Interference Studies

The interference studies were performed for Sb(III), Sb(V), Se(IV), Se(VI), V(IV), V(V), SO_4^{2-} and PO_4^{3-} ions. The extraction and elution of the Sb(III), Sb(V), Se(IV), Se(VI), V(IV) and V(V) were examined during the interference studies in conjunction with extraction of arsenicals. Firstly, $100.0 \mu\text{gL}^{-1}$ and $1000.0 \mu\text{gL}^{-1}$ of Sb(III), Sb(V), Se(IV), Se(VI), V(IV), V(V) and SO_4^{2-} , PO_4^{3-} , respectively, were added separately into $10.0 \mu\text{gL}^{-1}$ As(III), DMA, MMA and As(V) containing solution. The extraction experiments were performed under optimized conditions described in related part of the thesis. The extraction conditions were extraction time: 60 min, As concentration: $10.0 \mu\text{gL}^{-1}$, solution pH: 4.0, stirring speed: 700 rpm, solution volume: 15 mL. Desorption conditions were desorption time: 10 min, $150 \mu\text{L}$ 50.0 mM KH_2PO_4 .

3.1.5.4. Analytical Performance of the Method

The performance of the proposed analytical method was characterized in terms of the limit of detection (LOD_{3s}) and the limit of quantification (LOQ_{10s}). Also, the regression coefficients in the calibration plot were used to prove the correlation between the extracted amount of analytes and concentrations in a typical SPME experiment. Calibration plots were constructed to relate the variation of arsenic concentration as a function of the peak area. For this purpose various amounts of arsenicals spiked in ultra pure water ($0.10 \mu\text{gL}^{-1}$ to $10.0 \mu\text{gL}^{-1}$) and extraction/desorption to HPLC-ICPMS were performed under optimized experimental conditions. Similar calibration plots were also obtained in 0.010 M NaCl solution in order to compare the analytical performances of the extractions performed in ultra pure water and salted water. Extraction conditions were; solution pH: 4.0, extraction time: 60 min, stirring speed: 700 rpm, solution volume: 15.0 mL . Desorption conditions; desorption time: 10 min, $150 \mu\text{L}$ 50.0 mM KH_2PO_4 . Furthermore, the analytical performance of the developed method was tested via determining relative standard deviations of the peak areas for intra-day and inter-day extractions of the analytes with 10 and 4 fibers, respectively. The applied experimental parameters were identical to extraction/desorption conditions described above while the arsenic concentration of each investigated species was $10.0 \mu\text{gL}^{-1}$.

3.1.5.5. Method Validation

Validity of the developed method was tested by means of standard reference materials (Arsenic Species in Frozen Human Urine, NIST SRM 2669 and Trace Elements in Natural Waters, NIST SRM 1643e). In the validation experiments the extractions were performed in 1/10 diluted SRM samples. The applicability of the method to real samples was also shown by spike addition into bottled water, tap water, geothermal water, and urine sample (from a volunteer). The extractions were performed in 1/2 diluted samples in case of bottled and tap water, while 1/10 diluted urine samples were used for extraction of arsenicals. In order to eliminate possible matrix effect of the geothermal water, these samples were diluted further to 1/500. In all validation experiments extraction conditions were; extraction time: 60 min, solution pH: 4.0, stirring speed 700 rpm, solution volume: 15.0 mL. Desorption conditions; desorption time: 10 min, 150 μ L 50.0 mM KH_2PO_4 . Both standard addition method and aqueous calibration plots were applied to determine the species and concentration of arsenicals in the samples.

3.2. Results and Discussions

3.2.1. Characterization of Prepared SPME Fibers

As mentioned in Section 3.1.3, the new SPME fiber coatings were prepared in two main strategies, namely, sol-gel based SPME coatings and nanoparticles immobilized SPME coatings. In the sol-gel based coatings bare silica fiber was inserted directly into sol-gel solution when the reaction period was completed, the coated fiber was removed and dried. Another sol-gel based coating was also obtained in the same manner by controlled insertion/removal from sol-gel active solution with dip coater. The second method demonstrates an easy way for immobilization of previously synthesized nanoparticles via capillary templating approach which was described for the first time. Another method applied for nanoparticle immobilized SPME fiber coating is electrospinning method. In the mentioned method, electrospun nanofibers were

produced on the surface of a SPME fiber. The characterization results for the prepared SPME fibers were summarized below.

3.2.1.1. Sol-Gel Based SPME Fiber Coatings

Sol-gel based coatings of the silica fibers were achieved by the direct insertion of the silica fiber into sol-gel active solution. The coatings were obtained in two ways, manually inserting the fiber into solution or using dip coater. The effect of sol-gel constituents on fiber coating was tested at absence of the sol-gel active organic part (PDMS) of sol-gel solution. Various manual coated fibers are illustrated in Figure 3.5. Fiber coated by dipping into sol-gel solution containing only inorganic sol-gel active reagents (no PDMS) resulted in thinner coating which can be easily removed from the surface of the fiber. The addition of the PDMS produced thicker coating with more active sites on organic/inorganic polymer network. In addition, the manual coating process resulted in variations of the coating thickness throughout the fiber. Homogeneous coating is important to fiber to fiber reproducibility. For this reason, fiber coating process was performed in dip coater in ongoing study.

Optimization of the dip coating process was done for amine-functionalized fibers. The effect of the parameters such as repetitive coating, removal speed and viscosity of the PDMS on fiber coating thickness and morphology were investigated. The effect of removal speed of the fibers from sol-gel solution was studied at 10 mm/min and 1 mm/min moving speed of dip coater. In addition the effect of coating repetition was tested for single and double coating processes. The results of coating repetition at 10 mm/min are shown in Figure 3.6 and 3.7 for single and double layers, respectively. According to SEM images, the dip coating process is promising for the fabrication of homogeneous coatings. Additionally, the diameters after coating processes were determined as 126 μm and 140 μm for single and double coatings, respectively.

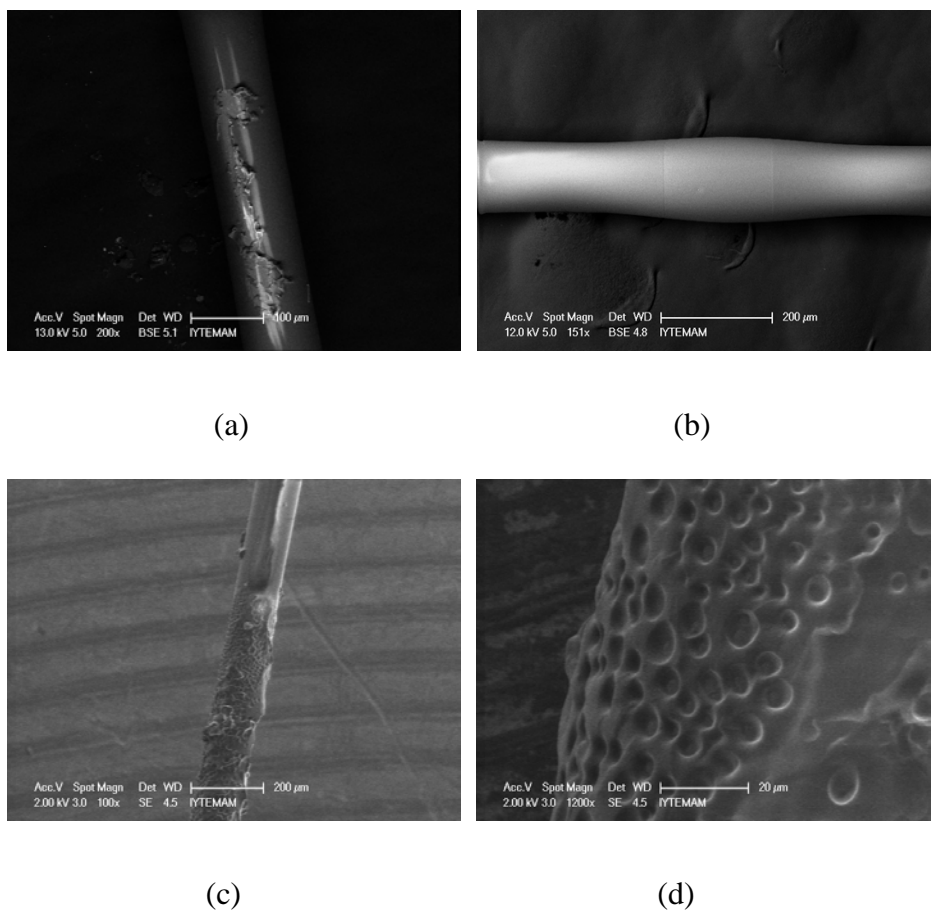


Figure 3.5. SEM images of various manually coated sol-gel based SPME fibers. a) amine-functionalized (no PDMS), b) amine-functionalized (with PDMS), c) and d) chloro-functionalized fibers.

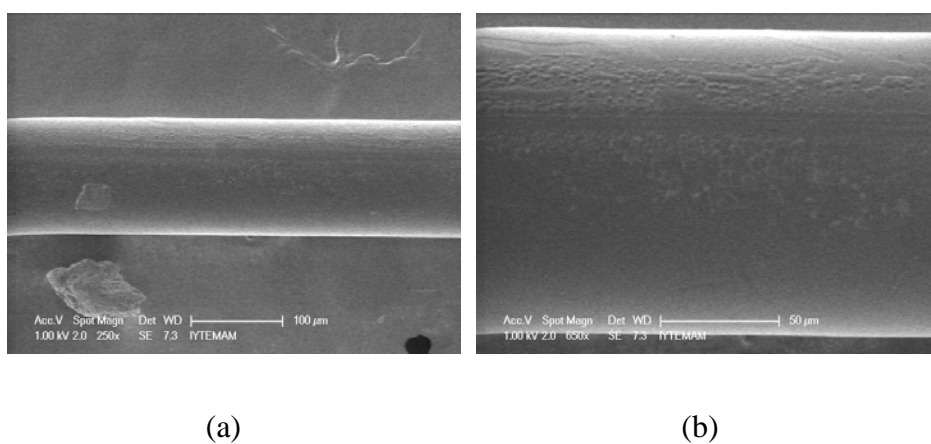
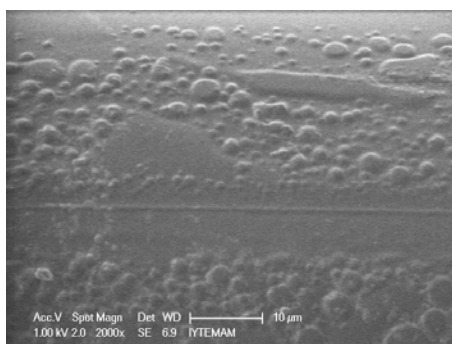


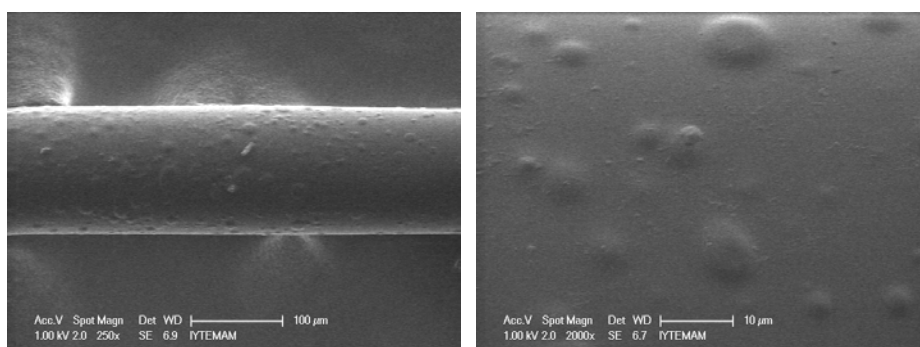
Figure 3.6. SEM images of amine-functionalized fibers (with dip coater) at various magnifications (10 mm/min removal speed, single layer coating) a) 250x, b) 650x and c) 2000x.

(cont. on next page)



(c)

Figure 3.6. (cont.)



(a)

(b)

Figure 3.7. SEM images of amine-functionalized fibers (with dip coater) at various magnifications (10 mm/min removal speed, double layer coating) a) 250x and b) 2000x.

SEM images obtained for fibers coated at 1 mm/min removal speed are given in Figure 3.8 and 3.9. Coating thicknesses were determined as 127 μm and 134 μm for single and double layer coatings, respectively. The comparison of the coating thickness obtained at 1 and 10 mm/min removal speed was not indicative of important effect from these parameters, while the homogeneity of the coating was clearly affected from the removal speed of the fiber from the sol-gel solution. The effect of the PDMS viscosity on the coating thickness and roughness was tested using low viscosity (25 000 cSt) and high viscosity (18 000 000- 22 000 000 cSt) PDMS. The results obtained for high viscosity PDMS are given in Figure 3.10. According to SEM images, the coating

thickness was not affected from viscosity of the PDMS. The most important outcome was the increased viscosity resulted in surface roughness on the SPME fibers.

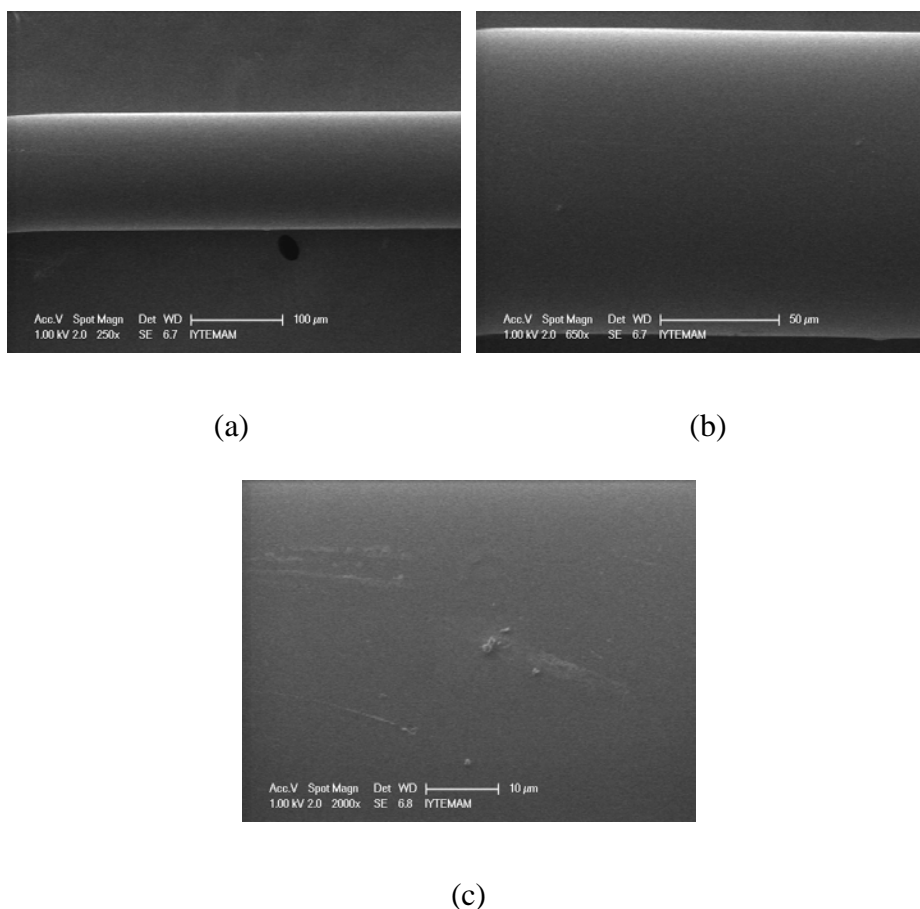
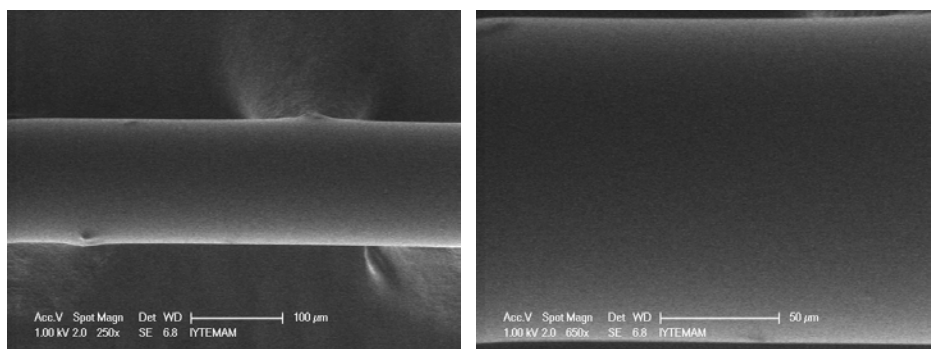


Figure 3.8. SEM images of amine-functionalized fibers (with dip coater) at various magnifications (1 mm/min removal speed, single layer coating) (a) 250x, (b) 650x and (c) 2000x.

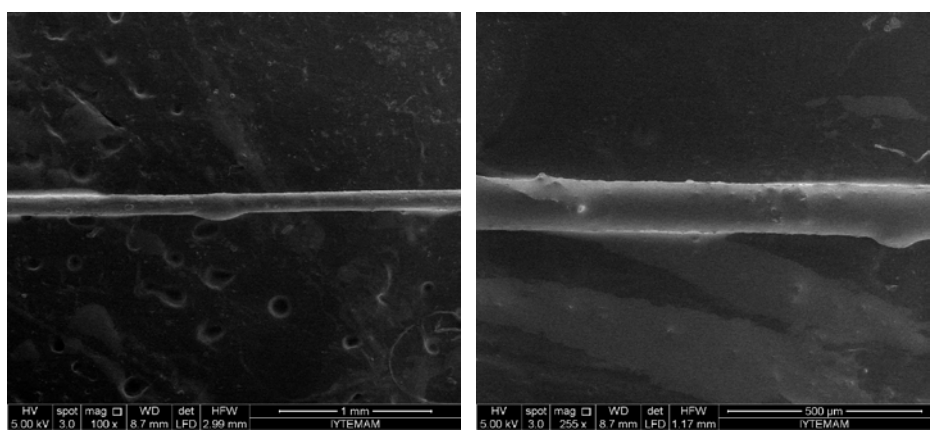
The effect of the PDMS viscosity on the coating thickness and roughness was tested using low viscosity (25 000 cSt) and high viscosity (18 000 000- 22 000 000 cSt) PDMS. The results obtained for high viscosity PDMS are given in Figure 3.10. According to SEM images, the coating thickness was not affected from viscosity of the PDMS. The most important outcome was the increased viscosity resulted in surface roughness on the SPME fibers.



(a)

(b)

Figure 3.9. SEM images of amine-functionalized fibers (with dip coater) at various magnifications (1 mm/min removal speed, double layer coating) a) 250x and b) 650x.



(a)

(b)

Figure 3.10. SEM images of amine-functionalized fibers (with dip coater) at various magnifications (1 mm/min removal speed, single layer coating, high viscosity PDMS) a) 100x, b) 255x.

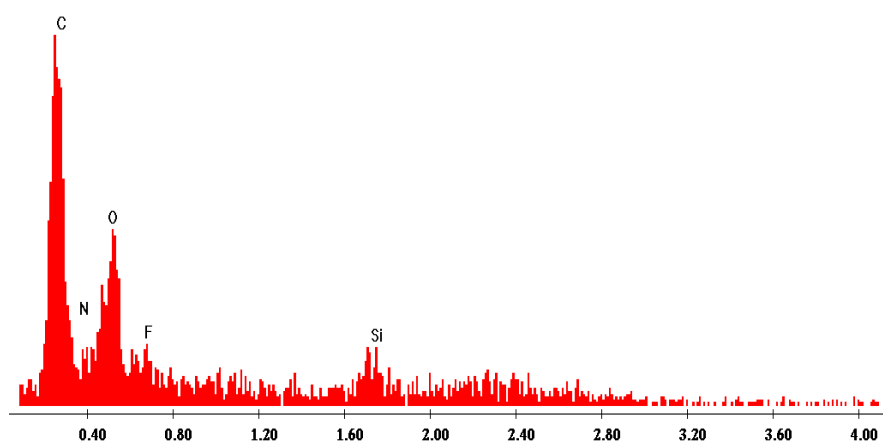
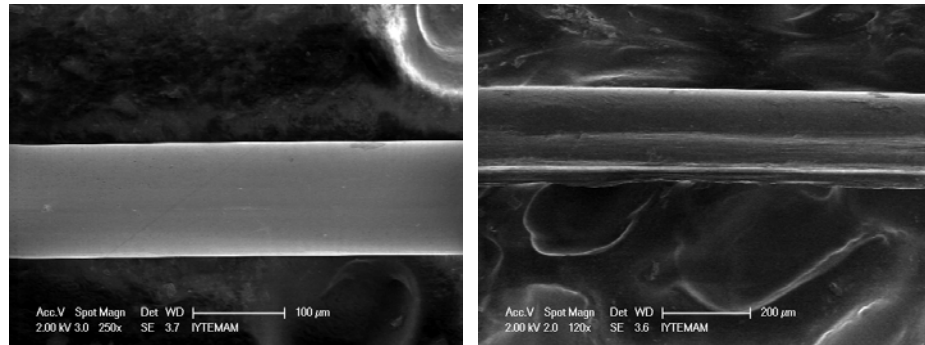


Figure 3.11. EDX spectrum of amine-functionalized fibers

3.2.1.2. Nanoparticles Immobilized SPME Fibers Prepared by Capillary Template Method

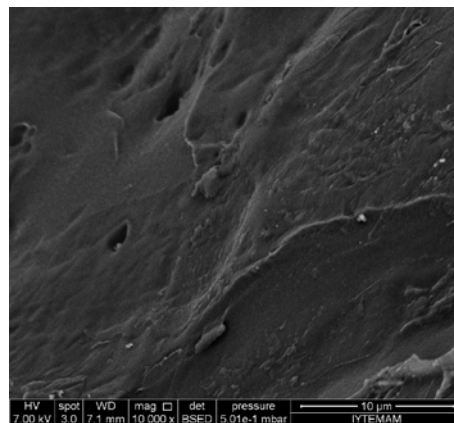
SEM images of the plain, the agarose-only, and the nanoiron-agarose fibers at different magnifications are given in Figure 3.12 and 3.13, respectively. The characteristic chain-like structure (Figure 3.14) reported for nanosized zerovalent iron particles in the previous study (Efecan et al. 2009) was not observed after immobilization of the nZVI into agarose matrix. This might have resulted from the oxidation of nZVI upon the immobilization process, as mentioned below based on XRD characterization. The SEM image shown in Figure 3.13(c) suggests that the iron nanoparticles were embedded completely inside the matrix. The diameters of the plain fiber and nanoiron-agarose fiber were measured as 125 μm and 220 μm , respectively. The presence of iron particles (K lines of Fe) was also validated by EDX analysis during SEM survey (Figure 3.15). The results reveal the weight percentage of C (29.7%), O (21.4%) and Na (1.0%) from agarose and Fe (47.3%) from immobilized iron nanoparticles. The XRD results of the agarose powder, synthesized nZVI, ground bare silica fiber and ground nanoiron-agarose coated SPME fibers were illustrated in Figure 3.16. XRD pattern of agarose powder indicates reflections at 2-theta 28, 35, 48, and 59. Iron nanoparticles showed a strong reflection at 2-theta 45 which is indicative that iron nanoparticles exist primarily as Fe^0 . After immobilization of the iron nanoparticles, the reflection of the zero valent state of the iron disappeared and reflections from iron oxide

particles (2-theta 36) were observed together with those of agarose, as well. As illustrated in SEM images of the prepared fibers, the iron nanoparticles were completely coated with agarose matrix which may result in their weak reflection responses.



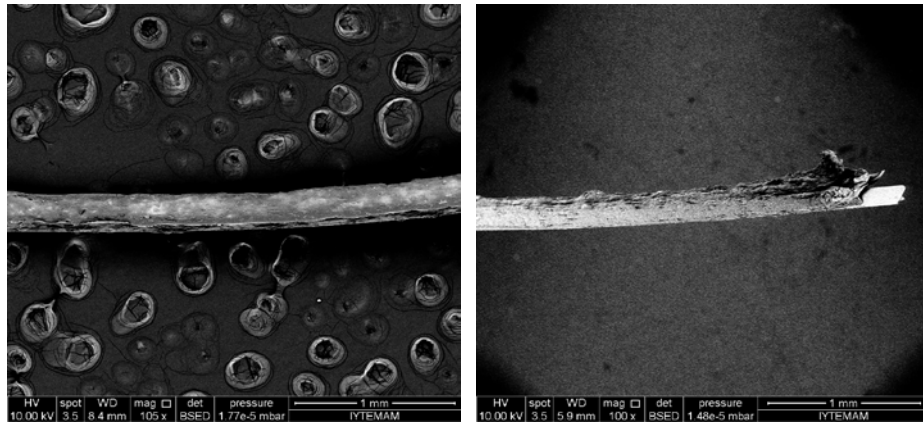
(a)

(b)



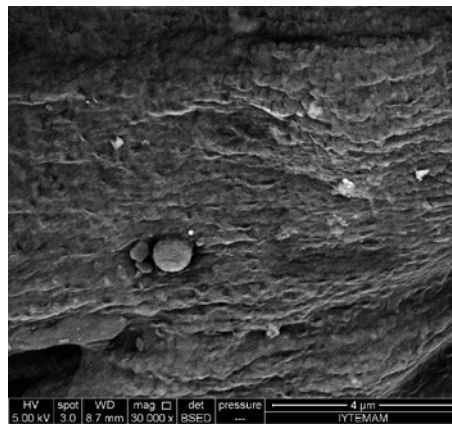
(c)

Figure 3.12. SEM images of a) bare silica fiber b) and c) agarose coated silica fiber at various magnifications.



(a)

(b)



(c)

Figure 3.13. SEM images of nZVI-agarose fibers at various magnifications a) 105x, b) 100x, c) 30000x.

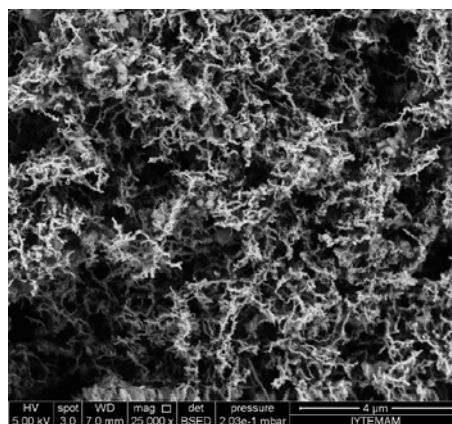
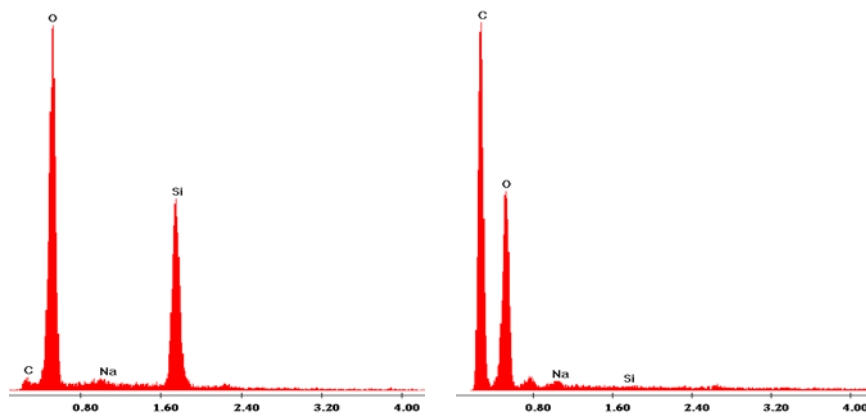
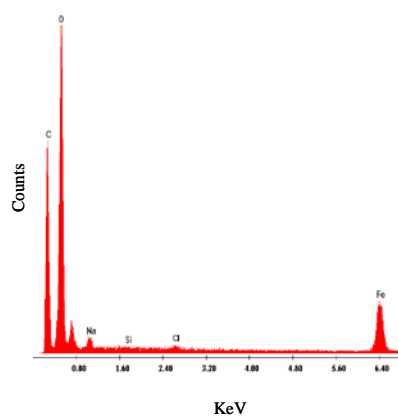


Figure 3.14. SEM images of the synthesized zerovalent iron nanoparticles



(a)

(b)



(c)

Figure 3.15. EDX spectra of a) bare silica fiber and b) agarose coated silica fiber and c) nanoiron-agarose coated silica fiber.

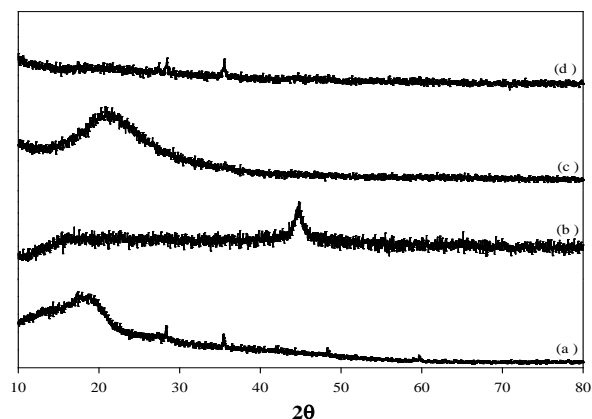
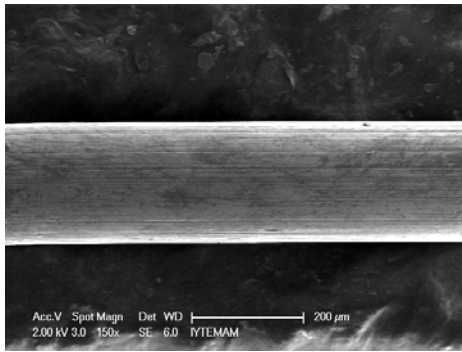


Figure 3.16. XRD pattern of the a) agarose powder, b) nZVI, c) ground silica fiber and d) ground nanoiron-agarose fiber.

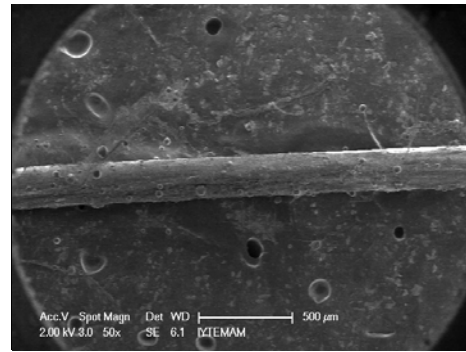
3.2.1.3. Electrospun Nanofiber Immobilized SPME Fibers

3.2.1.3.1. Electrospun ZnO Nanofibers

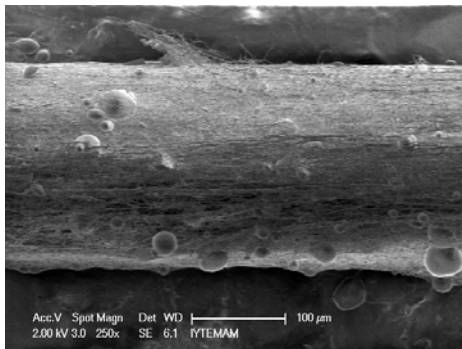
SEM images of plain fiber and PVA, zinc acetate-PVA, zinc acetate-cerium nitrate-PVA electrospun nanofiber coated fibers were shown in Figure 3.17 at various magnifications. The fiber material at this study was replaced by stainless steel to maintain conducting coating surface. Diameter of the steel fiber was determined as 200 μm . Steel fibers coated with PVA nanofibers demonstrated in Figure 3.17 was indicative of polymer network around the SPME fibers. Fiber coated with zinc acetate or cerium nitrate added PVA did not show important differences in morphology with respect to only PVA containing fibers. The application of calcination step on nanofiber coated fiber completely remove the PVA from the surface of fiber and ZnO or ZnO-CeO₂ nanofibers coated SPME fibers were produced (Figure 3.18). The continuum ZnO nanofibers with CeO₂ nanoparticles were clearly observed in the figure. In this method all functional groups are available on the surface of the SPME fiber for microextraction processes. For this reason, the shorter extraction time was expected to have a superior advantage. Additionally, on the light of the surface coating heterogeneity, it should be mentioned that such inhomogeneous coatings may result in elevated deviations during the extraction.



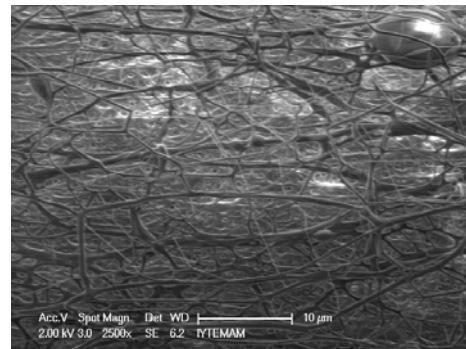
(a)



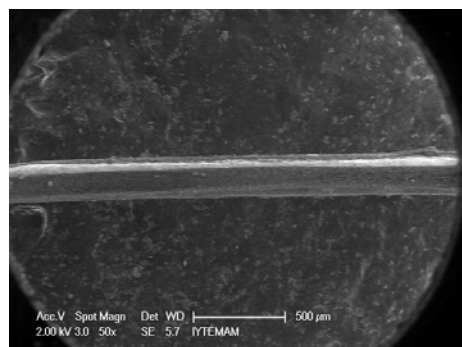
(b)



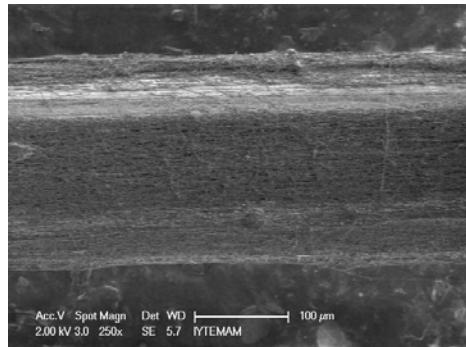
(c)



(d)



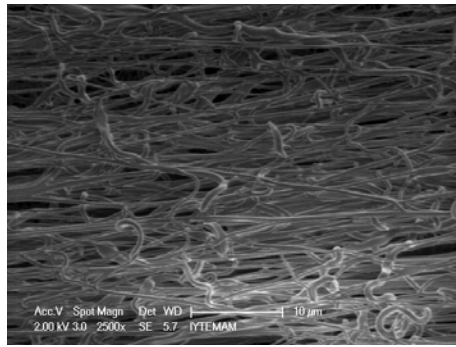
(e)



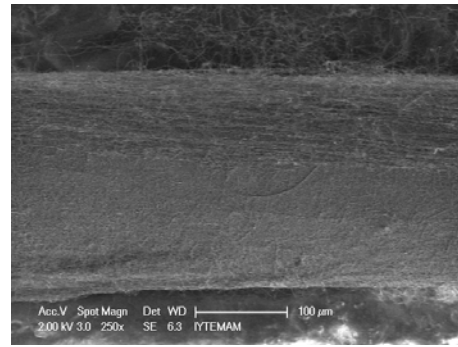
(f)

Figure 3.17. SEM images of electrospun coated fiber before calcination a) steel fiber, b), c) and d) PVA, e), f) and g) zinc acetate-PVA, h) and i) zinc acetate-cerium nitrate-PVA.

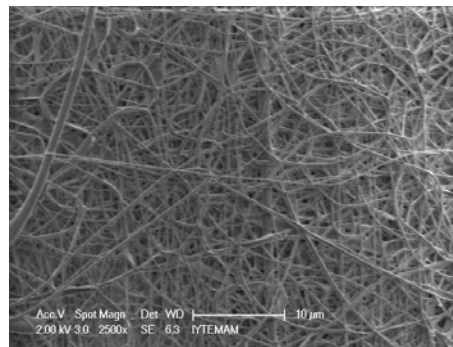
(cont. on next page)



(g)

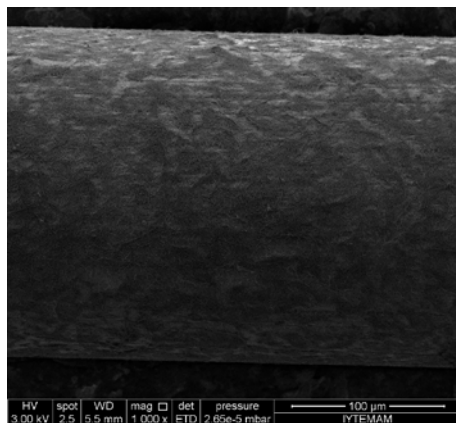


(h)

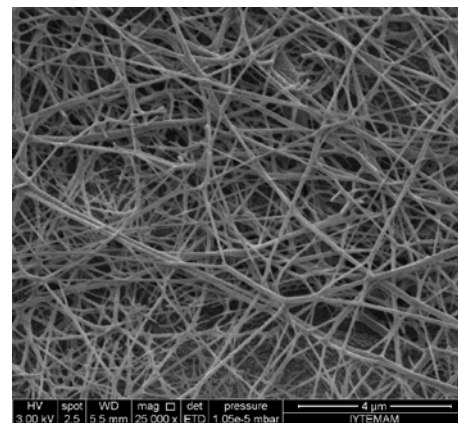


(i)

Figure 3.17. (cont.)



(a)



(b)

Figure 3.18. SEM images of a), b) and c) ZnO-CeO₂, d), e) and f) ZnO electrospun fibers after calcination.

(cont. on next page)

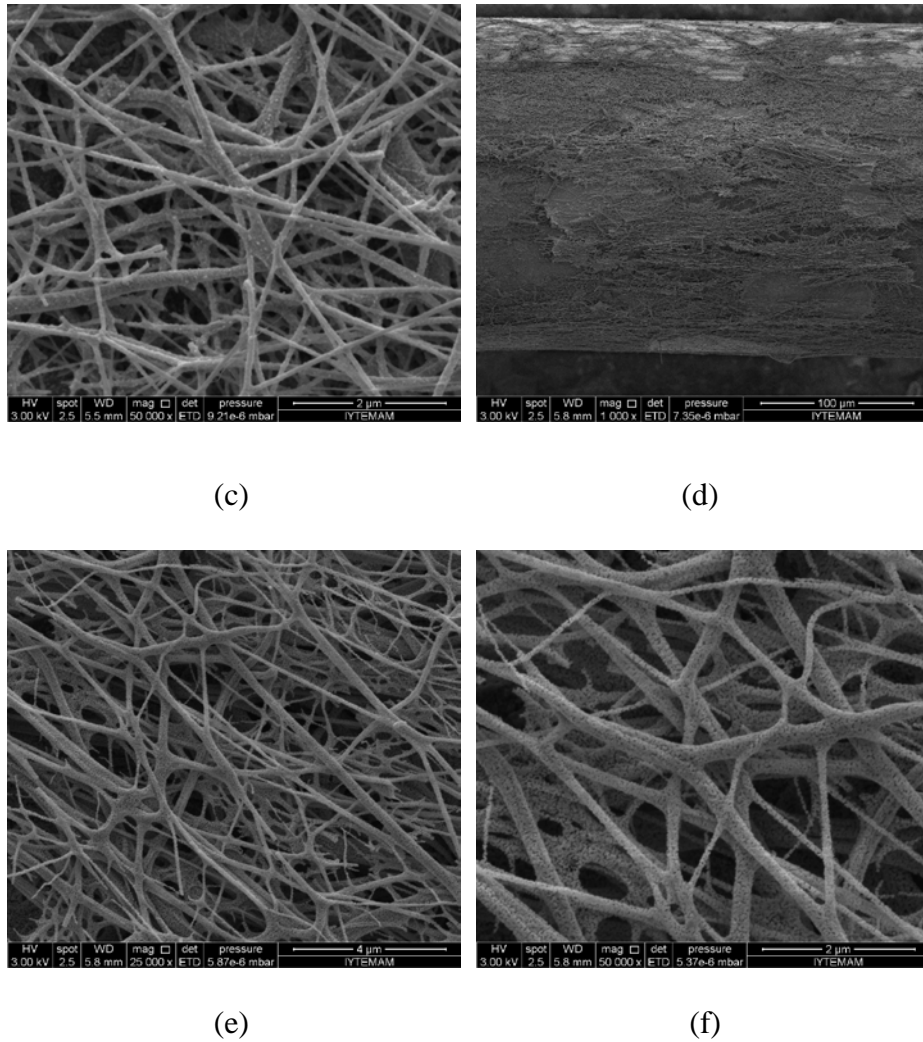


Figure 3.18. (cont.)

3.2.1.3.2. Electrospun Fe_2O_3 Nanofibers

The synthesis procedure for preparation of Fe_2O_3 nanofibers is outlined in the Section 3.1.3.4.2. For optimization of the electrospinning procedure, various parameters were tested. The effects of each parameter are summarized below.

3.2.1.3.2.1. Effect of Amount of $\text{FeCl}_3 \cdot 6\text{H}_2\text{O}$

Effect of the FeCl_3 amount was important in two general considerations. First of all, increasing the amount of a conductor in the polymer solution increases the spinnability of the solution. Secondly, increasing the amount of iron possibly will

increase the amount of iron on the resulting electrospun nanofibers. Therefore, after calcination step, Fe_2O_3 fibers will be thicker. According to the expectations listed above, the experiments were conducted with 0.50, 1.00, 1.50 and 2.50 g $\text{FeCl}_3 \cdot 6\text{H}_2\text{O}$. The electrospun nanofibers obtained in this experiment are shown in Figure 3.19- 3.22 for each tested iron amounts. First of all, as expected, increasing the amount of iron in the solution increased the spinnability of the solution. The most acceptable fibers were produced in solution containing 2.50 g $\text{FeCl}_3 \cdot 6\text{H}_2\text{O}$. Further increment of the iron amount was not tested due to solubility difficulties. The Fe_2O_3 nanofibers obtained after calcination are illustrated in the Figure 3.23. The most important outcome of the calcination was getting thinner fibers of Fe_2O_3 with respect to the PVP- FeCl_3 fibers and the structure was conserved during calcination.

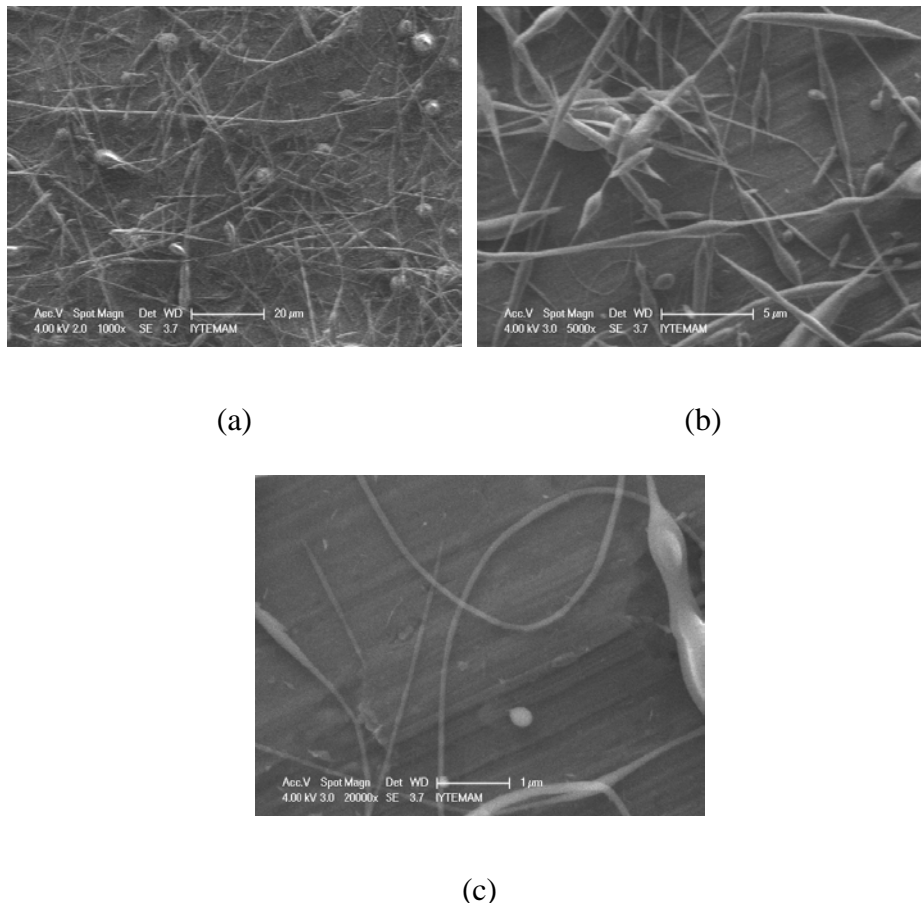
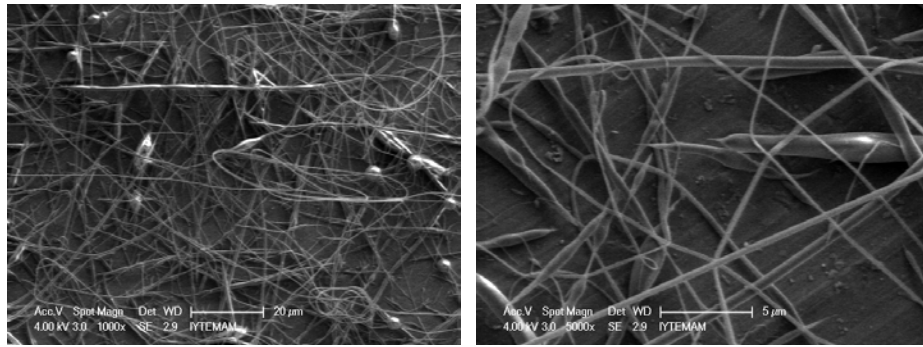


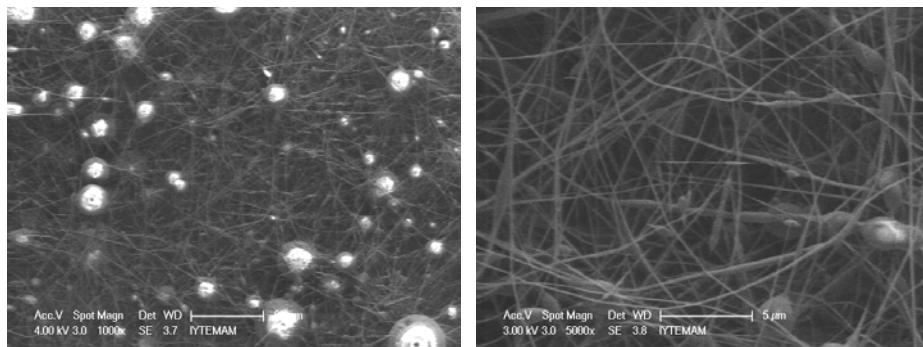
Figure 3.19. SEM images of PVP+ FeCl_3 electrospun fibers (11.50 g PVP/ 0.50 g $\text{FeCl}_3 \cdot 6\text{H}_2\text{O}$) at various magnifications (Spinning conditions: potential difference: 30 kV, feeding rate: 0.1 mL/h) a) 1000x, b) 5000x and c) 20000x.



(a)

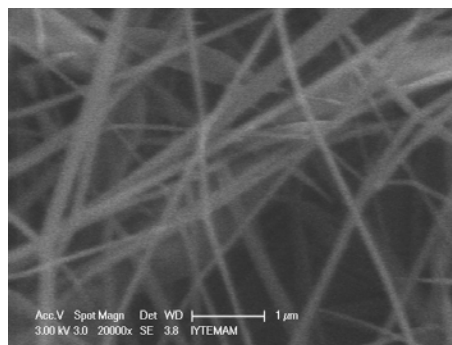
(b)

Figure 3.20. SEM images of PVP+FeCl₃ electrospun fibers (11.50 g PVP/ 1.00 g FeCl₃. 6H₂O) at various magnifications (Spinning conditions: potential difference: 30 kV, feeding rate: 0.1 mL/h) a) 1000x, b) 5000x.



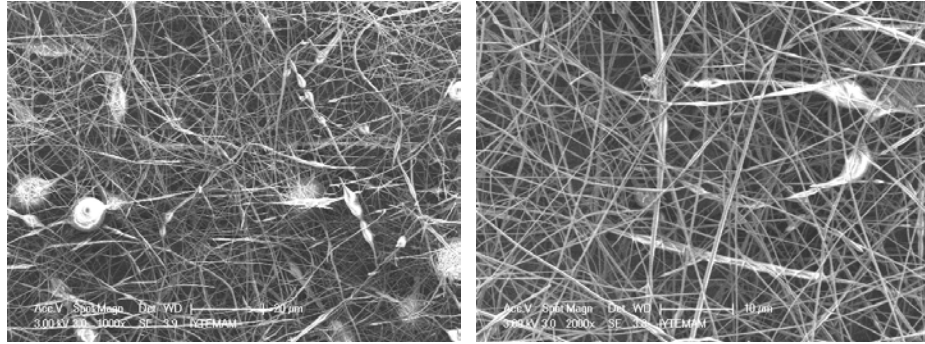
(a)

(b)



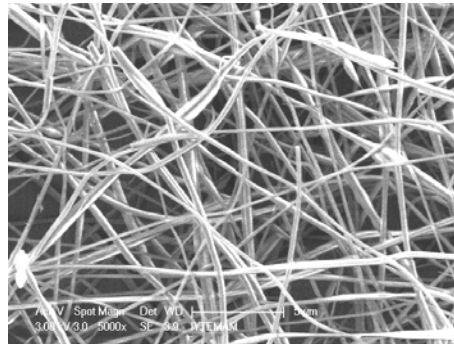
(c)

Figure 3.21. SEM images of PVP+FeCl₃ electrospun fibers (11.50 g PVP/ 1.50 g FeCl₃. 6H₂O) at various magnifications (Spinning conditions: potential difference: 30 kV, feeding rate: 0.1 mLh⁻¹) a) 1000x, b) 5000x and c) 20000x.



(a)

(b)



(c)

Figure 3.22. SEM images of PVP+FeCl₃ electrospun fibers (11.50 g PVP/ 2.50 g FeCl₃. 6H₂O) at various magnifications (Spinning conditions: potential difference: 30 kV, feeding rate: 0.1 mLh⁻¹) a) 1000x, b) 2000x and c) 5000x.

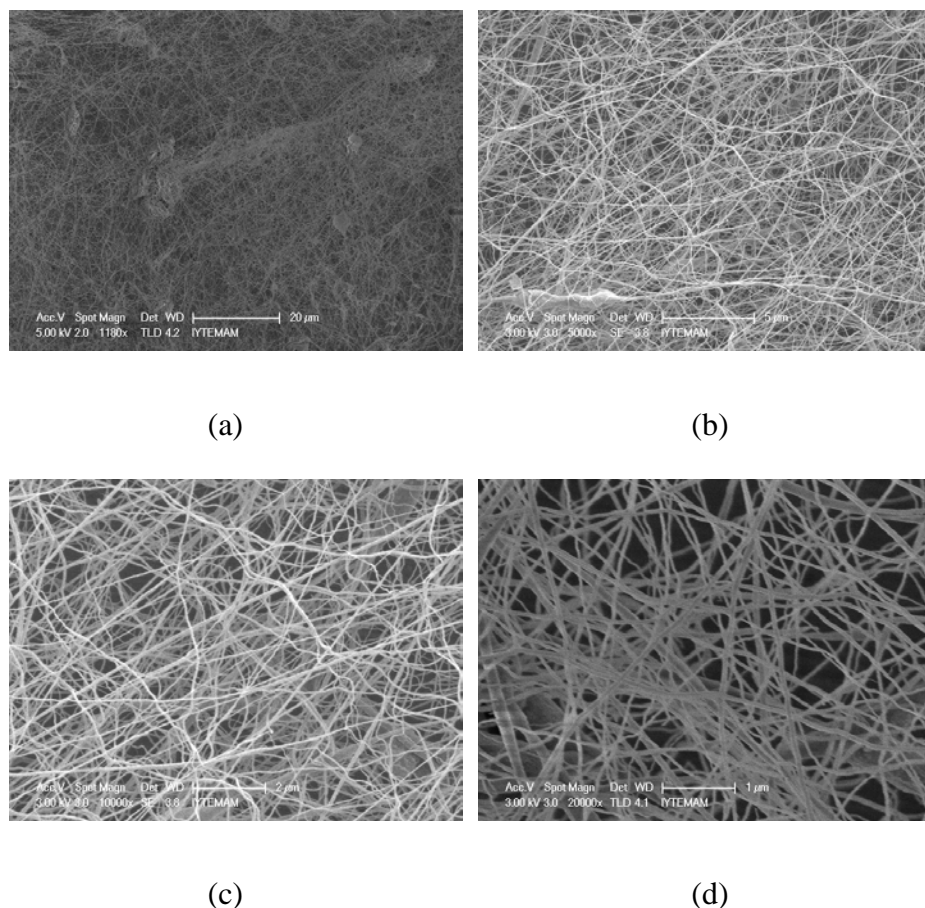
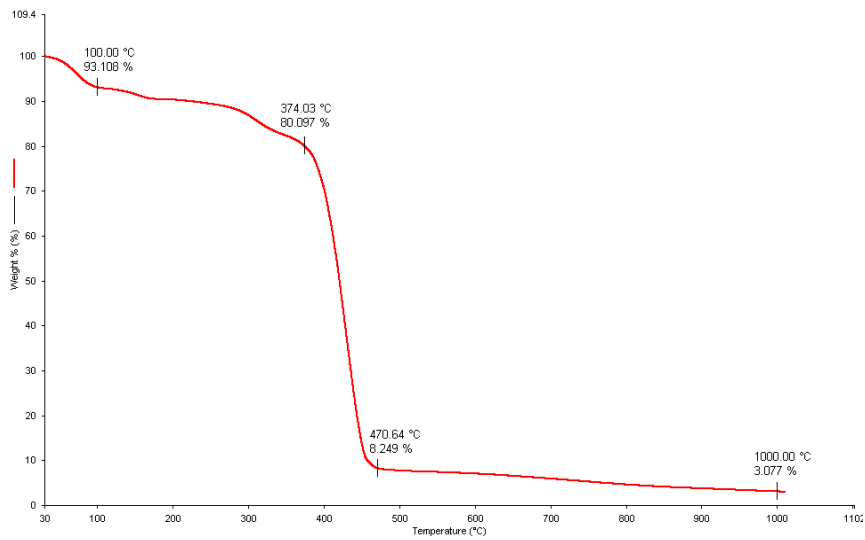
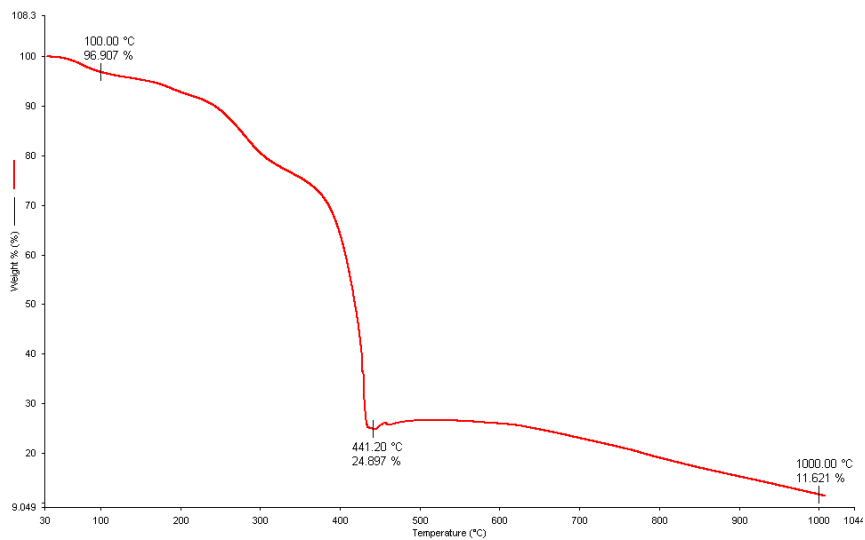


Figure 3.23. SEM images of PVP+FeCl₃ electrospun fibers after calcination (11.50 g PVP/ 2.50 g FeCl₃.6H₂O) at various magnifications (Spinning conditions: potential difference: 30 kV, feeding rate: 0.1 mLh⁻¹) a) 1180x, b) 5000x, c) 10000x and d) 20000x.

Thermal behaviors of the PVP nanofibers, PVP+FeCl₃ nanofibers (2.50 g FeCl₃.6H₂O containing) and calcinated fibers are demonstrated in the Figure 3.24. Two stage lost of the mass was observed in case of PVP fibers. The first lost is due to bonded water and the major lost between 374 and 470 °C can be explained as degradation of the polymer structure. In the thermogram of the PVP+FeCl₃ nanofibers, similar degradation of the polymeric part of the structure was observed in a combination with the small increase on weight percentage of the hybrid material after 440 °C. The reason for this behavior on the thermogram can be related to structural changes of inorganic part of the material. Therefore, it can be speculated that under elevated temperatures iron ions may convert to various iron oxide structures (Fe₂O₃ and Fe₂O₃FeO). Similarly, calcinated samples show the trend of increasing the weight percent as a result of structural changes.



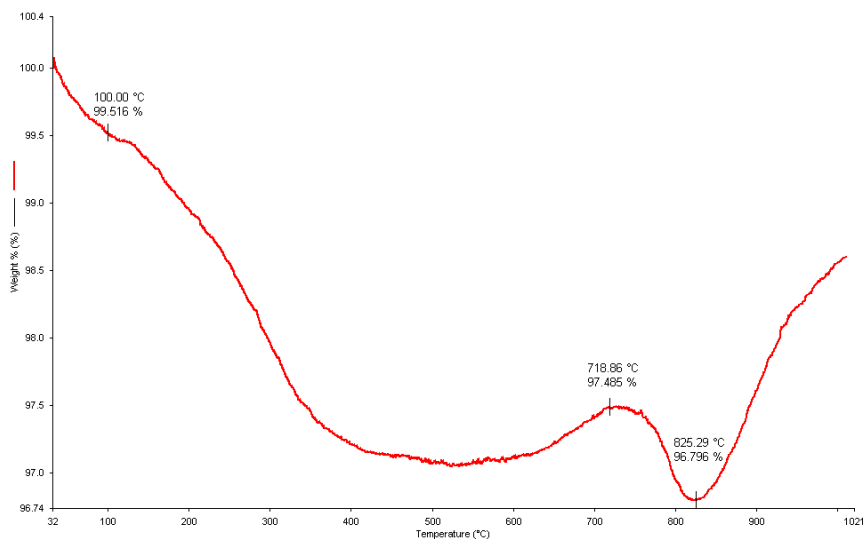
(a)



(b)

Figure 3.24. TGA curves of a) PVP, b) PVP+FeCl₃, and c) PVP+FeCl₃ after calcination

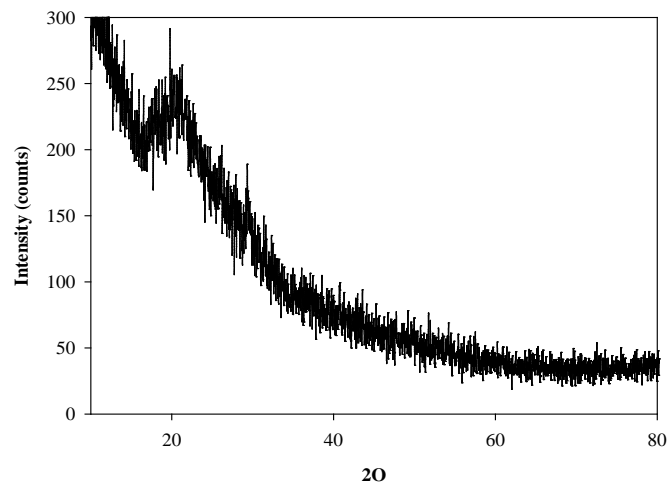
(cont. on next page)



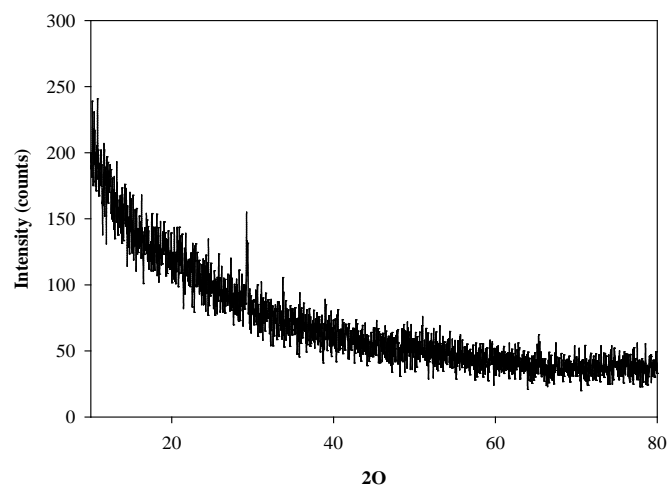
(c)

Figure 3.24. (cont.)

The XRD results of the PVP nanofibers, PVP+FeCl₃ nanofibers (2.50 g FeCl₃, 6H₂O containing) and calcinated fibers were illustrated in Figure 3.25. XRD pattern of PVP nanofibers and PVP+FeCl₃ nanofibers indicated reflections at 2-theta 29.4 which is most probably from crystalline structure of electrospun polymer. XRD pattern of calcinated fibers showed strong reflections at 2-theta 29.3, 33, 35.6, 40.7, 49.4 54, 62.3, 64 which are indicative that iron nanoparticles exist primarily as Fe₂O₃.



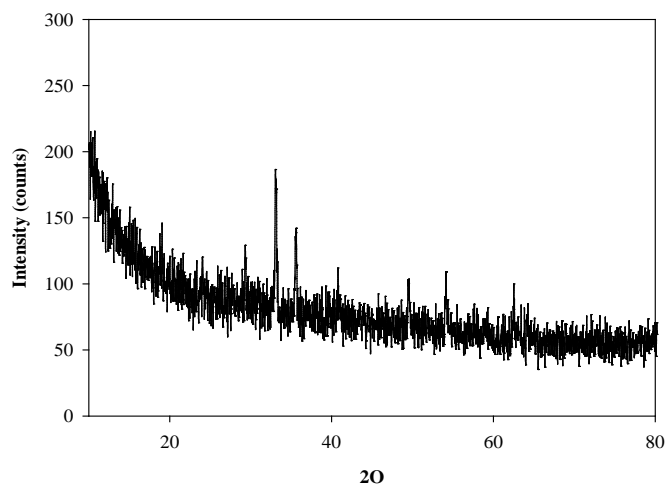
(a)



(b)

Figure 3.25. XRD pattern of the a) PVP, b) PVP+FeCl₃, and c) PVP+FeCl₃ after calcination

(cont. on next page)

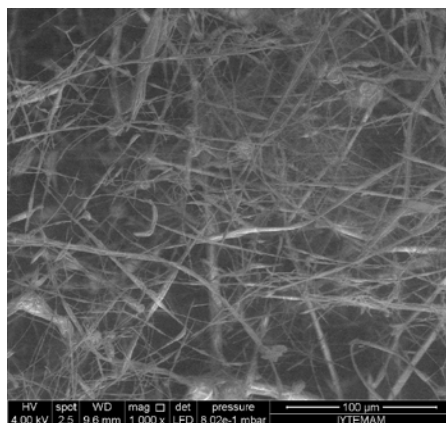


(c)

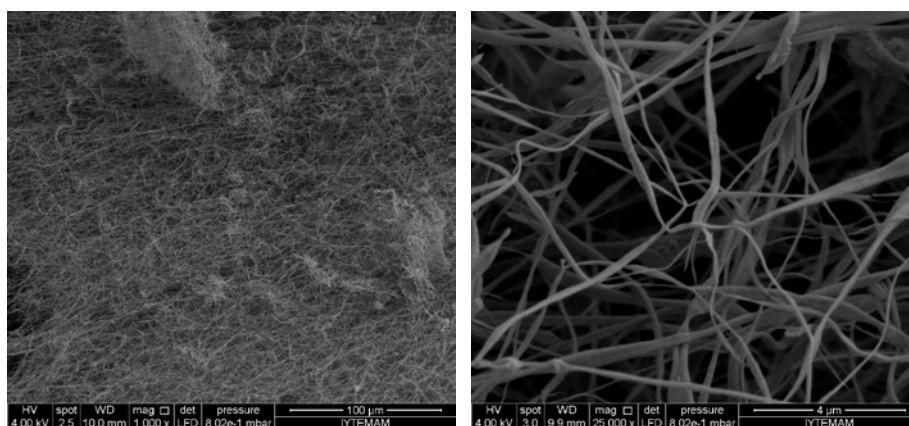
Figure 3.25. (cont.)

3.2.1.3.2.2. Effect of the Solvent

In effect of the solvent on electrospinning process experiment was carried with ethanol instead of water. Both the polarity and boiling point of the ethanol make it attractive solvent for spinning. Results obtained at various feeding rates for PVP+FeCl₃ nanofibers and calcinated fibers are illustrated in Figure 3.26-3.30. The SEM images showed that when ethanol was used as a solvent, the nanofibers were both inhomogeneous and thicker than nanofibers obtained from water based polymer solution.



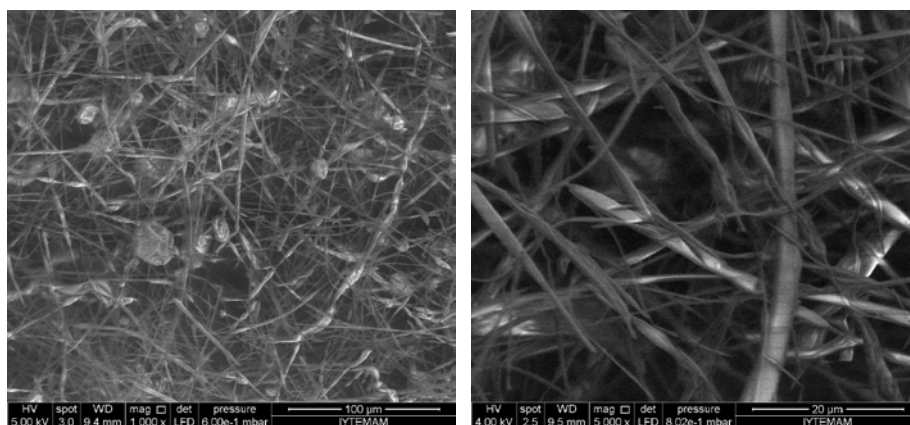
(a)



(b)

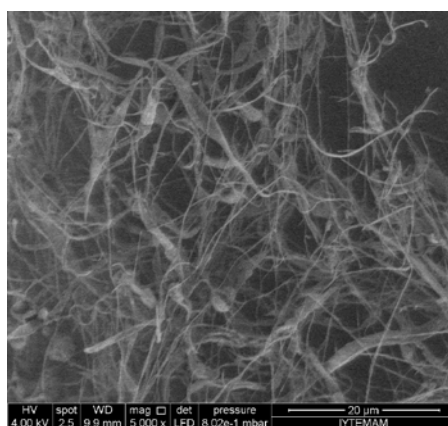
(c)

Figure 3.26. SEM images of PVP+FeCl₃ electrospun fibers a) before calcination, b) and c) after calcination (Spinning conditions: potential difference: 30 kV, feeding rate: 20.0 mLh⁻¹, amount of FeCl₃.6H₂O: 2.50 g, amount of PVP: 11.50 g).



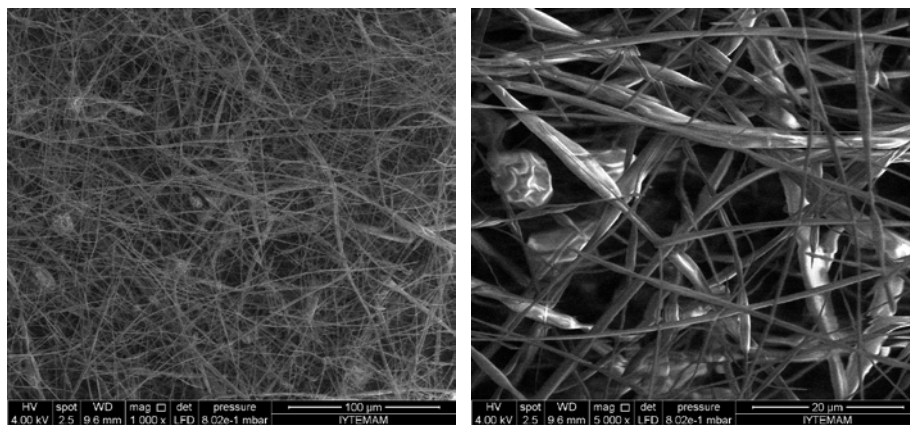
(a)

(b)



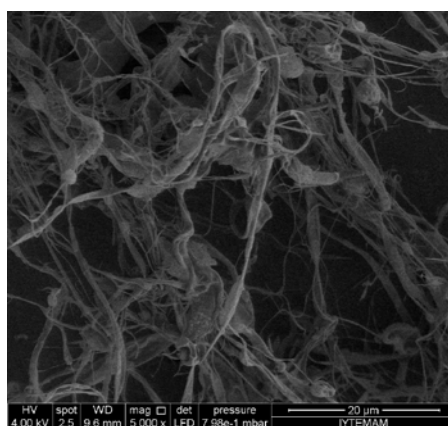
(c)

Figure 3.27. SEM images of PVP+FeCl₃ electrospun fibers a) and b) before calcination, c) after calcination (Spinning conditions: potential difference: 30 kV, feeding rate: 10.0 mLh⁻¹, amount of FeCl₃.6H₂O: 2.50 g, amount of PVP: 11.50 g).



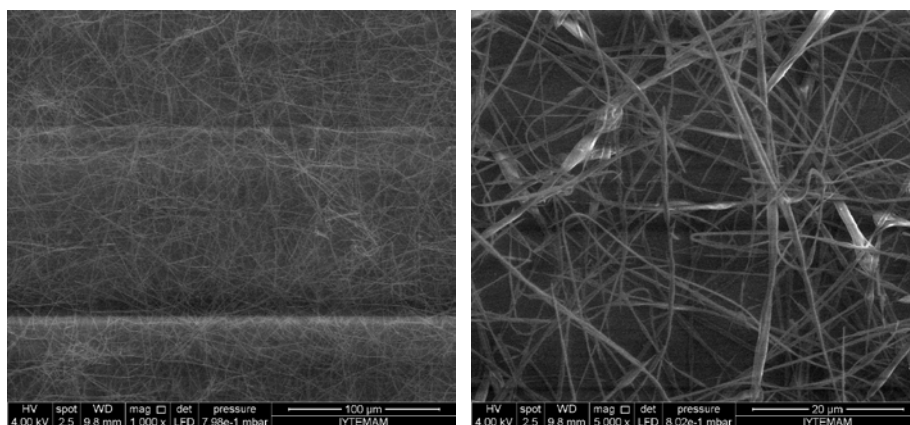
(a)

(b)



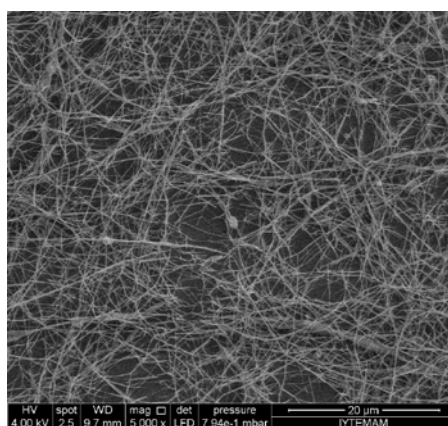
(c)

Figure 3.28. SEM images of PVP+FeCl₃ electrospun fibers a) and b) before calcination, c) after calcination (Spinning conditions: potential difference: 30 kV, feeding rate: 5.0 mLh⁻¹, amount of FeCl₃.6H₂O: 2.50 g, amount of PVP: 11.50 g).



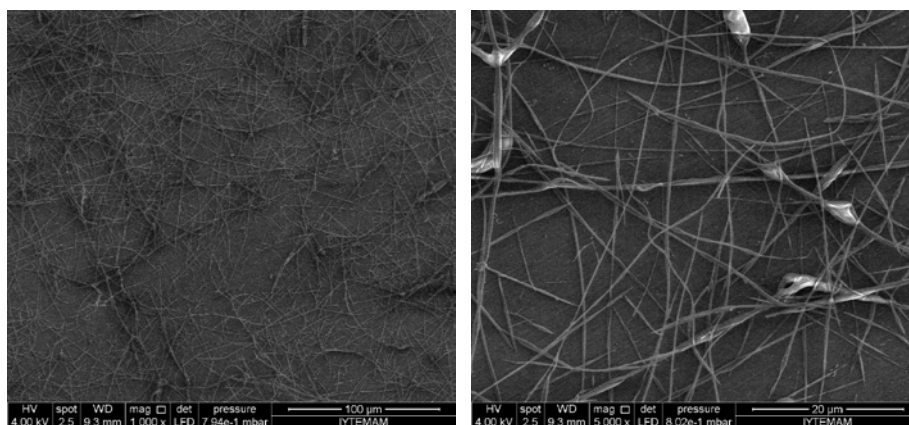
(a)

(b)



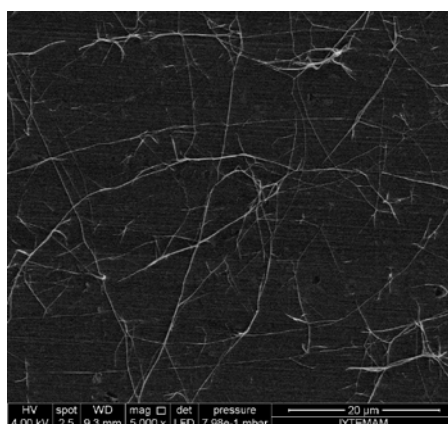
(c)

Figure 3.29. SEM images of PVP+FeCl₃ electrospun fibers a) and b) before calcination, c) after calcination (Spinning conditions: potential difference: 30 kV, feeding rate: 1.0 mLh⁻¹, amount of FeCl₃.6H₂O: 2.50 g, amount of PVP: 11.50 g).



(a)

(b)



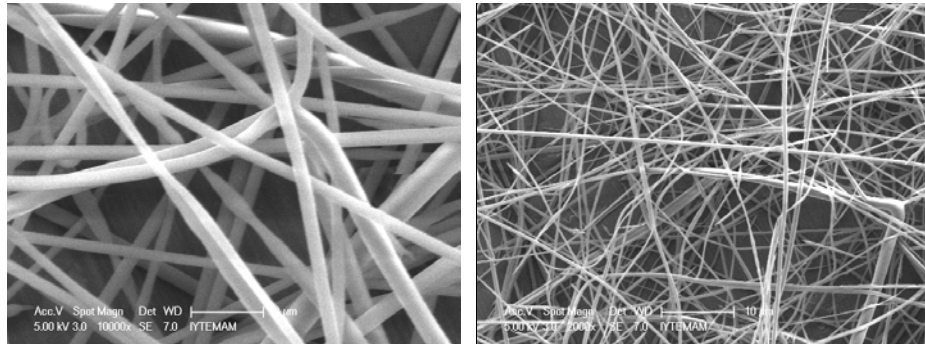
(c)

Figure 3.30. SEM images of PVP+FeCl₃ electrospun fibers a) and b) before calcination, c) after calcination (Spinning conditions: potential difference: 30 kV, feeding rate: 0.5 mLh⁻¹, amount of FeCl₃.6H₂O: 2.50 g, amount of PVP: 11.50 g).

3.2.1.3.2.3. Effect of the Feeding Rate

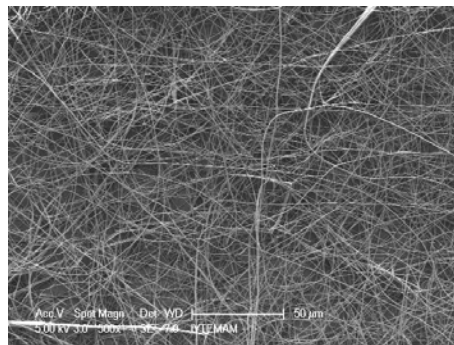
The effect of the feeding rate of the spinning solution was studied with polymer to iron compound ratio of 15.00 g/2.50 g prepared in water. Results obtained at various feeding rates for PVP+FeCl₃ nanofibers and calcinated fibers are illustrated in Figure 3.31-3.41. The most important outcome of the study is the effect of flow rate from the needle to the final diameter of the nanofibers. General trend was that decreasing the feeding rate increases the diameter of the fiber. The thinner fibers are expected to show

larger surface area which means more active sites on the surface. Another advantage of the higher feeding rates is the elevated nanofiber deposition in a shorter time.



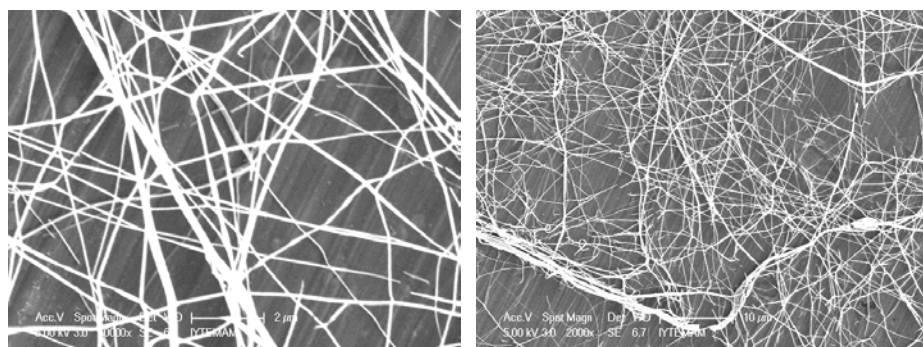
(a)

(b)



(c)

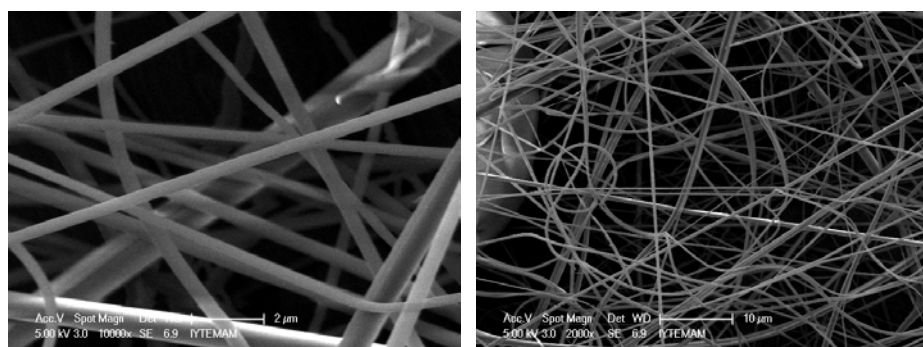
Figure 3.31. SEM images of PVP+FeCl₃ electrospun fibers at various magnifications (Spinning conditions: potential difference: 30 kV, feeding rate: 20.0 mLh⁻¹, amount of FeCl₃.6H₂O: 2.50 g, amount of PVP: 15.0 g) a) 10000x, b) 2000x and c) 500x.



(a)

(b)

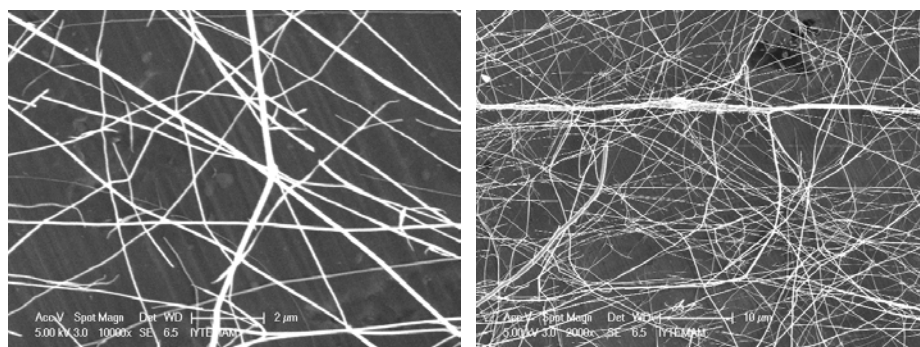
Figure 3.32. SEM images of PVP+FeCl₃ electrospun fibers after calcination at various magnifications (Spinning conditions: potential difference: 30 kV, feeding rate: 20.0 mLh⁻¹, amount of FeCl₃.6H₂O: 2.50 g, amount of PVP: 15.0 g). a) 10000x and b) 2000x.



(a)

(b)

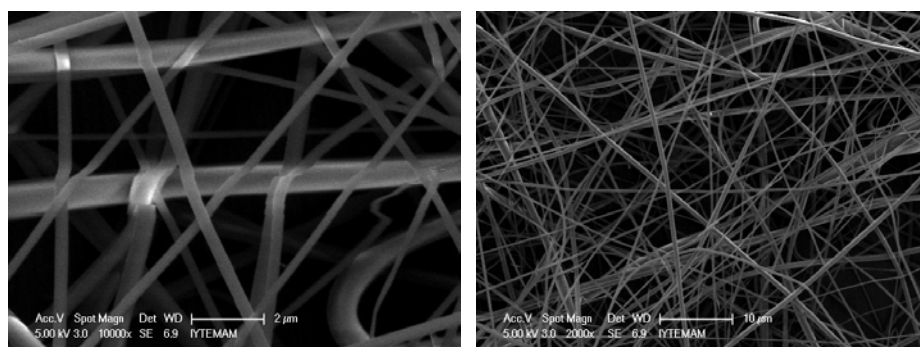
Figure 3.33. SEM images of PVP+FeCl₃ electrospun fibers at various magnifications (Spinning conditions: potential difference: 30 kV, feeding rate: 10.0 mLh⁻¹, amount of FeCl₃.6H₂O: 2.50 g, amount of PVP: 15.0 g) a) 10000x and b) 2000x.



(a)

(b)

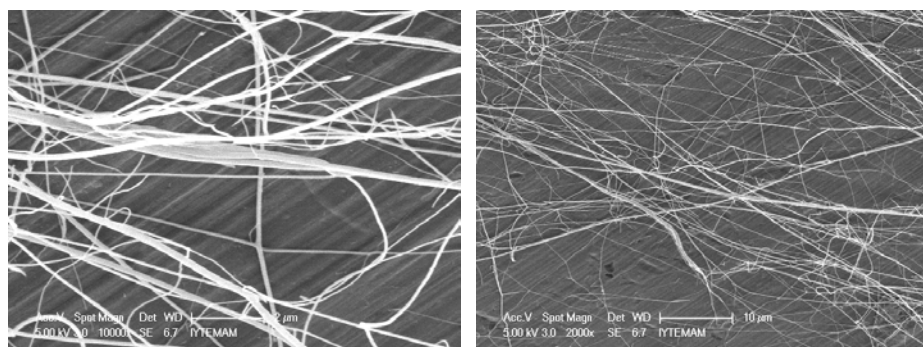
Figure 3.34. SEM images of PVP+FeCl₃ electrospun fibers after calcination at various magnifications (Spinning conditions: potential difference: 30 kV, feeding rate: 10.0 mLh⁻¹, amount of FeCl₃.6H₂O: 2.50 g, amount of PVP: 15.0 g) a) 10000x and b) 2000x.



(a)

(b)

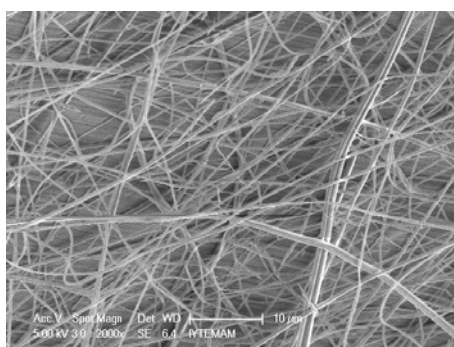
Figure 3.35. SEM images of PVP+FeCl₃ electrospun fibers at various magnifications (Spinning conditions: potential difference: 30 kV, feeding rate: 5.0 mLh⁻¹, amount of FeCl₃.6H₂O: 2.50 g, amount of PVP: 15.0 g) a) 10000x and b) 2000x.



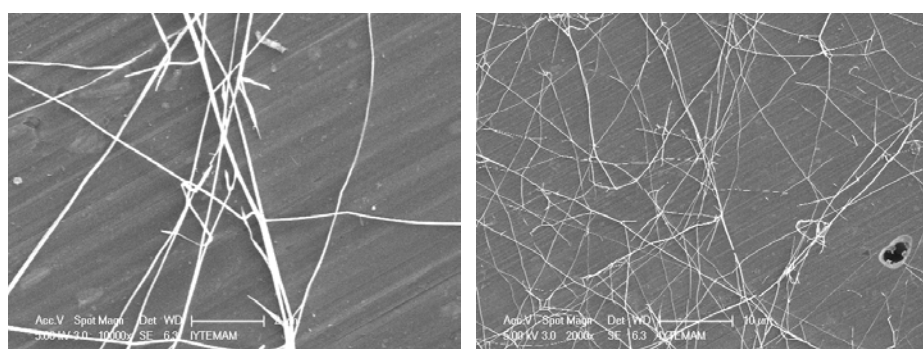
(a)

(b)

Figure 3.36. SEM images of PVP+FeCl₃ electrospun fibers after calcination at various magnifications (Spinning conditions: potential difference: 30 kV, feeding rate: 5.0 mLh⁻¹, amount of FeCl₃.6H₂O: 2.50 g, amount of PVP: 15.0 g) a) 10000x and b) 2000x.



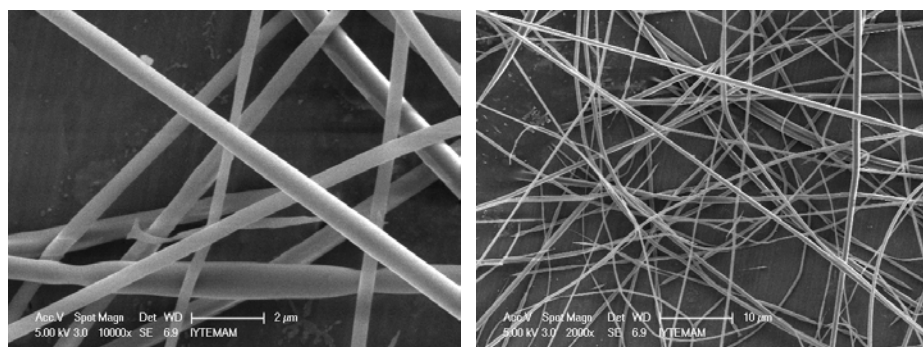
(a)



(b)

(c)

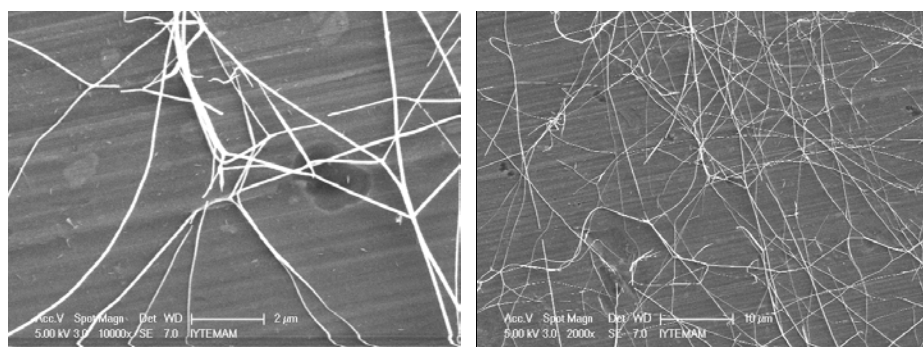
Figure 3.37. SEM images of PVP+FeCl₃ electrospun fibers a) before calcination b) and c) after calcination (Spinning conditions: potential difference: 30 kV, feeding rate: 1.0 mLh⁻¹, amount of FeCl₃.6H₂O: 2.50 g, amount of PVP: 15.0 g).



(a)

(b)

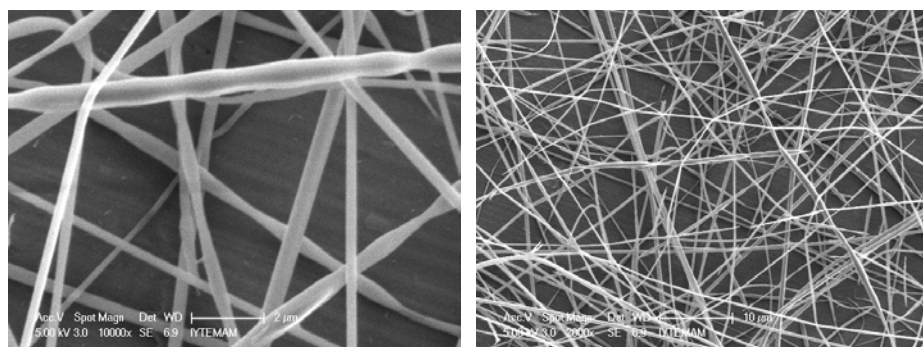
Figure 3.38. SEM images of PVP+FeCl₃ electrospun fibers at various magnifications (Spinning conditions: potential difference: 30 kV, feeding rate: 0.5 mLh⁻¹, amount of FeCl₃.6H₂O: 2.50 g, amount of PVP: 15.0 g) a) 10000x and b) 2000x.



(a)

(b)

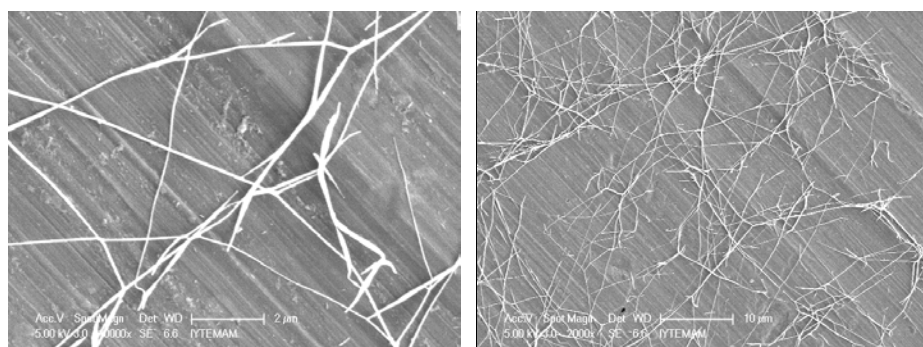
Figure 3.39. SEM images of PVP+FeCl₃ electrospun fibers after calcination at various magnifications (Spinning conditions: potential difference: 30 kV, feeding rate: 0.5 mLh⁻¹, amount of FeCl₃.6H₂O: 2.50 g, amount of PVP: 15.0 g) a) 10000x and b) 2000x.



(a)

(b)

Figure 3.40. SEM images of PVP+FeCl₃ electrospun fibers at various magnifications (Spinning conditions: potential difference: 30 kV, feeding rate: 0.1 mLh⁻¹, amount of FeCl₃.6H₂O: 2.50 g, amount of PVP: 15.0 g) a) 10000x and b) 2000x.



(a)

(b)

Figure 3.41. SEM images of PVP+FeCl₃ electrospun fibers after calcination at various magnifications (Spinning conditions: potential difference: 30 kV, feeding rate: 0.1 mLh⁻¹, amount of FeCl₃.6H₂O: 2.50 g, amount of PVP: 15.0 g) a) 10000x and b) 2000x.

3.2.2. Arsenic Speciation with Sol-Gel Based SPME Fibers

3.2.2.1. Optimization of Chromatographic Separation and Hydride Generation of Arsenic Species (HPLC-HGAAS)

In this study, the main goal was to develop the method for extraction of arsenic species with prepared amine-functionalized SPME fiber and separate each species in HPLC column prior to detection by HG-AAS. For this purpose, first of all, hydride generation ability of each arsenic species was optimized by varying the amount of NaBH_4 and HCl added into arsenic containing solutions. Results given in Figure 3.42 indicate that the each arsenic specie requires specific condition for maximum absorbance. As shown in the figure, maximum absorbance was obtained for As(III) and As(V) in 1.0% (w/v) L-Cysteine containing 1.0% (v/v) HCl solution. Strong reducing ability of L-Cysteine resulted in increased absorbance of As(V) due to the reduction to As(III). Maximum absorbance for DMA was obtained in 2.0% (v/v) HCl. In contrast to other arsenic species hydride generation of MMA was much more affected from acidity of the solution. The absorbance of the MMA which increases more than twice inspite of a small increment in HCl concentration from 1.0% to 2.0%. For the further studies the samples that were supposed to contain As(III) and/or As(V) were acidified with concentrated HCl in order to obtain 1.0% (v/v) HCl in the solutions. Additionally, L-Cysteine were added into As(III) and As(V) continig solutions in order to obtain 1.0% (w/v) L-Cysteine in final solutions. On the other hand, the samples that were supposed to contain DMA and MMA were only acidified with HCl to obtain 2.0% (v/v) HCl in the solutions.

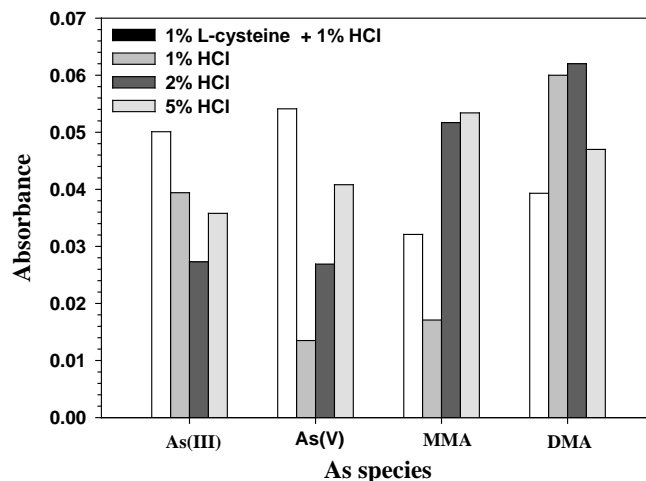


Figure 3.42. Optimization of hydride formation conditions of arsenic species (As concentration $5.0 \mu\text{gL}^{-1}$).

The second step in the study was the separation of the As(III), DMA, MMA and As(V) in an anion exchange column. For this purpose, each arsenic species was injected into HPLC column separately and retention times were determined after fractional collection (1 mL) of mobile phase from column exit. Each fraction was treated with HCl or HCl and L-Cysteine according to optimized conditions for hydride generation. Arsenic in the fractions was determined by HG-AAS the parameters of which were summarized in Table 3.1. The elution order of four arsenic species was As(III), DMA, MMA and As(V) from the anion exchange column. The retention mechanism of the arsenic species in the strong anion exchange column depends on the charge of the arsenicals under elution conditions. The structures and acidity dissociation constants of arsenical used throughout this study are given in Table 3.5.

Table 3.5. Arsenic species used throughout the study

As species	Structure	pKa	Reference
Arsenite As(III)	$\begin{array}{c} \text{OH} \\ \\ \text{As} \\ / \quad \backslash \\ \text{HO} \quad \text{OH} \end{array}$	9.2 12.1 13.4	Smith et al. 1998
Arsenate As(V)	$\begin{array}{c} \text{O} \\ \\ \text{OH} - \text{As} - \text{OH} \\ \\ \text{OH} \end{array}$	2.3 6.8 11.6	Larsen and Hansen 1992
Monomethylarsonic acid MMA	$\begin{array}{c} \text{O} \\ \\ \text{H}_3\text{C} - \text{As} - \text{OH} \\ \\ \text{OH} \end{array}$	3.6 8.2	Calatayud et al. 2010
Dimethylarsinic acid DMA	$\begin{array}{c} \text{O} \\ \\ \text{H}_3\text{C} - \text{As} - \text{OH} \\ \\ \text{CH}_3 \end{array}$	6.3	Calatayud et al. 2010
Arsenobetaine AsB	$\begin{array}{c} \text{CH}_3 \\ \\ \text{H}_3\text{C} - \text{As}^+ - \text{CH}_2 - \text{COO}^- \\ \\ \text{CH}_3 \end{array}$	2.2	Larsen and Hansen 1992

3.2.2.2. Speciation of Arsenic with Amine-Modified Fibers (Manual Coated)

Amine-, mercapto-, amine and mercapto-, vinyl-, chloro- silane modified sol-gel based coated fibers were used for extraction of four arsenic species, namely, As(III), DMA, MMA and As(V). Results showed that only amine-modified fibers show considerable extraction for As(V), DMA and MMA. Therefore, for optimization of the

extraction parameters, only amine-modified fibers were used. The extraction details were described in the experimental part of the study.

The calibration plots obtained after extraction of As(V), DMA and MMA from solution with manual coated amine-functionalized SPME fibers are given in Figures 3.43, 3.44 and 3.45, respectively. The results indicated wide linear dynamic range of calibration plots which are promising for extraction of various concentrations of arsenic species. However, considering the maximum allowable concentration of $10.0 \mu\text{gL}^{-1}$ recommended by World Health Organization (WHO) in 'Guidelines for Drinking-water Quality', the lowest concentrations in the obtained plots ($100.0 \mu\text{gL}^{-1}$) require further improvement. The enhancement of the detection limits of arsenicals is the main task of the succeeding section. In order to attain the desired levels of detection two strategies were followed. These approaches were replacement of the HPLC-HGAAS with HPLC-ICPMS and evolution on the extraction capability of the fibers.

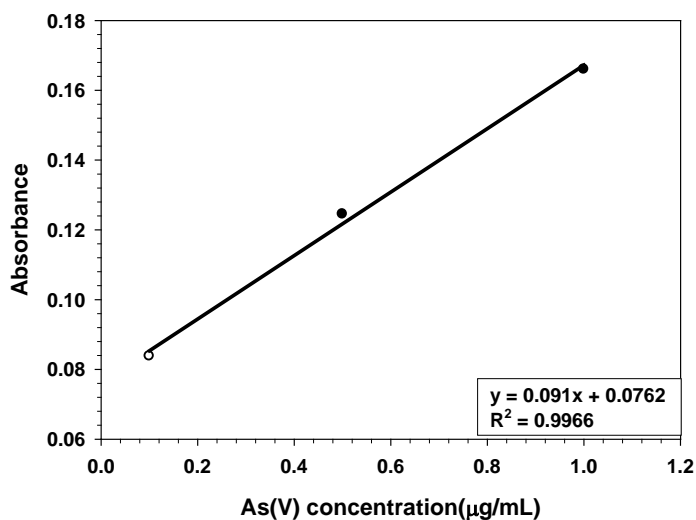


Figure 3.43. Calibration plot for As(V) extraction (Extraction conditions: solution volume: 15.0 mL, stirring speed: 200 rpm, solution pH: 3.0, extraction time: 60 min, temperature: 25 °C, desorption volume: 50 μL , desorption time 60 min).

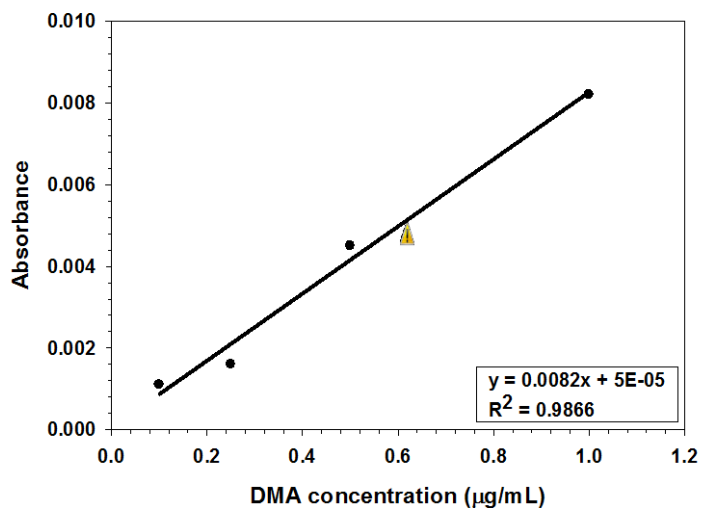


Figure 3.44. Calibration plot for DMA extraction (Extraction conditions: solution volume: 15.0 mL, stirring speed: 200 rpm, solution pH: 3.0, extraction time: 60 min, temperature: 25 °C, desorption volume: 50 µL, desorption time 60 min).

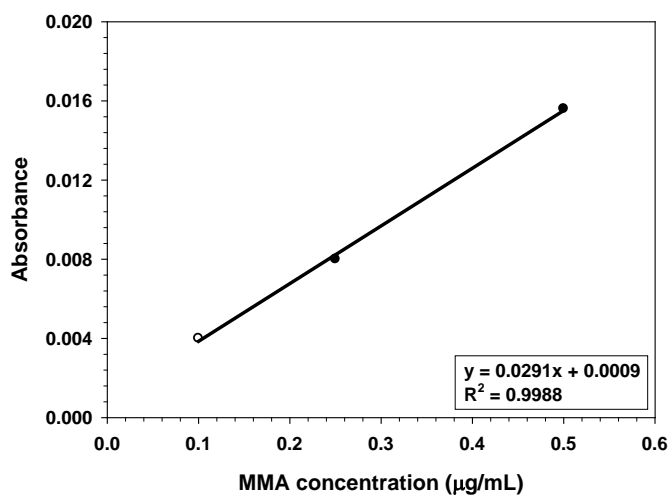


Figure 3.45. Calibration plot for MMA extraction (Extraction conditions: solution volume: 15.0 mL, stirring speed: 200 rpm, solution pH: 3.0, extraction time: 60 min, temperature: 25 °C, desorption volume: 50 µL, desorption time 60 min).

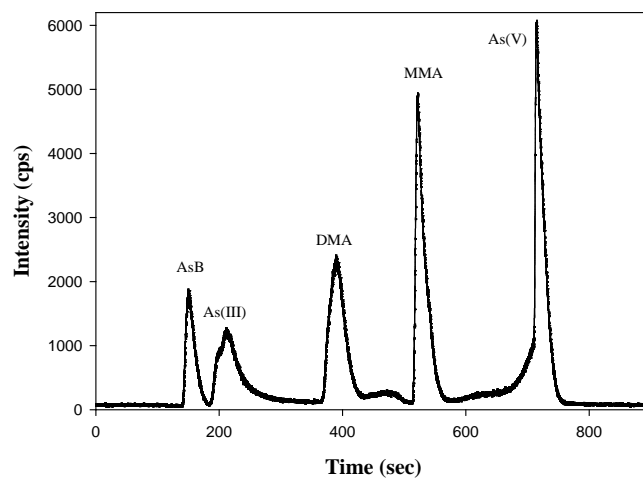
3.2.2.3. Speciation of Arsenic with Amine-Modified Fibers: Further Improvement on the Fibers

As explained in the preceding section, under the studied conditions the detection limit would not reach sufficiently lower values. There were two major contributors that are supposed to lead to inadequate detection levels. The first one was the detection method. The fractions collected from the exit of the anion exchange column were detected by HG-AAS where the samples were diluted with NaBH₄ solution, therefore the online determination of the eluted species without dilution is important. In this respect, using online connected HPLC-ICPMS, eliminates further dilution of analytes. The second main contributor was the fiber coating. Therefore, the optimization of the fiber coating is important. For this purpose the sol-gel based coating of the fiber was modified. As explained in Section 3.2.2.2, both sol-gel solution and fiber coating method was improved. Details of the modifications which were performed both on instrumentation and fiber coating are enlightened in this section.

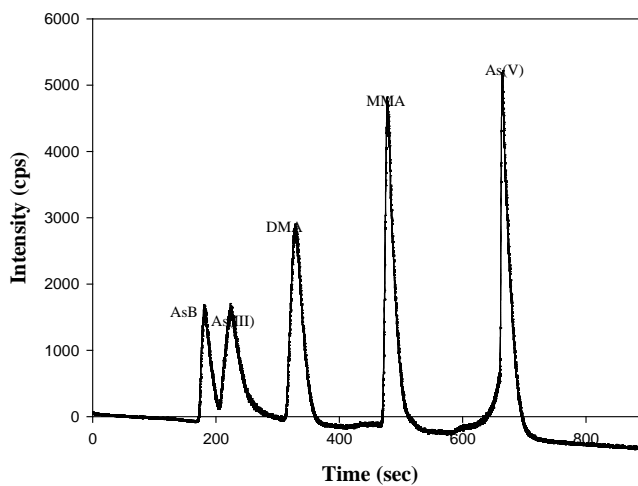
3.2.2.3.1. Optimization of Chromatographic Parameters for HPLC-ICPMS

Most of the buffers that are capable of separating arsenic species result in salt deposition on skimmer and sample cones of the ICP-MS. To prevent the formation of such depositions, ammonium carbonate solution was chosen as a proper eluent for chromatographic speciation. The elution order of the species in the following HPLC studies is AsB, As(III), DMA, MMA and As(V). The retention mechanism of the species was strongly controlled by the pH of the mobile phase and dissociation of acidic species. The pH dependent dissociations of arsenic species are given in Table 3.5. Depending on the ionic character of the column and the pH of the eluting buffer (pH 8.50) each arsenic species was eluted in accordance with its charge. Positively charged AsB was eluted first which was not retained by positively charged quaternary ammonium groups. As(III) is neutral at the working pH and has weak interaction with quaternary ammonium groups of the column; therefore, it was eluted second. Among the tested species, As(V) has the largest negative charge which results in higher affinity by the column bringing about the longest retention.

Various flow rates of the eluent were applied to optimize the separation of the five arsenic species (AsB, As(III), DMA, MMA and As(V)). Also, the effect of organic solvent on the peak intensity and the separation efficiency were investigated by the addition of different amounts of methanol to aqueous ammonium carbonate solution. Chromatograms obtained with 5 different flow rates (from 0.6 mLmin⁻¹ to 1.0 mLmin⁻¹) reveal that there is no improvement in the separation of adjacent AsB and As(III) peaks while other species were eluted from chromatogram with longer retention times. Although the addition of 2% (v/v) methanol to 10.0 mM ammonium carbonate resulted in superior separation of As(III) and AsB, the main outcome was asymmetry (formation of shoulder) on As(III) peak. Decreasing the methanol content in buffer to 1.0% and 0.5% (v/v) decreases the peak asymmetry; however, the results were not reproducible in separation of the peaks in eluents containing methanol. Decreasing the strength of the ammonium carbonate solution from 10.0 mM to 5.0 mM was not effective either for a further separation of these two species. Additionally, in contrast to several studies in literature suggesting the enhancement in peak intensities with the addition of a small amount of methanol (Vassileva et al. 2001), in this study, there was no evidence for such an increase in peak heights. As it is expected, the intensity enhancement was obtained by increasing the flow rate from 0.6 mLmin⁻¹ to 1.0 mLmin⁻¹. Consequently, 10.0 mM (NH₄)₂CO₃, (pH 8.50) for the first 4 min and 30.0 mM (NH₄)₂CO₃, (pH 8.50) for 4-13 min with a flow rate of 1.0 mLmin⁻¹ were chosen. Typical chromatograms obtained under these conditions are given in Figure 3.46.



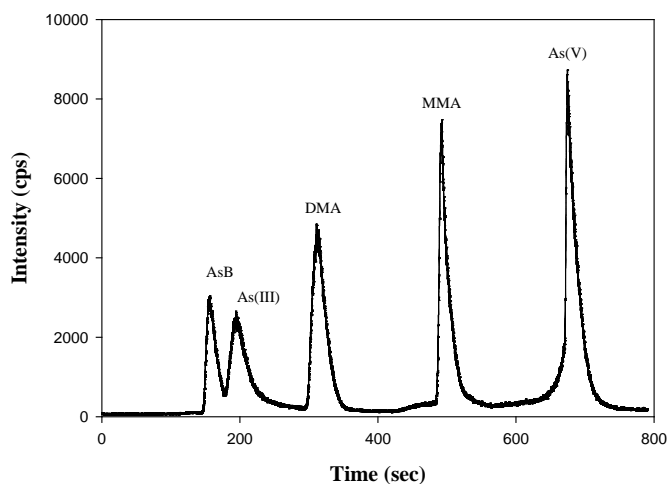
(a)



(b)

Figure 3.46. Optimization of chromatographic conditions in HPLC-ICPMS a) 2% Methanol added ammonium carbonate at 1 mL/min flow rate, b) ammonium carbonate at 0.7 mL/min flow rate and c) ammonium carbonate at 1 mL/min flow rate.

(cont. on next page)



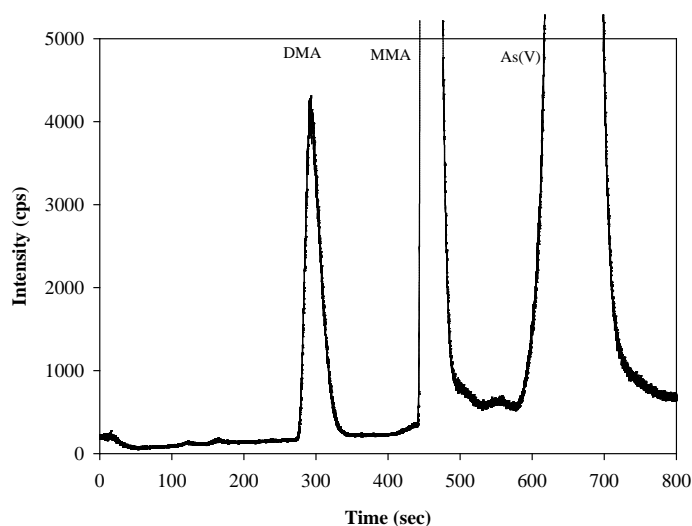
(c)

Figure 3.46. (cont.)

3.2.2.3.2. Optimization of Fiber Coating

In order to enhance the extraction of arsenicals by sol-gel based SPME fibers various parameters were tested. Firstly, to obtain homogeneous fiber coating, the manual coating process was replaced with coating by dip coater device. The fiber coating was made thicker by sequential coating of the bare fiber. However, there was no considerable enhancement of the extracted analytes even after ten successive loading of the sol-gel material on the surface of the fiber. Secondly, bare fibers were coated by electrospinning of sol-gel solution. In order to obtain a solution appropriate for electrospinning the preparation of sol-gel solution was modified. For this purpose 2.0 mL PDMS, 3.0 mL THF, 2.0 mL APTES and 0.50 mL PMHS were mixed in a 20 mL glass vial by continuous stirring. Sol-gel process was initiated by addition of 1.0 mL TFA solution containing 5% by volume H₂O. The reaction was continued for 48 h at room temperature (RT) followed by evaporation of THF until appropriate viscosity for electrospinning was achieved. Extraction capability of the electrospun coated fiber illustrated in Figure 3.47(a) shows that the electrospun coated fibers are promising for microextraction of arsenicals. However, when the fibers were prepared for the second time the extraction efficiency (Figure 3.47(b)) of the fibers was poor with respect to the first prepared fibers. The main outcome of the study is the trouble associated with the fiber-to-fiber reproducibility. To overcome this problem, the same fibers were prepared

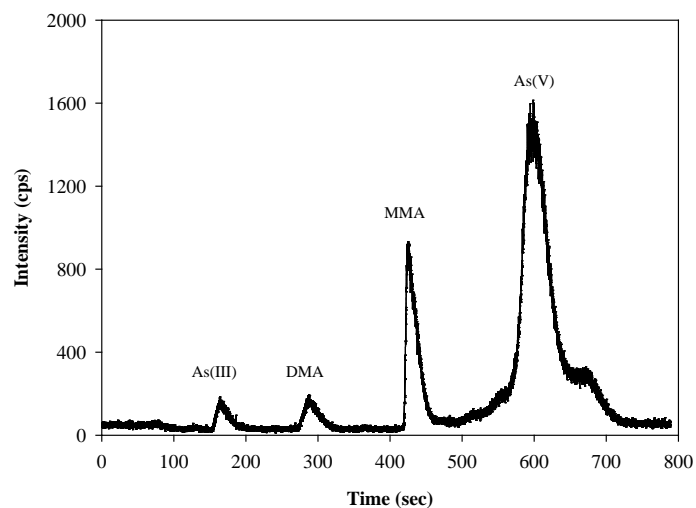
without addition of PMHS. As mentioned in the related experimental part of the study, PMHS was used as deactivator. Additionally, the PMHS control the surface polarity of the coating by endcapping the silanol groups. Thus, surface polarity decreases which results in hydrophobicity on the surface and most likely this effects the extraction ability of the coating. In order to prove this hypothesis, fibers were coated with the same amine containing sol-gel solution excluding addition of PMHS. Obtained chromatograms with two distinct non encapped amine-modified fibers are demonstrated in Figure 3.48. As it is seen, the fibers produced without addition of deactivator extracted quantitative amounts of each species in a more reproducible way. Therefore, the detection limitation problem has been alleviated.



(a)

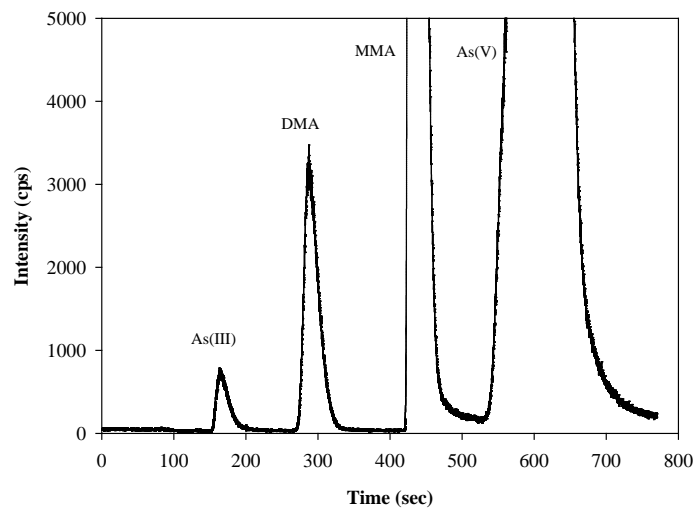
Figure 3.47. Chromatograms obtained after extraction with endcapped amine-modified fibers prepared in different times a) first prepared fiber and b) second prepared fiber (Extraction conditions; As concentration: $100.0 \mu\text{gL}^{-1}$, solution volume: 15.0 mL, stirring speed: 700 rpm, solution pH: 4.0, extraction time: 60 min, temperature: 25 °C, desorption volume: 150 μL , desorption time 15 min, desorption solution: 50.0 mM KH_2PO_4).

(cont. on next page)



(b)

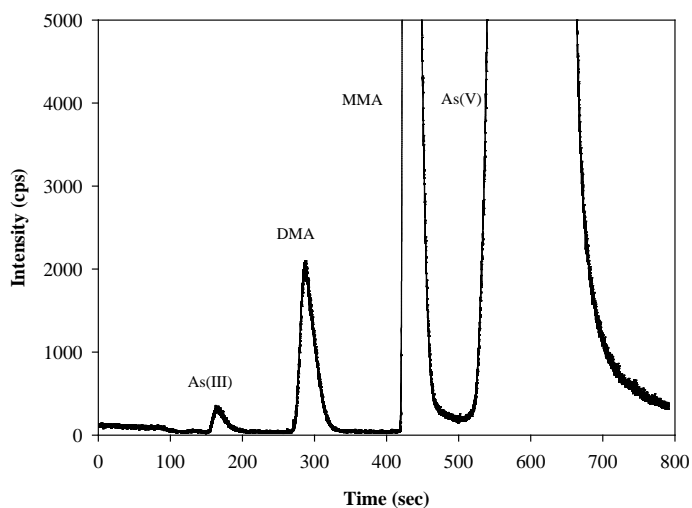
Figure 3.47. (cont.)



(a)

Figure 3.48. Chromatograms obtained after extraction with non endcapped amine-modified fibers prepared in different times a) first prepared fiber and b) second prepared fiber (Extraction conditions; As concentration: $100.0 \mu\text{gL}^{-1}$, solution volume: 15.0 mL, stirring speed: 700 rpm, solution pH: 4.0, extraction time: 60 min, temperature: 25 °C, desorption volume: 150 μL , desorption time 15 min, desorption solution: 50.0 mM KH_2PO_4).

(cont. on next page)



(b)

Figure 3.48. (cont.)

One of the main outcomes of the study is the difference of the extraction abilities of the fibers coated by the same sol-gel solution but different coating methods namely, electrospinning and dip coating. In order to verify the difference of the extraction capability of the coating obtained with two different methods, the amount of the APTES in the sol-gel solutions were varied. The microextraction results of arsenicals obtained by fibers coated with aforementioned methods and various amounts of APTES in coating solution are demonstrated in Figure 3.49 and 3.50. According to the results, electrospinning process produces more valuable fiber coatings even under same coating thicknesses obtained with both coating methods. Under the consideration of same coating thickness and sol-gel solution the only difference between these two methods is the application of the electric field in the electrospinning process. Amine functionality in the polymeric sol-gel solution is positively charged and it can be speculated that these functional groups most likely are oriented under influence of the electric field. Thus, amine groups on the electrospin coated fibers are self oriented and more available than the functional groups randomly distributed though the matrix where no electrical field is applied. The proposed mechanisms of the coatings were demonstrated in Figure 3.51.

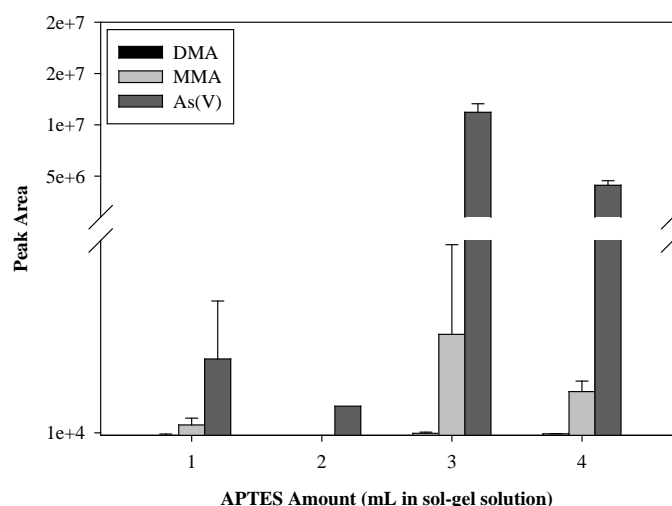


Figure 3.49. Effect of APTES amount in the sol-gel solution on extraction of the As(V) in dip coated fibers. (Extraction conditions; extraction time: 30 min, As concentration: $10.0 \mu\text{gL}^{-1}$, solution pH: 5.0, stirring speed: 700 rpm, solution volume: 15 mL, Desorption conditions; desorption time: 20 min, $150 \mu\text{L}$ 50.0 mM KH_2PO_4)

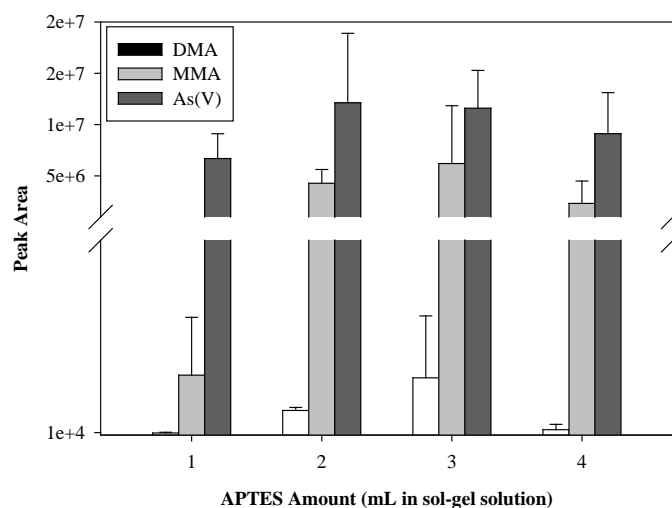


Figure 3.50. Effect of APTES amount in the sol-gel solution on extraction of the As(V) in electrospun coated fibers. (Extraction conditions; extraction time: 30 min, As concentration: $10.0 \mu\text{gL}^{-1}$, solution pH: 5.0, stirring speed: 700 rpm, solution volume: 15 mL, Desorption conditions; desorption time: 20 min, $150 \mu\text{L}$ 50.0 mM KH_2PO_4)

extraction was particularly independent from pH of the solution (Figure 3.53 and 3.54). Extraction of species was in agreement with the sorption characteristics of SPE part of the thesis. As expected from the results have been obtained in SPE part of the study As(III) was not retained by amine-modified SPME fibers. On the other hand, the extracted amounts of the analytes depend strongly on the interaction between the weak anion exchanger surface of the SPME coating and charge of the species. The correlation between the peak area and interaction of the species with fiber shows the trend of the extraction. The most and the least extracted species were As(V) and DMA, respectively. This finding is in agreement with the elution order of the analytes from strong anion exchange column used though the study.

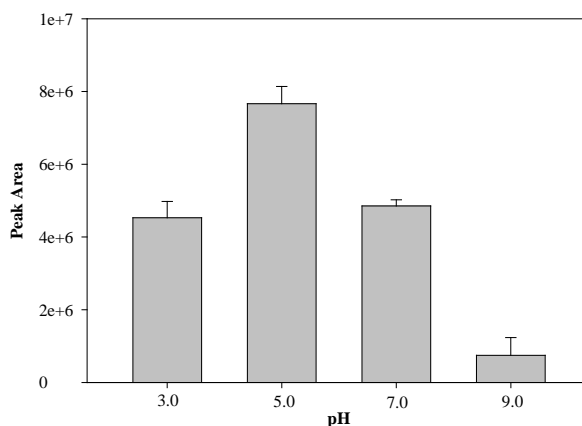


Figure 3.52. Effect of solution pH on extraction of As(V) (Extraction conditions: As(V) concentration: $10.0 \mu\text{gL}^{-1}$, solution volume: 15.0 mL, stirring speed: 700 rpm, extraction time: 60 min, temperature: 25 °C, desorption volume: 150 μL , desorption time 20 min, desorption solution: 50.0 mM KH_2PO_4)

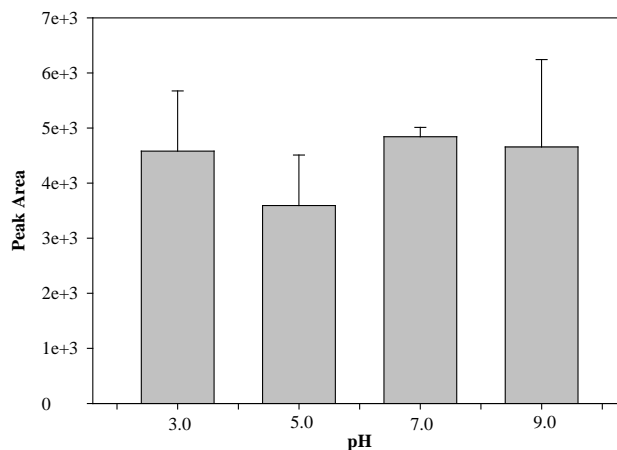


Figure 3.53. Effect of solution pH on extraction of DMA (Extraction conditions: As(V) concentration: $10.0 \mu\text{gL}^{-1}$, solution volume: 15.0 mL, stirring speed: 700 rpm, extraction time: 60 min, temperature: 25 °C, desorption volume: 150 μL , desorption time 20 min, desorption solution: 50.0 mM KH_2PO_4)

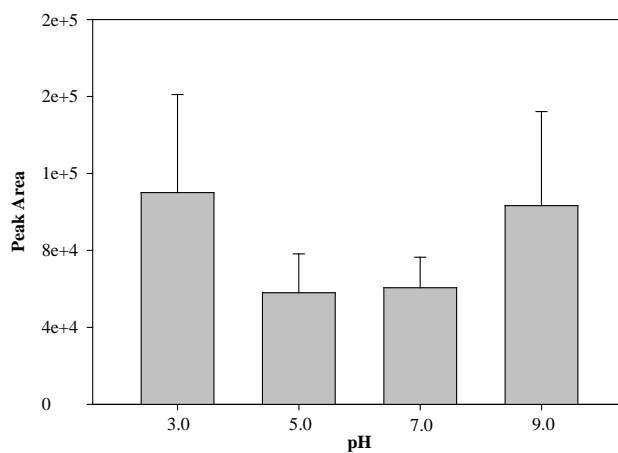


Figure 3.54. Effect of solution pH on extraction of MMA (Extraction conditions: As(V) concentration: $10.0 \mu\text{gL}^{-1}$, solution volume: 15.0 mL, stirring speed: 700 rpm, extraction time: 60 min, temperature: 25 °C, desorption volume: 150 μL , desorption time 20 min, desorption solution: 50.0 mM KH_2PO_4)

3.2.2.3.3.2. Effect of Agitation Time/Speed on Extraction of Arsenic Species

The effect of interaction time on extraction of each arsenic species are given in Figures 3.55, 3.56 and 3.57. For As(V), DMA and MMA species increasing the contact time resulted in increase of the extracted amount of analyte. Further increase in the interaction time (120 min) resulted in a decrease of extracted amount of analytes. Similar trend in sorption of As(V) was also observed with (NH₂)silicate in SPE part of the study. Results indicate that the contact time of the fiber and analyte solution is one of the most important optimization parameter. For the further study 30 min was chosen as extraction time.

The effect of stirring speed of the solution during the extraction of arsenic species was also investigated. The obtained results are given in Figures 3.58, 3.59 and 3.60. The most important outcome of the study was the inconsistency of the extracted amount of the arsenic species at various stirring speed. The maximum extraction was obtained for As(V) and MMA at 700 rpm while DMA was extracted in a larger amount under the static extraction conditions. When the solutions were stirred at 1000 rpm extracted amount of the arsenic species were decreased again due to formation of vortex in the solution. Another important point was extraction of DMA under static conditions. As can be seen from Figure 3.59, the maximum extraction of DMA was obtained with 30 min static extraction. Under the consideration of the limited number of functional sites available on the fiber, the kinetic of the interaction between functional groups and species is important. Kinetic of the extraction strongly depends on the strength of the electrostatic interaction between the arsenicals and protonated amine groups. The larger charge on the species (As(V) and MMA) results in larger interaction and fast extraction kinetic, while smaller negative charge (DMA) results in weaker interaction and slower extraction kinetic. The static extraction performed in this study decreases the probability for interaction of individual arsenicals with the active fiber surface. So the vacancies on the functional groups make these groups equally available for each species without consideration of the reaction kinetic. As a result, DMA can be extracted in a larger amount than the amount obtained with other extraction conditions, but almost in an equal amount as other two species. Considering the majority of the species 700 rpm was chosen as an optimum stirring speed for further studies.

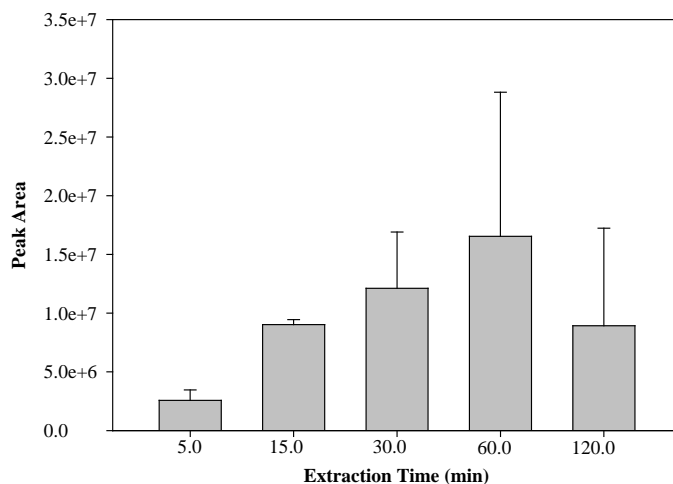


Figure 3.55. Effect of agitation time on extraction of As(V) (As concentration: 10.0 μgL^{-1} , solution pH: 5.0, solution volume: 15 mL, stirring speed: 700 rpm. Desorption conditions; desorption time: 20 min, 150 μL 50.0 mM KH_2PO_4)

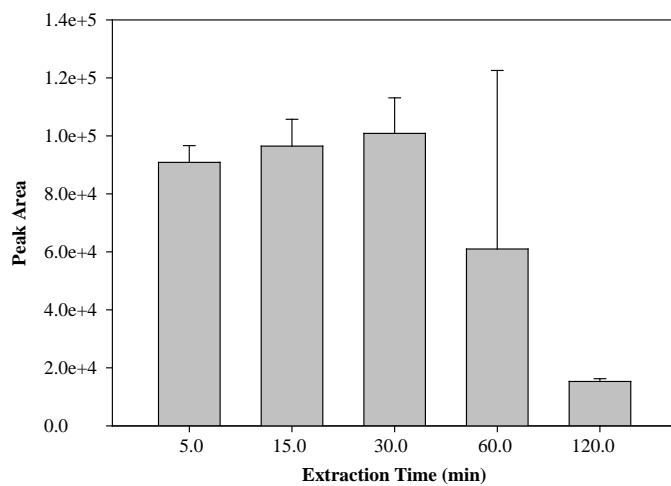


Figure 3.56. Effect of agitation time on extraction of DMA (As concentration: 10.0 μgL^{-1} , solution pH: 5.0, solution volume: 15 mL, stirring speed: 700 rpm. Desorption conditions; desorption time: 20 min, 150 μL 50.0 mM KH_2PO_4)

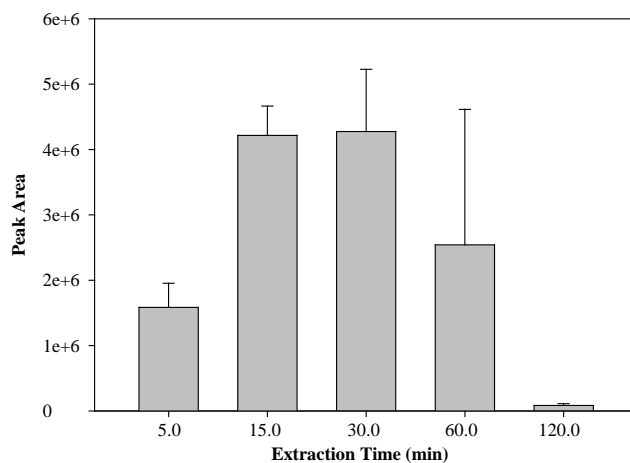


Figure 3.57. Effect of agitation time on extraction of MMA (As concentration: $10.0 \mu\text{gL}^{-1}$, solution pH: 5.0, solution volume: 15 mL, stirring speed: 700 rpm. Desorption conditions; desorption time: 20 min, $150 \mu\text{L}$ 50.0 mM KH_2PO_4)

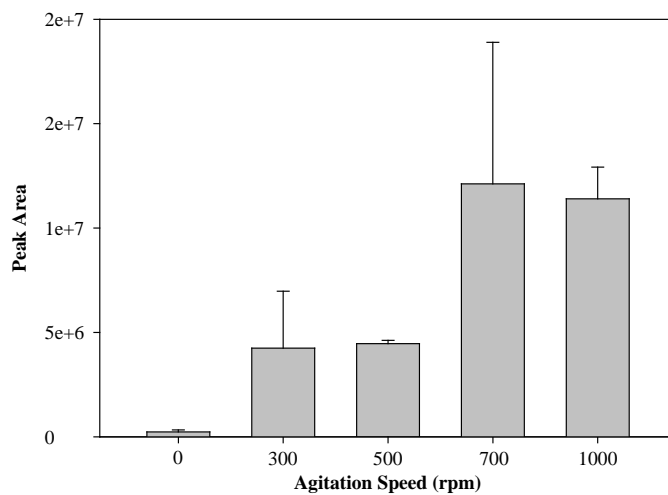


Figure 3.58. Effect of agitation speed on extraction of As(V) (Extraction conditions; extraction time: 30 min, As concentration: $10.0 \mu\text{gL}^{-1}$, solution pH: 5.0, solution volume: 15 mL, Desorption conditions; desorption time: 20 min, $150 \mu\text{L}$ 50.0 mM KH_2PO_4)

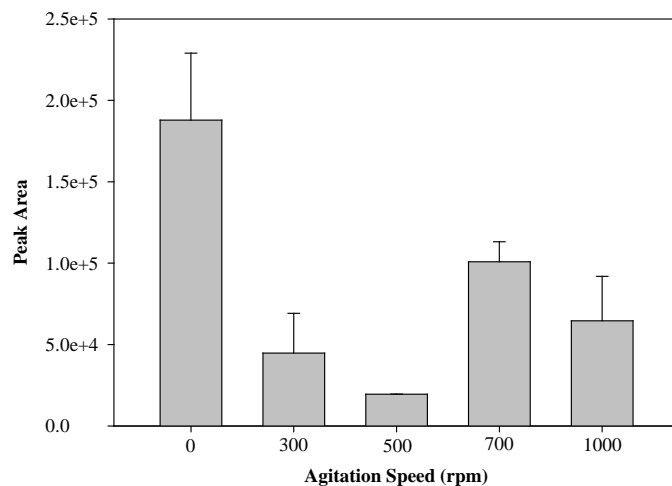


Figure 3.59. Effect of agitation speed on extraction of DMA (Extraction conditions; extraction time: 30 min, As concentration: $10.0 \mu\text{gL}^{-1}$, solution pH: 5.0, solution volume: 15 mL, Desorption conditions; desorption time: 20 min, $150 \mu\text{L}$ 50.0 mM KH_2PO_4)

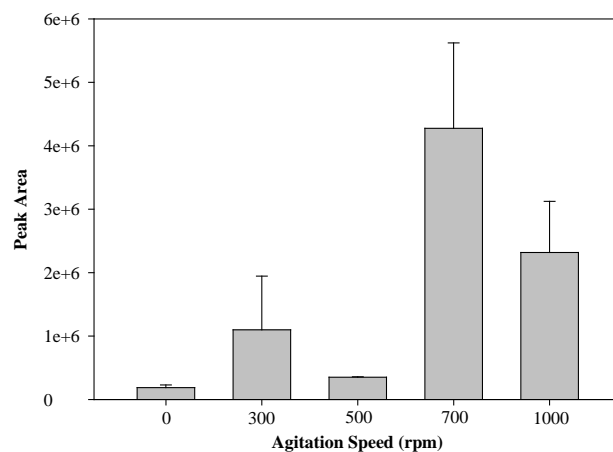


Figure 3.60. Effect of agitation speed on extraction of MMA (Extraction conditions; extraction time: 30 min, As concentration: $10.0 \mu\text{gL}^{-1}$, solution pH: 5.0, solution volume: 15 mL, Desorption conditions; desorption time: 20 min, $150 \mu\text{L}$ 50.0 mM KH_2PO_4)

3.2.2.3.3.3. Effect of Salt Concentration (Ionic Strength) on Extraction of Arsenic Species

The effect of NaCl concentration on extraction of arsenic species were studied in 1.0 M, 0.10 M, and 0.010 M NaCl solutions. The results were given in Figures 3.61, 3.62 and 3.63 indicate that increasing the ionic strength of the solution results in decrease in the extracted amount of each arsenical compound. It can be speculated that the decrease in the amount of the extracted analytes is related to competitive sorption of Cl⁻ ions by protonated amine groups. The amine groups were converted to surface inactive aminium salt (R-NH₃⁺Cl⁻). Therefore, the extractions of the arsenic species were decreased under chloride reach conditions.

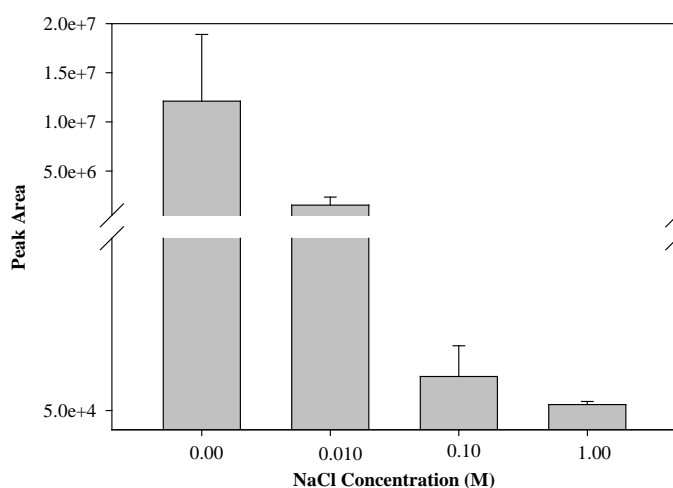


Figure 3.61. Effect of NaCl concentration on extraction of As(V). (Extraction conditions; extraction time: 30 min, As concentration: 10.0 μgL^{-1} , solution pH: 5.0, stirring speed: 700 rpm, solution volume: 15 mL, Desorption conditions; desorption time: 20 min, 150 μL 50.0 mM KH_2PO_4)

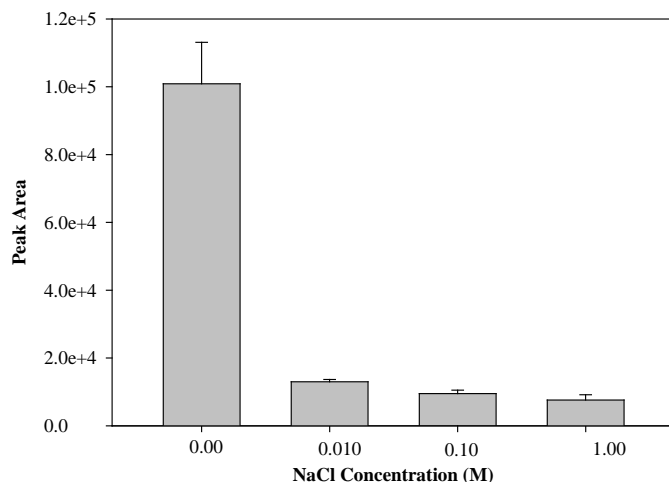


Figure 3.62. Effect of NaCl concentration on extraction of DMA. (Extraction conditions; extraction time: 30 min, As concentration: $10.0 \mu\text{gL}^{-1}$, solution pH: 5.0, stirring speed: 700 rpm, solution volume: 15 mL, Desorption conditions; desorption time: 20 min, $150 \mu\text{L}$ 50.0 mM KH_2PO_4)

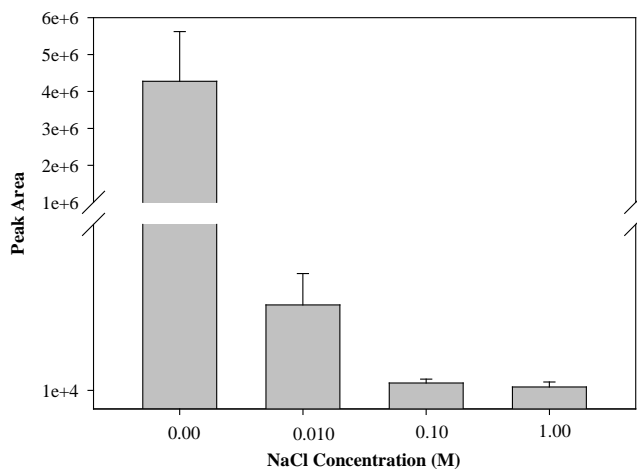


Figure 3.63. Effect of NaCl concentration on extraction of MMA. (Extraction conditions; extraction time: 30 min, As concentration: $10.0 \mu\text{gL}^{-1}$, solution pH: 5.0, stirring speed: 700 rpm, solution volume: 15 mL, Desorption conditions; desorption time: 20 min, $150 \mu\text{L}$ 50.0 mM KH_2PO_4)

3.2.2.3.3.4. Effect of Solution Temperature on Extraction of Arsenic Species

In the headspace microextractions of volatile compounds increasing the solution temperature increases the amounts of the extracted analytes (Pawliszyn 1999) by altering the equilibrium concentrations of analyte in the headspace and solution. In case of direct mode microextraction a prediction of the effect of the temperature on the extraction of analyte is not easy. It depends on the exothermic or endothermic nature of the extraction and as well as on the volatility of the analytes. In this study, the general trend in the effect of the solution temperature on the extraction of As(V), DMA and MMA is illustrated in Figure 3.64. Increasing the extraction temperature decreases the amount of extracted analytes. This finding shows the exothermic nature of the extraction of the analytes by the fibers. The effect of the temperature was more significant especially for MMA. Decrease of peak areas in orders of magnitude as increasing the extraction temperature was observed. For further study 20 °C was chosen as optimum extraction temperature.

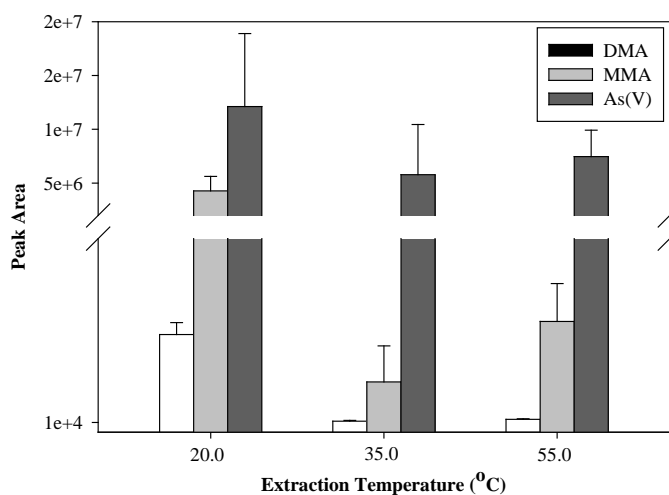


Figure 3.64. Effect of solution temperature on extraction of the arsenic species. (Extraction conditions; extraction time: 30 min, As concentration: 10.0 μgL^{-1} , solution pH: 5.0, stirring speed: 700 rpm, solution volume: 15 mL, Desorption conditions; desorption time: 20 min, 150 μL 50.0 mM KH_2PO_4)

3.2.2.3.4. Repetitive Use of the Fibers and Fiber Reproducibility

The one of the most important task in the SPME fiber production is to prepare stable fiber coatings. Results obtained from repetitive use of the same fiber are illustrated in Figure 3.65. Although the extracted analytes varied from one extraction to another there were significant amount of the extracted analytes, especially for As(V) and MMA. These results show potential for preparation of stable fiber coatings. On the other hand, the fiber to fiber reproducibility study which is shown in Figure 3.66 was indicative of the one of the main drawback of the SPME method which is mainly suffers from the reproducibility in preparation of the fibers.

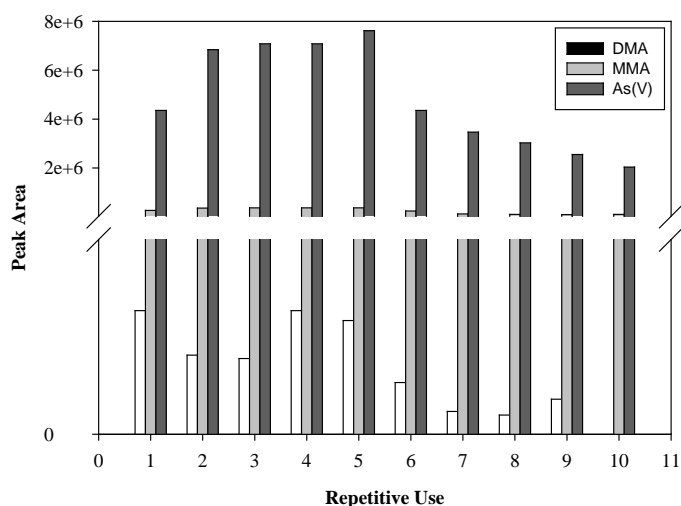


Figure 3.65. Repetitive use of the same fiber (Extraction conditions; extraction time: 30 min, As concentration: $10.0 \mu\text{gL}^{-1}$, solution pH: 5.0, stirring speed: 700 rpm, solution volume: 15 mL, Desorption conditions; desorption time: 20 min, $150 \mu\text{L}$ 50.0 mM KH_2PO_4 , Cleaning conditions; 10 min desorption into 15 mL 0.50 M KH_2PO_4 , 5 min cleaning in 15 mL upw, 2 min activation in 15 mL 0.10 M HNO_3 , 5 min conditioning at 110°C)

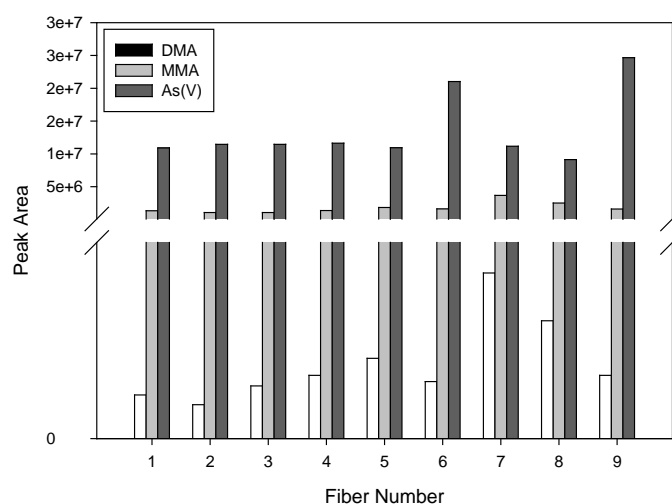


Figure 3.66. Fiber-to-fiber reproducibility (Extraction conditions; extraction time: 30 min, As concentration: $10.0 \mu\text{gL}^{-1}$, solution pH: 5.0, stirring speed: 700 rpm, solution volume: 15 mL, Desorption conditions; desorption time: 20 min, $150 \mu\text{L}$ 50.0 mM KH_2PO_4)

3.2.3. Arsenic Speciation with Nanoiron-Agarose SPME Fibers

The inorganic arsenic sorption ability of zero valent iron (Zhu et al. 2009) and FeOOH (Cumbal, L. and A.K. Sengupta. 2005) was already known and well studied for remediation of waters contaminated with arsenic. However, there is no report on the organoarsenic sorption behavior of the mentioned sorbents. In view of the affinity of the iron based sorbents for inorganic arsenic species the nZVI particles were synthesized and immobilized on the surface of the bare silica fiber by capillary templating method as a potential SPME fiber coating. The preparation and characterization of the nano-iron SPME fibers were given in the related part of the thesis. In order to show the applicability of the fibers for extraction of various arsenical species, microextraction was performed from solution containing AsB, As(III), DMA, MMA and As(V) and determined by HPLC-ICPMS configuration described in the preceding parts of the thesis. The preliminary results were demonstrated that the fibers were able to extract all arsenical species excluding AsB. Optimization of extraction and desorption parameters are explained in details in the subsequent parts of the thesis.

3.2.3.1. Optimization of Desorption Parameters

The success of the proposed methodology depends strongly on desorption of extracted arsenic species from the fibers. To find a suitable reagent, 0.100 M NaOH and two buffers (0.100 M $(\text{NH}_4)_2\text{CO}_3$ and 0.100 M KH_2PO_4) were tried. Although 0.100 M NaOH was successful in desorption of organoarsenic species, it was not suitable for HPLC due to peak broadening. Ammonium carbonate, on the other hand, was not capable of desorbing quantitative amounts of arsenic species from fibers. Fortunately, 0.100 M KH_2PO_4 was found to desorb arsenic species quantitatively with less perturbation in the chromatographic peaks compared to 0.100 M NaOH (results were not given). The next step was to find the optimum concentration of KH_2PO_4 that gives acceptable chromatographic peak shapes. For this purpose, various concentrations of KH_2PO_4 (25.0, 50.0, 75.0 and 100.0 mM) each spiked with arsenic mixture having a concentration of $50.0 \mu\text{gL}^{-1}$ was injected into anion exchange column and chromatograms were obtained. As shown in Figure 3.67, 50.0 mM KH_2PO_4 has demonstrated better performance in terms of peak asymmetry and peak broadening.

First of all the optimum desorption time of the analytes from the fibers was investigated. The fibers were immersed and statically desorbed in KH_2PO_4 for different durations such as 5, 10, 15 and 30 min; and 10 min was found to be optimum. In conclusion, the desorption of arsenic species from fibers were decided to be realized by immersing the fiber in $150.0 \mu\text{L}$ of 50.0 mM KH_2PO_4 solution for 10 min. In order to investigate the efficiency of desorption step further, the same fiber was immersed consecutively (10 min in each) in 5 different vials containing the desorption reagent ($150.0 \mu\text{L}$ of 50.0 mM KH_2PO_4). Figure 3.68 shows that the major portion of the analytes was desorbed in the first cycle, although there were still traces of the analytes on the fiber even after the 5th cycle. This finding suggested that there is a need for a final cleaning step before the next use of the fiber due to the non-exhaustive character of the desorption and this strategy was employed in further studies.

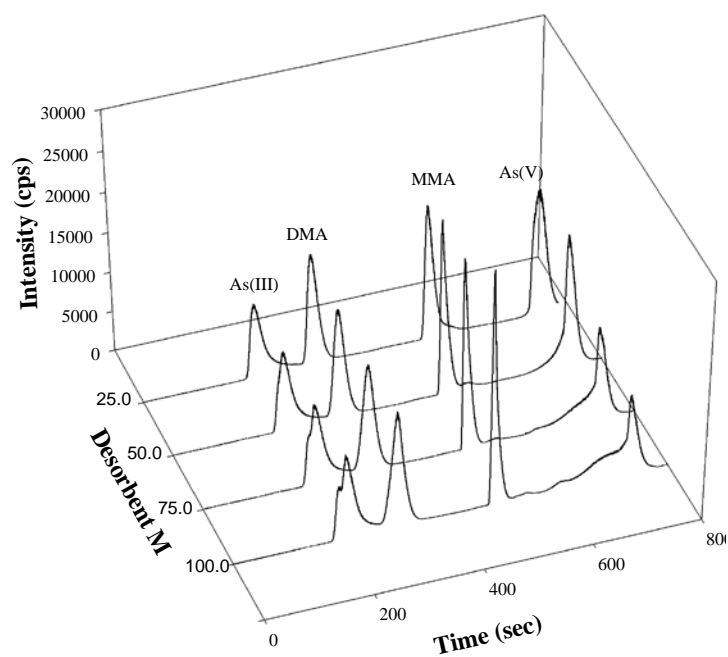


Figure 3.67. Effect of KH_2PO_4 concentration on arsenic peaks.

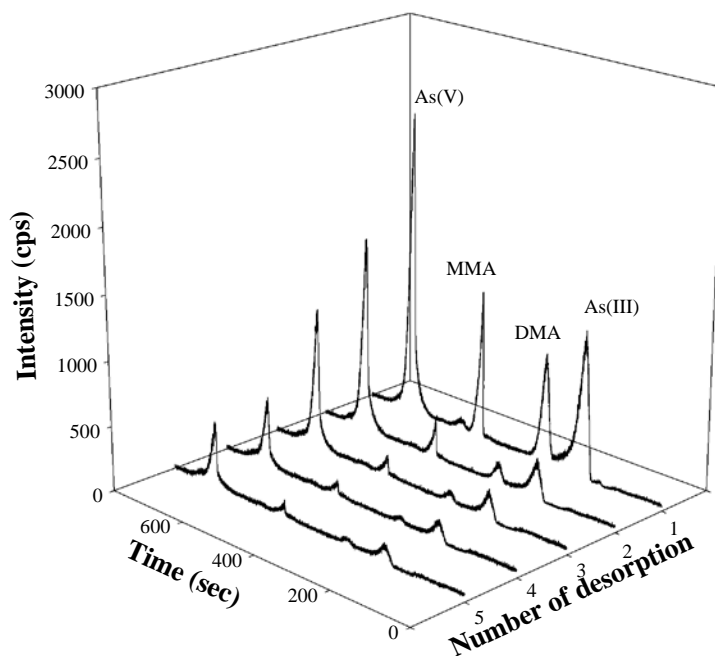


Figure 3.68. Repetitive desorption of As species from the same fiber. (Extraction conditions; extraction time: 30 min, As concentration: $10.0 \mu\text{gL}^{-1}$, solution pH: 7.0, solution volume: 15 mL; Desorption conditions; desorption time: 10 min, $150 \mu\text{L}$ 50.0 mM KH_2PO_4)

3.2.3.2. Optimization of Extraction Parameters

The developed SPME fibers were utilized for the determination of extraction parameters such as extraction pH, extraction time, agitation speed, and ionic strength. The optimized conditions were also applied to investigate fiber to fiber reproducibility.

3.2.3.2.1. Effect of pH on Extraction of Arsenic Species

The solution pH was expected to have a strong influence on the extraction of arsenic species since it affects both the charge on the surface of the fiber and the predominant form of arsenic in solution. Therefore, among the various parameters the priority was given to the optimization of extraction pH. The extraction efficiency using nanoiron-agarose as a function of solution pH was investigated at acidic, neutral, and basic pHs; namely, 4.0, 7.0 and 10.0 (Figure 3.69). The overall efficiency of extraction was maximized at pH 4.0 especially for As(V), DMA and MMA while pH 7.0 is optimum only for As(III) and not acceptable for the other arsenic species. None of the investigated arsenic species was effectively extracted under basic pH (10.0). For comparison, agarose fibers were also tested under the same experimental conditions and were shown to extract none of the arsenic species (Figure 3.70). In addition, AsB, the non-toxic form of arsenic, could not be extracted at any of the studied pHs by either nanoiron-agarose or agarose-fibers.

The effect of solution pH on the extraction can be rationalized by considering two phenomena; namely, the predominant forms of arsenic species at the indicated pH and also the possibility of variation of surface charge of the particles on the fiber. According to the previous report (Efecan et al. 2009), the Iso-Electric-Point (IEP) of nZVI particles was measured as 8.1-8.2. Thus, the surface of the fiber should be negatively charged at pH 10.0 where all arsenic species except AsB (which occurs in zwitterionic form) are also negatively charged. Therefore, no strong electrostatic interaction is expected at this pH. Lowering the pH to 7.0 results in the formation of less negative charge on As(V), DMA and MMA while As(III) is almost neutral. At the same time, the charge of the iron particles on the fiber surface is positive which attracts the negatively charged arsenic species in the solution. Although the further decrease in pH to 4.0 results in complete neutralization of As(III) and a reduced interaction with

positively charged surface of the fiber, the other species are still negatively charged and attracted strongly to the positively charged surface. Among the solution pHs investigated, pH 4.0 has been shown to be the optimum in terms of the amount of the arsenic species extracted. Therefore, the solution pH was adjusted to 4.0 in all the subsequent studies.

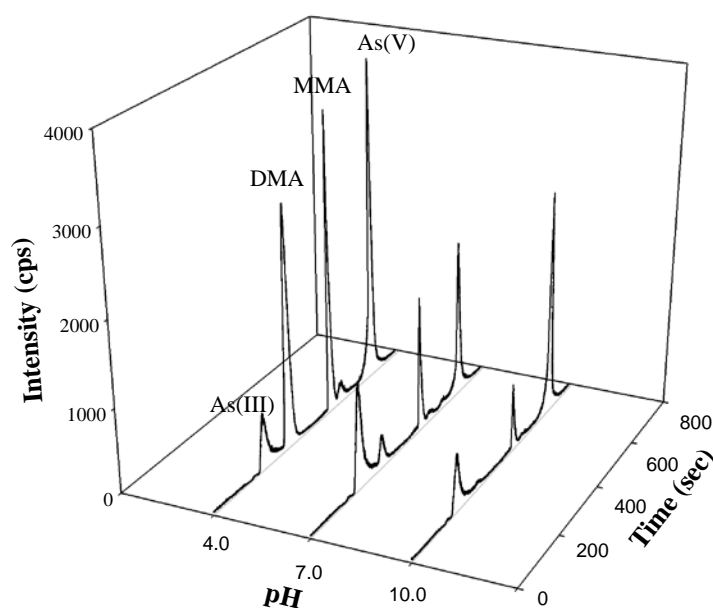


Figure 3.69. Effect of solution pH on extraction of As species by nanoiron-agarose fiber. (Extraction conditions; extraction time: 60 min, As concentration: $10.0 \mu\text{gL}^{-1}$, stirring speed: 300 rpm, solution volume: 15 mL, Desorption conditions; desorption time: 10 min, $150 \mu\text{L } 50.0 \text{ mM } \text{KH}_2\text{PO}_4$)

Generally speaking, the fixation mechanism of aqueous pollutants by iron nanoparticles is well known to encompass mainly two broad types: redox and surface sorption reactions. The redox mechanism is related to the zero-valent core of the nanoparticles and depends on the difference in reduction potentials between the contaminant and iron. Surface sorption, on the other hand, takes place between the pollutant entities in solution and the external oxyhydroxide groups (-OOH) of iron located in the shell of the nanoparticles. Arsenic possesses a more positive standard electrode potential relative to iron, and the amenability of As(III) and As(V) to reduction by nano iron core to form As(0) which was documented using high resolution X-ray photoelectron spectroscopy (HR-XPS) (Ramos et al. 2009). The oxyhydroxide layer on the external part of the

nanoparticles promotes arsenic sorption and/or coordination. Based on our characterization that showed iron nanoparticles to exist primarily as iron oxide, and the experimental observation of a pH-dependent retention, the operating fixation mechanism is most likely a surface sorption based on electrostatic attraction. Furthermore, in this study, the analytes were introduced into the HPLC column before and after extraction and the same retention times were observed for the inorganic arsenic species. This result eliminates the possibility of the reductive mechanism of extraction by produced fibers.

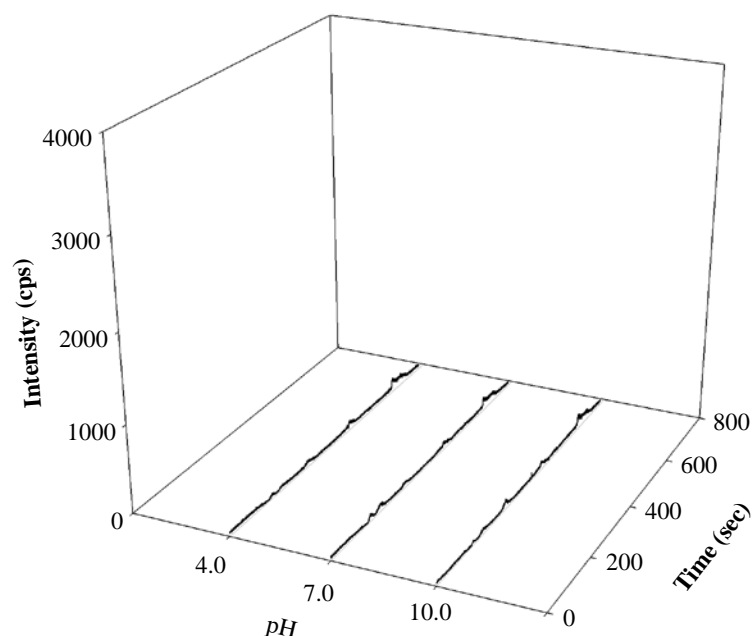


Figure 3.70. Effect of solution pH on extraction of As species by agarose fiber. (Extraction conditions; extraction time: 60 min, As concentration: $10.0 \mu\text{gL}^{-1}$, stirring speed: 300 rpm, solution volume: 15 mL, Desorption conditions; desorption time: 10 min, $150 \mu\text{L } 50.0 \text{ mM } \text{KH}_2\text{PO}_4$)

3.2.3.2.2. Effect of Agitation Time/Speed on Extraction of Arsenic Species

The agitation speed is one of the important parameters for the extraction procedure since the SPME fiber is immersed in the sample solution in a 20-mL vial. Agitation speeds of 300, 500, 700 and 1000 rpm were used to test this effect. According

to Figure 3.71, comparable extraction efficiencies were obtained at 500 and 700 rpm for DMA, MMA, and As(V) whereas maximum As(III) extraction was achieved at 700 rpm. A further increase in stirring speed to 1000 rpm resulted in a slight decrease in the amount of extracted analyte due to formation of vortex in the vial. Hence, 700 rpm was chosen as the optimum agitation speed in further studies in order to reach lower limits of detection for As(III) which is the most toxic form of all.

For evaluation of the effect of duration of interaction, immersion times of 1, 5, 15, 30 and 60 min were tested while holding the other parameters constant at the optimized values. In addition, in one study static extraction was also tested for a 5 min period. As demonstrated in Figure 3.72, an increase in the extraction time results in significant enhancement in the extracted amount of each arsenic species. Even at 60 min extraction time, equilibrium was not attained under the studied conditions; still, longer extraction times were not considered due to unreasonable time consumption. However, strict control of the extraction time was necessary throughout the study to overcome the possible deviations in extracted quantities of the analytes. This observation is very uncommon for head space analysis of solid phase microextraction. However, the diffusion-restricted extraction of each arsenic species was observed in the case of direct mode extraction applied in the present study. The extraction time of the fibers is mainly affected by the coating thickness, diffusion coefficient, and distribution constant of analyte between the fiber coating and the sample (Pawliszyn 1999). It should be mentioned here that the agarose coating on the fiber swells in just a few minutes when immersed in aqueous solution and the diameter of the fiber is doubled compared to its dry form. Nevertheless, the in-and-out motion of the fiber into the stainless steel injector was not affected from swelling of the coating.

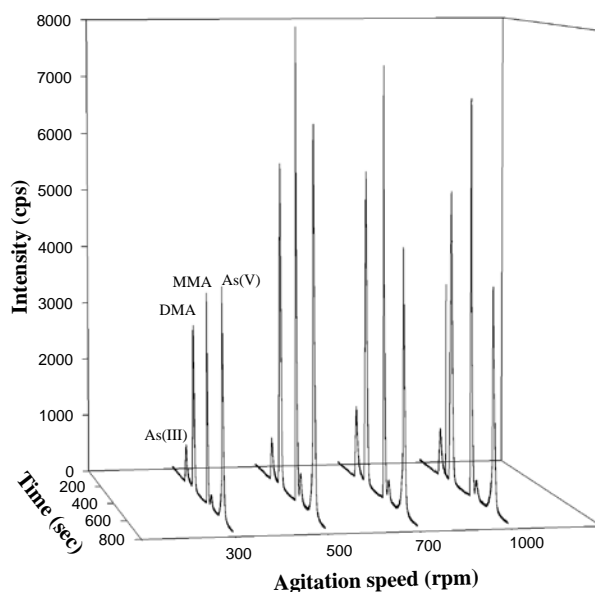


Figure 3.71. Effect of agitation speed on extraction of the As species. (Extraction conditions; extraction time: 60 min, As concentration: $10.0 \mu\text{gL}^{-1}$, solution pH: 4.0, solution volume: 15 mL, Desorption conditions; desorption time: 10 min, $150 \mu\text{L}$ 50.0 mM KH_2PO_4)

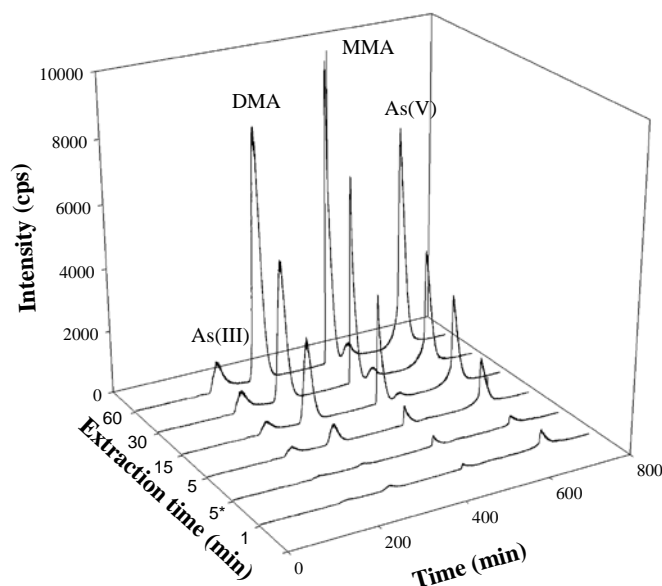


Figure 3.72. Effect of agitation time on extraction of the As species. (Extraction conditions; extraction time: 60 min, As concentration: $10.0 \mu\text{gL}^{-1}$, solution pH: 4.0, solution volume: 15 mL, stirring speed: 700 rpm. Desorption conditions; desorption time: 10 min, $150 \mu\text{L}$ 50.0 mM KH_2PO_4)

3.2.3.2.3. Effect of Salt Concentration (Ionic Strength) on Extraction of Arsenic Species

To investigate the effect of ionic strength on extraction of arsenic species, 10.0 μgL^{-1} concentrations of each arsenic species were prepared in 1.0 M, 0.10 M, 0.010 M and 0.0010 M NaCl and the solution pH was adjusted to 4.0. The results given in Figure 3.73 indicate that an enhanced extraction was achieved in the presence of NaCl matrix in comparison with the extraction performed in ultra pure water. This observation is in line with earlier results, especially in the case of organic species (Pawliszyn 1999). A NaCl concentration of 0.010 M was used in the subsequent studies.

The potential polyatomic interference due to the formation of $\text{Ar}^{40}\text{Cl}^{35}$ in the plasma at the same m/z : 75 during the measurement of monoistopic As^{75} by HPLC-ICPMS was also considered and prevented. For this purpose, a nanoiron-agarose fiber was immersed into 355.0 mgL^{-1} (0.010 M) Cl^{-} solution to test whether it extracted Cl^{-} under the optimized conditions used for arsenic speciation. In addition, octopole collision cell of the ICP-MS system was also used with He as the collision gas to overcome the potential interference of chloride ion on arsenic signal. With the experimental conditions explained above, no signal was observed at m/z :75 and m/z : 37 both in presence or absence of collision gas demonstrating that the affinity of the fiber for Cl^{-} ion was not appreciable (Figure 3.74). This finding is an indication of the an interference-free determination using the proposed methodology. In addition, the elution peak of Cl^{-} ion was determined by injection of 150 μL , 0.010 M NaCl solution into HPLC-ICPMS (Figure 3.75). The Cl^{-} ion peak was appeared around 500 sec in the chromatograms obtained at m/z : 37 (Figure 3.75(a) and Figure 3.75(c)). Chromatogram acquired at m/z : 75 (Figure 3.75(b)) shows a small peak related to $\text{Ar}^{40}\text{Cl}^{35}$ which was eliminated by additon of He gas into octopole collision cell (Figure 3.75(d)).

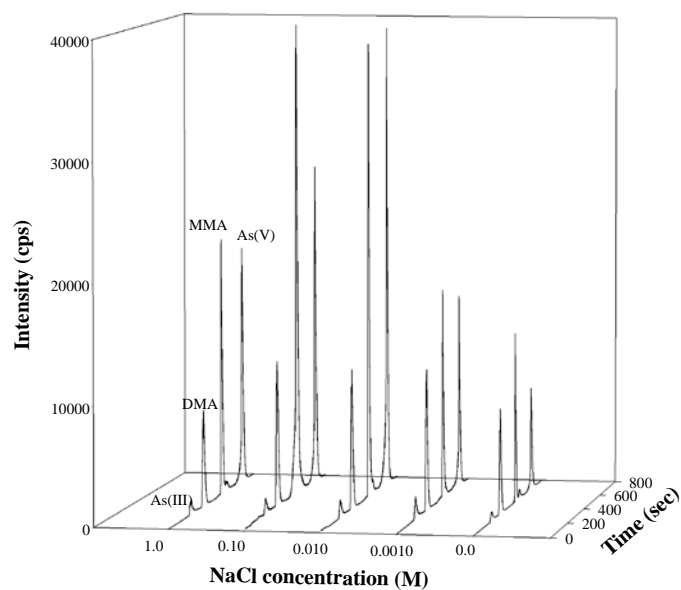


Figure 3.73. Effect of ionic strength on the extraction of the As species. (Extraction conditions; extraction time: 60 min, As concentration: $10.0 \mu\text{gL}^{-1}$, solution pH: 4.0, stirring speed: 700 rpm, solution volume: 15 mL, Desorption conditions; desorption time: 10 min, $150 \mu\text{L}$ 50.0 mM KH_2PO_4)

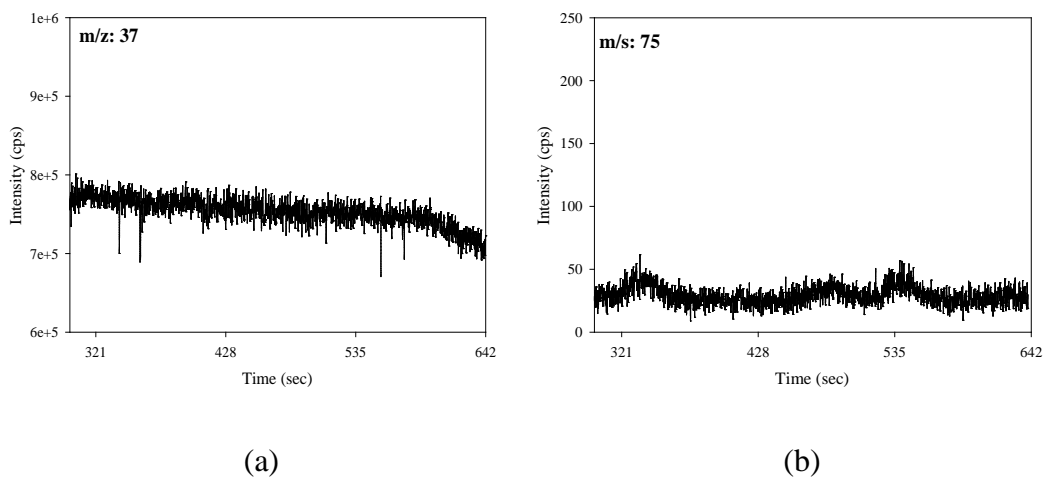
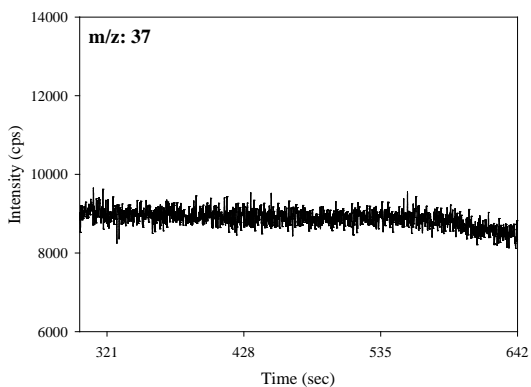
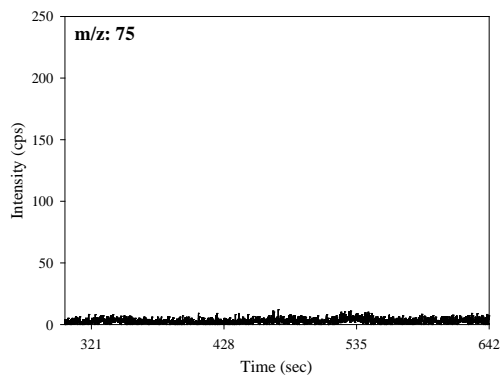


Figure 3.74. Chromatograms obtained with SPME-HPLC-ICPMS after inserting fiber into 0.010 M NaCl solution a) and b) no He in the octopole collision cell, c) and d) in the presence of He in the octopole collision cell.

(cont. on next page)

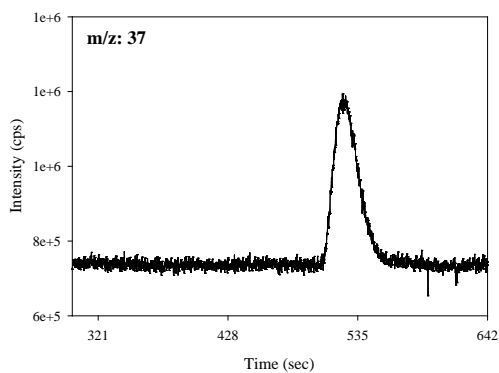


(c)

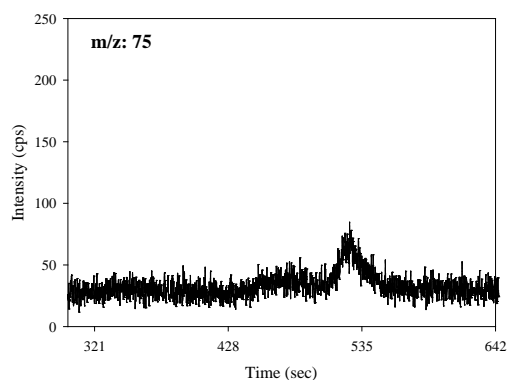


(d)

Figure 3.74. (cont.)



(a)



(b)

Figure 3.75. Chromatograms obtained after injection of 0.010 M NaCl to HPLC-ICPMS a) and b) no He in the octopole collision cell, c) and d) in the presence of He in the octopole collision cell.

(cont. on next page)

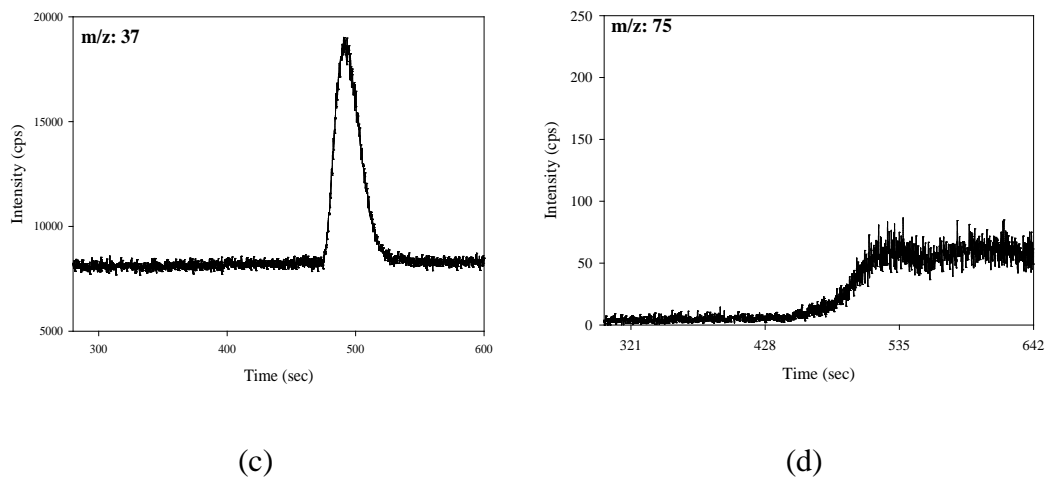


Figure 3.75. (cont.)

3.2.3.3. Interference Studies

Interference studies were performed for Sb(III), Sb(V), Se(IV), Se(VI), V(IV), V(V), SO_4^{2-} and PO_4^{3-} as described previously in Section 3.1.5.3. Table 3.8 demonstrated the effect of each species on extraction of As(III), DMA, MMA and As(V). Interfering case is described as $> 20\%$ decrease in peak area with respect to extraction performed excluding any interfering species. As understand from Table 3.8, Se(IV), V(IV), V(V), Sb(V) and PO_4^{3-} showed interference in extraction of all arsenic species. Se(VI) interfere only on extraction of organoarsenic species namely, DMA and MMA. In contrast to Se(VI), Sb(III) interfere on extraction of inorganic arsenic species namely, As(III) and As(V). On the other hand, addition of SO_4^{2-} ion shows interference on extraction of DMA and As(V).

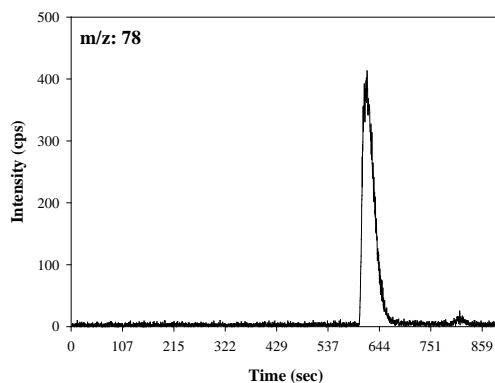
The extraction and elution of the Se(IV), Se(VI), V(IV), V(V), Sb(III) and Sb(V) were examined during the interference studies in conjunction with extraction of arsenicals. The chromatograms of the analytes (As(III), DMA, MMA and As(V)) after the extraction/desorption cycle in presence of the interfering species were acquired at m/z: 75. Apart from m/z: 75, the ions at m/z: 78, m/z 51 and m/z: 121 were detected in order examine the elution and extraction affinity of novel SPME fiber to Se(IV)/Se(VI), V(IV)/ V(V), and Sb(III)/Sb(V), respectively. The obtained chromatograms are demonstrated in Figures 3.76, 3.77 and 3.78. As it is understood from Figure 3.76, the novel fiber was also show considerdable extraction for Se(IV) while Se(VI) extraction

was less important. Similar results were obtained for extraction of V(IV) by the developed fiber. Both selenium and vanadium species were extracted in larger amount in their lower oxidation states. On the other hand, Sb(III) and Sb(V) showed similar trend both in the extraction by the fiber and elution from the column.

Table 3.6. Summary of the interference study; N: no interference, I: interference (Extraction conditions; extraction time: 60 min, As concentration: $10.0 \mu\text{gL}^{-1}$, solution pH: 4.0, stirring speed: 700 rpm, solution volume: 15 mL, Desorption conditions; desorption time: 10 min, $150 \mu\text{L}$ 50.0 mM KH_2PO_4)

Interfering species	As(III)	DMA	MMA	As(V)
Se(IV) ^a	I	I	I	I
Se(VI) ^a	N	I	I	N
V(IV) ^a	I	I	I	I
V(V) ^a	I	I	I	I
Sb(III) ^a	I	N	N	N
Sb(V) ^a	I	I	I	I
(SO_4^{2-}) ^b	I	N	I	N
(PO_4^{3-}) ^b	I	I	I	I

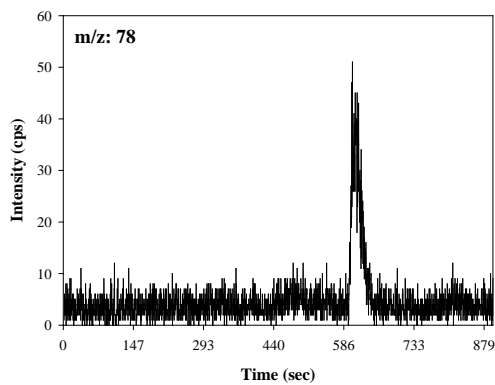
a: the concentration of the species was $100.0 \mu\text{gL}^{-1}$
b: the concentration of the species was $1000.0 \mu\text{gL}^{-1}$



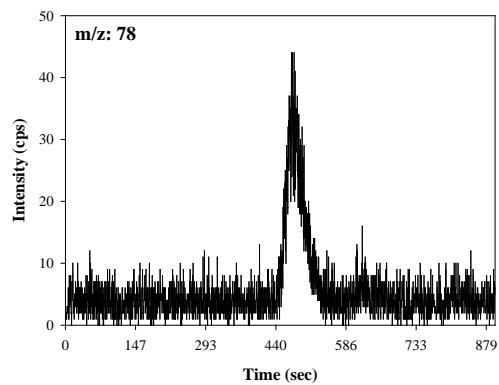
(a)

Figure 3.76. Selected ion monitoring chromatograms at m/z: 78 for selenium elution from HPLC-ICPMS obtained in selenium interference studies after extraction/desorption of arsenicals with nanoiron-agarose fibers a) Se(IV), b) Se(VI) and c) Se(VI) in the second data aquirement.

(cont. on next page)

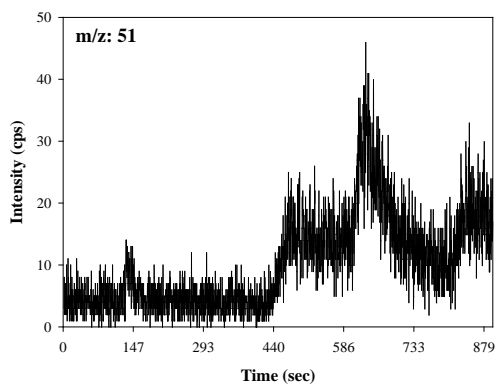


(b)

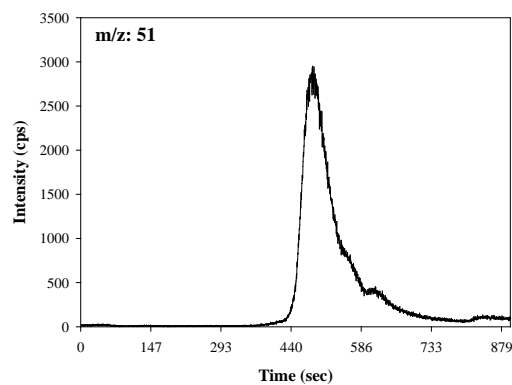


(c)

Figure 3.76. (cont.)



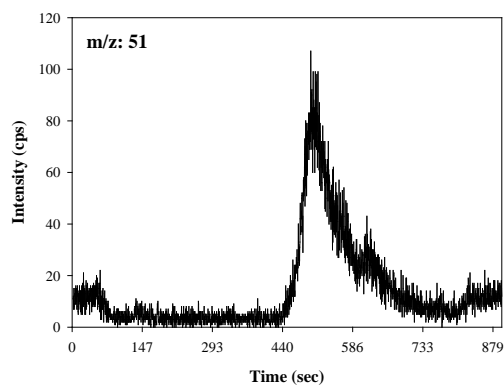
(a)



(b)

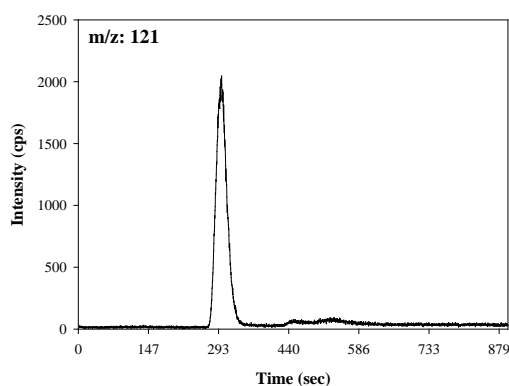
Figure 3.77. Selected ion monitoring chromatogram at m/z : 51 for vanadium elution from HPLC-ICPMS obtained in vanadium interference studies after extraction/desorption of arsenicals with nanoiron-agarose fibers a) V(IV), b) V(IV) in the second data acquisition and c) V(V)

(cont. on next page)

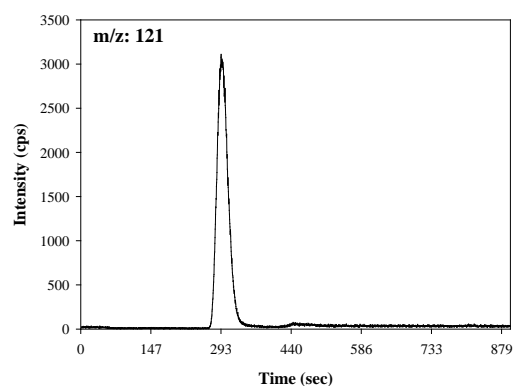


(c)

Figure 3.77. (cont.)



(a)



(b)

Figure 3.78. Selected ion monitoring chromatogram at m/z : 121 for antimony elution from HPLC-ICPMS obtained in antimony interference studies after extraction/desorption of arsenicals with nanoiron-agarose fibers a) Sb(III) and b) Sb(V).

3.2.3.4. Analytical Performance of the Method

Typical calibration line equations for each arsenic species obtained under optimized extraction condition with nanoiron-agarose fibers were given in Table 3.7 for both extraction conditions (ultra pure water and 0.010 M NaCl). The lower concentration of arsenicals in extraction solution was $0.10 \mu\text{gL}^{-1}$ while extraction from

10.0 μgL^{-1} was used as an upper point for the calibration. Obtained regression coefficients for each species showed good correlations between concentrations (x scale) and peak areas (y scale) of the extracted analytes, especially in the case of extractions in 0.010 M NaCl solution. In addition, the limit of detection (LOD), and the limit of quantification (LOQ) values for each As species were also calculated. In order to show the advantage of the developed method LOD and LOQ values of the HPLC-ICPMS without SPME were also determined (Table 3.8). The results have demonstrated that the developed SPME-HPLC-ICPMS methodology is superior in terms of detection limits with respect to the HPLC-ICPMS. Moreover, the analytical performance of the developed method was tested via relative standard deviations of the peak areas for intra-day and inter-day extractions of the analytes with 10 and 4 fibers, respectively (Table 3.9). The corresponding intra-day (and inter-day) RSDs were 15.5% (16.4%) for As(III), 8.3% (6.4%) for DMA, 7.3% (10.6%) for MMA and 6.5% (14.0%) for As(V).

Table 3.7. Typical calibration line equations obtained with prepared SPME fibers. (Extraction conditions; extraction time: 60 min, stirring speed: 700 rpm, solution volume: 15 mL, Desorption conditions; desorption time: 10 min, 150 μL 50.0 mM KH_2PO_4)

Species	Ultra-pure water				0.010 M NaCl	
	Equation	R ²	LOD μgL^{-1}	LOQ μgL^{-1}	Equation	R ²
As(III)	y= 20171x + 5792.7	0.9769	0.014	0.046	y= 28767x + 3072.2	0.9938
DMA	y= 243729x + 660.3	0.9991	0.006	0.021	y= 221457x - 5081.4	0.9994
MMA	y= 75657x + 28958	0.9843	0.022	0.073	y= 450683x + 22158	0.9984
As(V)	y= 296373x + 2408	0.9999	0.007	0.023	y= 468509x + 53620	0.9984

Table 3.8. Typical calibration line equations obtained with HPLC-ICPMS without extraction with SPME fiber

Species	Equation	R ²	LOD μgL^{-1}	LOQ μgL^{-1}
As(III)	y= 6441.6x - 811.72	0.9976	0.092	0.306
DMA	y= 9558.8x - 141.75	0.9998	0.104	0.346
MMA	y= 9958.9x - 524.01	0.9998	0.104	0.346
As(V)	y= 14578x - 48.05	0.9998	0.074	0.247

Table 3.9. Relative standard deviations obtained for inter-day and intra-day extractions (n= 4 and 10 for inter-day and intra-day extractions, respectively)

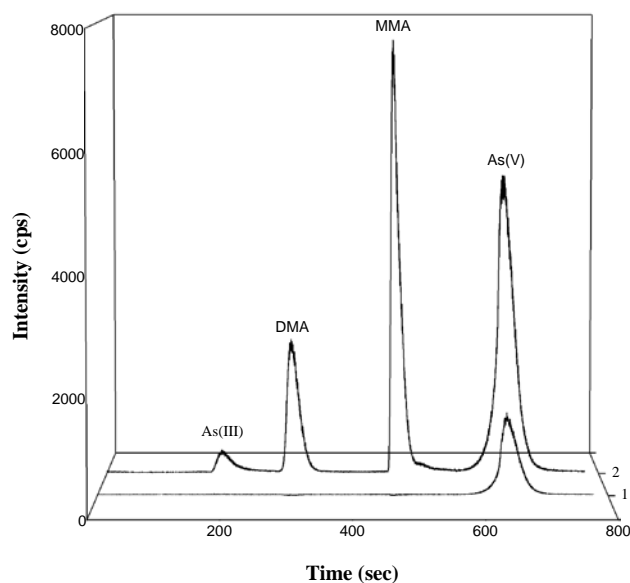
As Species	Inter-day RSD (%)	Intra-day RSD (%)
As(III)	15.5	16.4
DMA	8.3	6.4
MMA	7.3	10.6
As(V)	6.5	14.0

Extraction efficiency of the fibers was determined in order to verify the nature of extraction as being exhaustive or microextraction. In a typical experiment, extraction of As(III), DMA, MMA and As(V) was performed with nanoiron-agarose fibers under optimized conditions described before. The calibration plots of each species in ultra-pure water were obtained by injection of various concentrations of arsenicals into HPLC-ICPMS without extraction with SPME fiber. The solution containing arsenic species ($10.0 \mu\text{gL}^{-1}$ from each) was subjected to SPME procedure with nanoiron-agarose fibers. The concentration of the arsenicals in the original solution remaining after the extraction process was determined by HPLC-ICPMS. The extraction efficiency of the each species was found as 5.0%, 3.6%, 3.0% and 6.0% for As(III), DMA, MMA and As(V), respectively. The non-exhaustive nature of the extraction shows that the developed method is totally microextractive in nature.

3.2.3.5. Method Validation

The validation of the proposed method was performed by means of application to real samples and standard reference materials. Two different standard reference materials (SRM from NIST, Natural Water – Trace Elements, Cat. No. 1643e and Arsenic Species in Frozen Human Urine, Cat. No. 2669) were used for the validation of the method (Figure 3.79(a) and 3.79(b)). According to the results obtained and summarized in Table 3.10, with the proposed methodology, a good correlation between the certified and determined values was observed for all arsenic species. In addition to SRM analyses, tap water from IZTECH campus, geothermal water obtained from a well-known geothermal plant (Kızıldere/Aydın) and bottled water were analyzed for the

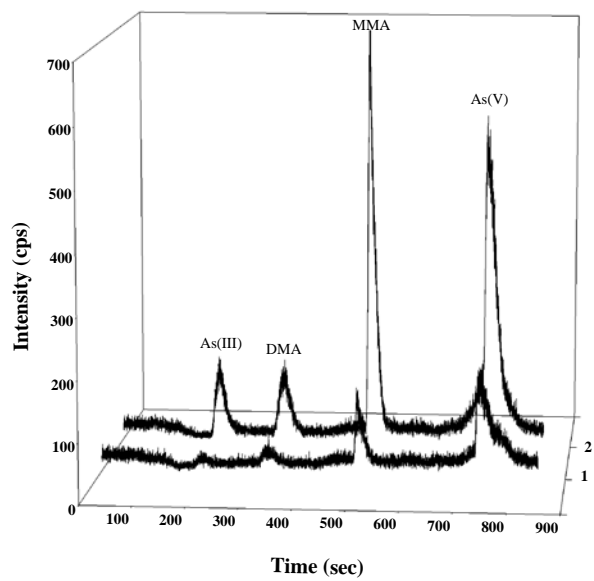
determination of arsenic species. The results are summarized in Table 3.11. The tap water (Figure 3.79(c)) and bottled water (Figure 3.79(d)) samples were expected to contain mainly inorganic As in higher oxidation state. As expected, due to the oxidizing conditions, all arsenicals were found in As(V) form at concentrations of $0.99 (\pm 0.14) \mu\text{gL}^{-1}$ and $1.57 (\pm 0.09) \mu\text{gL}^{-1}$ for tap water and bottled water, respectively. On the other hand, the geothermal water (Figure 3.79(e)) sample contained both As(III) ($235 \mu\text{gL}^{-1}$) and As(V) ($715 \mu\text{gL}^{-1}$) since reducing conditions prevail in ground waters. An unknown arsenic species was also observed in the chromatogram of geothermal water. Due to high sulfur content of the geothermal water (*ca.* 1000 mgL^{-1}), the new species most probably is the thioarsenate which is generally found in sulfidic waters (Planer and Wallschlager 2009; Planer et al. 2010).



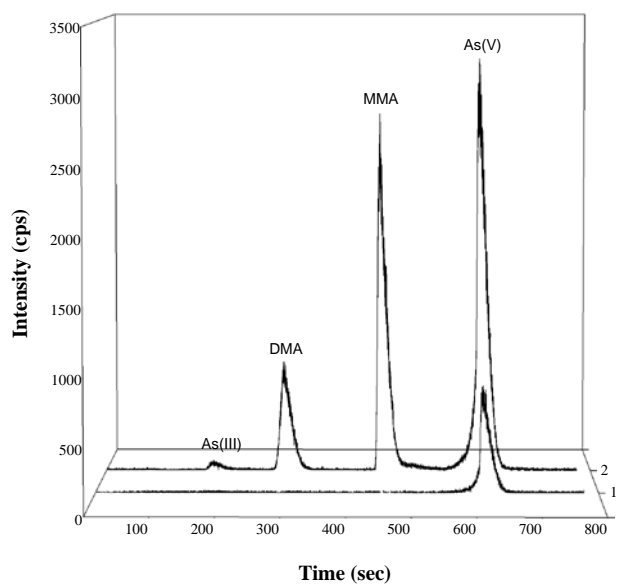
(a)

Figure 3.79. Chromatograms obtained from validation study for a) SRM 1643e (Natural Water, No.1: 10-fold diluted sample and No.2: spiked with $10.0 \mu\text{gL}^{-1}$ of each arsenic species), b) SRM 2669 (Human Urine, No.1: 10-fold diluted sample and No.2: spiked with $2.0 \mu\text{gL}^{-1}$ of each arsenic species), c) Tap water (No.1: 2-fold diluted sample and No.2: spiked with $1.0 \mu\text{gL}^{-1}$ of each arsenic species), d) Bottled water (No.1: 2-fold diluted sample and No.2: spiked with $2.0 \mu\text{gL}^{-1}$ of each arsenic species) and Geothermal water (No.1: 50-fold diluted sample and No.2: spiked with $10.0 \mu\text{gL}^{-1}$ of each arsenic species). (Extraction conditions; extraction time: 60 min, solution pH: 4.0, stirring speed 700 rpm, solution volume: 15 mL, Desorption conditions; desorption time: 10 min, $150 \mu\text{L } 50.0 \text{ mM } \text{KH}_2\text{PO}_4$)

(cont. on next page)



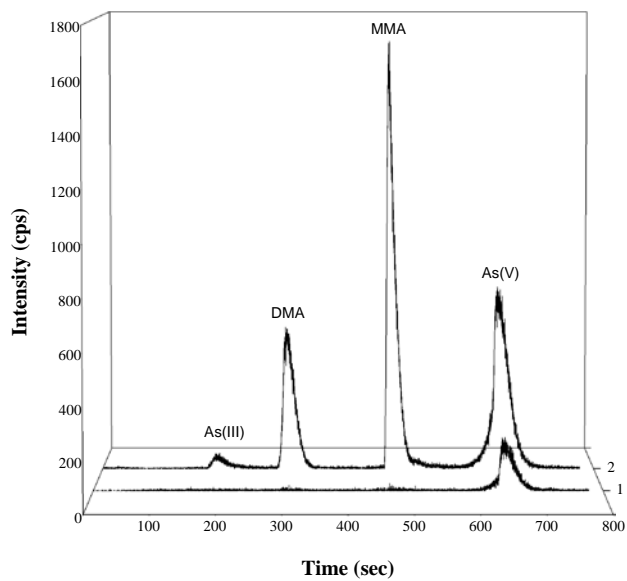
(b)



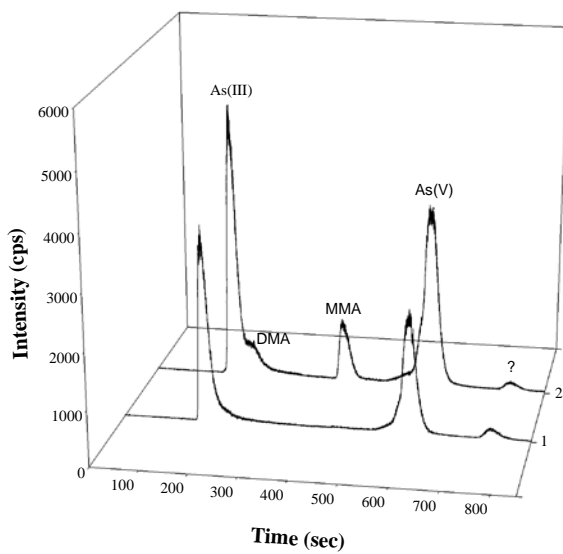
(c)

Figure 3.79. (cont.)

(cont. on next page)



(d)



(e)

Figure 3.79. (cont.)

Table 3.10. Method validation with novel SPME fibers. (Extraction conditions; extraction time: 60 min, solution pH: 4.0, stirring speed 700 rpm, solution volume: 15 mL, Desorption conditions; desorption time: 10 min, 150 μ L 50.0 mM KH_2PO_4 .)

As species	SRM 1643e ^a		SRM 2669 ^a	
	Determined μgL^{-1}	Certified μgL^{-1}	Determined μgL^{-1}	Certified μgL^{-1}
As(III)	ND*		4.56	5.03
DMA	ND		23.67	25.3
MMA	ND		6.17	7.18
As(V)	59.00	60.45**	6.15	6.16

a: extractions were performed in 1/10 diluted samples

* Not detected

** Speciation of arsenic in SRM 1643e was not indicated in the certificate.

Table 3.11. Sample applications with novel SPME fibers. (Extraction conditions; extraction time: 60 min, solution pH: 4.0, stirring speed 700 rpm, solution volume: 15 mL, Desorption conditions; desorption time: 10 min, 150 μ L 50.0 mM KH_2PO_4 , n=3)

As species	Bottled water ^a	Tap water ^a	Geothermal water ^b	Urine ^c
	μgL^{-1}	μgL^{-1}	μgL^{-1}	μgL^{-1}
As(III)	ND*	ND	235 (\pm 27)	ND
DMA	ND	ND	ND	0.34 (\pm 0.06)
MMA	ND	ND	ND	0.67 (\pm 0.05)
As(V)	1.57 (\pm 0.09)	0.99 (\pm 0.14)	715 (\pm 18)	ND

a: extractions were performed in 1/2 diluted samples

b: extractions were performed in 1/500 diluted samples

c: extractions were performed in 1/10 diluted samples

* Not detected

CHAPTER 4

CONCLUSIONS

The thesis progressed in two main routes, namely, solid phase extraction and solid phase microextraction. The solid phase extraction part of the study was performed with amine- and/or mercapto- functionalized silica for the speciation of As(III) and As(V). The solid phase microextraction part was about the preparation of stable and selective fiber coatings and their application for the determination of inorganic and organometallic arsenic species.

The main results of SPE studies can be summarized as follows:

A bifunctional sorbent, (NH₂+SH)silica, containing both amine and mercapto functionalities, was prepared by modification of silica gel with 3-(triethoxysilyl)propylamine and (3-mercaptopropyl)trimethoxysilane. In addition to the bifunctional sorbent, silica gel was modified individually with the functional mercapto- and amino-silanes. Moreover, monofunctional sorbents, namely (SH)silica and (NH₂)silica, were also mechanically mixed ((NH₂)silica+(SH)silica) for the sake of comparison of sorption performances. The prepared sorbents were used for sorption of As(III) and As(V), and the sorption results demonstrated the high specificity of the sorbents. For example, mercapto-functionalized (SH)silica shows selectivity only to As(III) and retains the species quantitatively at the pH of 1.0 and 9.0. The mechanism of sorption can be attributed to the chelate formation between the arsenite ions in the solution and the mercapto functional groups on the silica surface. Amine-functionalized (NH₂)silica, on the other hand, displays sorption only to As(V) at pH 3.0, due to electrostatic attraction between the protonated amine groups of the sorbent and H₂AsO₄⁻ ion which is the predominant species in the solution at this pH. The strong dependence of the sorption of (NH₂)silica on the solution pH necessitates the use of a buffer to fix the pH at 3.0 to prevent the possible increase of the pH to higher values where no sorption of As(V) occurs. Bifunctional (NH₂+SH)silica has shown superior sorption performance compared to the mono-functionalized sorbents in terms of solution pH, sorbent amount, reaction time, reaction temperature, and batch-to-batch reproducibility. Bifunctional (NH₂+SH)silica makes the speciation of As(III) and As(V) possible by

enabling the sorption of both As(III) and As(V) species at pH 3.0 and only As(III) at pH 1.0 or any pH higher than 4.0. As(V) can then be determined from the difference. Eluents, such as 0.05 M KIO₃ in 2.0 M HCl and 1.0% (w/w) L-cysteine can be used for the desorption of As(III) and As(V), respectively. However, simultaneous quantitative desorption of both As(III) and As(V) can only be achieved using 0.5 M NaOH, bearing in mind that this eluent restricts the use of the silica-based sorbents to only once. The validity of the proposed method was checked through the analysis of a standard reference material and a good correlation was obtained between the certified (26.67 μg L⁻¹) and determined (27.53±0.37 μg L⁻¹) values. Spike recovery tests realized with ultrapure water (93.0±2.3%) and drinking water (86.9±1.2%) also confirmed the applicability of the method.

SPME fibers were prepared mainly in two general approaches, namely, the sol-gel based modification and nanoparticle immobilization. The experience gained during the modification of silicate surface was used for preparation of the novel sol-gel based SPME fiber coatings. Homogeneity and coating thickness of the fibers was controlled by dip coating. In addition to the dip coated sol-gel based fibers, electrospinning was also used to prepare sol-gel coated SPME fibers. Nanoparticle immobilized fibers were produced by capillary template and electrospinning methods. Capillary template method was used for the first time to prepare SPME fiber coatings. This method has shown superior performance in controlling the thickness of coatings. The other advantages of the proposed method were the ease of preparing stable fiber coatings and inert matrix allowing the immobilization of various functional nanoparticles onto fiber, and also the fiber-to-fiber reproducibility obtained. Electrospun nanofiber coated SPME fibers were also promising for improved extraction time since all the functional groups of the nanofiber were available for extraction.

The amine-functionalized SPME fiber produced by sol-gel method was used for As(III), DMA, MMA and As(V) and all arsenic species except As(III) were extracted. Better detection limits were achieved with HPLC-ICPMS than HPLC-HGAAS. Optimization of amine-functionalized fiber coating revealed that the fibers coated by electrospinning process showed superior performance than dip coated fibers. The extracted amounts of analytes were shown to be affected from various parameters, namely, solution pH, ionic strength and extraction time.

Nanoiron-agarose fibers produced by capillary template method were used as novel stable and selective SPME fiber coating for the determination of various

inorganic and organoarsenic species; namely, As(III), DMA, MMA and As(V). Although the iron-based materials are well known for the removal of inorganic As(III) and As(V) from aqueous solutions, the extraction of the organoarsenicals, DMA and MMA, with iron nanoparticles was reported for the first time in literature. Extracted analytes were separated with anion exchange column and determined with online connection to ICP-MS. Optimization of the chromatographic conditions indicate that all arsenic species are well separated in 11 min by gradient elution program (0-4 min, 10 mM ammonium carbonate (pH 8.50), 4.1-12 min, 30 mM ammonium carbonate (pH 8.50)) at flow rate of 1.0 mL.min⁻¹. Extensive studies for extraction conditions have given the optimized parameters as; extraction pH: 4.0, agitation speed: 700 rpm, extraction time: 60 min. The fibers demonstrated reproducible extraction (< 10% rsd), good mechanical strength and good solvent resistivity. The validity of the proposed methodology was verified via the analysis of certified reference materials (SRM 1643e, Natural Water-Trace Elements, and SRM 2669, Arsenic Species in Frozen Human Urine) and through spike recovery tests. The values of percentage recovery for SRM 2669 were 90.7% for As(III), 99.8% for As(V), 93.6% for DMA, and 85.9% for MMA. A good correlation was also found between the certified (60.45 µgL⁻¹) and determined (59.00 µgL⁻¹) values for SRM 1643e. Moreover, the speciation capability of the method was demonstrated on various natural waters and biological fluids. Additionally, the developed method has been shown to possess superior performance figures than the available SPME fibers in terms of simultaneous determination capability of four critical arsenical compounds without requirement for a derivatization step.

Finally, it can be said that this study incorporates various multidisciplinary fields of chemistry such as analytical chemistry, nanoscience, organic chemistry and physical chemistry with the intention of preparation novel SPE sorbents and SPME fiber coatings. The main outcomes of the SPE study were the potential applicability of the prepared sorbents for both water remediation and analytical applications. The prepared SPE sorbents have potential for daily use as a resin for arsenic removal from waters without taking into consideration the form of arsenic. New SPME fiber coating strategies were introduced for the first time to prepare a variety of stable functional coatings. These suggest new ideas for the researchers in the related area for preparation of more specific coatings. Besides, the prepared fibers were effective in determination of four critical arsenic species in trace levels. The prepared SPME fibers are also promising to follow the arsenic metabolism in biological systems. It is hoped that the

aforementioned outcomes of the results of the thesis will be promising and directive for researchers in the related fields as well as for researchers from other disciplines.

REFERENCES

- Ackley, K.L., C. B'Hymer, K.L. Sutton, J.A. Caruso. 1999. Speciation of arsenic in fish tissue using microwave-assisted extraction followed by HPLC-ICP-MS. *Journal of Analytical Atomic Spectrometry* 14: 845-850.
- Afton, S., K. Kubachka, B. Catron, J.A. Caruso. 2008. Simultaneous characterization of selenium and arsenic analytes via ion-pairing reversed phase chromatography with inductively coupled plasma and electrospray ionization ion trap mass spectrometry for detection Applications to river water, plant extract and urine matrices. *Journal of Chromatography A* 1208: 156-163.
- Ahmad, U.K., A.R. Yacob, G. Selvaraju. 2008. A home-made SPME fiber coating for arson analysis. *The Malaysian Journal of Analytical Sciences* 12(1): 32-38.
- Alhooshani, K., T.Y. Kim, A. Kabir, A. Malik. 2005. Sol-gel approach to in situ creation of high pH-resistant surface-bonded organic-inorganic hybrid zirconia coating for capillary microextraction. *Journal of Chromatography A* 1062: 1-14.
- Ammann, A.A. 2010. Arsenic speciation by gradient anion exchange narrow bore ion chromatography and high resolution inductively coupled plasma mass spectrometry detection. *Journal of Chromatography A* 1217: 2111-2116.
- Arakaki, L.N.H. and C. Airoidi. 2000. Ethyleneimine in the synthetic routes of a new silylating agent: chelating ability of nitrogen and sulfur donor atoms after anchoring onto the surface of silica gel. *Polyhedron* 19: 367-373.
- Augusto, F., E. Carasek, R.G.C. Silva, S.R. Rivellino, A.D. Batista, E. Martendal. 2010. New sorbents for extraction and microextraction techniques. *Journal of Chromatography A* 1217: 2533-2542.
- Azenha, M., M. Ornelas, A.F. Silva. 2009. Solid-phase microextraction Ni-Ti fibers coated with functionalised silica particles immobilized in a sol-gel matrix. *Journal of Chromatography A* 1216: 2302-2306.
- Bagheri, H., E. Babanezhad, F. Khalilian. 2008. A novel sol-gel-based amino-functionalized fiber for headspace solid-phase microextraction of phenol and chlorophenols from environmental samples. *Analytica Chimica Acta* 616: 49-55.

- Bagheri, H., Z. Ayazi, E. Babanezhad. 2010. A sol-gel-based amino functionalized fiber for immersed solid-phase microextraction of organophosphorus pesticides from environmental samples. *Microchemical Journal* 94: 1-6.
- Bail, P., G. Stuebiger, H. Unterweger, G. Buchbauer, S. Krist. 2009. Characterization of volatile compounds and triacylglycerol profiles of nut oils using SPME-GC-MS and MALDI-TOF-MS. *European Journal of Lipid Science and Technology* 111: 170-182.
- Bianchi, F., F. Bisceglie, M. Careri, S.D. Berardino, A. Mangia, M. Musci. 2008. Innovative sol-gel coatings for solid-phase microextraction development of fibers for the determination of polycyclic aromatic hydrocarbons at trace level in water. *Journal of Chromatography A* 1196-1197: 15-22.
- Biazon, C.L., R. Brambilla, A. Rigacci, T.M. Pizzolato, J.H.Z. Santos. 2009. Combining silica-based adsorbents and SPME fibers in the extraction of the volatiles of beer: an exploratory study. *Analytical and Bioanalytical Chemistry* 394: 549-556.
- Blitz, I.P., J.P. Blitz, V.M. Gun'ko, D.J. Sheeran. 2007. Functionalized silicas: Structural characteristics and adsorption of Cu(II) and Pb(II). *Colloids and Surfaces A* 307: 83-92.
- Bohari, Y., G. Lobos, H. Pinochet, F. Pannier, A. Astruc, M. Potin-Gautier. 2002. Speciation of arsenic in plants by HPLC-HG-AFS: extraction optimisation on CRM materials and application to cultivated samples. *Journal of Environmental Monitoring* 4: 596-602.
- Boyacı, E., A.E. Eroğlu, T. Shahwan. 2010. Synthesis, characterization and application of a novel mercapto- and amine-bifunctionalized silica for speciation/sorption of inorganic arsenic prior to inductively coupled plasma mass spectrometric determination. *Talanta* 80: 1452-1460.
- Budziak, D., E. Martendal, E. Carasek. 2007. Preparation and application of NiTi alloy coated with ZrO₂ as a new fiber for solid-phase microextraction. *Journal of Chromatography A* 1164: 18-24.
- Budziak, D., E. Martendal, E. Carasek. 2009. Application of an NiTi alloy coated with ZrO₂ solid-phase microextraction fiber for determination of haloanisoles in red wine samples. *Microchimica Acta* 164: 197-202.

- Bundaleska, J.M., T. Stafilov, S. Arpadjan. 2005. Direct analysis of natural waters for arsenic species by hydride generation atomic absorption spectrometry. *International Journal of Environmental Analytical Chemistry* 85: 199-207.
- Burke, A.M., J.P. Hanrahan, D.A. Healy, J.R. Sodeau, J.D. Holmes, M.A. Morris. 2008. Large pore bi-functionalised mesoporous silica for metal ion pollution treatment. *Journal of Hazardous Materials* 164: 229-234.
- Calatayud, M., J. Gimeno, D. Velez, V. Devesa, R. Montoro. 2010. Characterization of the intestinal absorption of arsenate, monomethylarsonic acid, and dimethylarsinic acid using the Caco-2 cell line. *Chemical Research in Toxicology* 23: 547-556.
- Cao, D., J. Lu, J. Liu, G. Jiang. 2008. In situ fabrication of nanostructured titania coating on the surface of titanium wire: A new approach for preparation of solid-phase microextraction fiber. *Analytica Chimica Acta* 611: 56-61.
- Carpinteiro, M.I., I. Rodríguez, R. Cela, M. Ramil. 2009. Headspace solid-phase microextraction of halogenated toluenes in environmental aqueous samples with polypropylene microporous membranes. *Journal of Chromatography A* 1216: 2825-2831.
- Chaves, A.R., G. Chiericato, M.E.C. Queiroz. 2009. Solid-phase microextraction using poly(pyrrole) film and liquid chromatography with UV detection for analysis of antidepressants in plasma samples. *Journal of Chromatography B* 877: 587-593.
- Chen, W., J. Zeng, J. Chen, X. Huang, Y. Jiang, Y. Wang, X. Chen. 2009. High extraction efficiency for polar aromatic compounds in natural water samples using multiwalled carbon nanotubes/Nafion solid-phase microextraction coating. *Journal of Chromatography A* 1216 (52): 9143-9148.
- Choong, T.S.Y, T.G. Chuah, Y. Robiah, F.L.G. Koay, I. Azni. 2007. Arsenic toxicity, health hazards and removal techniques from water: an overview. *Desalination* 217: 139-166.
- Cui, X.Y., Z.Y. Gu, D.Q. Jiang, Y. Li, H.F. Wang, X.P. Yan. 2009. In situ hydrothermal growth of metal-organic framework 199 films on stainless steel fibers for solid-phase microextraction of gaseous benzene homologues *Analytical Chemistry* 8: 9771-9777.

- Cumbal, L. and A.K. Sengupta. 2005. Arsenic removal using polymer-supported hydrated iron(III) oxide nanoparticles: role of donnan membrane effect. *Environmental Science and Technology* 39: 6508-6515.
- Day, J.A., M. Montes-Bayón, A.P. Vonderheide, J.A. Caruso. 2002. A study of method robustness for arsenic speciation in drinking water samples by anion exchange HPLC-ICP-MS. *Analytical and Bioanalytical Chemistry* 373: 664-668.
- Djozan, D., M. Mahkam, B. Ebrahimi. 2009. Preparation and binding study of solid-phase microextraction fiber on the basis of ametryn-imprinted polymer Application to the selective extraction of persistent triazine herbicides in tap water, rice, maize and onion. *Journal of Chromatography A* 1216: 2211–2219.
- Dietz, C., T.P. Corona, Y.M. Albarran, C. Camara. 2003. SPME for on-line volatile organo-selenium speciation. *Journal of Analytical Atomic Spectrometry* 18: 467-473.
- Dietz, C., J. Sanz, C. Camara. 2006. Recent developments in solid-phase microextraction coatings and related techniques. *Journal of Chromatography A* 1103: 183–192.
- Dominguez, L., Z. Yue, J. Economy, C.L. Mangun. 2002. Design of polyvinyl alcohol mercaptyl fibers for arsenite chelation. *Reactive and Functional Polymers* 53: 205-215.
- Efecan, N., T. Shahwan, A.E. Eroğlu, I. Lieberwirth. 2009. Characterization of the uptake of aqueous Ni(2+) ions on nanoparticles of zero-valent iron (nZVI). *Desalination* 249: 1048–1054.
- El-Ashgar, N.M., I.M. El-Nahhal. 2005. Preconcentration and separation of copper(II) by 3-aminopropylpolysiloxane immobilized ligand system. *Journal of Sol-Gel Science and Technology* 34: 165-172.
- El-Nahhal, I.M., F.R. Zaggout, N.M. El-Ashgar. 2000. Uptake of divalent metal ions (Cu²⁺/Zn²⁺ and Cd²⁺) by polysiloxane immobilized monoamine ligand system. *Analytical Letters* 33: 2031-2053.
- El-Nahhal, I.M., B.A. El-Shetary, K.A.R. Salib, N.M. El-Ashgar, A.M. El-Hashash. 2001. Uptake of divalent metal ions (Cu²⁺, Ni²⁺, and Co²⁺) by polysiloxane immobilized triamine-thiol and thiol-acetate ligand system. *Analytical Letters* 34: 2189-2202.

- El-Nahhal, I.M., B.A. El-Shetary, K.A.R. Salib, N.M. El-Ashgar, A.M. El-Hashash. 2002. Polysiloxane-immobilized triamine ligand system, synthesis and applications. *Phosphorus, Sulfur, and Silicon and the Related Elements* 177: 741-753.
- El-Nahhal, I.M., N.M. El-Ashgar. 2007. A review on polysiloxane-immobilized ligand systems: Synthesis, characterization and applications. *Journal of Organometallic Chemistry* 692: 2861-2886.
- Erdem, A. and A.E. Eroğlu. 2005. Separation of trace antimony and arsenic prior to hydride generation atomic absorption spectrometric determination. *Talanta* 68: 86-92.
- Farhadi, K., R. Tahmasebi, R. Maleki. 2009. Preparation and application of the titania sol-gel coated anodized aluminum fibers for headspace solid phase microextraction of aromatic hydrocarbons from water samples. *Talanta* 77: 1285-1289.
- Gbatu, T.P., K.L. Sutton, J.A. Caruso. 1999. Development of new SPME fibers by sol-gel technology for SPME-HPLC determination of organometals. *Analytica Chimica Acta* 402: 67-79.
- Gbatu, T.P., O. Ceylan, K.L. Sutton, J.F. Rubinson, A. Galal, J.A. Caruso, H.B. Mark, Jr. 1999. Electrochemical control of solid phase micro-extraction using unique conducting polymer coated fibers. *Analytical Communications* 36: 203-205.
- Guibal, E., S. Milot, J.M. Tobin. 1998. Metal-anion sorption by chitosan beads: Equilibrium and kinetic studies. *Industrial and Engineering Chemical Research* 37:1453-1463.
- Hao, J., M.J. Han, X. Meng. 2009. Preparation and evaluation of thiol-functionalized activated alumina for arsenite removal from water. *Journal of Hazardous Materials* 167: 1215-1221.
- Hashemi, P., M. Shamizadeh, A. Badiei, A.R. Ghiasvand, K. Azizi. 2009. Study of the essential oil composition of cumin seeds by an amino ethyl-functionalized nanoporous SPME fiber. *Chromatographia* 70 (7/8): 1147-1151.
- He, J., Z. Liu, P. Dou, J. Liu, L. Ren, H.Y. Chen. 2009. Electrochemically deposited boronate affinity extracting phase for covalent solid phase microextraction of cis-diol biomolecules. *Talanta* 79: 746-751.

- Ho, K.Y., G. McKay, K.L. Yeung. 2003. Selective adsorbents from ordered mesoporous silica. *Langmuir* 19: 3019-3024.
- Howard, A.G. and L.E. Hunt. 1993. Coupled photooxidation hydride AAS detector for the HPLC of arsenic compounds. *Analytical Chemistry* 65: 2995-2998.
- Hu, W., F. Zheng, B. Hu. 2008. Simultaneous separation and speciation of inorganic As(III)/As(V) and Cr(III)/Cr(VI) in natural waters utilizing capillary microextraction on ordered mesoporous Al₂O₃ prior to their on-line determination by ICP-MS. *Journal of Hazardous Materials* 151: 58-64.
- Huang, C., B. Hu, Z. Jiang. 2007. Simultaneous speciation of inorganic arsenic and antimony in natural waters by dimercaptosuccinic acid modified mesoporous titanium dioxide micro-column on-line separation and inductively coupled plasma optical emission spectrometry determination. *Spectrochimica Acta, Part B* 62: 454-460.
- Huang, K.P., G.R. Wang, B.Y. Huang, C.Y. Liu. 2009. Preparation and application of ionic liquid-coated fused-silica capillary fibers for solid-phase microextraction. *Analytica Chimica Acta* 645: 42-47.
- Huck, C.W and G.K. Bonn. 2000. Recent developments in polymer-based sorbents for solid-phase extraction. *Journal of Chromatography A* 885: 51-72.
- Jal, P.K., S. Patel, B.K. Mishra. 2005. Chemical modification of silica surface by immobilization of functional groups for extractive concentration of metal ions. *Talanta* 62: 1005-1028.
- Jiang, R., F. Zhu, T. Luan, Y. Tong, H. Liu, G. Ouyang, J. Pawliszyn. 2009. Carbon nanotube-coated solid-phase microextraction metal fiber based on sol-gel technique. *Journal of Chromatography A* 1216: 4641-4647.
- Kannamkumarath, S.S., K. Wrobel, K. Wrobel, J.A. Caruso. 2004. Speciation of arsenic in different types of nuts by ion chromatography-inductively coupled plasma mass spectrometry. *Journal of Agriculture and Food Chemistry* 52: 1458-1463.
- Kataoka, H. 2010. Recent developments and applications of microextraction techniques in drug analysis. *Analytical and Bioanalytical Chemistry* 396: 339-364.

- Kaur, V., A.K. Malik, N. Verma. 2006. Applications of solid phase microextraction for the determination of metallic and organometallic species. *Journal of Separation Science* 29: 333–345.
- Kavitha, D. and C. Namasivayam. 2007. Recycling coir pith, an agricultural solid waste, for the removal of procion orange from wastewater. *Dyes and Pigments* 74:237-248.
- Killelea, D.R. and J.H. Aldstadt. 2002. Identification of dimethylchloroarsine near a former herbicide factory by headspace solid-phase microextraction gas chromatography-mass spectrometry. *Chemosphere* 48: 1003–1008.
- Kloskowski, A. and M. Pilarczyk. 2009. Membrane solid-phase microextractions A new concept of sorbent preparation. *Analytical Chemistry* 81: 7363–7367.
- Koning, S., H.G. Janssen, U.A. Brinkman. 2009. Modern methods of sample preparation for GC analysis. *Journal of Chromatography A* 69: 33-78.
- Kösters, J., R.A.D. Bone, B.P. Friedrich, B. Rothweiler, A.V. Hirner. 2003. Identification of organic arsenic, tin, antimony and tellurium compounds in environmental samples by GC-MS. *Journal of Molecular Structure* 661-662: 347–356.
- Kumar, A, Gaurav, A.K. Malik, D.K. Tewary, B. Singh. 2008. A review on development of solid phase microextraction fibers by sol–gel methods and their applications. *Analytica Chimica Acta* 610: 1–14.
- Kumaresan, M. and P. Riyazuddin. 2001. Overview of speciation chemistry of arsenic. *Current Science* 80: 837-846.
- Lambropoulou, D.A., I.K. Konstantinou, T.A. Albanis. 2007. Recent developments in headspace microextraction techniques for the analysis of environmental contaminants in different matrices. *Journal of Chromatography A* 1152: 70–96.
- Larsen, E.H. and S.H. Hansen. 1992. Separation of arsenic species by ion-pair and ion exchange high performance liquid chromatography. *Microchimica Acta* 109: 47-51.

- Leermakers, M., W. Baeyens, M. De Gieter, B. Smedts, C. Meert, H.C. De Bisschop, R. Morabito, Ph. Quevauviller. 2006. Toxic arsenic compounds in environmental samples: Speciation and validation. *Trends in Analytical Chemistry* 25: 1-10.
- Liu, W., Y. Hu, J. Zhao, Y. Xu, Y. Guan. 2006. Physically incorporated extraction phase of solid-phase microextraction by sol-gel technology. *Journal of Chromatography A* 1102: 37-43.
- Liu, W., L. Zhang, S. Chen, H. Duan, X. Chen, Z. Wei, G. Chen. 2009. A method by homemade OH/TSO-PMHS fibre solid-phase microextraction coupling with gas chromatography-mass spectrometry for analysis of antiestrogens in biological matrices. *Analytica Chimica Acta* 631: 47-53.
- Liu, X.D., S. Tokura, M. Haruki, N. Nishi, N. Sakairi. 2002. Surface modification of nonporous glass beads with chitosan and their adsorption property for transition metal ions. *Carbohydrate Polymers* 49: 103-108.
- Limousin, G., J.P. Gaudet, L. Charlet, S. Szenknect, V. Barthes, M. Krimissa. 2007. Sorption isotherms: A review on physical bases, modeling and measurement. *Applied Geochemistry* 22:249-275.
- Lin, B., T. Li, Y. Zhao, F.K. Huang, L. Guo, Y.Q. Feng. 2008. Preparation of a TiO₂ nanoparticle-deposited capillary column by liquid phase deposition and its application in phosphopeptide analysis. *Journal of Chromatography A* 1192: 95-102.
- Lord, H. and J. Pawliszyn. 2000. Evolution of solid-phase microextraction technology. *Journal of Chromatography A* 885: 153-193.
- Mandal, B.K. and K.T. Suzuki. 2002. Arsenic round the world: a review. *Talanta* 58: 201-235.
- Mattarozzi, M., M. Giannetto, A. Secchi, F. Bianchi. 2009. Novel coating for solid-phase microextraction: Electropolymerization of a molecular receptor functionalized with 2,2-bithiophene for the determination of environmental pollutants at trace levels. *Journal of Chromatography A* 1216: 3725-3730.
- Mester, Z. and J. Pawliszyn. 1999. Electrospray mass spectrometry of trimethyllead and triethyllead with in-tube solid phase microextraction sample introduction. *Rapid Communications in Mass Spectrometry* 13: 1999-2003.

- Mester, Z. and J. Pawliszyn. 2000. Speciation of dimethylarsinic acid and monomethylarsonic acid by solid-phase microextraction–gas chromatography–ion trap mass spectrometry. *Journal of Chromatography A* 873: 129–135.
- Mester, Z.; Sturgeon, R. E.; Lam, J. W. J. 2000. Sampling and determination of metal hydrides by solid phase microextraction thermal desorption inductively coupled plasma mass spectrometry. *Journal of Analytical Atomic Spectrometry* 15: 1461-1465.
- Mester, Z., R. Sturgeon, J. Pawliszyn. 2001. Solid phase microextraction as a tool for trace element speciation. *Spectrochimica Acta B* 56: 233-260.
- Mester, Z. and R. Sturgeon. 2005. Trace element speciation using solid phase microextraction. *Spectrochimica Acta B* 60: 1243–1269.
- Mohan, D. and C.U. 2007. Pittman Jr. Arsenic removal from water/wastewater using adsorbents-A critical review. *Journal of Hazardous Materials* 142: 1-53.
- Mollahosseini, A. and E. Noroozian. 2009. Polyphosphate-doped polypyrrole coated on steel fiber for the solid-phase microextraction of organochlorine pesticides in water. *Analytica Chimica Acta* 638: 169–174.
- Musteata, M.L., F.M. Musteata, J. Pawliszyn. 2007. Biocompatible solid-phase microextraction coatings based on polyacrylonitrile and solid-phase extraction phases. *Analytical Chemistry* 79: 6903-6911.
- Nerín, C., J. Salafranca, M. Aznar, R. Batlle. 2009. Critical review on recent developments in solventless techniques for extraction of analytes. *Analytical and Bioanalytical Chemistry* 393: 809–833.
- Pawliszyn, J. 1999. Application of solid phase microextraction. Cornwall, UK: Royal Society of Chemistry
- Perez, M.C., J. Moreda-Pineiro, P. Lopez-Mahia, S. Muniategui-Lorenzo, E. Fernandez-Fernandez, D. Prada-Rodriguez. 2008. Pressurized liquid extraction followed by high performance liquid chromatography coupled to hydride generation atomic fluorescence spectrometry for arsenic and selenium speciation in atmospheric particulate matter. *Journal of Chromatography A* 1215: 15-20.

- Planer-Friedrich, B., D. Wallschläger. 2009. A critical investigation of hydride generation-based arsenic speciation in sulfidic waters. *Environmental Science and Technology* 43: 5007–5013.
- Planer-Friedrich, B., E. Suess, A.C. Scheinost, D. Wallschläger. 2010. Arsenic speciation in sulfidic waters: reconciling contradictory spectroscopic and chromatographic evidence. *Analytical Chemistry* 82: 10228–10235.
- Prasad, B.B., K. Tiwari, M. Singh, P.S. Sharma, A.K. Patel, S. Srivastava. 2008. Molecularly imprinted polymer-based solid-phase microextraction fiber coupled with molecularly imprinted polymer-based sensor for ultratrace analysis of ascorbic acid. *Journal of Chromatography A* 1198–1199: 59–66.
- Puangnam, M. and F. Unob. 2008. Preparation and use of chemically modified MCM-41 and silica gel as selective adsorbents for Hg(II) ions. *Journal of Hazardous Materials* 154: 578–587.
- Ramos, M.A.V., W. Yan, X. Li, B.E. Koel, W. Zhang. 2009. Simultaneous oxidation and reduction of arsenic by zero-valent iron nanoparticles: understanding the significance of the core-shell structure. *Journal of Physical Chemistry C* 113: 14591–14594.
- Risticvic, S., V.H. Niri, D. Vuckovic, J. Pawliszyn. 2009. Recent developments in solid-phase microextraction. *Analytical and Bioanalytical Chemistry* 393: 781–795.
- Roerdink, A.R., J.H. Aldstadt. 2004. Sensitive method for the determination of roxarsone using solid-phase microextraction with multi-detector gas chromatography. *Journal of Chromatography A* 1057: 177–183.
- Shearrow, A.M., S. Bhansali, A. Malik. 2009. Ionic liquid-mediated bis[(3-methyldimethoxysilyl)propyl] polypropylene oxide-based polar sol–gel coatings for capillary microextraction. *Journal of Chromatography A* 1216: 6349–6355.
- Shen, S. J. Lee, W.R. Cullen, X.C. Le, M. Weinfeld. 2009. Arsenite and its mono- and dimethylated trivalent metabolites enhance the formation of benzo[α]pyrene diol epoxide-dna adducts in xeroderma pigmentosum complementation group a cells. *Chemical Research in Toxicology* 22: 382–390.

- Shi, Z.G., F. Chen, J. Xing, Y.Q. Feng. 2009. Carbon monolith: preparation, characterization and application as microextraction fiber. *Journal of Chromatography A* 1216: 5333–5339.
- Silva, R.G.C. and F. Augusto. 2005. Highly porous solid-phase microextraction fiber coating based on poly(ethylene glycol)-modified ormosils synthesized by sol–gel technology. *Journal of Chromatography A* 1072: 7–12.
- Smith, E., R. Naidu, A.M. Alston. 1998. Arsenic in the soil environment: a review. *Advances in Agronomy* 64: 149-195.
- Sur, R. and L. Dunemann. 2004. Method for the determination of five toxicologically relevant arsenic species in human urine by liquid chromatography–hydride generation atomic absorption spectrometry. *Journal of Chromatography B* 807: 169-176.
- Szostek, B. and J.H. Aldstadt. 1998. Determination of organoarsenicals in the environment by solidphase microextraction–gas chromatography–mass spectrometry. *Journal of Chromatography A* 807: 253–263.
- Şeker, A., T. Shahwan, A.E. Eroğlu, S. Yılmaz, Z. Demirel, M.C. Dalay. 2008. Equilibrium, thermodynamic and kinetic studies for the biosorption of aqueous lead(II) and nickel(II) ions on *Spirulina platensis*. *Journal of Hazardous Materials* 154:973-980.
- Tamer, U., B. Yates, A. Galal, T. Gbatu, R. LaRue, C. Schmiesing, K. Temsamani, O. Ceylan, H.B. Mark Jr. 2003. Electrochemically aided control of solid phase micro-extraction (EASPM) using conducting polymer-coated solid substrates applicable to neutral analytes. *Microchimica Acta* 143: 205–215.
- Tan, F., H. Zhao, X. Li, X. Quan, J. Chen, X. Xiang, X. Zhang. 2009. Preparation and evaluation of molecularly imprinted solid-phase microextraction fibers for selective extraction of bisphenol A in complex samples. *Journal of Chromatography A* 1216: 5647–5654.
- Tong, H., N. Sze, B. Thomson, S. Nacson, J. Pawliszyn. 2002. Solid phase microextraction with matrix assisted laser desorption/ionization introduction to mass spectrometry and ion mobility spectrometry. *Analyst* 127: 1207-1210.
- Tsalev, D.L., M. Sperling, B. Welz. 2000. Flow-injection hydride generation atomic absorption spectrometric study of the automated on-line pre-reduction of arsenate,

- methylarsonate and dimethylarsinate and high-performance liquid chromatographic separation of their L-cysteine complexes. *Talanta* 51: 1059-1068.
- Tsalev, D.L., M. Sperling, B. Welz. 2000. On-line UV-photooxidation with peroxodisulfate for automated flow injection and for high-performance liquid chromatography coupled to hydride generation atomic absorption spectrometry. *Spectrochimica Acta Part B* 55: 339-353.
- Tuzen, M., D. Çıtak, D. Mendil, M. Soylak. 2009. Arsenic speciation in natural water samples by coprecipitation-hydride generation atomic absorption spectrometry combination. *Talanta* 78: 52-56.
- United States Environmental Protection Agency, USEPA, Doc. EPA 815-P-01-001, 1999.
- Vassileva, E., A. Becker, J.A.C. Broekaert. 2001. Determination of arsenic and selenium species in groundwater and soil extracts by ion chromatography coupled to inductively coupled plasma mass spectrometry. *Analytica Chimica Acta* 441: 135-146.
- Vidal, L., A. Chisvert, A. Canals, E. Psillakis, A. Lapkin, F. Acosta, K.J. Edler, J.A. Holdaway, F. Marken. 2008. Chemically surface-modified carbon nanoparticle carrier for phenolic pollutants: Extraction and electrochemical determination of benzophenone-3 and triclosan. *Analytica Chimica Acta* 616: 28-35.
- Vuckovic, D., R. Shirey, Y. Chen, L. Sidisky, C. Aurand, K. Stenerson, J. Pawliszyn. 2009. *In vitro* evaluation of new biocompatible coatings for solid-phase microextraction: Implications for drug analysis and *in vivo* sampling applications. *Analytica Chimica Acta* 638: 175-185.
- Wang, Z., C. Xiao, C. Wu, H. Han. 2000. High-performance polyethylene glycol-coated solid-phase microextraction fibers using sol-gel technology. *Journal of Chromatography A* 893: 157-168.
- Wu, J., Z. Mester, J. Pawliszyn. 2000. Speciation of organoarsenic compounds by polypyrrole-coated capillary in-tube solid phase microextraction coupled with liquid chromatography/electrospray ionization mass spectrometry. *Analytica Chimica Acta* 424: 211-222.

- Wu, J.H. Y. Zhao, T. Li, C. Xu, K. Xiao, Y.Q. Feng, L. Guo. 2010. The use of liquid phase deposition prepared phosphonate grafted silica nanoparticle-deposited capillaries in the enrichment of phosphopeptides. *Journal of Separation Sciences* 33: 1806–1815.
- Yates, B.J., K.R. Temsamani, Ö. Ceylan, S. Öztemiz, T.P. Gbatu, R.A. LaRue, U. Tamer, H.B. Mark. 2002. Electrochemical control of solid phase micro-extraction: conducting polymer coated film material applicable for preconcentration/analysis of neutral species. *Talanta* 58: 739-745.
- Yu, J., L. Dong, C. Wu, L. Wu, J. Xing. 2002. Hydroxyfullerene as a novel coating for solid-phase microextraction fiber with sol-gel technology. *Journal of Chromatography A* 978: 37-48.
- Yu, J., C. Wu, J. Xing. 2004. Development of new solid-phase microextraction fibers by sol-gel technology for the determination of organophosphorus pesticide multiresidues in food. *Journal of Chromatography A* 1036: 101–111.
- Yu, Q. W., Q. Ma, Y.Q. Feng. 2011. Temperature-response polymer coating for in-tube solid-phase microextraction coupled to high-performance liquid chromatography. *Talanta* 84: 1019–1025.
- Zewe, J.W., J.K. Steach, S.V. Olesik. 2010. Electrospun fibers for solid-phase microextraction. *Analytical Chemistry* 82: 5341–5348.
- Zhang, Z., M.J. Yang, J. Pawliszyn. 1994. Solid-phase microextraction. *Analytical Chemistry* 66 (17): 844-853.
- Zhang, W., Y. Sun, C. Wu, J. Xing, J. Li. 2009. Polymer-functionalized single-walled carbon nanotubes as a novel sol-gel solid-phase microextraction coated fiber for determination of polybrominated diphenyl ethers in water samples with gas chromatography-electron capture detection. *Analytical Chemistry* 81: 2912–2920.
- Zheng, Z., W. Qiu, Z. Huang. 2001. Solid-phase microextraction using fused-silica fibers coated with sol-gel-derived hydroxy-crown ether. *Analytical Chemistry* 73: 2429-2436.
- Zheng, F. and B. Hu. 2009. Dual silica monolithic capillary microextraction (CME) on-line coupled with ICP-MS for sequential determination of inorganic arsenic and selenium species in natural waters. *Journal of Analytical Atomic Spectrometry* 24: 1051–1061.

Zhu, H., J. Yongfeng, X. Wu, H. Wang. 2009. Removal of arsenic from water by supported nano zero-valent iron on activated carbon. *Journal of Hazardous Materials* 172: 1591–1596.

Zhu, Y., S. Zhang, Y. Tang, M. Guo, C. Jin, T. Qi. 2010. Electrochemical solid-phase nanoextraction of copper(II) on a magnesium oxinate-modified carbon paste electrode by cyclic voltammetry. *Journal of Solid State Electrochemistry* 14: 1609–1614.

VITA

PERSONAL INFORMATION

Surname, Name: BOYACI EZEL

Nationality: Turkish (TC)

Date and Place of Birth: 18.08.1976, Shumen/Bulgaria

Marital Status: Single

Phone: +90 (232) 420 6203

E-mail: ezelboyaci@hotmail.com

EDUCATION

Degree Institution Year of Graduation

MSc İzmir Institute of Technology 2008

BSc İzmir Institute of Technology 2005

WORK EXPERIENCE

Year Place Enrollment

2005-2011 İzmir Institute of Technology, Research Assistant

2004 İzmir Refik Saydam National Public Health Agency, Trainee

FOREIGN LANGUAGES

English (Advanced), Bulgarian (Native)

PUBLICATIONS

Ezel Boyacı, Ali Çağır, Talal Shahwan, Ahmet E. Eroğlu. Synthesis, characterization and application of a novel mercapto- and amine-bifunctionalized silica for speciation/sorption of inorganic arsenic prior to inductively coupled plasma mass spectrometric determination, Talanta 85 (1517–1525) 2011.

T. Shahwan, S. Abu Sirriah, M. Nairat, E. Boyacı, A.E. Eroğlu, T.B. Scott, K.R. Hallam. Green synthesis of iron nanoparticles and their application as a Fenton-like catalyst for the degradation of aqueous cationic and anionic dyes, Chemical Engineering Journal 172 (258–266) 2011.

Nesrin Horzum, Ezel Boyacı, Ahmet E. Eroğlu, Talal Shahwan, and Mustafa M. Demir. Sorption Efficiency of Chitosan Nanofibers toward Metal Ions at Low Concentrations, Biomacromolecules 11 (3301–3308) 2010.

Ezel Boyacı, Ahmet E. Eroğlu, Talal Shahwan. Sorption of As(V) from waters using chitosan and chitosan-immobilized sodium silicate prior to atomic spectrometric determination, Talanta 80 (1452-1460) 2010.

AWARDS

2nd rank in graduation from BSc (İzmir Institute of Technology, Department of Chemistry)

ExTech 2010 best poster presentation (12th. International Symposium on Advances in Extraction Technologies, 19-22 September 2010, Poznan University of Life Sciences, Poznan, Poland)

I. Trace Analysis Workshop (EsAn-2010) 3th award for poster presentation (22-25 April 2010- Pamukkale University Faculty of Arts and Sciences, Department of Chemistry, Denizli, Turkey)